

Fitness-based classification of phytoplankton species from the southern North Sea

Von der Fakultät für Mathematik und Naturwissenschaften
der Carl von Ossietzky Universität Oldenburg
zur Erlangung des Grades und Titels eines
Doktor der Naturwissenschaften (Dr. rer. nat.)
angenommene Dissertation

von

Dipl.-Biol. Nico Grüner,
geboren am 19. September 1979
in Emsdetten.

Erstgutachter: PD Dr. Jan A. Freund
Zweitgutachterin: Prof. Dr. Karen H. Wiltshire
Tag der Disputation: 21.03.2017

Abstract

The determination of the ecological niche and the grouping of species into generalists and specialists are established ecological concepts carried out even today. However, a new method of ecological niche reconstruction is introduced in this thesis, and this new method, called the optimal niche estimate, reconstructs the ecological niche in a new manner by taking the fitness of the species into account. An application of this method to a subset of the Helgoland Roads data, a marine long-term time series, resulted in optimal niches for different phytoplankton species. A niche volume was computed with the environmental conditions at the times of fastest growth for every species, allowing for an estimation of the range in which the analysed species showed their highest fitness. The time series of 23 selected species, mainly diatoms and dinoflagellates from the Helgoland Roads data were analysed and the volume of the optimal niche was interpreted in a way comparable to the classical ecological niche introduced by Hutchinson (1957). Species with a large optimal niche showed their highest growth rates in a wide range of environmental conditions, while species with a small optimal niche had their times of fastest growth distributed over a small range of the environmental parameters. A general tendency that the analysed species are more often classified as specialists than as generalists was identified.

The optimal niche estimate was applied to different periods of sampling and to different combinations of the environmental factors to identify the sensitivity of the computation. Finally, this method was used to test for some global hypotheses with an increased number of analysed species. It was shown that the number of presence days per year had no impact on the size of the optimal niche, but that species with a large number of time points with fastest growth in this time series tended to have larger optimal niches. Additionally, the variability of the environmental parameters were analysed, and it was shown that species that had their times of fastest growth in the period of the year with a high variability had larger optimal niches than species

with their times of fastest growth in the period with small variability. Lastly, a splitting of the time series into sections and a ‘running’ niche analysis were carried out to investigate the reported regime shifts, as opposed to a trend an abrupt change in the environment. These customizations of the optimal niche estimate clearly identified anomalies in the different time periods and supported the detected regime shifts for the southern North Sea.

Zusammenfassung

Die Bestimmung der ökologischen Nische und die Einteilung von Arten in Generalisten und Spezialisten sind etablierte ökologische Konzepte. Diese Dissertation führt eine neue Methode zur Bestimmung der ökologischen Nische ein. Diese neue Methode, die Bestimmung der optimalen Nische, nutzte ein Maß für die Fitness, um die optimale Nische zu bestimmen. Die Anwendung dieser Methode auf die Helgoland Reede Daten, eine marine Langzeit-Datenreihe, klassifizierte die ausgewählten Arten anhand der Größe ihrer Nischen. Mit Hilfe der Umweltparameter zum Zeitpunkt des schnellsten Wachstums der einzelnen Arten wurde das Nischenvolumen berechnet und das zeigte wiederum, wie groß der Bereich ist, in dem die einzelnen Arten ihre größte Fitness hatten. Dieses Nischenvolumen wurde in einer ähnlichen Weise wie die von Hutchinson eingeführte ökologische Nische interpretiert, erweiterte diese Interpretation aber um einen Fitnessparameter. Zusätzlich wurde durch das Hinzufügen von zwei biotischen Faktoren – einem Maß für den Fraßdruck und einem Maß für die intra- und interspezifische Konkurrenz – zu den abiotischen Faktoren eine neue Perspektive für die Nischenanalyse eröffnet. 23 ausgewählte Arten der Helgoland Reede Daten, hauptsächlich Diatomeen und Dinoflagellaten, wurden mit der neuen Methode untersucht. Arten mit einer großen optimalen Nische hatten die Zeitpunkte des schnellsten Wachstums über einen weiten Bereich der Umgebungsparameter verteilt und Arten mit einer kleinen optimalen Nische hatten die Zeitpunkte des schnellsten Wachstums über einen engen Bereich verteilt. In dieser Untersuchung wurde deutlich, dass die Mehrzahl der ausgewählten Arten eine Tendenz zum Spezialisten hatte.

Diese neue Methode wurde auf verschiedene Kombinationen der Umweltparameter und auf verschiedene Abschnitte der Zeitreihe angewandt, um den Einfluss der Zusammensetzung des Datensatzes zu untersuchen. Weiterhin wurden verschiedene globale Hypothesen mit einer größeren Anzahl an Arten getestet. Es wurde gezeigt,

dass die Anzahl der Tage, an denen die einzelnen Arten in der Zeitreihe gefunden wurden, keinen Einfluss auf die Nischengröße hatte und dass Arten mit einer großen Anzahl an Zeitpunkten des schnellsten Wachstums eine Tendenz zu größeren Nischen hatten. Zusätzlich wurde die Variabilität in den Umgebungsparametern untersucht und festgestellt, dass die Arten mit den Zeitpunkten des schnellsten Wachstums im Bereich größerer Variabilität auch größere Nischen hatten. Letztendlich wurde die neue Methode auf verschiedene Zeitabschnitte angewandt und zusätzlich eine gleitende Nischenanalyse durchgeführt, um die bereits beschriebenen „Regime Shifts“ (eine Änderung der Umwelt innerhalb eines kurzen Zeitraumes im Gegensatz zum Trend) zu untersuchen. Diese Anpassung der Methode zeigte deutlich, dass die Folgen der „Regime Shifts“ in der südlichen Nordsee erkannt werden konnten.

Contents

1. Introduction	10
2. Phytoplankton	21
3. Helgoland	25
3.1. Habitat	25
3.2. The island, the station, and the data	27
4. Phytoplankton abundance data and the extraction of the fitness parameter	47
4.1. The Idea	47
4.2. The phytoplankton abundance curve	47
4.3. Parameters considered for the niche classification	49
4.4. The inflection point	54
5. Processing the data	59
5.1. Outline of the method	59
5.2. Detection of the inflection points	60
5.3. Principal component analysis and visualization	62
5.4. Statistics	73
5.5. Sensitivity of the optimal niche to the extracted number of principal components	77
5.6. Results	79
6. Variation of the biotic database	82
6.1. Transformation of the abundance data	82
6.2. Different compositions of the environmental dataset	83
6.2.1. Approaches	83

6.2.2.	Computation with different biotic data - 1967 until 2008	85
6.2.3.	Computation with different biotic data - 1974 until 2008	91
6.2.4.	Differences and similarities between the approaches with varied environmental factors	107
7.	Ecological interpretation of the results	115
7.1.	Consequences of the inclusion of all biotic data for the 23 selected species	115
7.2.	Analysing an increased number of species to test some general ecological hypotheses	133
7.2.1.	How these species were analysed	133
7.2.2.	Hypothesis 1: <i>Species with a small ONE are specialists and thus have a lower number of presence days per year than those with a big ONE</i>	134
7.2.3.	Hypothesis 2: <i>The size of the optimal niche is positively correlated with the number of inflection points</i>	137
7.2.4.	Hypothesis 3: <i>Species with inflection points in summer face more variable environmental conditions than species with inflection points in spring and therefore have a bigger ONE</i> . .	139
8.	Niche changes against the backdrop of regime shifts in the North Sea	145
8.1.	Changes in the context of the reported regime shifts	145
8.1.1.	Modification of the ONE method	145
8.1.2.	Results	148
8.1.3.	Discussion	151
8.2.	Sliding window analysis	152
9.	Discussion of the newly developed method	157
9.1.	Summary	157
9.2.	Why the new method?	157
9.3.	Advantages of the new method	163
A.	Appendix	165
A.1.	Graphs of the 23 selected species	165

A.2. Species list	177
List of Figures	181
References	189
Danksagung, Lebenslauf, Erklärung	218

1. Introduction

The term *ecology* was introduced by Haeckel (1866), who understood it as the interaction of organisms with their environment. Nowadays, a classification of this interaction is often done through an analysis of the ecological niche. The traditional concept of the ecological niche is widely known and has gone through various refinements and adaptations. Wake et al. (2009) point out that the expression *niche* was used for the first time by Johnson (1910) in his book ‘Determinate evolution in the color-pattern of lady-beetles’. However, the introduction of the ecological niche concept is usually attributed to Joseph Grinnell, who explained the distribution of mammals and birds (Grinnell, 1914) and the distribution of the California Thrasher (*Toxostoma redivivum*) based on the niche concept (Grinnell, 1917). After Grinnell’s introduction of the term, Elton (1971) used the phrase in another way. These two authors had different ideas of the niche. The Grinnellian niche was determined by analysing noninteractive and nonconsumable variables in the multidimensional niche space. These factors, like temperature, cannot be changed by the species. The Eltonian niche was characterized by the analysis of variables related to ecological interactions and resource consumption (Soberón, 2007). Thirty years after Elton’s interpretation of the niche, the niche concept was popularized by Hutchinson (1957), who defined the niche in a rather abstract way. He introduced the definition that the niche is constructed by the resources used by or influencing a species:

We may now introduce another variable (...) until all of the ecological factors relative to S_1 have been considered. In this way an n -dimensional hypervolume is defined, every point in which corresponds to a state of the environment which would permit the species S_1 to exist indefinitely. For any species S_1 , this hypervolume \mathbf{N}_1 will be called the fundamental niche of S_1 . Similarly for a second species S_2 the fundamental niche will be a similarly defined hypervolume \mathbf{N}_2 .

It will be apparent that if this procedure could be carried out, all X_n variables, both physical and biological, being considered, the fundamental niche of any species will completely define its ecological properties. The fundamental niche defined in this way is merely an abstract formalization of what is usually meant by an ecological niche. Hutchinson (1957, p. 416)

This was the first approach to explain the niche as a high-dimensional structure of all environmental factors relevant for a species. Because of the inclusion of several environmental factors, this theoretical concept is well suited for multivariate time series analysis, and a method for the classification of a comparable ecological niche is developed in this thesis. Hutchinson refined this concept of the ecological niche (Hutchinson, 1957) by introducing two different kinds of niches: the *fundamental* and the *realized* niche. The fundamental niche (Hutchinson credits Robert MacArthur with coining this term) has to be seen as the ecological niche of a species without any biological interaction. No competition or grazing is included in this interpretation, and it is thus nearly impossible to find this kind of niche in the ‘real’ world. However, in laboratory experiments, a detection of this fundamental niche can be realized through an exclusion of competition and grazing. The realized niche is what should be expected when considering these biological interactions, and this niche is, therefore, the one that can be found in the habitat. Due to the biological interaction (competition, predation, etc.), this niche is usually smaller than the fundamental niche. Exceptions can be considered as some effects of facilitation (e.g. mutualism) leading to a realized niche that is larger than the fundamental one. In experimental ecology, the transition from the fundamental to the realized niche is often paralleled by the step from laboratory experiments to fieldwork. While in a typical laboratory experiment all but a few abiotic factors are kept constant and biotic factors are preferably excluded, all factors in the field including the biotic or interaction milieu (McGill et al., 2006) (competitors, predators, and prey) are dynamic quantities prone to fluctuation. Therefore, reconstructions of the fundamental niche from laboratory experiments may vastly differ from corresponding reconstructions of the realized niche from field data.

Hutchinson’s theoretical concept had a strong influence on the ecological research community, and the analysis of the ecological niche has been carried out in many

different ways. Nonetheless, this theoretical and high dimensional niche is hard to detect in experiments, because one has to sample all environmental factors relevant for the species. This is impossible, because all factors and the combination of factors relevant for the species cannot be known and even if it were possible, it would cost a lot of time and money to sample all of them. By measuring an array of factors considered important for the species, one can get a reliable estimate of this kind of ecological niche.

This thesis classifies the ecological niche using a method based on real data sampled at Helgoland, Germany's only offshore island. Helgoland lies at a distance of 65 km off the coast in the German Bight (Bauerfeind et al., 1990). The sampling station is at Helgoland Roads, an old position of a buoy, and sampling has been carried out since 1962 (Franke et al., 2004). All factors (except the microbiological time series) sampled along with the Helgoland Roads Data (HRD) are included and enable a reliable estimation of the ecological niche. A detailed overview of the time series sampled at Helgoland Roads can be found in a special issue of 'Helgoland Marine Research' (Wiltshire, 2004). One may argue whether these are all relevant factors, but proxies for potentially missing data can be considered as included, because they are correlated with the sampled data (e.g. salinity and nitrate as proxies for coastal water masses). Based on a reconstruction of species-specific ecological niches from field data and the inclusion of biotic and abiotic data, this thesis aims at classifying the realized niche of selected phytoplankton species.

The utilization of marine phytoplankton data for niche analysis has not been done often for a number of reasons. Most importantly, a long and densely sampled species dataset is needed, because a reconstruction of the ecological niche can only be done if the waxing and waning of the abundances are measured and if the changed conditions throughout the year are included as well. This is a great and expensive effort, especially due to the work force required. Therefore, there are just a few adequate time series for a niche analysis worldwide. Additionally, the environmental factors have to be included in this series of measurements.

Phytoplankton forms the basis of the marine food web, and changes in this phylum have a strong influence on the higher trophic levels of the food web. This influence will pass through the food web until it reaches humans. Lower phytoplankton abundances can result in a decrease in fish stocks, while higher abundances of some

phytoplankton species can lead to harmful algal blooms representing a possible danger for man and fish (Smayda 1997a and Smayda 1997b). The most important fact about this phylum is that these photosynthetic species "emit much of the oxygen that permeates our atmosphere" (Falkowski, 2012, p. S17).

The seasonal dynamic of phytoplankton is well known (for details, see Chapter 2), and especially the dynamic blooms are characteristic of these species. These blooms occur in spring and summer (or autumn), and are connected with seasonal dynamics of the environmental parameters, the nutrients, and the species grazing on phytoplankton, mainly species from the zooplankton. These dynamics can be identified for every year, and it is thus possible to identify an average of 73 blooms for the species analysed from the HRD in this thesis (maximum number of blooms 133; minimum number of blooms 21). These numbers reflect that not all species show the same blooming pattern—while some species bloom only once every year, others bloom twice or even thrice.

There are various methods to identify an ecological niche, but the methodological approaches can be very different. One main difference between the approaches is the concept behind the analysed niche. Hutchinson (1978) (cited in Newsome et al. (2007)) distinguished between scenopoetic and bionomic factors, where the scenopoetic factors set the bioclimatic stage (area with its characteristics) in which a species performs and the bionomic factors define the resource the species uses. Soberón (2007) and Soberón and Nakamura (2009) utilized this to distinguish between the Eltonian and the Grinnellian niche determining methods by the set of variables used. The Hutchinsonian niche, which is a combination of these two approaches, has been investigated in this thesis. In early ecological niche research and even today, the niche was often determined through laboratory experiments and the range of a single parameter was investigated. These experiments were often conducted to identify in what range of temperature a species can survive, or in what range of salinity a species reproduces. This can lead to artefacts in the measurements, because results from the laboratory cannot be transferred to field data without restrictions. This is because the environment is the driving force for the realized ecological niche and the interaction between different environmental factors can restrict the species to a niche never identified through laboratory experiments.

Today, the methods of niche reconstruction have undergone a profound change and sophisticated multivariate statistical tools are applied. The following statistical methods for describing the ecological niche can be found in the literature, often focusing on different conceptual aspects. Colwell and Futuyma (1971) set up a model where the species are sampled in the field and the environmental parameters are measured. The species numbers in the different resource states (e.g. soil moisture) are counted, and the distribution of the species along this gradient is used to calculate the niche breadth (and niche overlap) with the help of a measure for the uniformity of the distribution of the individuals. This method shows the range where the species can be found and, hence, the breadth of the ecological niche. Niche overlap is the joint use of a resource by two or more species, i.e. where the distributions overlap (Colwell and Futuyma, 1971).

Green (1974) (refinement of a method published in Green (1971)) developed a multivariate statistical method to reconstruct the Hutchinsonian niche. Based on a multiple discriminant analysis, this method reduces the dimensionality of the dataset, followed by a grouping of species with respect to the environmental factors. Mollusc species in different lakes were sampled, and the corresponding environmental parameters were measured. With this dataset of species presence, the method gives a grouping of the species where the groups consist of species with similar presence patterns. The method developed in this thesis also uses a dimension reduction, but the reconstruction of the niche is done in a completely different way, which will be outlined in the following paragraphs. Additionally, Green (1974) took only the presence into account and postulated: "If a species is present, one can conclude that the species can live there, and that the total niche for the species must include that point in ecological space" (Green, 1974, p. 545). This is of course true; however, as shown below, it is a completely different viewpoint of the niche than that proposed in this thesis.

Feinsinger et al. (1981) used the proportional similarity index to quantify the niche breadth. In this approach, the niche is quantified with reference to the supply of the resources. A species exploiting the resource as it is found in the habitat shows a wider niche than a species utilizing the resources in a different way, i.e. a species with a wide niche exploits the resource as it is supplied. This approach opens a completely different perspective on the ecological niche and is not followed in this

thesis. Because of the strongly fluctuating character of this habitat in the German Bight, applying this approach to the Helgoland Roads Data is nearly impossible. Due to the seasons and the resulting aforementioned fluctuation in the phytoplankton abundance and in the nutrients, the species numbers and the resource concentrations are changing too fast.

Another multivariate approach was carried out by ter Braak (1986) and ter Braak and Verdonschot (1995) by determining species-environment relationships using a newly developed ordination method—the canonical correspondence analysis. It was developed to "extract synthetic environmental gradients from ecological data sets. The gradients are the basis for succinctly describing and visualizing the differential habitat preferences (niches) of taxa via an ordination diagram" (ter Braak and Verdonschot, 1995, p. 255).

A relatively recent method measures the distance between the average habitat conditions used by a species and the average habitat conditions of the sampling area or period (Hausser, 1995). Since this method determines the marginality (i.e. the deviation of the average habitat conditions) of a given species, it is called outlying mean index (OMI) analysis (Dolédec et al., 2000). The niche parameters position and breadth are calculated by an ordination technique, weighting the environmental factors by the species' abundance. Niche position is specified by the distance between the mean habitat conditions used by the species and the mean habitat conditions of the sampling site. Therefore, niche position describes the position of the niche in the original dataset. To be exact, the ordination technique reduces the dimension of the original dataset and, therefore, the niche is computed on this subset. Niche breadth describes the tolerance of a species with respect to the environmental parameters in the habitat, i.e. the expansion of the niche in the subspace. The OMI was used to analyse the niche characteristics of unicellular eukaryotes and the niche of orchids of east Macedonia (Heino and Soininen, 2006; Tsiftsis et al., 2008). Additionally, Gebühr et al. (2009) applied this method to a marine dataset for a yearly abundance-based reconstruction of the niche with a species from the HRD. The main disadvantage of a yearly niche reconstruction in a strongly fluctuating environment is the interannual variability. This makes it difficult to compare the niches for different years, because this reconstruction results in a completely different niche due to the change of the environment. The niche in one year can be larger

than in another year because of a broader scale in the environmental factors. Additionally, this disadvantage makes it difficult to distinguish short-term fluctuations from trends or regime shifts (DeYoung et al., 2008, see Section 3.1 for more details).

Hooper et al. (2008) extracted positive ranges of the population growth rate of the zooplankton species *Daphnia magna* at different pH values and calcium. The values with positive growth rates were used to define the ecological niche of the population. They analysed these ranges in the laboratory, tested the gained results against field data, and predicted the species distribution in a large sample set of lakes from England and Wales. Using positive growth rates is an interesting approach because here one is not concentrating on the abundance anymore, but instead analysing a niche also involving the overall physiological properties of a species. This represents an extraction of environmental conditions where the species performs well and therefore shows a high fitness. This idea, although realized in a different way, is comparable in the broadest sense to the concept of niche classification put forward in this thesis. The underlying understanding of the niche, the use of field data for the classification, and the inclusion of a different species-specific parameter can be seen as similarities.

Hutchinson's notion explains the niche through indefinite existence, but considering the seasonal fluctuation of the phytoplankton counts, how would it be possible to extract the conditions in which a species can exist forever? The waxing and waning of species in the seasonal cycle makes it impossible to determine the parameters at which a species exists forever. Consequently, the Hutchinsonian concept had to be revised. This thesis focuses on special conditions of phytoplankton growth and not on mere abundance, unlike the majority of niche classification methods. This special condition is the time of fastest net growth and represents the phase where the species apparently experiences optimal growth conditions. These are definitely advantageous situations for the species. The extraction of the times of fastest growth even widens the idea of an indefinite existence to conditions that are optimal for the species, especially for a strong fluctuating environment where indefinite existence would be hard to determine. Hence, the new method was named the *Optimal Niche Estimate* (in the following abbreviated as ONE), and the adaptation of the ecological niche concept to the idea of an optimal niche was developed in this direction.

This completely new approach to niche classification has some advantages over the previously developed methods. ONE not only determines the realized niche using

environmental data, but also introduces the notion of fitness into the niche concept, thus enabling a reconstruction of the fitness-based realized niche.

Fitness (first introduced by Darwin (1859)) can be described as the performance of a species or genus in relation to an environmental factor or the success of a second generation. Examples include bodyweight in relation to food supply, the metabolic rate in relation to temperature, and the ratio of reproduction rate to temperature. The fitness notion used in this thesis can be seen as a species population average (or an average of the part of the population found in the investigated area). Of course, it is not possible to determine the individual fitness with this dataset, and we cannot be sure if there is any genetic variation included. Some species can potentially be divided into strains that might be adapted to different conditions. The analysis of these strains is not a part of the time series, but one has to keep in mind that this variation could have an influence on the results. For example, *Paralia sulcata* showed a change in presence timing (change from presence in winter to presence throughout the year) connected with a change in the competitive milieu (Gebühr et al., 2009). This could be the result of different strains growing at different times and favouring different conditions. An analysis of the 18S rRNA (Gebühr, 2010) showed a clear genetic differentiation between species isolated in January and from October to December (if a season is mentioned in this thesis, it refers to the Northern Hemisphere).

The volume of an ecological niche is computed with ONE. In two dimensions, this niche volume is a subset of the environmental dataset (gray ellipse in Figure 1.1). The times of fastest growth and hence the optimal growth conditions are highlighted in this subset. This characterization of an ecological niche is quite different from what was done before, and introduces the following new idea: In ONE, the spread of the optimal niche is characterized with respect to the environmental dataset. This can be seen as an approach in spirit similar to the Hutchinsonian niche, but with a different interpretation. The optimal niche has to be seen as a smaller part of the Hutchinsonian niche because the range where species grow fastest will probably be only a subset of the conditions where indefinite existence is possible. This shows the difference in these concepts, because the optimal niche concentrates on maximal fitness within a specific period, not on indefinite existence. By concentrating on the maximal fitness of the species, the interpretation of the optimal niche has to be done

in a different way. One can identify species that show their fastest growth only under special conditions (red and blue ellipses in Figure 1.1) as well as species that are capable of growing fast at many diverse compositions of the environmental conditions (green ellipse in Figure 1.1). These times of fastest growth can be extracted for every bloom event (rapid increase in phytoplankton cell counts) and every species. Hence, the conditions found at these times can be compared to the global conditions found in the habitat, and a classification into specialist and generalist can then be reached. Another essential difference from Hutchinson's idea is that, for practical reasons, the ONE constructs the niche in a new subspace of the dataset and not as an n-dimensional hypervolume.

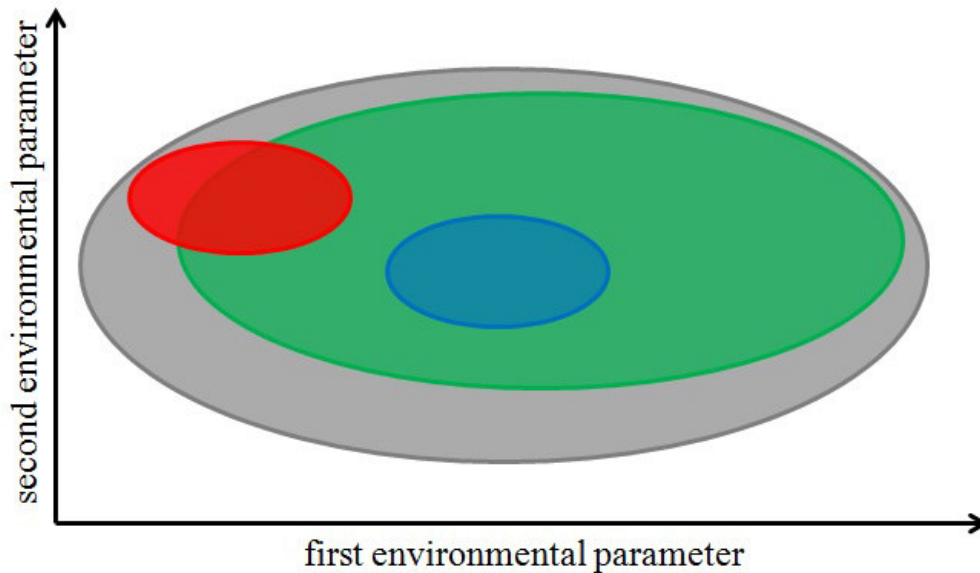


Figure 1.1.: Sketch of different concepts of niche classification; gray: environmental conditions; green: generalist - occupying nearly the whole range of the environmental conditions; blue: specialist or generalist - found at the average environmental conditions (centre) but only in a small range; red: specialist - found in a small range and at the border of the environmental conditions (extended after Gebühr (2010))

Another somewhat related interpretation of specialist and generalist can be found using the approach presented in Dolédec et al. (2000). A species that is found at the average conditions of the habitat is classified as a generalist (blue and green ellipses in Figure 1.1) and a species at the border of the cluster of the environmental

conditions is seen as a specialist (red ellipse in Figure 1.1). This is called the niche position (Dolédec et al., 2000). It includes the traditional concepts of large and small niches as a classification of how broad the range of environmental conditions is where a species is found based on abundance. This is determining the so-called niche breadth. As Figure 1.1 suggests, niche position and breadth are anti-correlated since the more peripheral it is the smaller the ellipse will be. In ONE, the niche position is not analysed, but in Chapter 8 the centre of the ellipsoids is used to determine a drift of the niche in different sections of the time series. A species showing the highest growth rates in a small range of the average environmental conditions is considered a specialist in ONE. This is done because a small range is considered a strong result, and just lying at the centre does not necessarily mean that the species is a generalist, because a generalist should utilize the different combinations of the environmental conditions over their whole range. Therefore, the volume or the breadth has more power to classify a species than the position.

In summary, this thesis introduces a fitness-based reconstruction of the realized ecological niche from multivariate field data. The results of this niche classification are not directly comparable to previous niche estimates, as the optimal niche evaluates a species based on its performance rather than its presence. The fitness-based niche is ecologically more meaningful than the abundance-based niche, because indefinite existence (Hutchinson, 1957) is rather a question of fitness than abundance. Identifying fitness with sheer abundance can be misleading, since the highest abundance specifies a moment when net growth ceases. Several other reasons may explain the stagnation and subsequent decline of the population size, for instance, increased grazing pressure or viral infection, and it is possible that reduced net growth expressing poor physiological fitness is only one of them but a not-so-unlikely one. By contrast, the fastest net growth can only be explained by high fitness—sufficiently high to overcompensate for all losses. The usage of field data leads to the realized niche and decouples the niche reconstruction from the laboratory.

This thesis shows how this new kind of ecological niche is classified. After the explanation of the ecology of phytoplankton in Chapter 2, Chapter 3 explains the characteristics of the habitat, shows the selected data, and gives an ecological overview of the selected species. Chapter 4 reviews the main characteristics of the phytoplankton time series. Additionally, the differences between abundance- and fitness-

based analyses are detailed by an application of these concepts to one exemplarily species through a stepwise procedure. The extraction of this novel fitness descriptor is explained, and following this specification of the idea and procedure, Chapter 5 explains the details of the newly developed method and ends with the results for every selected species. This result is a classification of each species, and thus a range of specialization is given for every species. This shows the size of the optimal niche for the selected species. Chapter 6 shows a modification of the method to different sets of biotic data and discusses the results for every approach. This comparison reveals the influence of this adaptation. This was done because the zooplankton (included as an environmental parameter for phytoplankton) was sampled with a different time resolution. The inclusion of zooplankton and the total abundance of the selected phytoplankton as biotic environmental factors improve the classification of the optimal niche. After the methodological procedures, Chapter 7 discusses the results for the species ecologically. The characteristics of the optimal niche are illustrated and a species-specific classification is conducted. Additionally, through an increase in the analysed species number to 115, some hypotheses for the concurring phytoplankton community are tested. These hypotheses are as follows:

- 1) Species with a small ONE are specialists and thus have a lower number of presence days per year than those with a big ONE.
- 2) The size of the optimal niche is positively correlated with the number of inflection points.
- 3) Species with inflection points in summer face more variable environmental conditions than species with inflection points in spring and therefore have a bigger ONE.

Another extension of the method is shown in Chapter 8 where the change in the niche characteristics is analysed within the framework of the reported regime shifts (see Section 3.1 for more details). This shows that a segmentation of the HRD into subsets with respect to the regime shift years enables a visualization of the changes in the habitat and in the species-specific optimal niche. The last Chapter 9 presents a general discussion of the advantages and limitations of this new method and includes an outlook with open questions.

2. Phytoplankton

To understand life in the sea, it is necessary to understand the life cycles and the ecological influences on phytoplankton. Phytoplankton have many shapes and forms, and can be found single-celled or in chains. They can float in the water column (pelagic species) or lie on the sea floor (benthic species) (Fogg, 1991). These manifold characteristics are reflected in the phytoplankton life cycle (Reid et al., 1990). The typical phytoplankton dynamics are the yearly succession of species with the corresponding nutrient depletion (Gillbricht, 1988) and the recurring algal blooms (Figure 2.1). These blooms are characterized by a fast mass development of the individual numbers and a steep decline after reaching the maximum.

One can identify some phytoplankton blooms every year at Helgoland and in the German Bight, the area investigated in this work (Hoppenrath et al., 2009). The first bloom starts in spring and is dominated by diatoms. This bloom is favoured by replenishment through recycling and only sparse consumption of nutrients throughout winter. The turbulent conditions during winter rebuild these nutrient stocks through resuspension. The days get longer, and since most of phytoplankton species are autotrophic and photosynthetic organisms (Raven et al., 2000), this leads to an increased growth through improved availability of light. The last condition is the stratification of the water column through the elevation of temperature (Townsend et al., 1994). This causes the species to stay in the upper part of the water column, leading to a prolonged exposure to light. A steep increase in the species number is the result, and the bloom reaches its maximum in about two weeks. Afterwards, the individual numbers start to decline because of a high grazing pressure from the now-dominant zooplankton. These zooplankton establish a large population and start reducing the phytoplankton population. With reference to the diatoms, this zooplankton bloom is time-delayed. Another reason for the decline of the diatom bloom is the depletion of silicate. Moreover, viral or parasitic infections of the phy-

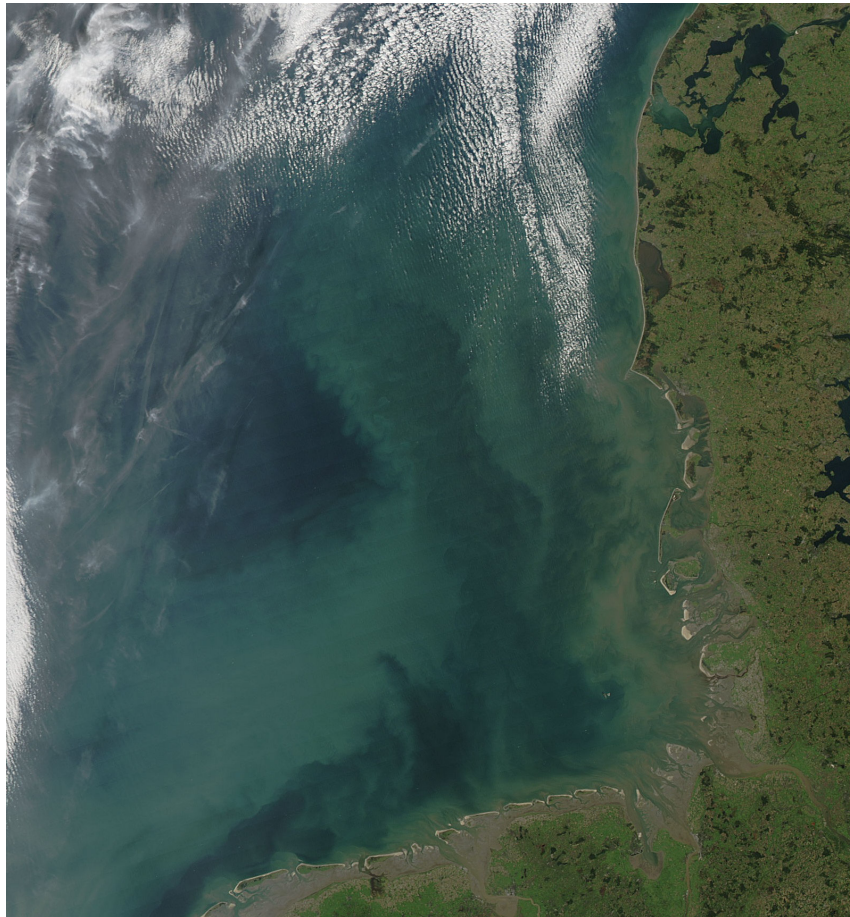


Figure 2.1.: Phytoplankton blooms in the North Sea in late October 2011 with brownish sediment clouds close to the coast; NASA images, courtesy Jeff Schmaltz, MODIS Rapid Response Team, Goddard Space Flight Center - detail from the original picture

toplankton species probably reduce the fitness or even the cell counts (Brussaard, 2004; Llewellyn et al., 2008; Tillmann et al., 1999). This spring bloom is normally followed by a summer bloom dominated by dinoflagellates, because only silicate is depleted and the concentration of the other nutrients is still high enough for the dinoflagellates to grow (Löder et al., 2011). This short summer bloom is followed by a period of nearly no growth, and through turbulence and mixing, nutrients are rebuilt again. In late summer or autumn, the last bloom of the year follows dominated by diatoms again. The following turbulent condition reduces the phytoplankton growth, and the bloom declines (Hoppenrath et al., 2009). The special conditions at Helgoland can exhibit some differences in these dynamics, because the water is usually well mixed at the shallow sampling station at Helgoland Roads (Wiltshire et al., 2008).

This dynamic characteristic is important for the niche analysis done in this thesis. Because of the waxing and waning, it is possible to identify times of fastest growth and relate these times to the corresponding environmental conditions. This enables the reconstruction of the fitness-based realized niche of phytoplankton.

The distribution of phytoplankton species still lacks a detailed overview; however, there are some regular sampling stations where it is identified which species are found at this spot. Besides, there were many cruises where species were sampled and the distribution of species in these transects was determined (e.g. the Continuous Plankton Recorder Survey (Warner and Hays, 1994)). Some species are presumably globally distributed, while others are restricted to distinct areas. However, this information is often hard to find.

Some phytoplankton species are used as model organisms for microbiological research, such as investigating the production of exudates (Paul et al., 2009), the vulnerability to viruses (Llewellyn et al., 2008), or the investigation of predator-prey relationships (Gutiérrez-Rodríguez et al., 2011). Some phytoplankton species are used for the determination of water quality (Shi et al., 2012), or the bacterial community found in combination with phytoplankton species is studied (Rink et al., 2011).

These investigations are meant to understand the community and life cycle of phytoplankton. Additionally, a lot of modelling is done in this field of plankton research to understand the succession of phytoplankton and the dynamics in this

ecosystem. These modelling approaches are often done in the framework of nutrient-phytoplankton-zooplankton (NPZ) models (Franks, 2002) where interactions of these parameter are studied. Moreover, the phytoplankton dynamics in the German Bight were modelled (Brandt and Wirtz, 2010) with an NPZ model coupled with the General Estuarine Transport Model (GETM, Stips et al. 2004) and help to understand the activity in this part of the North Sea. The application of trait-based models to understand which functional traits are driving the dynamics of the phytoplankton population is regularly done (Litchman and Klausmeier, 2008). The traits are used to define functional groups of species (i.e. different species with similar characteristics), and this allows the modelling of different kinds of species without a concentration on single species. Trade-offs between the characteristics of different functional groups can be used to model the impact of a changing environment or which functional group is able to outcompete the other under which circumstances.

3. Helgoland

3.1. Habitat

The North Sea is one of the greatest neritic shelf seas in the world (Huthnance, 1991) with an area of 575 300 km² and a water mass of 40 300 km³ (ICES, 1983). It is mainly a shallow basin with a mean depth of approximately 100 m and can be divided into different water masses, the main ones being the North Atlantic, Channel, Skagerak, Scottish Channel, English coastal, and Continental coastal masses (Lee, 1980). The nutrient-rich water from the Atlantic has a strong influence on the northern part of the North Sea (Radach, 1992). Helgoland is Germany's only offshore island and situated in the German Bight, with the shortest distance to the coast being about 65 km (Bauerfeind et al., 1990). The German Bight is part of the Continental coastal water mass, which is comprised of the southern part of the North Sea and a shallow coastal area with a high influence of fresh water inflow through river discharge. The main rivers discharging into the German Bight are Ems, Weser, and Elbe, carrying nutrients and suspended load with the fresh water into the German Bight. Radach and Pätsch (2007) showed that 4.3% of the phosphorous and 9.4% of the nitrogen input into the entire North Sea are through rivers and that the main nutrient inflow comes through the advective flows. However, the highest nutrient loads are found in the area close to the continental coast (Radach, 1992). The special position of Helgoland far from the coast makes it ideally suitable for the sampling of a time series where the coastal conditions, especially the influence of freshwater inflow, are not as pronounced as for the islands in the German Wadden Sea. Nevertheless, the influence of the river Elbe can sometime be shown at Helgoland. Following times with a high river discharge, the diluted Elbe plume sometimes reaches the island (Hickel, 1998). This water carries nutrients and water with a lower salinity, which can have an influence on the species community at Helgoland. This can lead to an

advantageous composition of the environmental factors for species that tolerate this lower salinity or need higher concentration of nutrients.

The North Sea water body has undergone some dramatic changes throughout the sampling period and analyses for regime shifts were done for different areas, species groups, and datasets (Kraberg et al., 2011). In marine ecosystems, a regime shift is an abrupt change in the environment (Lees et al., 2006), not just in a few measured parameters. A regime shift has to be seen in contrast to long-term trends or fluctuations with extended autocorrelations (red noise), and it is detected as a pronounced change in a short time period compared to the regimes before and after the shift (DeYoung et al., 2008; Rudnick and Davis, 2003). Beaugrand (2004), Weijerman et al. (2005), and Wiltshire et al. (2008) utilized datasets for a regime shift detection and concluded that these shifts happened around 1979 and 1988. A regime shift for the year 1998 is discussed, but evidence for a shift in this year can be found (Weijerman et al., 2005). A regime shift analysis carried out in this thesis (Chapter 8) and published as part of Freund et al. (2012) provides strong evidence for a pronounced shift in this year. While the regime shift in the year 1979 is seen in relation to large-scale changes in the atmospheric pressure system over the North Atlantic (East Atlantic teleconnection pattern) and influences of a great salinity anomaly of 1978 (Dickson et al., 1988; Lindeboom et al., 1995), the other regime shifts were connected with two pulses of oceanic inflow into the North Sea in 1988 and in 1998, which coincided with warm water advected northward along the West European shelf edge (Reid et al., 2001). Beaugrand (2004), Beaugrand and Ibanez (2004), and Schlüter et al. (2008) identified climatic factors as the main drivers for the shift in the year 1988. Weijerman et al. (2005) described the ocean climate conditions, weather, and temperature as reasons for the shift in the year 1988.

The two main currents flowing into the North Sea come from the North Atlantic Ocean and the Channel. The outflow of water occurs mainly through the current close to the Norwegian coast. Central currents distribute the water in the North Sea. These currents are important for understanding the regime shifts and the propagation of these changes in the environment across the whole North Sea. One main hydrographic event in the Atlantic Ocean was a great salinity anomaly between 1968 and 1982 (Dickson et al., 1988). Because of small currents, this anomaly spread

across the North Sea and was detected in the southern continental North Sea around the year 1979. This low-salinity event was connected with fresher water input and therefore changed conditions for phytoplankton growth. These changed conditions resulted in a pronounced reduction of the phytoplankton biomass (Edwards et al., 2002).

3.2. The island, the station, and the data



Figure 3.1.: The island of Helgoland and its position in the German Bight with marked sampling station Helgoland Roads in the inset; map from Teeling et al. (2016, p. 4), Creative Commons Attribution License - <https://creativecommons.org/licenses/by/4.0>

The biological station on Helgoland was founded in 1892 (Werner, 1993) as the ‘Königliche Biologische Anstalt auf Helgoland’. Biological research had been carried out at the station since then with the exception of the time during the evacuation of

the island in the context of World War I and II. However, even before the sampling of the HRD, first data were recorded as early 1873 (Wiltshire and Manly, 2004) through a continuous measurement of sea surface temperature. In 1963 a programme on North Sea ecosystem research was initiated by the former director of the Biologische Anstalt Helgoland (BAH) Otto Kinne, who realized the need for a detailed sampling to answer questions of trophic interactions in the German Bight (Hagmeier, 1998). This was the start of the Helgoland Roads project (although the programme was announced in 1963, the first samples belonging to the Helgoland Roads data date from the beginning of 1962). This time series is exceptional on a global scale. Today, with its high frequency (three days of sampling per week for the first 10 years, five days per week afterwards) and over 50 years of sampling, it is one of the most impressive ones in the world. The location of the sampling site is situated between the two islands at the former position of an old buoy, the ‘Kabeltonne’ (54°11.3' N; 7°54.0' E, Figure 3.1) and has never been changed since the beginning.

Since 1962 water samples are taken regularly (Franke et al., 2004). The sampling of zooplankton was initiated in 1974, with three days of sampling per week (Greve et al., 2004). Additionally, microbial parameters (Gerdtts et al., 2004) and macrozoobenthos (Franke and Gutow, 2004) are sampled on the island, but these time series were not used for the analyses in this thesis. Taken from the surface, the water samples are seen as representative of the entire water column, which is generally well mixed as a result of strong tidal currents and the shallow environment (Hickel, 1998). Identification and quantification of the phytoplankton community, the photometric determination of inorganic nutrients (nitrite, nitrate, ammonia, phosphate), and the measurement of temperature and salinity have been carried out since the beginning of the time series (Wiltshire, 2004). Only silicate and Secchi depth were included a few years later. This long-term dataset was reviewed and quality-controlled by Raabe and Wiltshire (2009) through a careful comparison with other available datasets (e.g. BSH (Hamburg), ICES (Copenhagen), and MUDAB (Hamburg)) for the North Sea and a reanalysis of the calibrations. The quality of the phytoplankton data was controlled by Wiltshire and Dürselen (2004) through a comparison of the electronic database with the original lists recorded by the different persons and through an inclusion of available metadata.

Not all identified phytoplankton species from the HRD were found every year:

Some were found only a few times or with relatively small cell counts. A subset of this large number of species was selected for the subsequent analysis through personal communication with HRD experts by selecting species suitable for an analysis of the whole HRD time series. The selected species should be found in the time series for some years and have comparatively high abundances. Additionally, these species should represent an important portion of the phytoplankton community. Therefore, a selection of 23 species was used for the analysis presented in this thesis. Two species were pooled to genus level due to lower abundances (Hoppenrath, 2004).

The following 21 species and two genera were chosen for the following analyses (the three-letter abbreviations used in the remainder of this thesis are presented on the right side marked by an arrow):

<i>Ceratium furca</i> (Ehrenberg)	⇒ CFC
<i>Ceratium fusus</i> (Ehrenberg)	⇒ CFS
<i>Ceratium horridum</i> (Cleve)	⇒ CHR
<i>Ceratium lineatum</i> (Ehrenberg)	⇒ CLN
<i>Ceratium tripos</i> (O.F. Müller)	⇒ CTR
<i>Eucampia zodiacus</i> (Ehrenberg)	⇒ EZD
<i>Guinardia delicatula</i> (Cleve)	⇒ GDL
<i>Guinardia striata</i> (Stolterfoth)	⇒ GST
<i>Noctiluca scintillans</i> (Macartney)	⇒ NSC
<i>Odontella aurita</i> (Lyngbye)	⇒ OAR
<i>Odontella regia</i> (Schultze)	⇒ ORG
<i>Odontella rhombus</i> (Ehrenberg)	⇒ ORH
<i>Odontella sinensis</i> (Greville)	⇒ OSN
<i>Paralia sulcata</i> (Ehrenberg)	⇒ PSL
<i>Phaeocystis</i> ssp.	⇒ PHS
<i>Porosira glacialis</i> (Grunow)	⇒ PGL
<i>Prorocentrum micans</i> (Ehrenberg)	⇒ PMS
<i>Protoperdinium depressum</i> (Bailey)	⇒ PDP
<i>Scrippsiella</i> ssp.	⇒ SCG
<i>Skeletonema costatum</i> (Greville)	⇒ SCS
<i>Thalassionema nitzschioides</i> (Grunow)	⇒ TNT

3. Helgoland

Thalassiosira rotula (Meunier) ⇒ TRT
Torodinium robustum (Kofoid & Swezy) ⇒ TRB

Owing to missing values of Secchi depth and silicate concentrations during the period from 1962–67, the long-term data of the phytoplankton and the physico-chemical parameters from 1968 to 2008 were used. Sunshine duration and wind speed (Beaufort scale) were provided by Germany’s National Meteorological Service (Deutscher Wetterdienst, DWD, Climate data - online). The environmental variables included in the analysis are thus as follows:

1. Temperature (Figure 3.2)

Temperature showed typical distribution for the temperate regions in the northern hemisphere with cold winters and warm summers. Because of the heat capacity and the corresponding buffering of the water, water temperature followed air temperature with small lag. The coldest temperatures were reached in February and the highest in August.

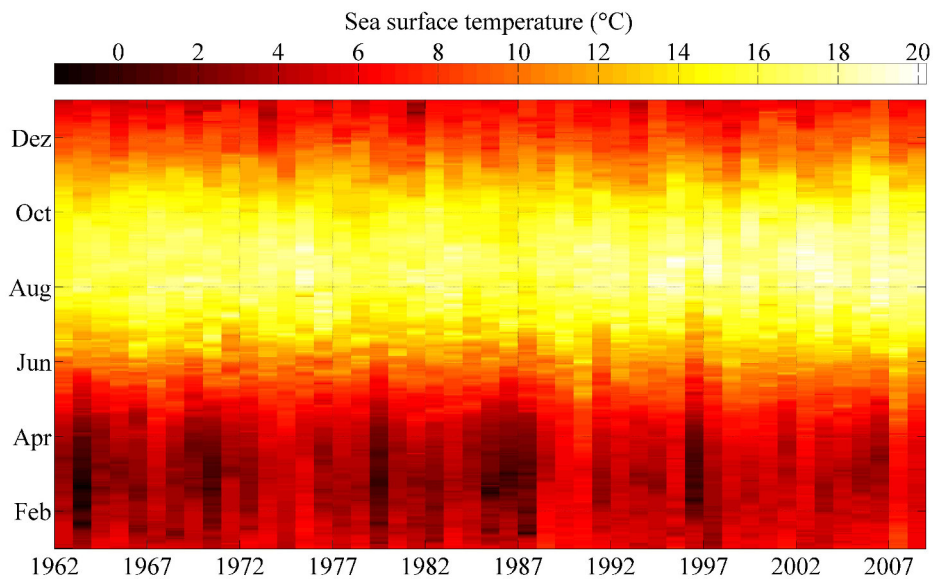


Figure 3.2.: Sea surface temperature at Helgoland

2. Secchi depth (Figure 3.3)

The Secchi depth is a measure for the turbidity of the water column. It is

measured with the help of a disc, the Secchi disc, which is lowered into the water. The Secchi depth is the depth where it cannot be seen from the surface anymore (Tyler, 1968). The water turbidity was lowest in the summer months when high Secchi depths could be observed in the period between the two phytoplankton blooms. The turbidity was highest in winter, because the wind was strongest in this season and led to resuspension of detritus, benthic phytoplankton species, and other material on the sea floor. Short periods of strong wind could lead to a high turbidity throughout the whole year, which can be seen in the patchiness of Figure 3.3.

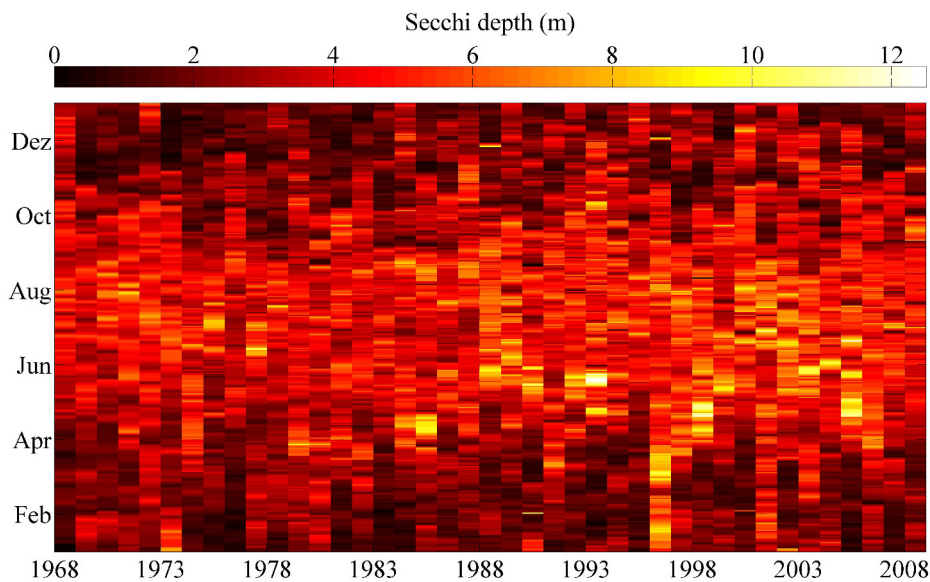


Figure 3.3.: Secchi depth at Helgoland

3. Salinity (Figure 3.4)

The salinity around Helgoland is usually around 32, but dips could be observed. These dips can be caused by strong rainfall, because the sampling was done at a very shallow place between the two islands of Helgoland. Another reason for the reduction in salinity was a temporarily strong influence of coastal waters. Several rivers discharge into the North Sea, which is why these coastal waters have a lower salinity.

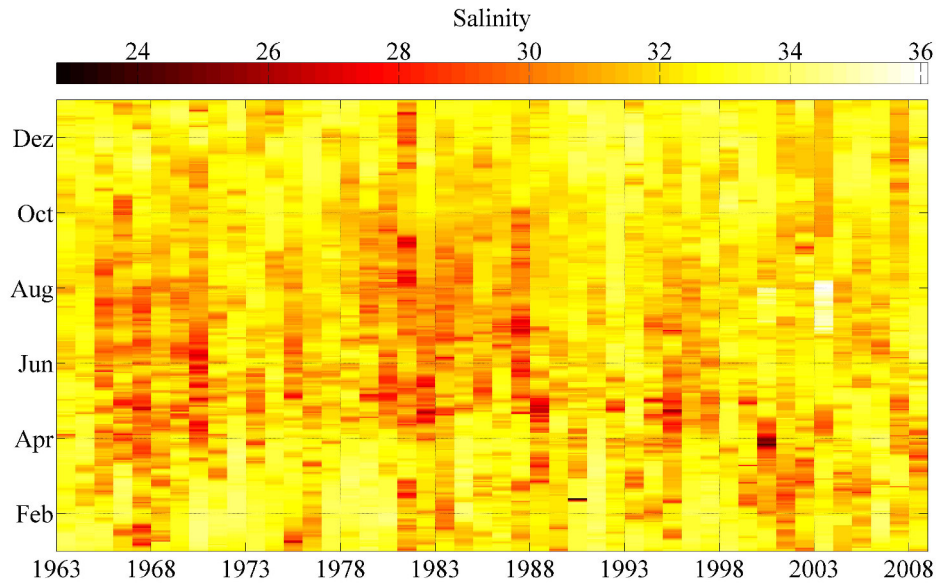


Figure 3.4.: Salinity at Helgoland

4. Concentrations of total dissolved inorganic nitrogen (DIN) calculated as the sum of ammonium, nitrate, and nitrite (Figure 3.5)

The highest DIN concentrations were found between February and May. This nutrient is consumed by phytoplankton species during phytoplankton blooms and is slowly resuspended and rebuilt throughout the winter.

5. Phosphate (Figure 3.6)

High phosphate concentrations were found between October and May with a clearly visible period of lower concentration in late spring and summer. This was caused by the phytoplankton species. The rebuilding and the resuspension of this nutrient happened quickly. One can see that the concentration from the beginning of the spring bloom was reached again in October.

6. Silicate (Figure 3.7)

High silicate concentrations were found from October until May, and this was caused by the phytoplankton species, too. The rebuilding of this nutrient was a continuous process, and the highest concentrations were found before the onset of the diatom spring bloom.

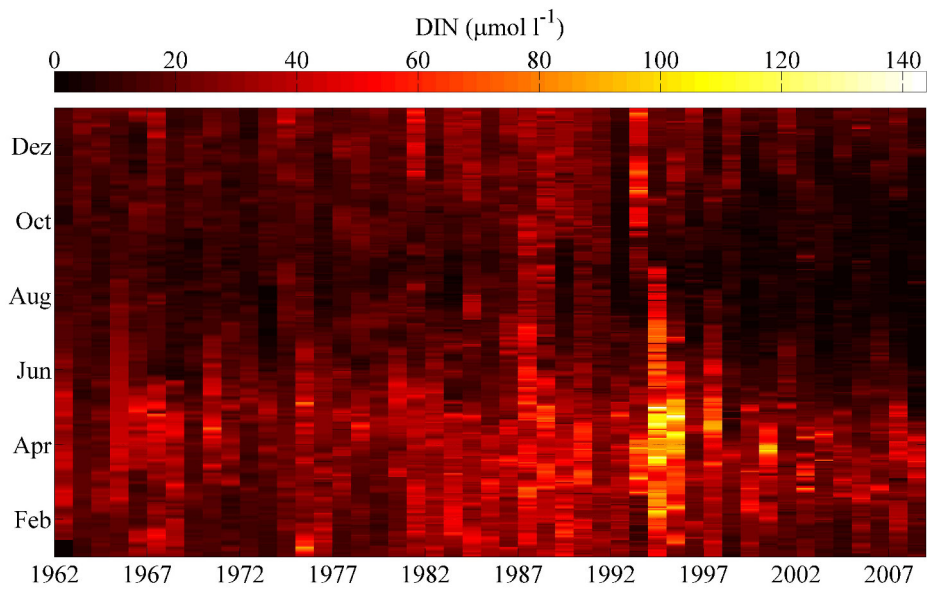


Figure 3.5.: DIN concentration at Helgoland

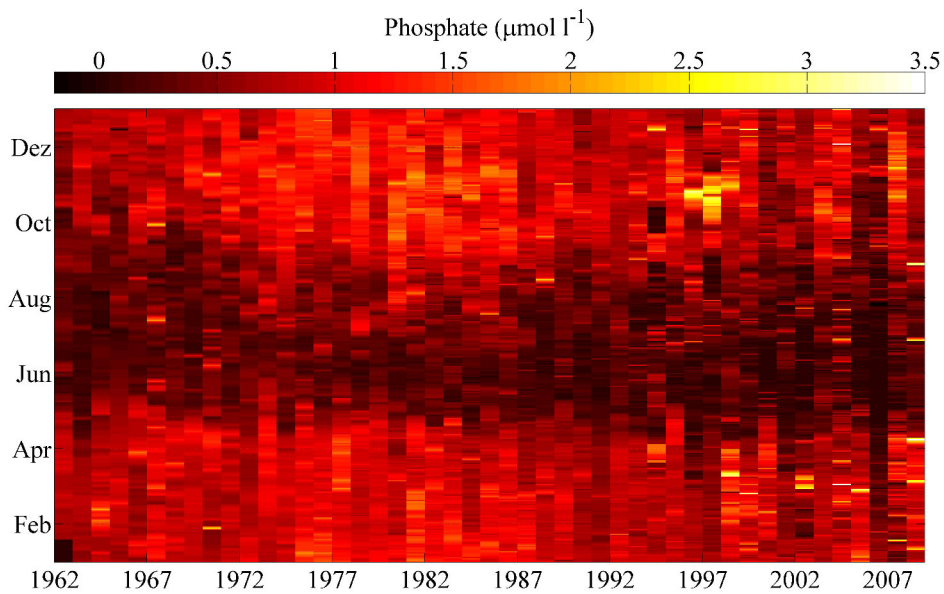


Figure 3.6.: Phosphate concentration at Helgoland

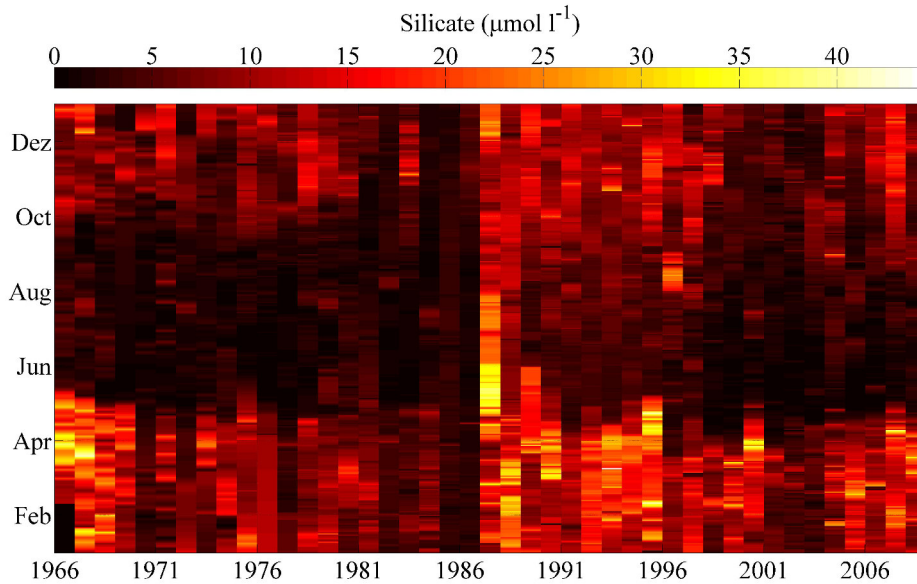


Figure 3.7.: Silicate concentration at Helgoland

7. Sunshine duration (Figure 3.8)

The longest sunshine durations were found in summer and the shortest in winter, because sunny days were more often found in summer. Additionally, days are longer in summer and that makes long sunshine duration more likely.

8. Wind speed (Figure 3.9)

The wind speed at Helgoland was very patchy, but one can see a darker band for the summer month in Figure 3.9. This reflects that stronger winds were found in the winter. Especially larger yellow areas in this figure can be found only for the winter months, meaning that events with high wind speed throughout several consecutive days were only found in this time of the year.

The subsequent analyses were based on a species-environment relationship, and biotic interaction plays a considerable role in this framework (McGill et al., 2006). Competition and grazing are two important environmental factors that influence the phytoplankton growth. Competition between different species will most likely prefer the species that is better adapted to the environment (e.g. species adapted to warmer temperature will replace other species in the warmer months), and graz-

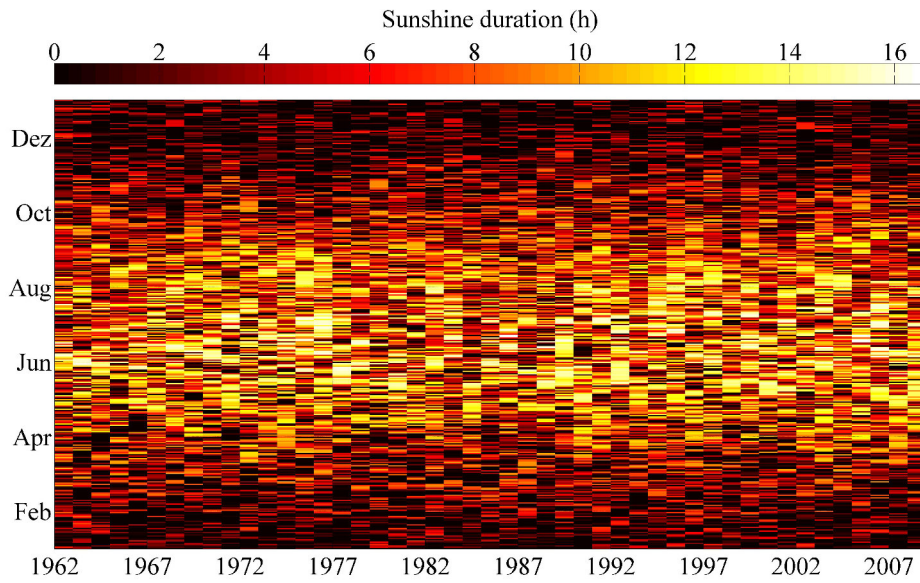


Figure 3.8.: Sunshine duration at Helgoland

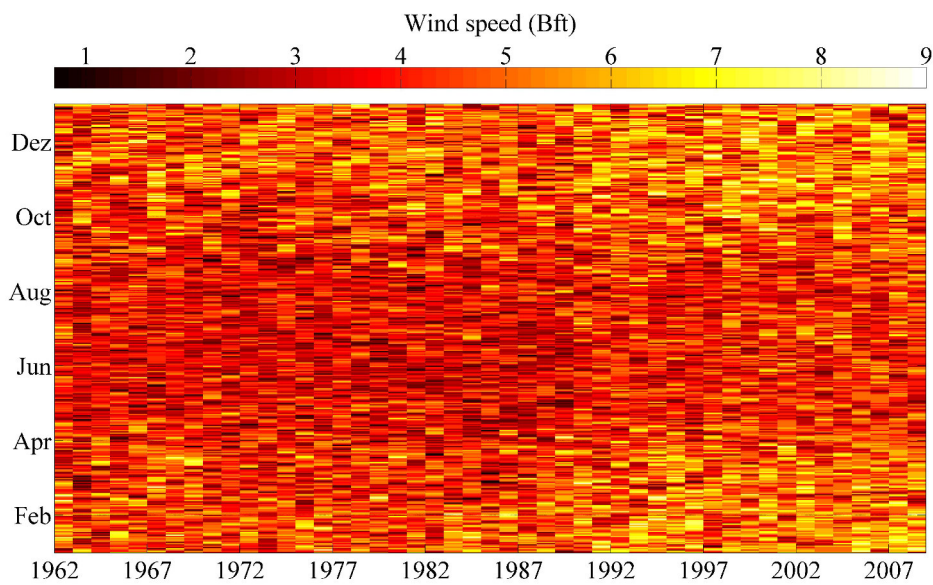


Figure 3.9.: Wind speed at Helgoland

ing preferences of a zooplankton species may reduce the cell counts of one distinct species only. Therefore, a measure for these interactions had to be included. Competition and grazing were added as two different time series—the zooplankton time series and the competitive milieu. The competitive milieu, named after the interaction milieu from McGill et al. (2006), as a measure for the intra- and interspecific competition was included through the sum of the abundances of all 23 selected phytoplankton species. It includes the grazing of the dinoflagellates on the diatoms. The mixotrophic phytoplankton species can use light for their metabolism and prey on other phytoplankton species or ingest organic compounds, whereas the heterotrophic species prey only on other species or ingest organic compounds. These different diets result in a different dependence on the included biotic factors.

Owing to the later start of zooplankton sampling (Figure 3.10) in 1974 (Greve et al., 2004), different analyses were carried out in this thesis—one analysis without the zooplankton time series on a longer time scale and another with the influence of the grazers. This reduced the investigated time period to 34 years (1974–2006) and expanded the number of environmental factors to 10 (the eight mentioned on page 30 ff., the phytoplankton and the zooplankton time series). Zooplankton was included as the sum of all zooplankton species sampled at Helgoland Roads with a Nansen net (mesh size 150 μm) except *Noctiluca scintillans*, because *N. scintillans* was part of the species analysed in this thesis and included in the other biotic time series (see Chapter 6).

The trophy, which determines the nutritional status of a species, was adopted for all dinoflagellates from Löder et al. (2011), who considered species with a lack of chloroplasts as heterotrophic.

If not stated otherwise, information about the different analysed species shown in the following listing were taken from Hoppenrath et al. (2009). The graphs for the selected species show the colour-coded logarithmic abundances. These were calculated separately for every species, and blue represents low while green indicates high abundance. The years 1962–2008 are plotted on the x-axis, and the months bottom up from January through December on the y-axis. Larger and labelled version of these graphs can be found in the appendix (see A. Appendix section A.1).

This listing serves as a short overview of the different species and will be revisited later in the context of the ecological niches for these species.

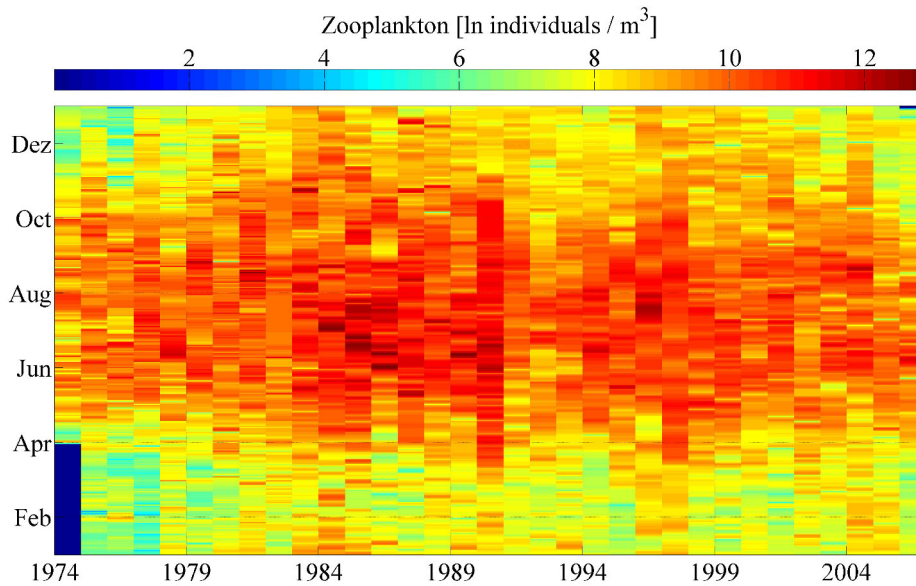


Figure 3.10.: Logarithmic zooplankton abundance at Helgoland

Diatoms

Eucampia zodiacus The chain-forming diatom *Eucampia zodiacus* (Figures 3.11 and A.1) is adapted to higher temperatures (Resende et al., 2007, 2005). This species occurred throughout the whole year and bloomed sporadically in autumn. It is a cosmopolitan, neritic species from temperate areas.

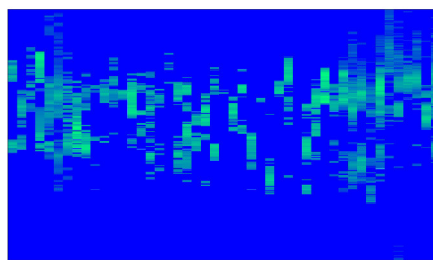
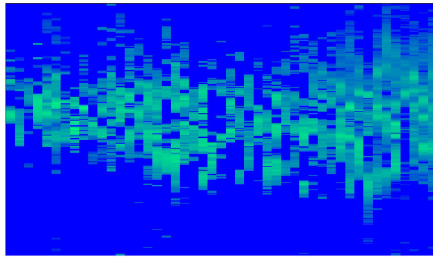


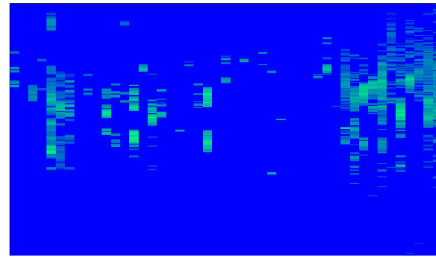
Figure 3.11.: Logarithmic abundances of *Eucampia zodiacus* at Helgoland

Guinardia delicatula, *G. striata* The *Guinardia* species (Figure 3.12) occur as

chains and single-celled. *Guinardia delicatula* (Figures 3.12 a and A.2) can form blooms at Helgoland and occurred throughout the whole year even though it was more abundant in the warmer months. Schlüter et al. (2012) showed a clear tendency towards higher water temperatures for this species. *Guinardia striata* (Figures 3.12 b and A.3) was identified almost throughout the whole year, but had its highest abundance around summer.



(a) *Guinardia delicatula*

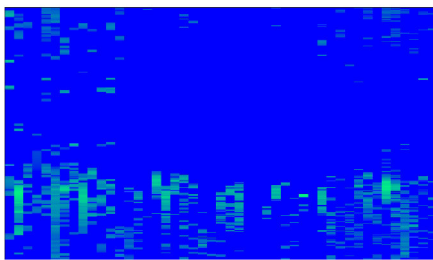


(b) *Guinardia striata*

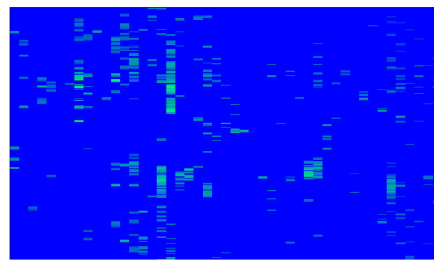
Figure 3.12.: Logarithmic abundances of the *Guinardia* species at Helgoland

Odontella aurita, O. regia, O. rhombus, O. sinensis The *Odontella* species (Figure 3.13) can be found in chains or as single cells. *Odontella aurita* (Figures 3.13 a and A.4) was identified in the water column from November to April, and it stayed the rest of the year in the benthos. Blooms were found in spring. The neritic *O. regia* (Figures 3.13 b and A.5) was found throughout the year at Helgoland. It is a typical species for the coastal regions of the southern North Sea. *Odontella rhombus* (Figures 3.13 c and A.6), named after its typical shape, was not found very frequently in the Helgoland Roads data due to its normal occurrence as a benthic species. However, this species can be found in the water column after turbulent conditions. *Odontella sinensis* (Figures 3.13 d and A.7) invaded the North Sea in 1903 (Ostenfeld, 1909) and the first records from Helgoland are from this year, too. Today, this species is often present throughout the year at the coastal regions of the southern North Sea.

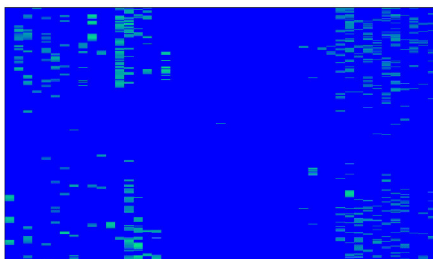
Paralia sulcata The diatom *Paralia sulcata* (Figures 3.14 and A.8) was found



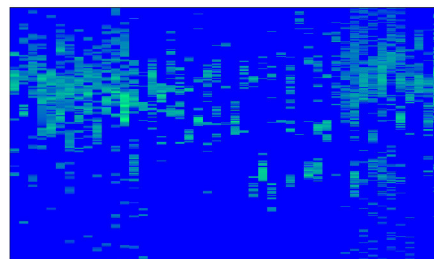
(a) *Odontella aurita*



(b) *Odontella regia*



(c) *Odontella rhombus*



(d) *Odontella sinensis*

Figure 3.13.: Logarithmic abundances of the *Odontella* species at Helgoland

throughout the year at Helgoland Roads, but, as shown by Gebühr et al. (2009) and later in this thesis, it changed the intraannual timing. Some new *Paralia* species were described recently (MacGillivray and Kaczmarska, 2012), but their global occurrence is still unclear.

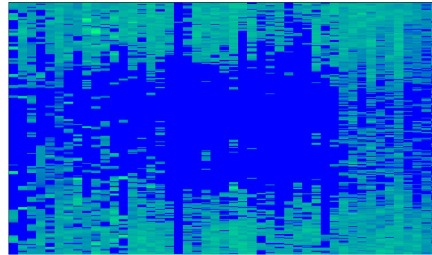


Figure 3.14.: Logarithmic abundances of *Paralia sulcata* at Helgoland

Porosira glacialis The literature shows that *Porosira glacialis* (Figures 3.15 and A.9) can be found from November to August at Helgoland Roads, with its highest abundance in winter and spring, but in the used time series, it was found very sparsely. This species can form loose chains or is found single-celled.

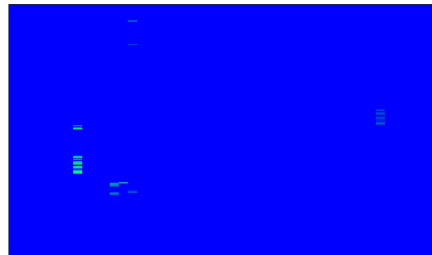


Figure 3.15.: Logarithmic abundances of *Porosira glacialis* at Helgoland

Skeletonema costatum The species *Skeletonema costatum* (Figures 3.16 and A.10) was found throughout the year. Its highest abundance was detected in late autumn or in winter. One cannot be completely sure that all species detected as *S. costatum* were members of this species, because *S. marinoi* could also have

been inaccurately detected as *S. costatum*. Morphologically, these species are not distinguishable from each other.

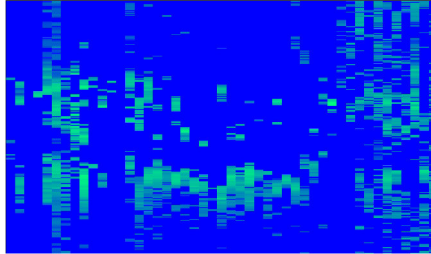


Figure 3.16.: Logarithmic abundances of *Skeletonema costatum* at Helgoland

Thalassionema nitzschioides The cosmopolitan species *Thalassionema nitzschioides* (Figures 3.17 and A.11) was found throughout the year at Helgoland Roads. Normally, this species has its highest abundance in spring, but at Helgoland it was detected with comparatively high abundance in the colder months.

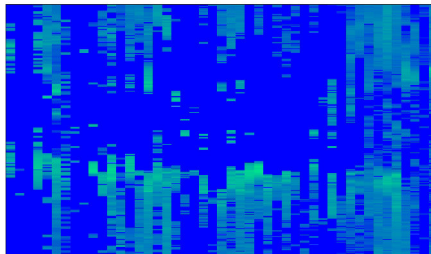


Figure 3.17.: Logarithmic abundances of *Thalassionema nitzschioides* at Helgoland

Thalassiosira rotula The diatom *Thalassiosira rotula* (Figures 3.18 and A.12) was found in the beginning and at the end of this time series. Its highest abundance was detected in spring and autumn, as reported by Widdicombe et al. (2010) for the western English Channel. Krawiec (1982) described *T. rotula* as eurythermal (tolerating a wide range of temperatures) and moderately

euryhaline (tolerating a wide range of salinity). Cloern and Dufford (2005) detected *T. nodulolineata* in the San Francisco Bay in a broad salinity range.

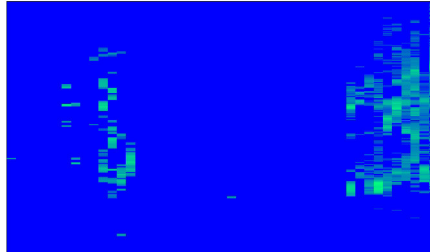
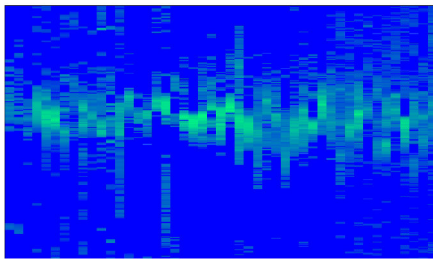


Figure 3.18.: Logarithmic abundances of *Thalassiosira rotula* at Helgoland

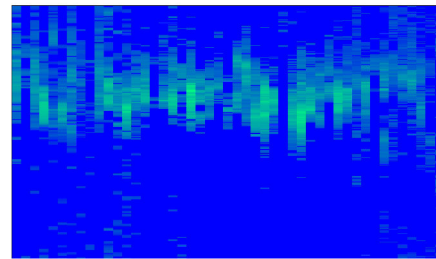
Dinoflagellates

Ceratium fusus, *C. furca*, *C. horridum*, *C. lineatum*, *C. tripos* The mixotrophic dinoflagellates of the genus *Ceratium* (Figure 3.19) were found in large numbers in the Helgoland Roads data. All members of this group have chloroplasts and are abundant over the whole year. The highest abundances were typically found in the warmer period. *Ceratium fusus* (Figures 3.19 a and A.13) formed dense blooms in the summer months and was detected all year round. It is a typical warm water species for this area (Hesse et al., 1989). *Ceratium furca* (Figures 3.19 b and A.14) also formed blooms and was found over the whole year with highest abundances in summer. *Ceratium horridum* (Figures 3.19 c and A.15) is a common species of the North Sea, identified over the whole year with peak abundances in the second half of the year. *Ceratium lineatum* (Figures 3.19 d and A.16) was found in the northern oceans and regularly detected in the North Sea with its highest abundances in summer. *Ceratium tripos* (Figures 3.19 e and A.17) was not as common as *C. furca* or *C. fusus*, but it was found regularly in the Helgoland Roads data, typically in summer.

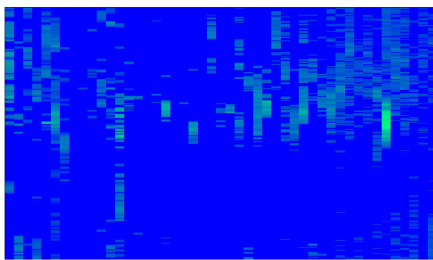
Noctiluca scintillans The heterotrophic dinoflagellate *Noctiluca scintillans* (Figures 3.20 and A.18) preys on other species and exhibits a diverse diet (Fock



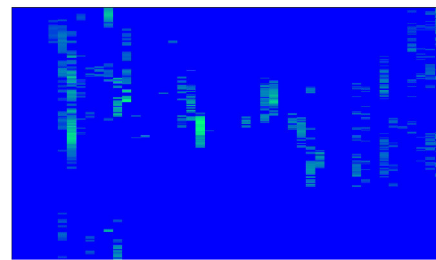
(a) *Ceratium fusus*



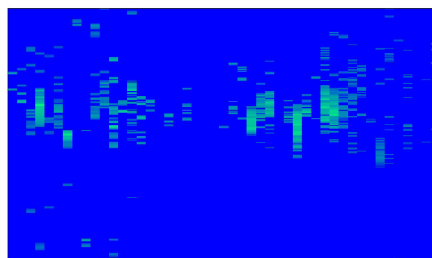
(b) *Ceratium furca*



(c) *Ceratium horridum*



(d) *Ceratium lineatum*



(e) *Ceratium tripos*

Figure 3.19.: Logarithmic abundances of the *Ceratium* species at Helgoland

and Greve, 2002). This species has to be seen as an atypical representative of the analyses conducted in this work, because, together with *Protoperidinium depressum*, it was the only heterotrophic species analysed in this thesis. This species was found throughout the whole year. It can form blooms that colour the water in summer and is well known to be responsible for the marine phosphorescence in the North Sea.

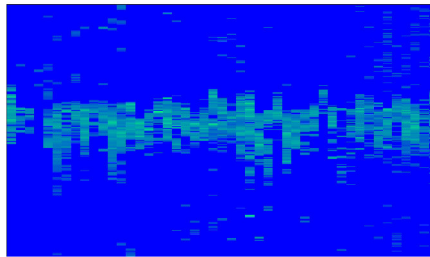


Figure 3.20.: Logarithmic abundances of *Noctiluca scintillans* at Helgoland

Prorocentrum micans The dinoflagellate *Prorocentrum micans* (Figures 3.21 and A.19) is a widely distributed mixotrophic species common in the North Sea. This species formed dense blooms around summer and autumn. These characteristics were reported by Resende et al. (2007) and Widdicombe et al. (2010), too.

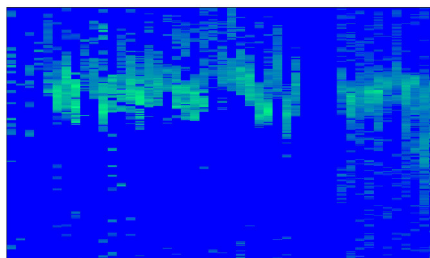


Figure 3.21.: Logarithmic abundances of *Prorocentrum micans* at Helgoland

Protoperidinium depressum The heterotrophic *Protoperidinium depressum* (Fig-

ures 3.22 and A.20) is distributed worldwide and also common in the North Sea. It was detected throughout the year with higher abundances in the warmer period.

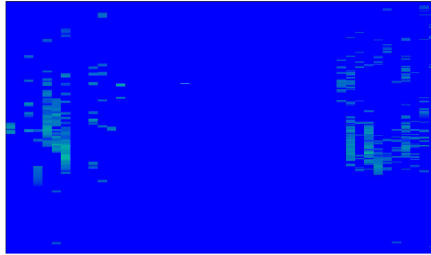


Figure 3.22.: Logarithmic abundances of *Protoperdinium depressum* at Helgoland

***Scrippsiella* ssp.** The mixotrophic dinoflagellate *Scrippsiella* ssp. (Figures 3.23 and A.21) was not detected throughout the whole investigation period. This species was only found during the last 10 years of sampling. During these 10 years, the bloom events were concentrated around July and August. The same pattern was found by Terenko and Terenko (2009) for *Scrippsiella trochoidea* in the brackish Black Sea.



Figure 3.23.: Logarithmic abundances of *Scrippsiella* ssp. at Helgoland

Torodinium robustum The mixotrophic *Torodinium robustum* (Figures 3.24 and A.22) was not detected regularly, and when this species was detected, cell

counts were often low. Although the seasonality is not clear, this species was found throughout the year at the end of this time series.

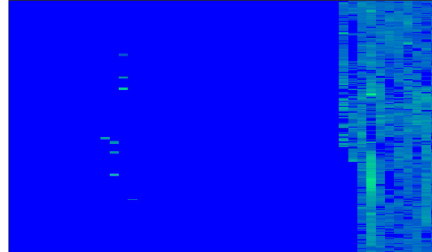


Figure 3.24.: Logarithmic abundances of *Torodinium robustum* at Helgoland

Haptophyte

Phaeocystis ssp. The haptophyte *Phaeocystis* ssp. (Figures A.23 and A.23) is known for forming blooms in spring, especially after the diatom spring bloom. It sometimes forms blooms in autumn, too. Jordan and Chamberlain (1997) and Peperzak et al. (1998) identified the same characteristics for the Dutch coastal zone of the North Sea. As the members of this algal group are hard to identify to species level, all species were pooled together and the complete genus was used for the analyses conducted in this thesis. *Phaeocystis* ssp. can form large blooms in summer and is a known producer of foam (Riegman et al., 1992).

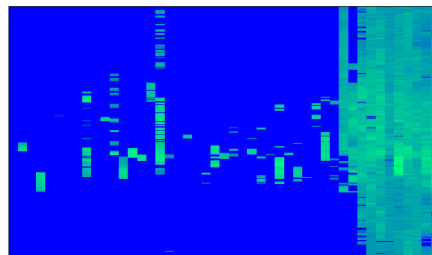


Figure 3.25.: Logarithmic abundances of *Phaeocystis* ssp. at Helgoland

4. Phytoplankton abundance data and the extraction of the fitness parameter

4.1. The Idea

The Helgoland Roads data set is exceptionally detailed and an excellent basis for an investigation of phytoplankton ecology. Even though this time series represents the phytoplankton community at Helgoland, some species are considered globally distributed and, therefore, some of the analyses are likely of general relevance. The ecological classification of these phytoplankton species was done by reconstructing their fitness-based ecological niche as indicated previously (see Chapter 1).

This fitness-based ecological niche should not be misinterpreted as a location or place in the habitat; it is rather a position and volume in the abstract space of relevant environmental factors. As mentioned before, Hutchinson defined the niche with indefinite existence and did not explicitly include the fitness of species in this concept. To do this, an adaptation of Hutchinson's niche concept was carried out. Another difference was that a species-specific fitness-based ecological niche had to be estimated. This difference was especially methodologically important, because this estimation had to be done from an empirical abundance time series of phytoplankton species. The following sections show how the idea was put forward and explain the steps taken to arrive at the conclusive classification parameter.

4.2. The phytoplankton abundance curve

The phytoplankton abundance at Helgoland Roads is characterized by waxing and waning (Figure 4.1), where blooms, caused by a mass development of cell counts, are regularly found, and these peaks are followed by the rapid decline in the abundance.

Some species show these blooms in spring or autumn, others in summer (see Chapter 2). To use this time series for the classification of a value describing the fitness, one had to find a procedure that could deal with these patterns.

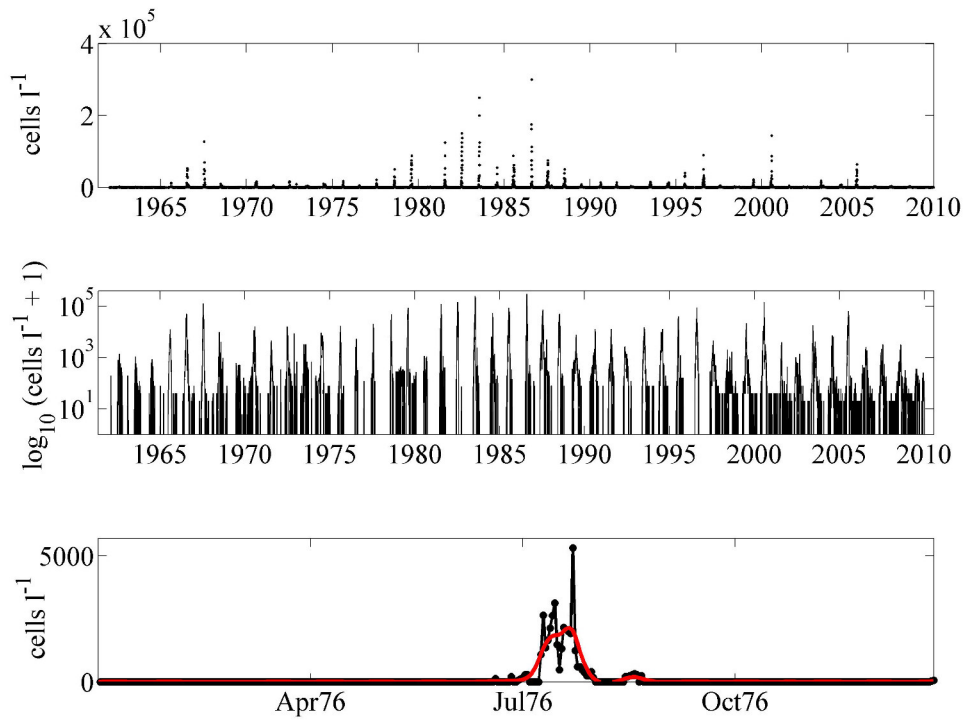


Figure 4.1.: Abundance data from *C. fusus*, upper panel: complete time series of cell counts; middle panel: complete time series of cell counts on a logarithmic scale; lower panel: black - raw cell counts for the year 1976, red - smoothed cell counts for the year 1976

Figure 4.1 shows the dynamics of the phytoplankton abundance curve for all years. The upper panel displays the raw abundance data, and the middle panel shows this raw data on a logarithmic scale. The lower panel highlights the year 1976 with an included smoothed abundance curve. All panels of Figure 4.1 are related to *Ceratium fusus*. One can see clearly the blooms in the different years and the yearly cell counts varied over three orders of magnitude (cf. Figure 1 in Mieruch et al. 2010). The species-specific fitness was computed with the help of time series

like the one shown in Figure 4.1.

4.3. Parameters considered for the niche classification

Based on the fitness of a given species, multivariate environmental time series were processed to yield the species-specific niche. However, for the estimation of the ecological niche, obviously all relevant factors were needed. This will be shown in Chapter 5 in detail, but for a better visualization and for the explanation of the procedure, only one environmental parameter is shown in the following for the development of the method to estimate a fitness-based ecological niche. Temperature was chosen as environmental factor for this exemplarily visualization.

As a first step towards the extraction of a suitable fitness estimate, the raw abundance curve was considered for the classification and the values where the species is present were extracted (Figure 4.2). This graph shows the range of temperature a species faced throughout all years and the temperature distribution for the whole time series. These histograms were normalized and show the species-unspecific temperature statistics for the whole time series and the presence statistics for *Ceratium fusus*. If f_i is the frequency in temperature bin i and a_i is the abundance in temperature bin i , the normalized statistics for the whole time series is $\pi_i = \frac{f_i}{\sum_{j=1}^n f_j}$ and

n is the total number of bins. This is shown as the blue histogram in Figure 4.2.

With $\theta(x) = \begin{cases} 1 & \text{if } x > 0 \\ 0 & \text{if } x = 0 \end{cases}$ the species-specific presence statistic is $p_i = \frac{f_i \theta(a_i)}{\sum_{j=1}^n f_j \theta(a_j)}$ and shown as the red histogram in Figure 4.2.

With this measure, one could see if the species was present at cold or warm temperature and one could use this information for the fitness niche of the species. The disadvantage in this case was that every extracted value for the species was taken as equally important, and no information about the abundance was included. The presence included periods where the species was present with only low abundance. These periods with low abundance represented likely conditions that were not beneficial for the species. This was because low abundances could be the consequence of the depletion of required nutrients, high grazing pressure through other species, or unfavourable climatic conditions.

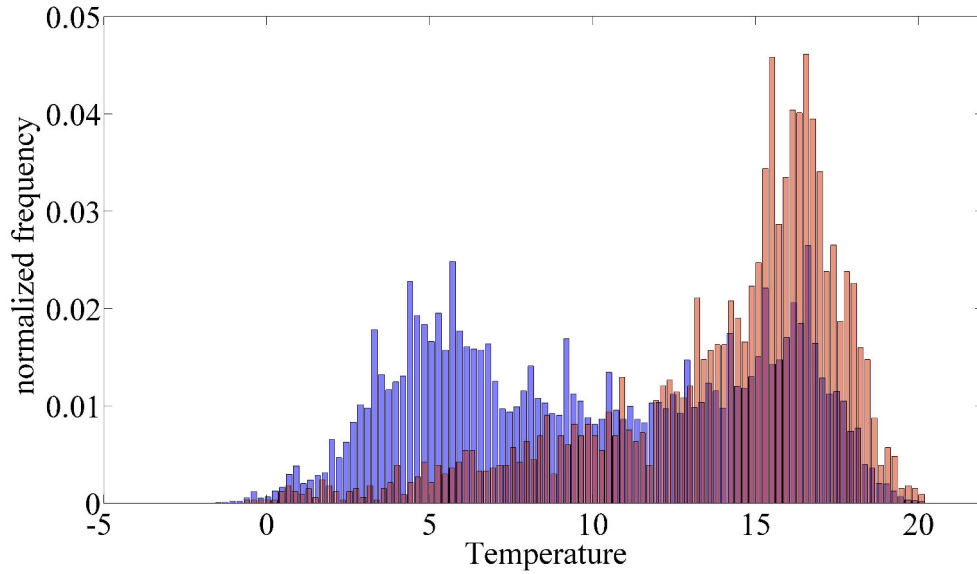


Figure 4.2.: Histogram of the temperatures where *Ceratium fusus* is present in red; histogram of the temperature for the whole time series in blue

Figure 4.2 shows the distribution of the temperature and the distribution of the temperature where the species *Ceratium fusus* was present. One can see that this species was present between -2°C and 20°C and had its highest abundance around 17°C . Due to the differently shaped histogram for the temperatures found in the whole time series (blue histogram in Figure 4.2), this reflects the timing of this species. The temperature histogram exhibits two peaks, but *C. fusus* is hardly found at the peak at low temperatures and, therefore, the species-specific histogram reflects that this species was typically found in summer (compare Boersma et al., 2016). Considering this parameter for the classification of the fitness-based niche, one would have considered every moment where the species was present as a moment with high fitness. This is obviously not the case, because a species can be present at the aforementioned unfavourable conditions (depletion of nutrients, grazing, unfavourable climate), but it will probably not be present with high abundance. Including these days with low abundance in the analysis, actually taking them as equally important, would thus mean including suboptimal conditions, which cannot be a measure for high fitness.

Weighting the abiotic factor with the abundance led to another classification (Figure 4.3). The weighting algorithm used here divided the temperature linearly into 100 bins and summarized all abundances found in the corresponding temperature bin. A normalization was done afterwards through a division with the total abundance. With the previously introduced variables, the abundance statistic was $p_i = \frac{f_i a_i}{\sum_{j=1}^n f_j a_j}$. The weighting emphasized periods where the abundances were higher as well as suppressed periods where the abundances were low. The weighted temperature again showed a concentration at elevated temperatures with a peak around 17°C, which was strongly influenced by a small number of samples (compare Figure 4.1) with very high cell counts.

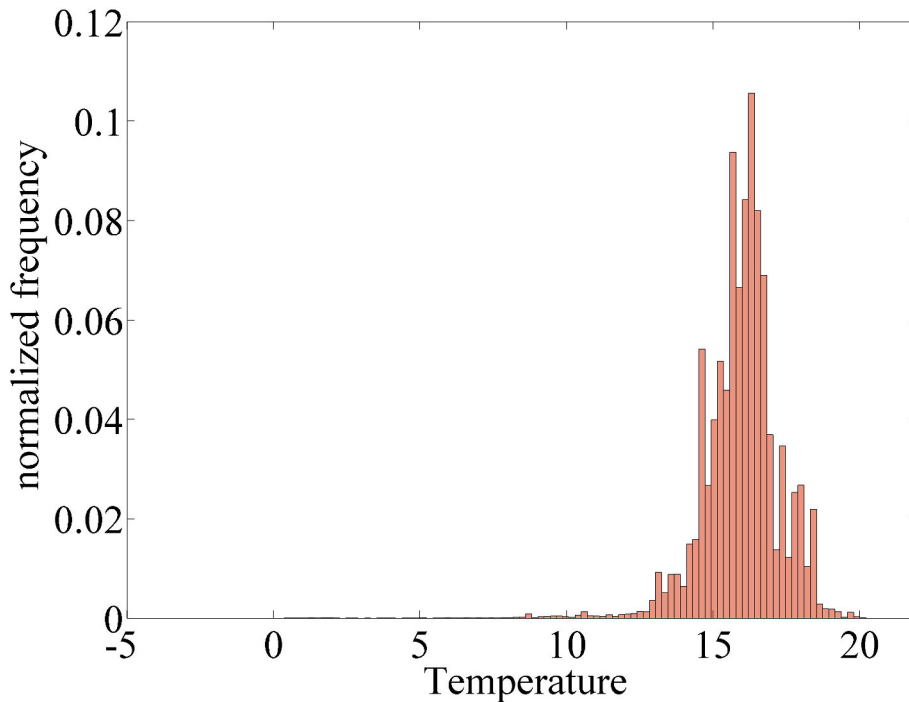


Figure 4.3.: Histogram of temperatures weighted with the species abundance for *C. fusus*

If one had chosen to weight with abundance, it would have emphasized the bloom maxima. However, through the weighting, times with lower abundances were included and considered as (less) important, too. Performing this abundance-weighted

approach in a univariate way was still an incomplete, but promising approach, because it considered periods with high abundance as more important than periods with low abundance. This could be seen as a simple fitness measure, because high cell counts can only be reached when the conditions are good. One could use this for a classification of the ecological niche for the phytoplankton species, but this measure still emphasized periods with zero net growth. Therefore, another approach was considered more useful.

The Outlying Mean Index (OMI) method developed by Dolédec et al. (2000) weighted the abiotic factors with the abundance. Obviously, the analysis was done in a multivariate way and not only was a single factor used for the classification. The OMI did this in a way comparable to the abundance-based approach, and an application of the OMI was carried out with the Helgoland Roads data (Gebühr et al., 2009). As mentioned before, the OMI specified the niche position by the distance between the habitat conditions used by the species and the mean habitat conditions. The niche breadth was the tolerance of a species with respect to the environmental conditions. The OMI was an abundance-based approach and this method considered high abundance as a measure for suitable conditions for the species. This could be explained in a univariate way with Figures 4.2 and 4.3, where the niche distance was the range between the mean temperature (around 10°C) and the mean of the temperature where the species was abundant (around 17°C). The niche breadth could then be interpreted as the range of temperature in Figure 4.3. A critical discussion of taking the mean temperature for ecological time series analysis was made in Boersma et al. (2016).

The analysis by Gebühr et al. (2009) indicated that the OMI can be used to determine the range where a species can survive and where it finds suitable conditions. With the help of the abundance, one could weigh the environmental factors and identify suitable environmental conditions. This weighted factor could be taken as a descriptor for the conditions needed by the species: The most suitable conditions are found where numbers are high. This is intuitively plausible, because high abundance can only be reached where the environmental conditions are suitable for the species. Obviously, these conditions cannot be critical; otherwise no species would exist. These suitable conditions are therefore a good measure for niche classification, especially for relatively stable populations where the high abundance can directly

be connected with high fitness, but if one considers a fluctuating population (Figure 4.1) for the phytoplankton at Helgoland, one can argue if this is the best method for a characterization of the species. When extracting not only suitable but also optimal growth conditions for a species, one would not focus on the highest abundance. A disadvantage of highest abundance is that the net growth is zero and the population starts to decline. Therefore, these conditions can be suitable but not optimal. Optimal conditions can be found before the abundance reaches its maximum, where the highest growth rate can be found.

To extend the search for a fitness parameter, the same analysis was performed with the local maxima of the abundance curve (Figure 4.4). The local maxima described the timing during the growth phase where the species reached the highest cell counts.

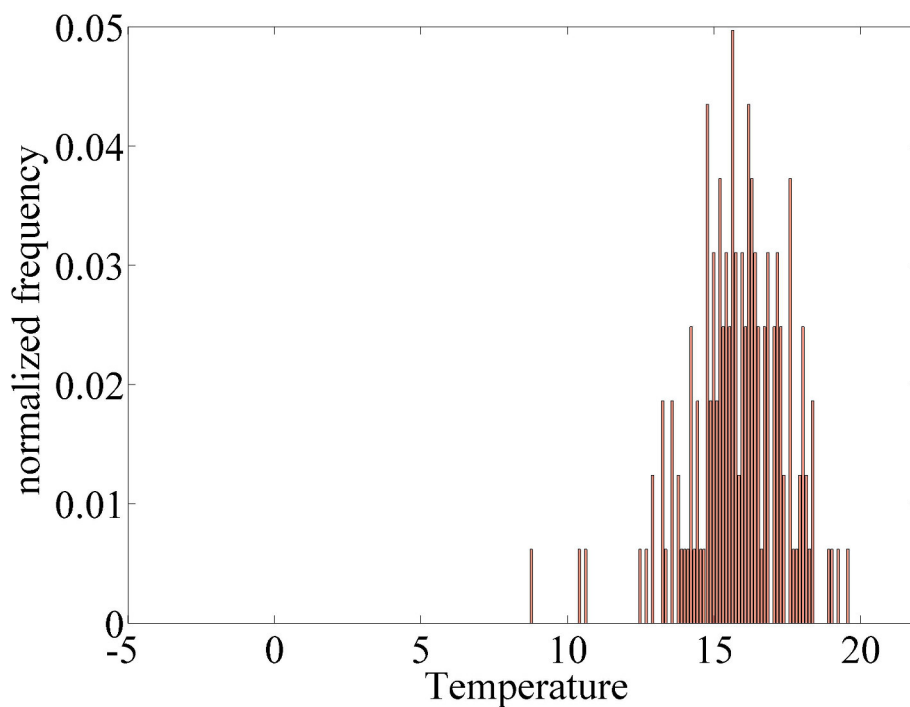


Figure 4.4.: Histogram of temperatures at the local maxima for *C. fusus*. Only local maxima higher than the acceptance threshold of 1% from the global maximum were taken into account

Figure 4.4 shows the normalized distribution of the temperatures found at the

local maxima of the abundance curve for *C. fusus* for the whole time series. Most of the maxima were found at temperatures between 14°C and 18°C, reflecting a species showing high abundances in the warmer period of the year. This result seemed to express the ecology of the species in a more precise way, because the temperature range where the species were found with high cell counts for that specific growth phase was emphasized; however, it still had disadvantages. It highlighted a moment where net growth was zero and the cell numbers were about to decline. Therefore, probably not the best conditions for the species were found at these moments.

4.4. The inflection point

The maxima of the phytoplankton curve represent moments where net growth is zero. This indicates conditions where dying and reproduction of individuals is in equilibrium, which is why the cell counts of species remain static. Therefore, one should consider a different approach that emphasizes conditions where cell counts are on the rise, and place the emphasis on the ascending part of the abundance curve, because these are the moments where net growth is positive.

Considering the whole ascending part still leads to drawbacks, because one has to determine where the ascending part starts. This is not a technical problem, but an ecological one. One has to define a starting point of the ascending part, which is inevitably an artificial one. One could consider, for example, the first day with abundance above zero as a starting point, the day with the first exponential growth, or the day where the abundance reaches a preset threshold. To avoid including this a priori information and to introduce an approach to extract a parameter that represents optimal conditions for the species, the extraction of a single characteristic time point of the phytoplankton abundance curve was carried out.

Apparently, the best conditions can be found at the steepest slope of the abundance curve where net growth takes its highest values—the ascending inflection point. This point is, therefore, a perfect descriptor for the phase during the species' growth that represents these optimal conditions and is perfectly suited to arrive at a fitness-based classification.

To apply this idea to fluctuating raw abundance data, the first step was a smooth-

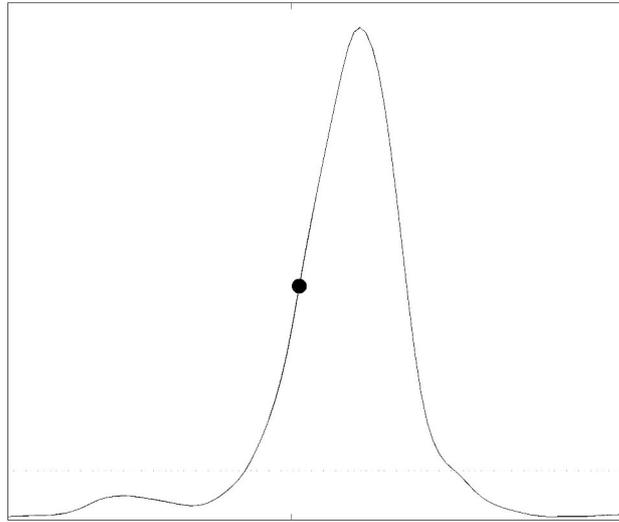


Figure 4.5.: Illustration of an inflection point; section of the smoothed abundance curve from *Ceratium fusus* of the year 1987

ing of the time series to reduce the noise in these data (see Section 5.2). After this smoothing, an extraction of the ascending inflection points was processed (Figure 4.5).

This inflection point has some advantages over the aforementioned methods (presence, weighted abundance, local maxima):

1. A single point can easily be used in subsequent analyses. It is just one point in time and can be easily shown in x/y-plots.
2. The interpretation of this inflection point is evident. The steepest slope is found at this point, reflecting the highest net growth. Thus, the conditions at this point have to be favourable for the species and most probably reflect highest fitness.
3. The environmental parameters at the times of fastest growth can be directly extracted, and a set of ideal growth conditions can be put together.
4. For a multivariate approach, this point can be used to extract a subset of the

environmental parameters reflecting conditions where a species performs best (see Chapter 5).

5. To the best of my knowledge, no one has considered this optimal single point for an analysis of phytoplankton before. Hence, incorporating the fitness with a parameter based on this idea has not been done before. Only the start of bloom, maximum of bloom, first exponential bloom day (Wiltshire et al., 2008), mean diatom day (Wiltshire et al., 2008; Wiltshire and Manly, 2004), cardinal dates for the mass development (Rolinski et al., 2007), and other values have been used to date (see Ji et al. (2010) for a detailed overview).

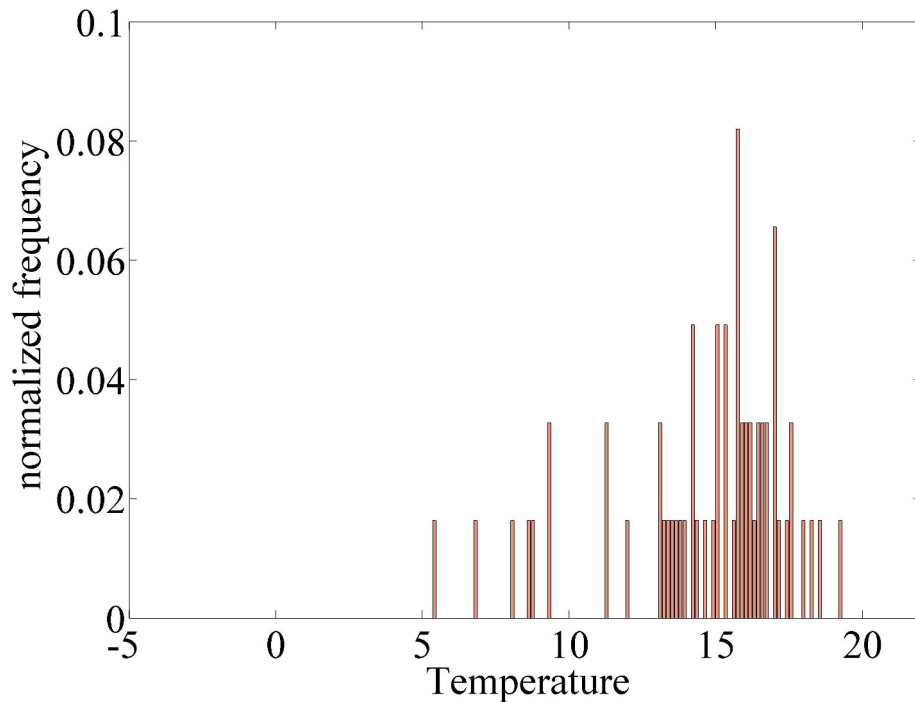


Figure 4.6.: Histogram of temperatures at the inflection points for *C. fusus*.

To compare the fitness-based approach with the aforementioned approaches, the water temperatures at the inflection points were extracted (Figure 4.6). Due to non-equidistant sampling, the computation of the temperature at the inflection points was done with linearly interpolated abiotic data. This had to be done because the

smoothing and the incorporated interpolating of the biotic data could have led to a date of an inflection point which, due to the missing weekends or other seldom events leading to missing data, was not found in the measured temperature data.

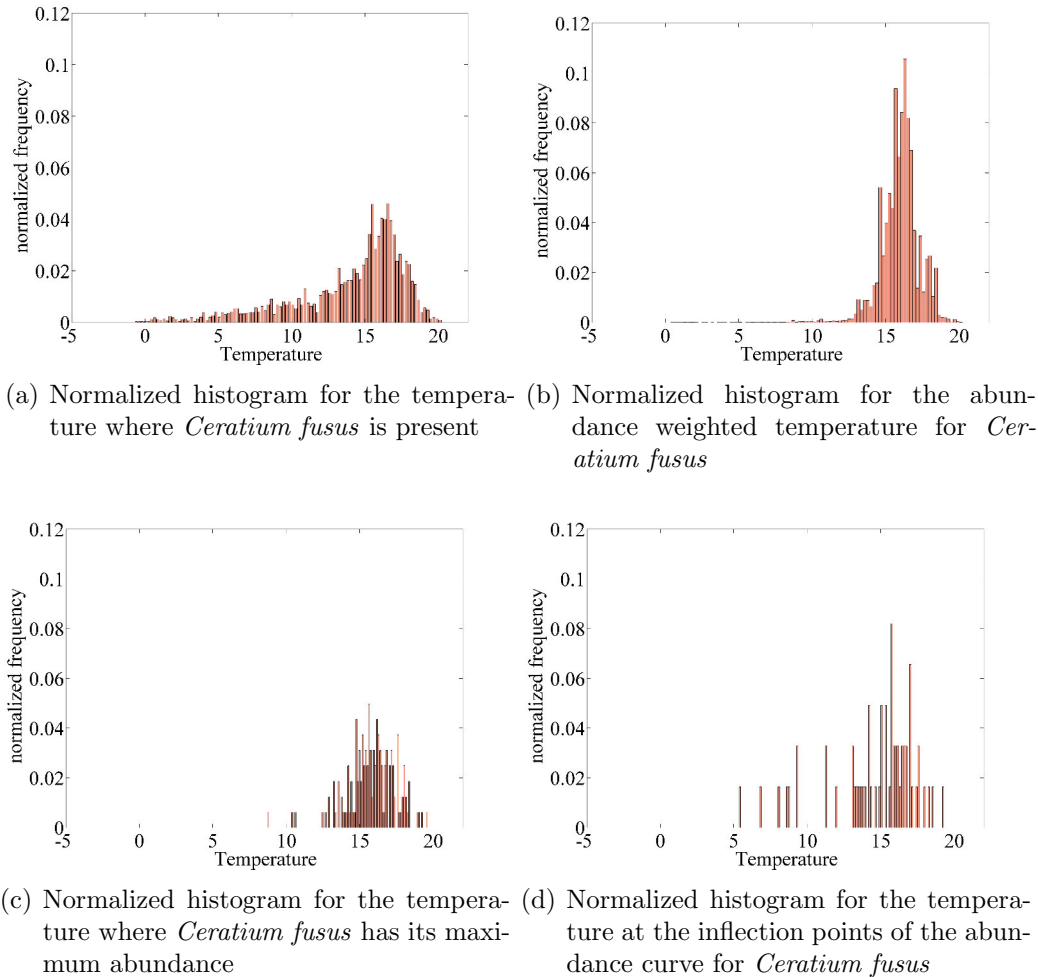


Figure 4.7.: Normalized histograms for the different approaches

Figure 4.6 shows the temperature histogram of the inflection points for *Ceratium fusus*. This species had its highest growth rates distributed over a broad range (from 5°C to 19°C), but the small number of inflection points between 5°C and 12°C was probably caused by a few small blooms at these temperatures. It can be seen clearly that the inflection points were concentrated at temperatures between 14°C and 17°C. This was the same range found for the extraction of temperatures at the

local maxima and the abundance-weighted temperature. Due to some criteria (see Section 5.2) the inflection points had to fulfil, the number of resulting inflection points was lower than the number of local maxima. With this inflection point, one got a measure (here for temperature again) for the range where a species showed its best performance, i.e. had its highest fitness.

Figure 4.7 shows all histograms for the different approaches, and one can see clearly that the number of extracted temperature values decreased from (a) to (d). All histograms are comparable in shape and have their maxima at summer temperatures, but the inflection point extracted a time in the growth phase that could have been directly connected with the fitness.

Here temperature was chosen as the best factor for an explanation of the extraction of the appropriate parameter. However, this section should just be seen as an explanation of the development of this method and how the idea of an optimal niche analysis grew. Temperature certainly plays a role in the ecology of phytoplankton (Boyd et al., 2013) and the temperature at the inflection points was recently successfully used to answer the question ‘Projecting effects of climate change on marine systems: is the mean all that matters?’ (Boersma et al., 2016). Our argument to use this method was: ”Net population growth rates are highest at this inflection point, thus, we propose that the growing conditions for the taxon are optimal on this day. This might not be completely accurate as a variety of factors, such as nutrient availability, light conditions and predation, influence growth of phytoplankton, but there is no a priori reason to assume that the estimate is biased” (Boersma et al., 2016, p. 2).

Because of these reasons and the growth phase argument, the analyses were done with the inflection point. The development of the method for multivariate environmental time series is put forward in the next chapter.

5. Processing the data

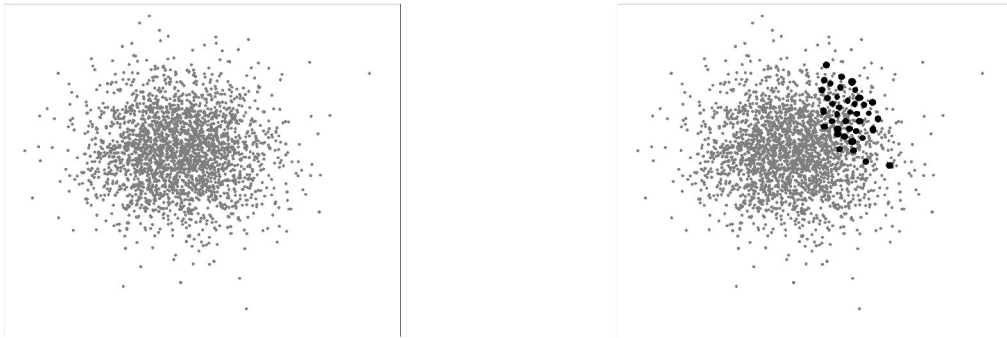
5.1. Outline of the method

In this chapter, the multifactorial approach of the new method is presented. If not stated otherwise, examples are computed for *Ceratium fusus*. Some parts of this description were published in *Limnology & Oceanography: Methods* (Grüner et al., 2011).

The idea behind taking the inflection points was described in Chapter 4 and the advantages of these points were explained in detail. The characterization of the ecological niche for every single species will be shown in the following sections. As explained before, the optimal niche is a collection of all environmental factors where the species attains its highest growth rate and is a subset in the high-dimensional abstract space of environmental factors. The factors included temperature, salinity, Secchi depth, wind speed, sunshine duration, silicate, phosphate, dissolved inorganic nitrogen, and the competitive milieu (see Section 3.2). This resulted in a nine-dimensional data series in which the optimal niche for the chosen species was reconstructed.

As a tool for proper reduction of dimensionality, a principal component analysis (PCA) was performed with the nine-dimensional data series. The PCA is an ordination method that applies an orthogonal transformation to the original dataset, thus transforming it into linearly uncorrelated data series. A restriction to a smaller number of these uncorrelated variables enabled the reduction of the dimensions (see Section 5.3). This allowed for a visualization of the results and confined the estimation error of the niche volume. To estimate the niche spread compared to the spread of the ‘all points’ (AP) cluster (the dataset projected onto the first three principal components, Figure 5.1 a), a highlighting of the inflection points (black circles in Figure 5.1 b) in this reduced dataset was done. The volumes of these two

clusters (AP and the inflection point cluster), computed with the principal axis of a corresponding covariance ellipsoid, were used as measures for their size (see Section 5.3).



(a) Sketch of the AP cluster, artificial data

(b) Sketch of the AP cluster with highlighted inflection points, artificial data

Figure 5.1.: (a) Sketch of the empirical ‘all points’ cluster in the space defined by the first two principal components, in (b) the inflection points are highlighted as black circles; reduction to two dimensions with a sketch of principal component 1 vs. principal component 2

After these computations, the volume of the inflection point ellipsoid was normalized to the volume of the AP cluster, whereupon the resulting number gave a measure for the spread of the inflection points. To test for the statistical significance, a resampling procedure was carried out (see Section 5.4). A classification of the phytoplankton species could then be reached with this measure. A step-by-step description of the developed method is provided in the next sections.

5.2. Detection of the inflection points

For every species, the computation of inflection points was based on the raw abundance time series. First, the abundance time series was pretreated by a smoothing spline algorithm to reduce the noisiness of the data, thereby enabling the detection of the inflection points. This smoothing was based on an algorithm from Reinsch (1967) customized and provided by Mieruch et al. (2010). Second, the data were nor-

malized year-by-year to the respective annual maximum. This was because peaks of the cell counts varied strongly between the years (Mieruch et al., 2010) and fluctuations at relatively low cell counts had to be omitted to exclude inflection points found at these, compared to the annual maximum, low cell counts. These inflection points were omitted, because short and small peaks indicated a short period where the species faced good conditions. However, if the species was not able to establish a stable bloom, these conditions could not have been optimal. Therefore, only inflection points at relevant cell counts were taken into account. Third, the inflection points were computed via the derivatives. The first derivative had to be greater than zero. The second derivative had to be zero at this point (necessary condition) and had to change its sign from positive to negative to detect an inflection point at the turning from left to right (sufficient condition)—the inflection point on the ascending part of the abundance curve. This was as follows:

- $f' > 0$,
- $f'' = 0$,
- f'' : sign $+ \rightarrow -$.

These inflection points (Figure 5.2) were extracted for the whole time series for every species. Because abundance data exhibited high variability on short time scales, a bloom with two connected peaks with a distance of about 5–20 days could appear. These interspersed dips presumably resulted from algal patches drifting through the narrow channel between the two islands at Helgoland. In general, it was possible to detect more than one inflection point per year, particularly for species with a spring and a summer bloom. The final result of this computation was a list containing the times of maximal net growth (highest fitness) for each investigated species.

The following rules were set for these extracted inflection points:

1. To exclude inflection points at relatively low values of smoothed cell counts, an acceptance threshold at 10% of the annual maximum was set. The choice of a percentage was due to the aforementioned large interannual variation of peaks.

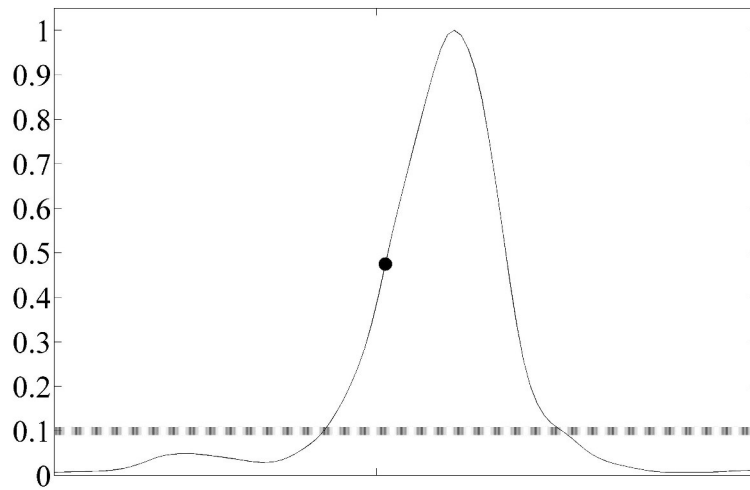


Figure 5.2.: Extracted inflection point (black circle) for *C. fusus* in summer 1987; dotted line: 10 % of the annual maximum

2. Only inflection points on ascending parts of the abundance curve were considered.
3. After one detected inflection point, the abundance curve had to fall below 10 % of the annual maximum before accepting the next point. This was done because in some cases two closely connected peaks appear, i.e. one bloom with two local maxima. To exclude two inflection points with a distance of only a few days, the first inflection point was extracted in this case.

5.3. Principal component analysis and visualization

It is complicated to visualize a large number of factors (a total of nine: 8 abiotic environmental factors, plus the biotic competitive milieu, i.e. the sum of the 23 selected species). Therefore, to reduce this high dimensionality, a principal component analysis (PCA) of the multivariate data series comprising all considered environmental factors was performed (Handl, 2002; Jolliffe, 2002; McGarigal et al., 2000). A PCA is an ordination method that is often applied with the aim to reduce high dimensional data where a PCA replaces n variables (factors) by n orthogonal linear combinations

of them. The reduction following the computation of the principal components is accomplished by a projection of the dataset onto the first few principal components. Geometrically, a PCA translates the origin of the coordinate system into the data cloud's centroid (defined by the vector of mean values) and aligns the basis vectors with the principal axes via an orthogonal transformation (Figure 5.3).

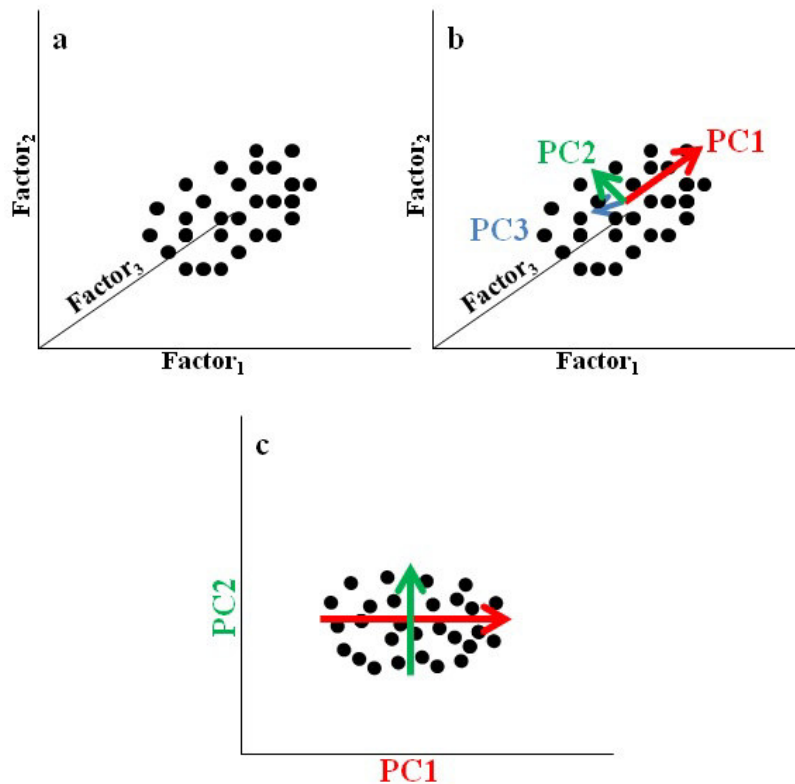


Figure 5.3.: Geometrical view of the PCA; a: original dataset, b: original dataset with the principal components, c: transformed dataset with a projection onto two dimensions

A normalization of the environmental factors to zero mean and a standard deviation of one was carried out to give an equal weight to the environmental factors. Hence, every environmental factor was considered equally important for phytoplankton growth. Additionally, this normalization made the scale invariant, i.e. environmental factors units and scales did not influence the PCA. One could bias

the analysis by giving certain factors more weight than the other. However, since there were no a priori information as to how to do that, an unbiased analysis was chosen.

The linear combinations were ranked with respect to their corresponding eigenvalues representing their share of total variance, i.e. the first PC contributed the major share to the total variance, the second PC contributed the second major share, and so on. Afterwards, one could consider a reduction in the dataset based on a suitable criterion. To mention but a few, the scree-plot criterion determines the number of axes by a visual assessment (Cattell, 1966). The plot of components ranked in decreasing order with respect to their related eigenvalue reveals a steep decrease for the first components, while the plot approaches zero asymptotically for the latter ones. This can be compared to a scree, and only components on the left side of the ‘elbow’ (the bend where the slope changes) should be retained. As an alternative, following the Kaiser-Guttman rule (Guttman, 1954; Kaiser, 1960, sometimes called the latent root criterion), only principal components (PCs) with an eigenvalue larger or equal to one should be retained. Due to the normalization prior to the PCA, PCs with an eigenvalue larger than one explained more variance than a single original variable (dotted line in Figure 5.4). Therefore, the Kaiser-Guttman rule was chosen for the following procedure.

As mentioned before, some climate data from Germany’s National Meteorological Service (DWD) were included in the analysis, because these were considered important environmental factors for phytoplankton growth. Light is certainly an important factor for phytoplankton growth. Here sunshine duration was included to account for this relevant factor. An inclusion of a measure for the irradiance was not included, but sunshine duration is highly correlated with this factor. The turbidity of the water column is also a measure for the light availability for the phytoplankton species, but such a strong correlation between irradiance and Secchi depth is not necessary. Strong turbidity in the water column can be caused by growing phytoplankton during times where the light conditions are good, and it can result in a self-shading where the growing species in the upper layer face good light conditions and grow fast while the species in the lower layers do not get enough light (Lorenzen, 1972; Shigesada and Okubo, 1981).

However, the selection of the environmental factors for the PCA should be done

with care, because through an inclusion of irrelevant factors for the phytoplankton growth, the reduction to lower dimensions might cause misinterpretations through unimportant information in the principal components. One should keep in mind that the PCA is a statistical method that sorts the original data series with respect to their variance and does not analyse any causal relationships.

When applying a PCA, the data should fulfil some qualifications to be sure that the results are not misleading or wrong. The data should follow a multivariate normal distribution. Figure 5.6 shows, on the one hand, non-normal tendencies and, on the other, the large number of data points (more than 10,000) leading to a reliable estimation. This is because an increasing number of data points leads usually to a decreasing estimation error (e.g. Pierce and Running, 1988; Slawnych et al., 1997; Vanvoorhis and Morgan, 2007). Included factors with larger variances have a higher influence on the PCA, but through the implemented normalization, the variances are the same for all factors. Thus, factors with a high variance are not overrepresented in this PCA.

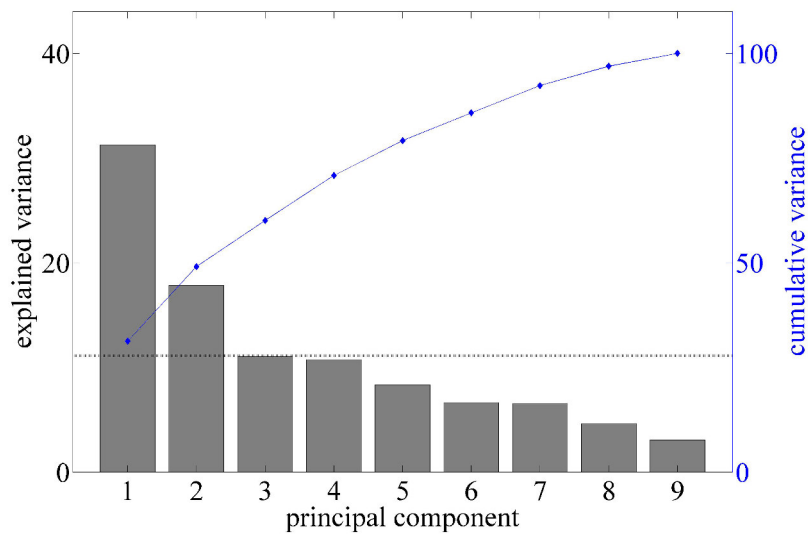


Figure 5.4.: Explained and cumulative variance for the principal components; dotted line shows the Kaiser-Guttman criterion

Figure 5.4 shows how the variance was distributed among the principal components. This was the share of the total variance each principal component accounted

5. Processing the data

for and showed the consequences of dimension reduction. The cumulative variance contained the variance explained by the considered PCs. The first two PCs explained a large proportion of the variance (PC1: 31.25 %, PC2: 17.81 %, PC3: 11.02 %) and the third PC was slightly below the Kaiser-Guttman rule. Every PC with an eigenvalue larger than one should be excluded after this criterion; here it corresponded to 11.11 % explained variance. This criterion was not followed strictly, and three PCs were selected for the analysis. One reason for selecting three PCs was that an appropriate solution for the problem of selecting a sufficient number of PCs had to be found. The problem was that selecting too few PCs would have led to a loss of information, whereas selecting too many PCs would have led to an increasing estimation error for the following steps of the procedure (see Section 5.5 for a test of the sensitivity to the selection of different numbers of PCs).

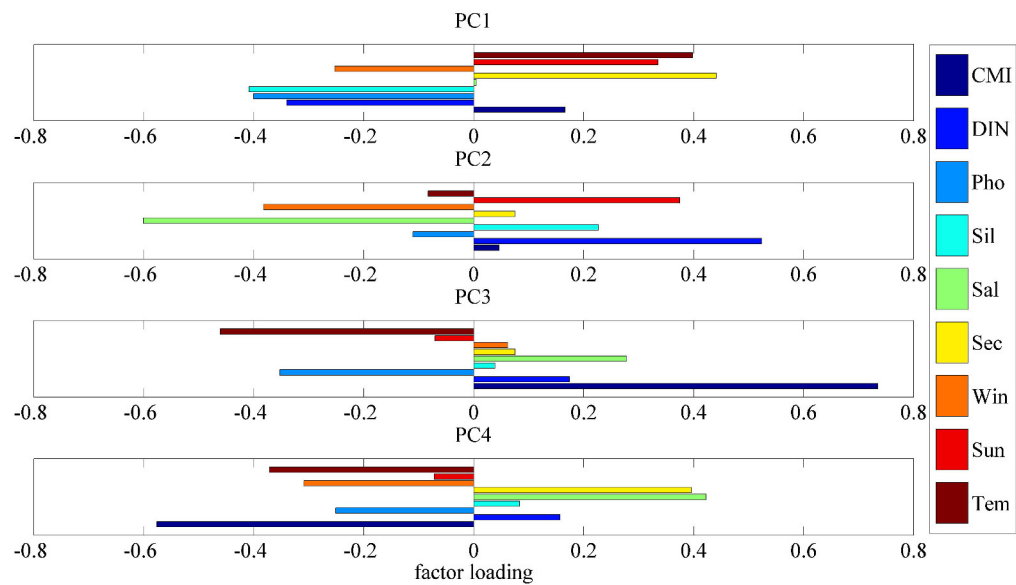


Figure 5.5.: Factor loadings of the first four principal components; Tem: temperature, Sun: sunshine duration, Win: wind speed, Sec: Secchi depth, Sal: salinity, Sil: silicate, Pho: phosphate, DIN: dissolved inorganic nitrogen, CMI: competitive milieu

Another important point was how the new variables were composed of the original ones. Every PC is a linear combination of the original variables and the linear

coefficients of this combination are called factor loadings (FL). These factor loadings are shown in Figure 5.5, which shows the share of every original variable represented by the PCs. The main factors accounting for the variance in the new subspace could be identified. The factors with the main influence on the first PC were temperature, sunshine duration and Secchi depth on the negative side, and DIN, phosphate and silicate on the positive side. The factors on the negative side were mainly physical parameters necessary for phytoplankton growth while the factors on the positive side were mainly identified as the nutrients. The opposite signs indicated that the mentioned physical parameters and the nutrients were anti-correlated. This is an interesting aspect, but it can be explained with the waxing and waning of these factors throughout the year. Some nutrients were depleted simultaneously, and some of the environmental factors showed strong correlations. Since different groups of factors were identified, these patterns were found in the FLs of the PCA. The second PC was composed in a completely different way. Salinity and wind speed had the highest influence on the positive side of PC2, and DIN and sunshine duration on the negative side. No clear separation in physical parameters or nutrients could be seen for the second PC.

In Figure 5.6, projections of the time series onto the first two principal components are shown. The light grey points reflect the environmental conditions for the whole dataset and are species-unspecific, because the whole dataset was used for this ordination method. One can see that the cluster has two regions with a higher density and becomes sparser near the edges, a pattern which could be seen in a comparable limnological study (Salmaso, 2003). The extracted inflection points (the highly species-specific instants of fastest growth) were included afterwards. One can see in Figure 5.7 that, here for *Ceratium fusus*, the species-specific conditions were concentrated in a small region of the ‘all point’ cluster (AP cluster), with the exception of some outliers. This allowed a comparison of the AP cluster reflecting general environmental variability and the species-specific cluster.

Figure 5.8 shows the estimation of the cluster’s size, while the ellipses indicate the distribution of the respective points. These ellipses were computed via a procedure similar to the PCA, and the corresponding volume (in 2d: area) was calculated as a measure for the effective spread of the times of fastest growth. The varying lengths of the principal axes reflected different spreads of the hypervolume in different di-

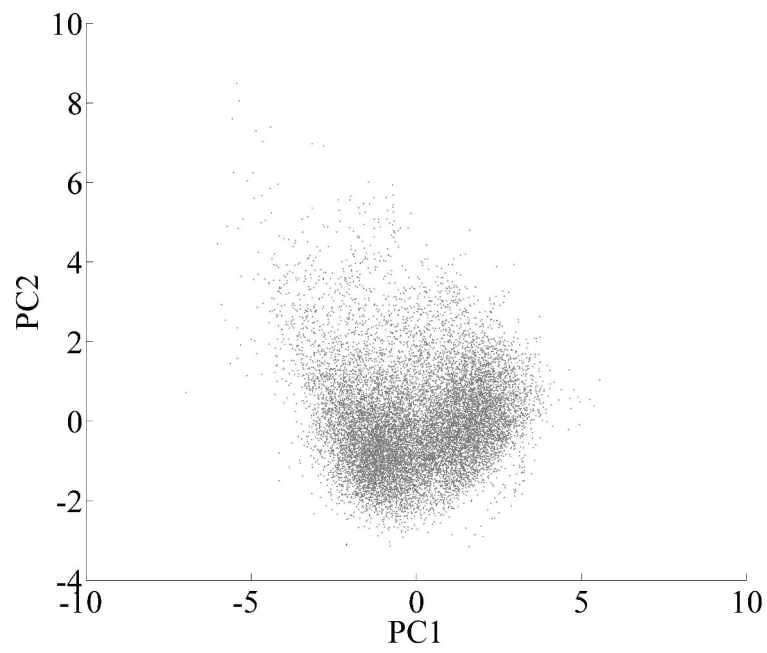


Figure 5.6.: ‘All points’ cluster projected onto the first three principal components resulting from the PCA; for a better visualization, only two dimensions are shown; all environmental factors were used for this computation

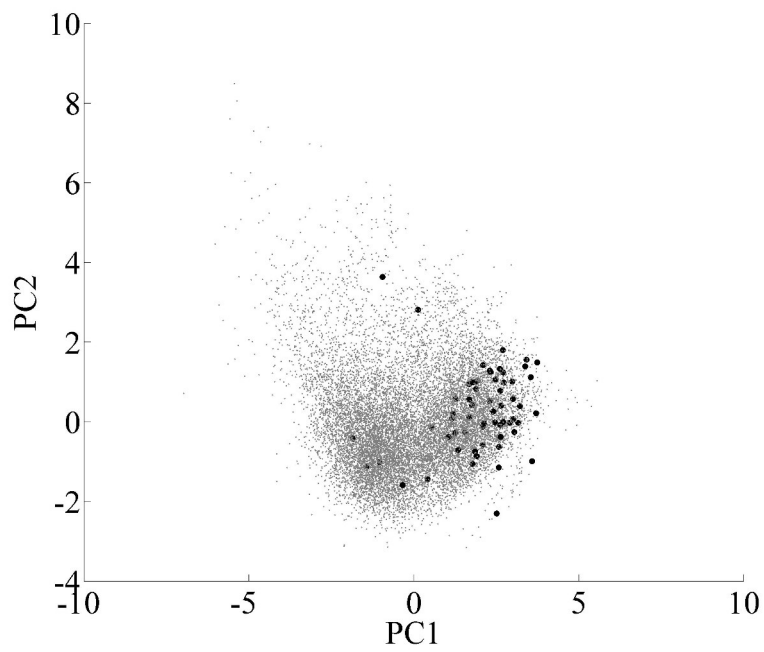


Figure 5.7.: ‘All points’ cluster (grey dots) with highlighted inflection points (black circles)

rections of projection space. In order to obtain one quantity for the niche spread, the product of the axes lengths was computed. This quantity was the volume (up to a dimension specific geometric factor, e.g. π for 2d and $\frac{4}{3}\pi$ for 3d) of the covariance ellipsoid that was estimated from the inflection point cluster. Since the length of the i -th principal axis was given by the square root of the i -th eigenvalue λ_i of the covariance matrix (Brandt, 1999), the product of the first n principal axis lengths was given by the expression $\prod_{i=1}^n \sqrt{\lambda_i}$. With the lengths of the longest and shortest ellipsoids' semi-axis, further characterization of the shape and identification of artefacts was possible, for instance, when one ellipsoid had a very truncated shape reflected by a large disparity between the length of the semi-axis. The estimation of a covariance matrix was repeated with the whole dataset, and the volume of the related ellipsoid (AP ellipsoid) in projection space for the AP cluster was computed. An illustration of these ellipsoids is shown in Figure 5.8. These ellipsoids are shown as ellipses here, because only two dimensions are shown.

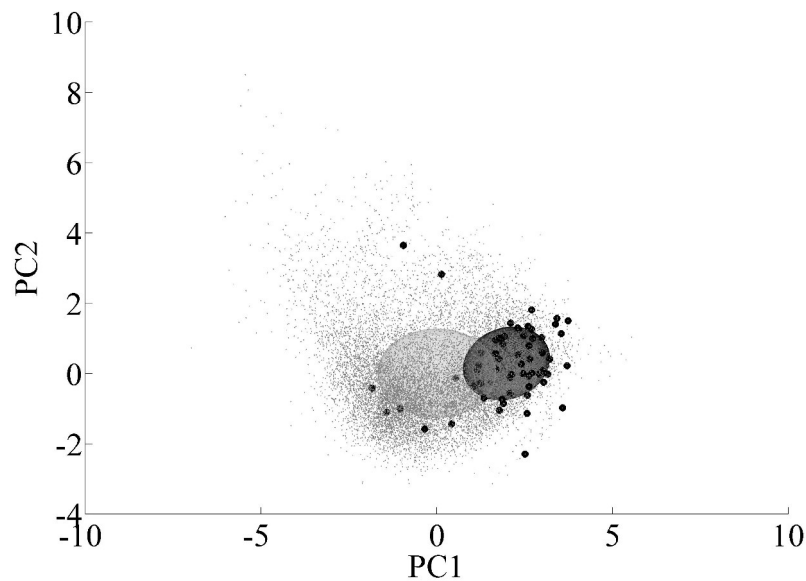
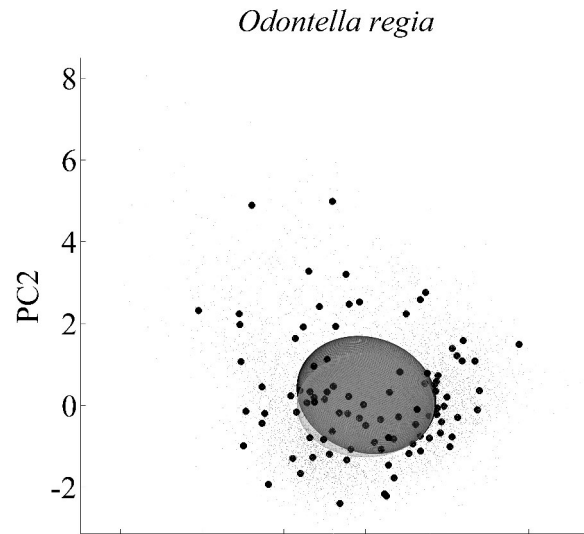


Figure 5.8.: ‘All points’ cluster (grey dots) with corresponding ellipse (grey ellipse) and highlighted inflection points (black circles) with corresponding ellipse (dark ellipse) for *Ceratium fusus*

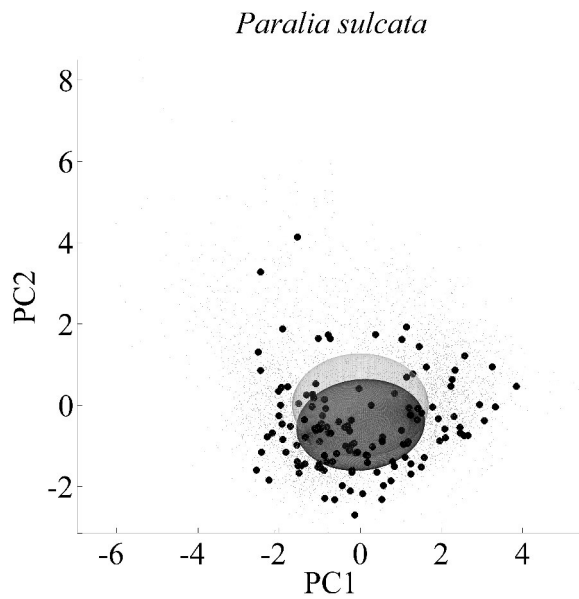
The light grey AP ellipsoid in Figures 5.8 and 5.9 is species-unspecific and is identical in both figures. In contrast, the black ellipsoids, related to species-specific inflection points (filled black circles), exhibit significant variation, thereby demonstrating their species-specific character. A normalization of the inflection point ellipsoid to the AP ellipsoid was executed, and thus the ratio varied on a scale between 0 and the order of 1. In spite of this normalization, special distribution could lead to a volume higher than one if all points were found on or close to the edge. A benefit of this standardization was that the dimension-specific geometrical factor dropped out when computing the ratio.

Figures 5.8 and 5.9 show the covariance ellipsoids for three different species. It can be seen that the inflection points were distributed completely differently. *Ceratium fusus* (Figure 5.8) had the smallest ellipsoid, and the inflection points were distributed over a small area of the AP cluster. In contrast, Figure 5.9 shows that the inflection points for *Odontella regia* and *Paralia sulcata* were scattered over the whole AP cluster and the ellipsoids were correspondingly large. Another important point was that the centroid of the ellipsoids was different for the three species. The ellipsoid for *Odontella regia* was more or less congruent with the AP cluster, while the inflection point ellipsoid for *P. sulcata* was shifted to negative values of the ordinate.

The pronounced shift in the inflection point ellipsoid for *Ceratium fusus* in Figure 5.8 to the outer border of the AP cluster could be interpreted in biological terms. Deviation from the mean, i.e. the centroid of the AP cluster, represented non-average conditions found in the habitat, and thus *C. fusus* was found at these special conditions. Figure 1.1 and the related text on Page 18f. show the concept and the interpretation behind this finding. The aforementioned outlying mean index (Dolédec et al., 2000) classified *C. fusus* as a specialist, too, because the niche was comparatively small and was found at the outer margin of the AP cluster. Owing to the small volume, this species was classified as a specialist in this thesis, the position was not used here. As mentioned before, the two measures of niche breadth (volume) and position are anti-correlated, since the more peripheral it is, the smaller the niche must be.



(a) 'All points' cluster and highlighted inflection points for *Odontella regia*



(b) 'All points' cluster and highlighted inflection points for *Paralia sulcata*

Figure 5.9.: 'All points' cluster (for better visualization of the ellipses as very tiny grey dots, same distribution as in Figures 5.7 and 5.8) with corresponding ellipse (grey ellipse) and highlighted inflection points (black circles) with corresponding ellipse (dark ellipse) for two different species.

5.4. Statistics

To measure the size of the ecological niche of the species, the volume of the inflection point ellipsoid had to be assessed. However, obtained values left an uncertainty resulting from the fact that the estimation of covariance ellipsoids from a (possibly) small number of points introduce considerable estimation errors. To identify the range of these statistical fluctuations, a resampling (or Monte Carlo) method (Metropolis and Ulam, 1949) was adopted. This is a procedure where repeated random sampling is used to assess the statistical significance. Here it was done in the following manner: The same number of points used to estimate the inflection point ellipsoid was picked randomly from the AP cluster to compute the corresponding volume. This step was repeated 10 000 times to sample the null hypothesis, which assumed that the inflection points were scattered randomly (independent and identically distributed) across the AP cluster. This null hypothesis implied that the volume of the inflection point ellipsoid was identical to the volume of the AP ellipsoid within statistical fluctuations. Binning the volumes resulting from the 10 000 random pickings generated histograms like those shown in Figure 5.10. The black arrow indicates the volume of the inflection point ellipsoid obtained for *Ceratium fusus*, while the grey bars show the statistics for the volumes computed with the resampling procedure. The p-value was directly calculated as the fraction of resampled ellipsoids, which had a volume identical to or smaller than the inflection point ellipsoid.

Figure 5.11 (upper panel) shows the results of a simulation with various choices for the number of points. For a given number of points, its related vertical column corresponds to a specific histogram as in Figure 5.10 (in top view) with height (counts per bin) coded by grey level. As before, the resamples were calculated 10 000 times for each chosen number of points, and as expected, with increasing number of points, the observed contraction of the null statistics opened space for statistically significant normalized volumes. To show the statistical range of the null hypothesis, the standard quantiles in addition to mean and median were plotted. Species with smaller normalized volumes were relatively safe to identify, but species with larger normalized volumes were harder to detect since the resampling histogram exhibits long tails that pushed the upper quantiles to relatively large values. As a more prac-

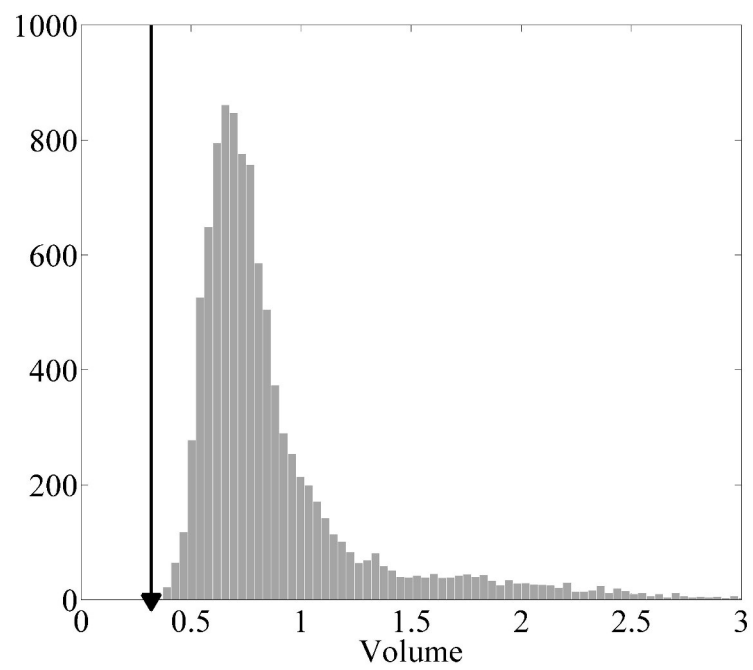


Figure 5.10.: Histogram of the null hypothesis resulting from the resampling procedure; black arrow indicates the volume found for the analysed species (*Ceratium fusus*)

tical approach, a specialization range (displaying the need for special conditions) was introduced. This measure was constructed corresponding to Figure 5.11: the species' niche volumes were extracted and normalized to the quantiles. The number of resamples resulting in a smaller volume than the species' niche volume is subtracted by 5 000 and then divided by 4 500. With n as the resample's number for the species volume, it was calculated using:

- $ROS = \frac{n-5000}{4500}$.

In this perspective, the 5 % quantile (resample number 500) corresponds to -1, the median (resample 5000) to 0 and the 95 % quantile (resample 9500) to 1. Based on this procedure, a range of specialization was obtained: Species with -1 and below were classified as species having their inflection points at special conditions, species with 1 and above were classified as species with inflection points at conditions distributed over the whole cluster, and species with a range of specialization close to 0 were somewhere in between. The range of specialization is illustrated with values -1, 0 and 1 along the right axis of the upper panel in Figure 5.11. This range showed the specialization and *C. fusus* was classified with -1.11 as a species with special needs. *Odontella regia* was found close to the median with -0.11 and *P. sulcata* on the upper end with 0.74.

Some studies attempting to classify species have suffered from type II errors (often called β , error of the second kind, or false negative). Especially Telford et al. (2006) criticized that the analysis of freshwater sediment diatoms by Pither and Aarssen (2005) had led to a misclassification of these species because of a high type II error. In the context of this thesis, this error would result in rejecting a truly small niche as not significant. The power of a statistical test ($1 - \beta$) increases with sample size, i.e. the probability to correctly identify a significantly small niche. To estimate if rejecting a truly small ellipsoid, the aforementioned Telford et al. (2006) was followed by quantifying the type II error through a simulation technique. A similar simulation was performed here, and the type II error was quantified for an artificial species with the construction of a small inflection point ellipsoid. Because the subset was selected to represent a specialized species with a very small ellipsoid, the results of the resampling should have been below the acceptance threshold, shown as the blue line in the upper panel of Figure 5.11. Therefore, the fraction of resamples

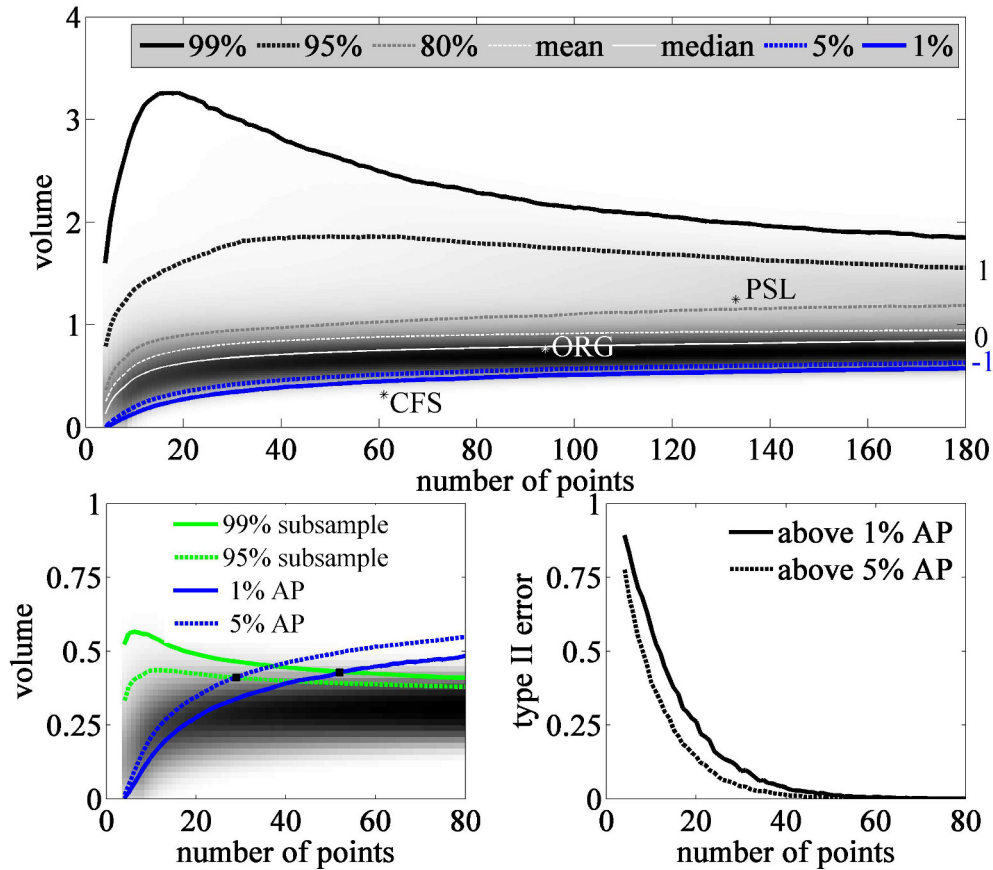


Figure 5.11.: Upper panel: Simulation of the resampling procedure with the original AP cluster; lines show the different quantiles (grey box in the top), the median, and the mean of the normalized volumes. 10 000 resamples were computed with different numbers of points simulating an artificial inflection points ellipsoid (this number is shown on the x-axis). The volume along the y-axis was normalized to the volume of the AP cluster (CFS: *C. fusus*, ORG: *O. regia*, PSL: *P. sulcata*). The range of specialization is indicated on the right side fenced between values -1 and 1. Lower left panel: Simulation of the resampling procedure with different number of points taken out of an AP cluster subset with constructed volume 0.32, i.e. an artificial species with inflection points concentrated in a small region. Blue lines same as in the top panel, green lines reflect the subsamples, and the black squares identify the type II error of 5% and 1% respectively. Lower right panel: Type II error as a function of the number of points; the two curves correspond to the different acceptance thresholds.

that fell above the acceptance threshold reflected false negatives, which estimated the type II error. To go into detail, we picked 8 312 points out of the AP cluster (a total of 14 968 points), thus forming a subset with a normalized volume of 0.32, i.e. the volume of the smallest inflection point ellipsoid found by analysing all species mentioned in Section 3.2. Again, this subset was resampled by randomly picking a given number of points (which was variable but way below the total number of points) and by computing the corresponding volume. The statistics of the null hypothesis were generated by 10 000 repetitions of this procedure, and the results are shown as the blackish area in lower left panel of Figure 5.11. The green line represents the upper quantiles of volumes for the subsample. Volumes above the blue lines in the lower left panel of Figure 5.11 were therefore identified as false negatives. The values resulting for various numbers of points are plotted in the lower right panel of Figure 5.11. This was the fraction of volumes that fell above the blue lines and represented the amount of volumes identified as false negative. Already and beyond 30 inflection points, a type II error smaller than 5 % was found. Therefore, even with a comparatively small number of inflection points, the risk of rejecting a true small niche was low.

5.5. Sensitivity of the optimal niche to the extracted number of principal components

To test for the sensitivity to the dimension reduction, i.e. the number of extracted principal components, and to find out which quantity of PCs was optimal (see Section 5.3), the introduced method was computed for three different species and three different dimensions. This enabled the detection of the optimal number of PCs that represented enough information and did not lead to a high estimation error. On the one hand, taking too few axes would mean losing an amount of total variance while the dimension reduction would not reflect the environmental parameters correctly. On the other hand, using more axes than needed would lead to an increasing estimation error of the covariance ellipsoids needed for the determination of the niche volumes.

In Table 5.1, the results for two, three, and four dimensions are compiled. The

5. Processing the data

Table 5.1.: Computations for different dimensions; d: dimension, λ_{max} and λ_{min} : length of the longest and shortest semi-axis, n: number of inflection points

	<i>Ceratium fusus</i>			<i>Odontella regia</i>			<i>Paralia sulcata</i>		
d	2	3	4	2	3	4	2	3	4
norm.	0.598	0.319	0.222	1.148	0.765	1.072	0.833	1.245	0.816
volume									
λ_{max}	1.191	1.2613	1.2083	1.7985	1.7405	1.8169	1.6439	1.8062	1.6903
λ_{min}	1.0204	0.5055	0.465	1.5538	0.6601	0.7542	1.295	1.1015	0.6859
p-value	0.002	$< 10^{-6}$	0.016	0.903	0.456	0.802	0.058	0.836	0.689
n		61			94			133	

method was continued with three dimensions, and with representation of 60% from the total variance. Moreover, three dimensions had the advantage that the results could be shown graphically. The main point here was to show that the results for a species with a small niche were convincing for three axes. Table 5.1 shows that the p-value was lowest, which was the optimal solution. The estimation error was higher for four axes, and the significance test failed more often, shown by the higher p-value. The decreasing trend towards a smaller normalized volume for the specialist with the dimension was expected due to the addition of axis with lower explained variance. This showed the advantage of the dimension reduction to lowering the risk of a high estimation error.

The calculated volumes were different between the three analysed species. The length of the semi-axis explained the spread in the subspace. An extreme value for one of these lengths indicated an extremely (small or large) axis and could be useful in the interpretation of volumes, but here we did not have such an extreme value for one of the axes. The normalized volume for *C. fusus* was larger for only two dimensions; for three and four, it stayed more or less constant on a smaller value. The spread of the cluster for *O. regia* was the smallest for three dimensions; two dimensions and four dimensions showed a trend towards larger volumes. *Paralia sulcata* showed the largest volume for three dimensions, because *P. sulcata* changed the timing of presence over the whole dataset and the optimal niche was expected to show a broad spread.

This showed that the choice of three dimensions was not only supported by the aforementioned criteria, but also by this comparison.

5.6. Results

Table 5.2 shows the results of applying the optimal niche estimate (ONE) to a wider spectrum of species computed with the competitive milieu. No zooplankton was included yet, and the computation was done exactly as described above.

Table 5.2 shows that most of the species had small optimal niches. Only four species had a positive value for the range of specialization, while two of them reached a relatively large value. This reflects the characteristics of the grey area in Figure 5.11 and the easier detection of species at the lower border of the range of specialization. That species tend to be classified in the lower range could be seen as a negative aspect of this computation. Comparison with the ‘all points’ cluster means that the null hypothesis was biased towards large niches (generalists) because a rejection of the null hypothesis allowed only for the detection of small niches. As Figure 5.11 shows, some species (here *Phaeocystis* ssp., *P. sulcata*, and *P. depressum*) were found in the upper range of the distribution. These species were found in the whole range of the environmental conditions and were therefore not restricted to some special conditions. These species seemed to be well adapted to the environment and showed their highest growth rates in average conditions. Table 5.2 shows that the dinoflagellates were more specialized than the diatoms. The competitive pressure on the diatoms in spring was stronger than on the dinoflagellates in summer, and the environmental conditions were more variable in the summer months and, therefore, this was counterintuitive. However, another source of variability was introduced through the second bloom of the diatoms (larger N in Table 5.2) in late summer or autumn and explained this classification.

Additionally, Figure 5.12 shows the resample statistics (see Section 5.4) performed with all species. This figure illustrates Table 5.2, showing the range where the species were found. One can see *P. depressum* and *P. sulcata* on top of the 80% quantile, as well as an aggregation where most species are found. This aggregation shows similar characteristic for some of these species. A discussion of the results will be done in a comparative way in Subsection 6.2.4 with the inclusion of different approaches (Chapter 6).

Table 5.2.: Results for ONE with the inclusion of the interaction milieu; N: number of inflection points, λ_{max} : length of the longest semi-axis, λ_{min} : length of the shortest semi-axis, diatoms in light grey, dinoflagellates in dark grey and the haptophyte in white

Species	volume ONE ellipsoid	p-value	N	λ_{max}	λ_{min}	range of special-ization
<i>Guinardia striata</i>	0.21621	< 0.001	53	1.2597	0.51744	-1.1109
<i>Ceratium fusus</i>	0.31945	< 0.001	61	1.2613	0.50554	-1.1107
<i>Scrippsiella</i> ssp.	0.3263	0.008	29	1.9514	0.49944	-1.0931
<i>Ceratium tripos</i>	0.32643	< 0.001	62	1.3523	0.47201	-1.1109
<i>Prorocentrum micans</i>	0.34973	< 0.001	53	1.2681	0.66045	-1.1098
<i>Ceratium furca</i>	0.39892	0.0011	66	1.3089	0.6197	-1.1084
<i>Eucampia zodiacus</i>	0.41604	0.0026	68	1.2201	0.70488	-1.1051
<i>Ceratium horridum</i>	0.43165	< 0.001	91	1.7476	0.49488	-1.11
<i>Thalassiosira rotula</i>	0.49195	0.058	48	1.8377	0.53918	-0.982
<i>Guinardia delicatula</i>	0.49429	0.0081	93	1.3471	0.81146	-1.0929
<i>Porosira glacialis</i>	0.52157	0.2872	21	1.6074	0.57701	-0.47267
<i>Odontella rhombus</i>	0.53141	0.0114	120	1.5411	0.58491	-1.0856
<i>Torodinium robustum</i>	0.54439	0.0644	68	1.7731	0.59857	-0.96778
<i>Noctiluca scintillans</i>	0.55803	0.1037	61	1.4783	0.70482	-0.88044
<i>Ceratium lineatum</i>	0.60652	0.1591	72	1.4564	0.72427	-0.75733
<i>Odontella aurita</i>	0.63923	0.2319	71	1.6746	0.63345	-0.59556
<i>Skeletonema costatum</i>	0.70182	0.3218	91	1.9656	0.58573	-0.39578
<i>Thalassionema nitzschioides</i>	0.75259	0.4317	89	1.7835	0.60071	-0.15156
<i>Odontella regia</i>	0.76456	0.4542	94	1.7405	0.66012	-0.10156
<i>Odontella sinensis</i>	0.83243	0.5657	102	1.5671	0.82792	0.14622
<i>Phaeocystis</i> ssp.	0.89224	0.6903	67	1.5282	1.0201	0.42311
<i>Paralia sulcata</i>	1.2452	0.8318	133	1.8062	1.1015	0.73756
<i>Protoperidinium depressum</i>	1.4357	0.9006	64	2.1412	0.86551	0.89044

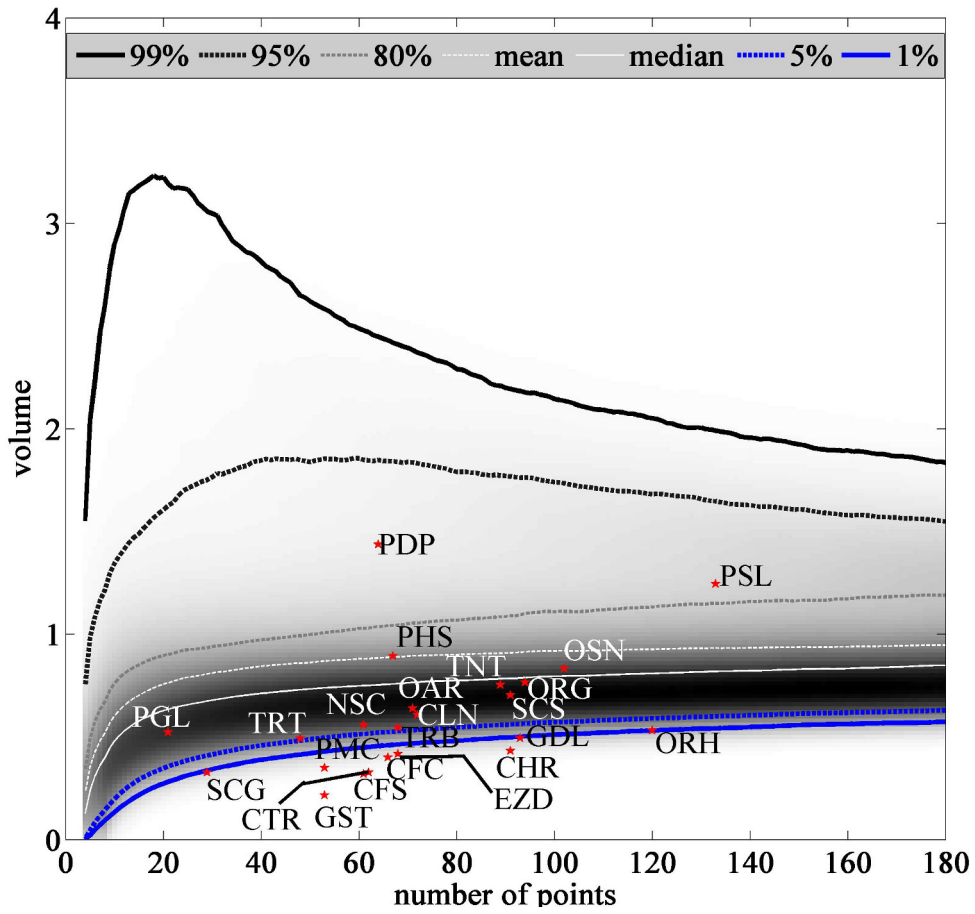


Figure 5.12.: Simulation of the resampling procedure

6. Variation of the biotic database

6.1. Transformation of the abundance data

The aforementioned extraction of the inflection points was based on the raw abundance data and hence a measure for the net growth of the population. To compute the per capita growth rate, which was often done to discuss the response per individual, one had to extract the inflection points of the logarithmic transformed abundance curve because:

- $\dot{x} = r(x) \cdot x$
- $\Rightarrow \frac{\dot{x}}{x} = \frac{d \ln x}{dt} = r(x),$

$r(x)$ was the per capita growth rate of population x and \dot{x} the population growth rate. Solving the equation with the logarithmic abundance data led to the per capita growth rate. This extraction of the inflection points via the log-transformed abundance curve resulted in different inflection points. This transformation compressed high and stretched low cell counts. This rescaling led to problems in the detection of the inflection points by emphasizing the short but pronounced fluctuations at the bottom line. This resulted in a very high number of inflection points compared to the number extracted with the untransformed data. Figure 6.1 shows the differences of the two extractions for the same year. It can be seen that the untransformed approach extracted two inflection points and the log-transformed approach extracted four. Two inflection points were found at similar dates in both approaches, but they were shifted by a few days in the transformed approach and two additional points were extracted. With an adjustment of the acceptance threshold, the number of inflection points extracted with the log-transformed data could be reduced and the number would be nearly the same. However, it was questionable that all these points represented a high fitness of the species. ONE was analysing the ecological niche of

a species where it had its fastest growth, without concentrating on the individual level. Therefore, it was adequate and self-explanatory to extract the inflection points of the raw abundance curve.

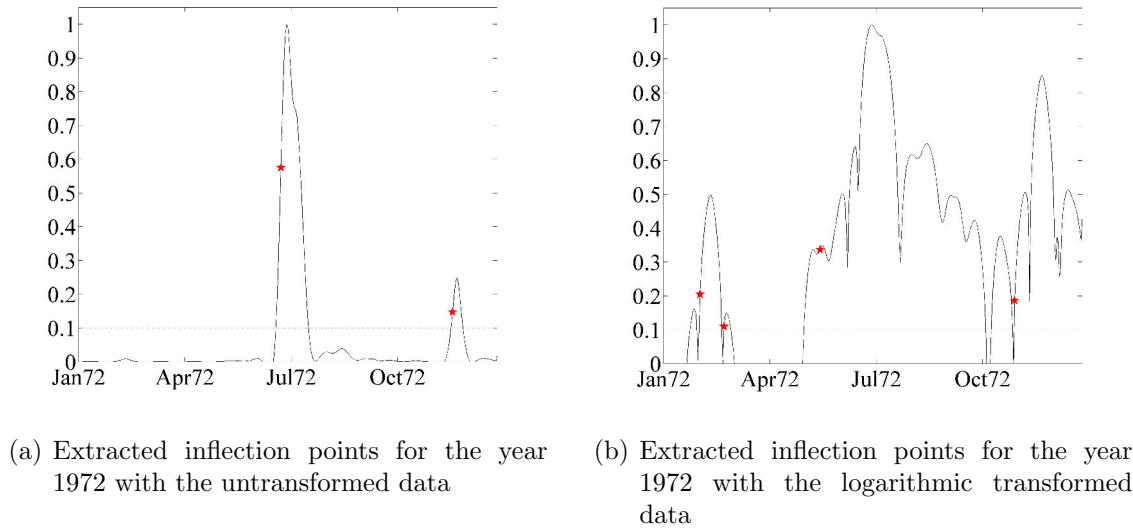


Figure 6.1.: Extracted inflection points without and with logarithmic transformed data for *Ceratium fusus*

6.2. Different compositions of the environmental dataset

6.2.1. Approaches

To test this method for the influence of the abiotic factors and to determine the influence of competition and grazing on the niche reconstruction, this section will show the analysis of different applications of ONE. Therefore, several principal component analyses (PCAs) with different compositions of environmental factors were performed.

The competitive milieu was extracted as explained in Section 3.2 as a quantity for intra- and interspecific competition. It was the sum of the abundances of all 23 selected phytoplankton species. The zooplankton data were included as the sum of

all recorded species without *Noctiluca scintillans*, because this species was treated as a member of the 23 analysed species here and hence already included in the biotic dataset. Unless otherwise stated, the further steps of ONE were carried out in the same manner as explained before (Chapter 5).

It has to be kept in mind that the zooplankton sampling started in 1974 (cf. Chapter 3), meaning that the time series had to be shortened for related analyses. To reach a fair comparison, normal ONE (cf. Chapter 5) and ONE without the competitive milieu were also performed on the shortened dataset. This allowed comparing the approaches, and the results helped to understand the effects of including or excluding different biotic factors.

By including all available time series, the ecological niche for every single species could be reconstructed, but the importance of competition and grazing could only be determined through a comparison of differently composed datasets. Therefore, different compositions of the environmental datasets were computed to identify the influence of these time series on the method. The exclusion of the biotic time series, the inclusion of only one of these time series, and the inclusion of both helped to identify what effect these time series had on the computation, thus helping to isolate the influence of the biotic from the abiotic time series.

These tests were carried out by using four additional set-ups (five in total, notation with reference to McGill et al. (2006)) of the previously explained method:

XL:	Without any biological information	⇒ 1967 until 2008
CL:	With the competitive milieu (Chapter 5)	⇒ 1967 until 2008
XS:	Without any biological information	⇒ 1974 until 2008
CS:	With the competitive milieu	⇒ 1974 until 2008
CZS:	With the competitive milieu and zooplankton	⇒ 1974 until 2008

The identifiers were selected to explain the used datasets. These will be used in Subsection 6.2.4 for the discussion of the results:

- X: without biological data,
- C: with the competitive milieu,
- Z: with zooplankton,
- S: for the short period,

L: for the long period.

To help clarify this comparison in the following sections, the results will only be shown graphically for *Ceratium fusus* and not for all of the 23 analysed species. An illustration of the aforementioned ellipsoids and the histograms (see Sections 5.3 and 5.4) for the resampling procedures will be done for this species in the following approaches. The results for all species will be shown in a corresponding table and will be combined in one graph.

6.2.2. Computation with different biotic data - 1967 until 2008

XL: Exclusion of all biotic factors

The exclusion of all abiotic factors resulted in an eight-dimensional PCA. Figure 6.2 shows the factor loadings (details in Section 5.3) for the first four principal components (PCs). Nearly all factor loadings had comparable values for the first PC (except the sign), but the representation of wind speed was less pronounced and only salinity had hardly any influence on the composition of the first PC. The nutrients and wind speed were on the same side, and all other physico-chemical parameters were on the opposite side.

As mentioned in Section 5.2, this could be explained with the waxing and waning of these factors throughout the year. The nutrients were depleted simultaneously, and factors like temperature and sunshine duration showed strong correlations. As one could identify different groups of factors, these groups were also found in the factor loadings (FLs) of the PCA. Salinity had the highest contribution to the second, temperature to the third, and silicate to the fourth PC.

Figure 6.3 shows the explained and cumulative variances distributed among the eight principal components (PC1: 34.5 %, PC2: 20.0 %, PC3: 12.2 %, PC4: 9.5 %). The first three PCs were above the Kaiser-Guttman rule (dotted line). Therefore, the following analysis was carried out with three dimensions. Figure 6.4 shows the distribution of the inflection points in comparison with the ‘all points’ cluster and the corresponding ellipsoids. It can be seen that with the exception of some outliers, the inflection points for *C. fusus* were distributed over a small area of the ‘all points’

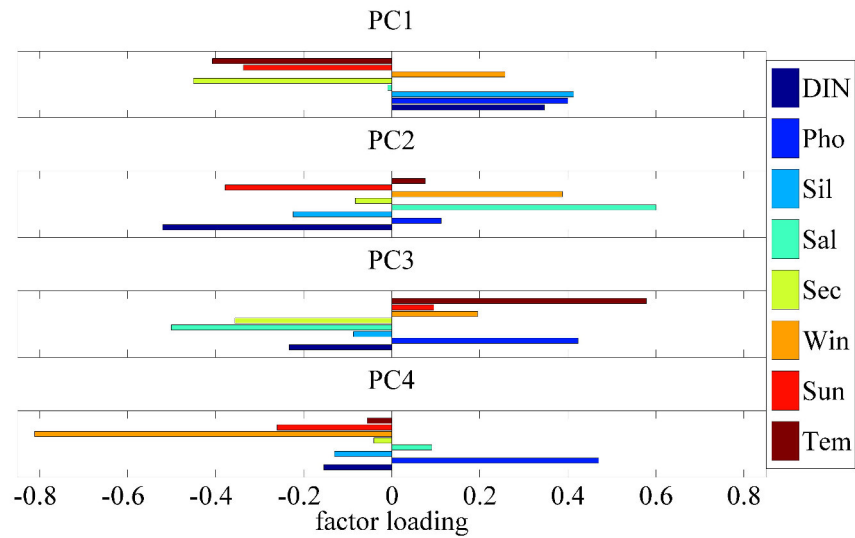


Figure 6.2.: Factor loadings of the first four PCs for the approach without biological interaction; Tem: temperature, Sun: sunshine duration, Win: wind speed, Sec: Secchi depth, Sal: salinity, Sil: silicate, Pho: phosphate, DIN: dissolved inorganic nitrogen

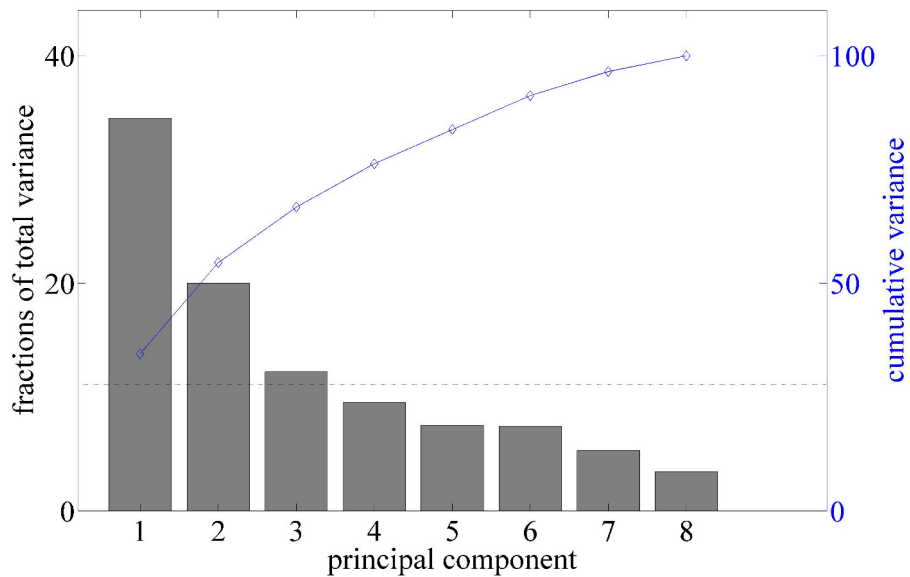


Figure 6.3.: Explained and cumulative variance for the eight PCs, dotted line: Kaiser-Guttman rule

(AP) cluster, and the ellipsoids supported this visual impression well. The results for all species are summarized in Table 6.1. The statistics for the computation are shown in Figure 6.5. Of course, the volume found for *C. fusus* was still significantly small, but the histogram approached the Gaussian distribution (see Figure 5.10). This fact can also be seen in Figure 6.6 at the more symmetrical quantile lines at the grey area that is darker in the middle. The consequences of this change in the distribution can also be seen in figure (Figure 6.6). Through the shifting of the mean, it was easier to reach a statistically significant small niche volume, and it was getting harder to reach a high p-value. This can be seen in Tables 6.1 and 5.2.

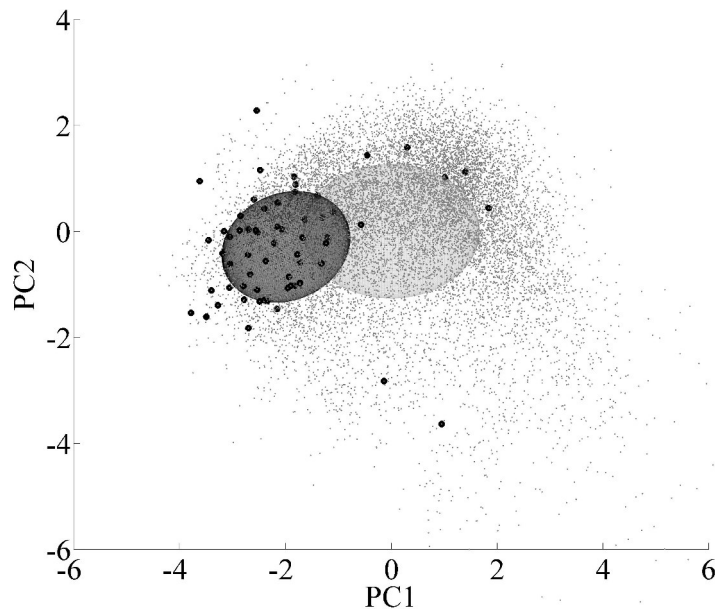


Figure 6.4.: ‘All points’ cluster (grey) and highlighted inflection points (black) with the correlation ellipses (same colour) for the approach without biological interaction for *Ceratium fusus*

The simulation of the resampling procedure (Figure 6.6) shows where the species can be found in the range of the randomized sampling. There were 15 species below the 5% quantile and nine below the 1% quantile, which showed that a lot of species were classified as more specialized. Table 6.1 shows the complete results of the computations without biological interactions. It can be seen that there were no

species in the upper range of specialization.

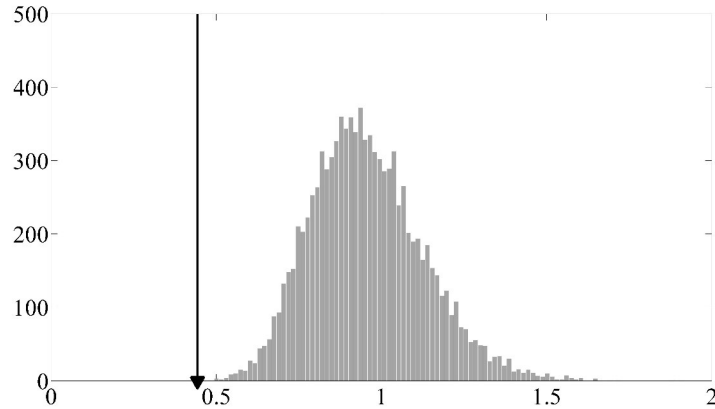


Figure 6.5.: Histogram for the resampling procedure without biological interaction for *C. fusus*, black arrow points at the volume found for the analysed species

The results of the approach without biological interactions on the long time scale were summarized in Table 6.1. The data were ranked with respect to increasing volumes of the ONE ellipsoids, and these values were in a range between 0.25845 for *Guinardia striata* and 1.0187 for *Thalassionema nitzschioides*. Most species were found in the lower range of the spectrum of specialization (cf. Figure 6.6), supported by the p-value and the range of specialization (ROS). Owing to the same time frame, the inflection points were distributed in the same way as shown in Chapter 5 and ranged from 21 for *Porosira glacialis* to 133 for *Paralia sulcata*. The longest and shortest semi-axes were similar for all species. Only *Scrippsiella* ssp. showed an imbalance between the two semi-axes. Compared to the other species, the ellipsoid had an oblate shape. This showed that the inflection points for this species were distributed along one axis, but because of the spatial orientation of the ellipsoid this axis was not one of the principal axis. Therefore, it was hard to say what causes the special shape. The species' results were extracted and normalized to the quantiles from the resampling procedure: The 5 % quantile corresponded to -1, the median to 0, and the 95 % quantile to 1. The ROS showed that 15 species are below -1 and therefore classified as specialists. The other species were above this value, but no species was close to 1 and thus no generalists could be found with this approach.

Table 6.1.: Results for the computation with the exclusion of all biotic factors sorted by the volume of the ONE ellipsoid in an ascending order; N: number of inflection points, λ_{max} : length of the longest semi-axis, λ_{min} : length of the shortest semi-axis, diatoms in light grey, dinoflagellates in dark grey and the haptophyte in white

Species	volume ONE ellipsoid	p-value	N	λ_{max}	λ_{min}	range of specialization
<i>Guinardia striata</i>	0.25845	< 0.001	53	1.2686	0.57717	-1.1109
<i>Prorocentrum micans</i>	0.41046	< 0.001	53	1.2567	0.68262	-1.1109
<i>Porosira glacialis</i>	0.41283	0.0141	21	1.4009	0.51703	-1.0796
<i>Ceratium fusus</i>	0.44372	< 0.001	61	1.2666	0.66985	-1.1109
<i>Scrippsiella</i> ssp.	0.47637	0.0107	29	1.929	0.67018	-1.0871
<i>Ceratium furca</i>	0.49801	< 0.001	66	1.3	0.71439	-1.1107
<i>Ceratium tripos</i>	0.50318	< 0.001	62	1.3572	0.63942	-1.1098
<i>Eucampia zodiacus</i>	0.52096	< 0.001	68	1.2392	0.8517	-1.1107
<i>Guinardia delicatula</i>	0.54241	< 0.001	93	1.349	0.84998	-1.1109
<i>Ceratium horridum</i>	0.59672	< 0.001	91	1.7408	0.66818	-1.1096
<i>Protoperidinium depressum</i>	0.63155	0.0109	64	1.7379	0.81697	-1.0867
<i>Phaeocystis</i> ssp.	0.66869	0.0226	67	1.4836	0.89571	-1.0607
<i>Noctiluca scintillans</i>	0.68128	0.0373	61	1.4841	0.84533	-1.028
<i>Paralia sulcata</i>	0.69024	0.0029	133	1.5095	0.82325	-1.1044
<i>Ceratium lineatum</i>	0.71942	0.0469	72	1.4495	0.83821	-1.0067
<i>Thalassiosira rotula</i>	0.78882	0.2153	48	1.8356	0.85054	-0.63244
<i>Torodinium robustum</i>	0.79365	0.1499	68	1.7858	0.83797	-0.77778
<i>Odontella rhombus</i>	0.85453	0.1612	120	1.5393	0.92748	-0.75267
<i>Odontella sinensis</i>	0.86904	0.232	102	1.5696	0.85136	-0.59533
<i>Odontella aurita</i>	0.94079	0.4708	71	1.706	0.90257	-0.064667
<i>Odontella regia</i>	0.94176	0.439	94	1.7326	0.8035	-0.13533
<i>Skeletonema costatum</i>	0.99565	0.5908	91	1.9599	0.81567	0.202
<i>Thalassionema nitzschioides</i>	1.0187	0.6442	89	1.7852	0.79435	0.32067

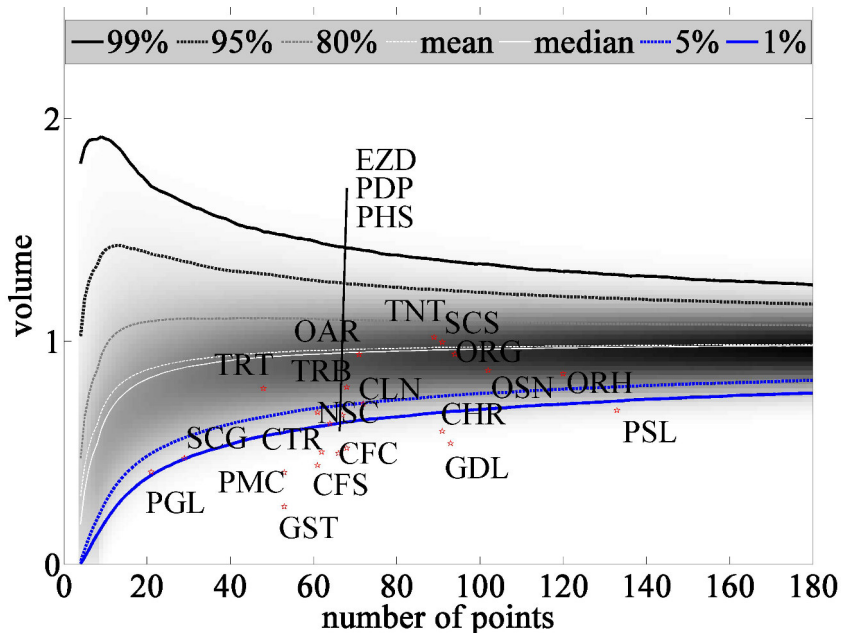


Figure 6.6.: Simulation of the resampling procedure without biological interaction; abbreviation of the species can be found in Chapter 3

No clear trend of grouping into diatoms and dinoflagellates was found in the upper part of the table, but the species found with large ONE volumes at the lower end were diatoms. The diatoms are known to form blooms in spring and late summer or autumn, and through temporal variability, these species face a broad range of environmental conditions (Wiltshire and Dürselen, 2004). Excluding the biological interaction did not have a strong influence on these species, because the times of maximal growth were mainly found at times when grazing was still low and the competition with dinoflagellates was not strong (Hoppenrath et al., 2009). Intra-specific competition between the diatoms led to different species that outcompete the other in different years, but throughout the years most of these diatoms often showed the fastest growth in this time of the year. This led to the aforementioned facing of a broader range of the environmental conditions. None of the dinoflagellates on the list were found to have large ONE volumes. These species were often found in summer when the spring bloom was over and the environmental conditions were highly variable. This is interesting because the variable conditions should have led to a large niche. The variability of the environmental conditions was highest between

March and August, because, among other things, the nutrients were depleted and, later in the interval, became available again (Hoppenrath et al., 2009; Reid et al., 1990) and the temperature rose (a detailed analysis of the temporal variability can be found in Subsection 7.2.4). But through the restriction to a very narrow time window in the year, these species showed their highest growth rates within a narrow range of the environmental conditions.

CL: Computation with the competitive milieu

The computation of ONE with the inclusion of the competitive milieu was already explained in detail in Chapter 5.

Computation with the competitive milieu and zooplankton

Due to the shorter sampling of the zooplankton time series, it was not possible to do this analysis on the long time scale from 1967 until 2008.

Summary for the computations from 1967 until 2008

The aforementioned computations resulted in different ecological niches for the selected species, and the PCA resulted in different factor loadings. The environmental factors and the nutrients were represented equally in both approaches, but the competitive milieu included in the second approach (CL) had a considerable share of PC3 and PC4 and was also represented in PC1. The competitive milieu had the lowest influence of all included environmental factors in PC2. When excluding the competitive milieu, it could be seen that the eight species with the greatest ecological niches were exclusively diatoms. Furthermore, the range from the smallest to the largest niche size was wider for the approach with the included biotic time series. The results are discussed in Subsection 6.2.4.

6.2.3. Computation with different biotic data - 1974 until 2008

XS: Exclusion of all biotic factors

The aforementioned approaches and the inclusion of zooplankton were also applied to the shorter time series. This enabled a comparison of the derived results and

helped to understand the influence of the biotic components. A computation of the PCA with factors of different length was not possible, and therefore, all computations had to be redone with the shorter time frame. Through the reduction of the length of the time series, the PCA led to different results, because the number of samples was reduced from 14 968 to 10 337. This influenced all steps of the computation and a safe comparison could not be guaranteed any more. The reduction in the length and the varying number of included factors changed the composition of the principal components, thereby leading to changes in the results of the PCA. Consequently, the size of the ecological niches were computed on a changed basis.

The first approach was the exclusion of all biotic factors; just the eight physico-chemical parameters were used. Figure 6.7 shows the factor loadings, i.e. the contribution of the abiotic factors to the linear combinations. All factors contributed with nearly equal weight (neglecting the sign) to the first PC; only the wind speed was represented less. Temperature, sunshine duration, and Secchi depth were positive, while the other factors had a negative sign. As mentioned before, this was a representation of the different characteristics of the environmental factors. The nutrients were correlated and the climatic variables were correlated, too. Salinity and dissolved inorganic nitrogen had the highest contribution to the second PC, temperature, phosphate, and salinity to the third. The fourth PC was dominated by the influence of silicate.

The explained variance (Figure 6.8) of the eight PCs was analogue to the comparable approach on the longer time scale, because the intraannual dynamics of the different time series were not changed through the shortening. The first PC represented 33.8%, the second 20.3%, the third 12.6%, and the fourth PC 9.5% of the variance. The Kaiser-Guttman rule once again supported the reduction to three PCs. The fourth PC was clearly below the Kaiser-Guttman rule and was considered unimportant in the next steps. Figure 6.9 shows the distribution of the all points cluster and the ONE cluster. One can see clearly the narrow distribution of the inflection point cluster, this is also represented by the ellipsoids.

The histogram in Figure 6.10 illustrates the statistical significance of this result and the distribution obtained from the resampling procedure. The result for *Ceratium fusus* was clearly statistically significant. The resampling statistics (Figure 6.11) show the distribution of the species' result. There were 13 species below the

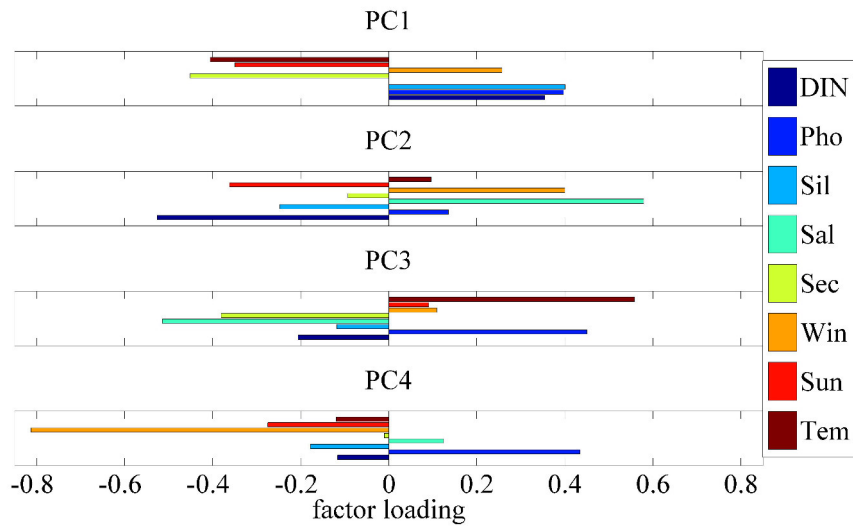


Figure 6.7.: Factor loadings of the first four PCs for the approach without biological interaction and shortened time frame; Tem: temperature, Sun: sunshine duration, Win: wind speed, Sec: Secchi depth, Sal: salinity, Sil: silicate, Pho: phosphate, DIN: dissolved inorganic nitrogen

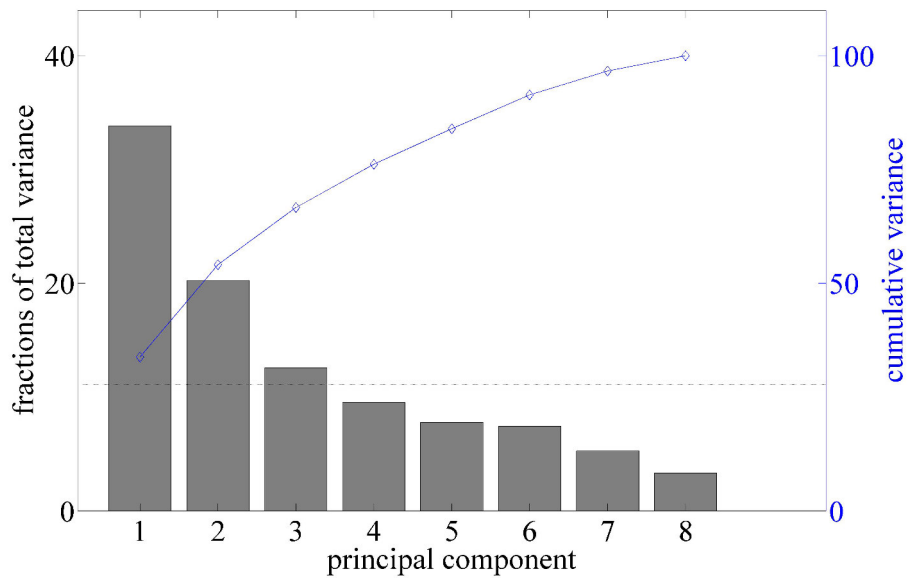


Figure 6.8.: Explained and cumulative variance for the eight PCs for the approach without biological interaction for *Ceratium fusus* and the short time series, dotted line: Kaiser-Guttman rule

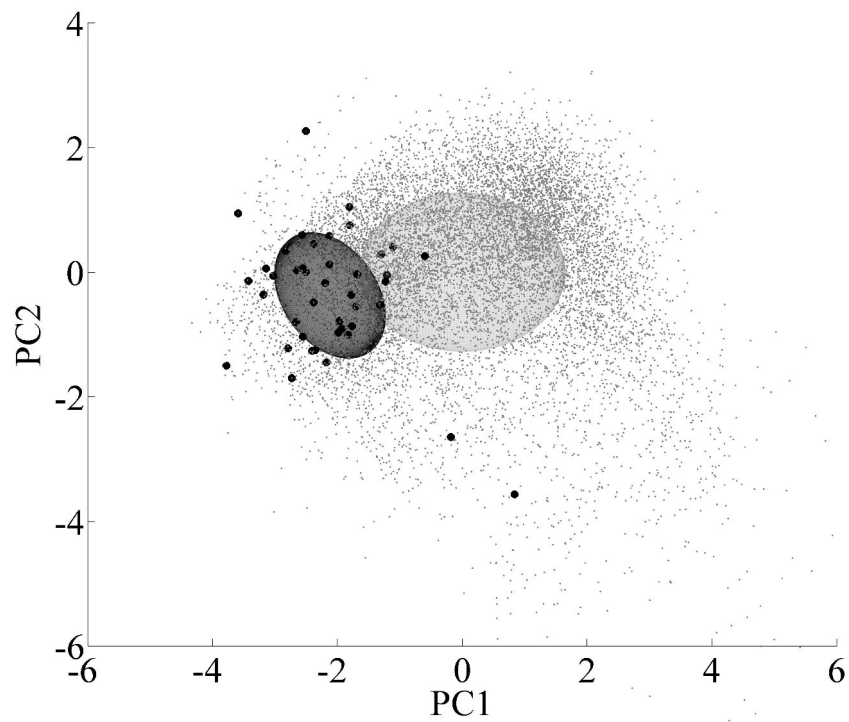


Figure 6.9.: ‘All points’ clusters (grey) and highlighted inflection points (black) with the correlation ellipses (same colour) for the approach without biological interaction for *Ceratium fusus* and the short time series

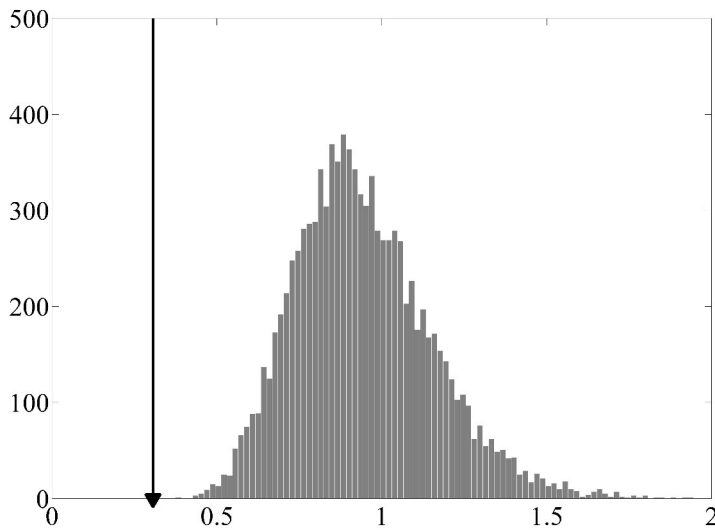


Figure 6.10.: Histogram for the resampling procedure without biological interaction for *C. fusus*, black arrow points at the volume found for the analysed species for the approach without biological interaction and the short time series

5% and 10 below the 1% quantile, but no species was found in the upper range of specialization.

Table 6.2 shows the results of all previous steps in the analysis without any biological interaction on the shorter time series. One can see that the species sorting resulted in a very similar table with minor changes in ranks when compared to Table 6.1. Species found to be more specialized in the analysis with the longer time series were also found to be more specialized in this analysis with the shorter time frame. This showed that the dependence on the length was not crucial for the classification of the species in this approach. The number of inflection points was, of course, reduced and ranged from 16 for *Porosira glacialis* to 93 for *Paralia sulcata*. The ROS showed again that a lot of species were identified as more specialized, but no species was found on the upper range of the spectrum.

Again, the grouping showed that the diatoms were found in the upper range of the ONE volumes. In the lower range, there was a mixture of diatoms and dinoflagellates. These results were similar to the longer time series. Hence, the shortening of the time

Table 6.2.: Results for the computation with the exclusion of all biotic factors and the short time series sorted by the volume of the ONE ellipsoid in ascending order; N: number of inflection points, λ_{max} : length of the longest semi-axis, λ_{min} : length of the shortest semi-axis, diatoms in light grey, dinoflagellates in dark grey and the haptophyte in white

Species	volume ONE ellipsoid	p-value	N	λ_{max}	λ_{min}	range of special-ization
<i>Guinardia striata</i>	0.28157	< 0.001	43	1.3211	0.59572	-1.1109
<i>Porosira glacialis</i>	0.28519	0.0031	16	1.4288	0.57819	-1.104
<i>Ceratium fusus</i>	0.30676	< 0.001	42	1.2183	0.64724	-1.1109
<i>Ceratium furca</i>	0.35229	< 0.001	44	1.2453	0.60238	-1.1109
<i>Prorocentrum micans</i>	0.36699	< 0.001	41	1.2756	0.57339	-1.1109
<i>Scrippsiella</i> ssp.	0.45305	0.0121	26	1.9412	0.69395	-1.084
<i>Ceratium tripos</i>	0.47723	0.0012	44	1.2783	0.64809	-1.1082
<i>Eucampia zodiacus</i>	0.53093	0.0021	53	1.1751	0.87382	-1.1062
<i>Guinardia delicatula</i>	0.55774	< 0.001	79	1.3808	0.83189	-1.11
<i>Protoperidinium depressum</i>	0.57446	0.0143	44	1.7925	0.67403	-1.0791
<i>Paralia sulcata</i>	0.60279	< 0.001	93	1.4742	0.75817	-1.1102
<i>Ceratium horridum</i>	0.61593	0.0076	68	1.7797	0.6601	-1.094
<i>Phaeocystis</i> ssp.	0.66123	0.0388	54	1.5	0.92622	-1.0247
<i>Noctiluca scintillans</i>	0.68201	0.0685	50	1.5429	0.85116	-0.95867
<i>Torodinium robustum</i>	0.70006	0.0773	51	1.7695	0.82073	-0.93911
<i>Ceratium lineatum</i>	0.70901	0.0871	51	1.3956	0.81634	-0.91733
<i>Odontella aurita</i>	0.77325	0.1718	52	1.7013	0.7604	-0.72911
<i>Thalassiosira rotula</i>	0.88721	0.4778	32	1.9592	0.90864	-0.049111
<i>Odontella rhombus</i>	0.8942	0.3129	91	1.5972	0.90134	-0.41556
<i>Odontella regia</i>	0.92827	0.4282	78	1.6713	0.82235	-0.15933
<i>Odontella sinensis</i>	1.0026	0.6193	83	1.6201	0.93727	0.26533
<i>Skeletonema costatum</i>	1.0257	0.6696	70	1.8926	0.85342	0.37711
<i>Thalassionema nitzschoides</i>	1.0346	0.6816	70	1.7781	0.77997	0.40378

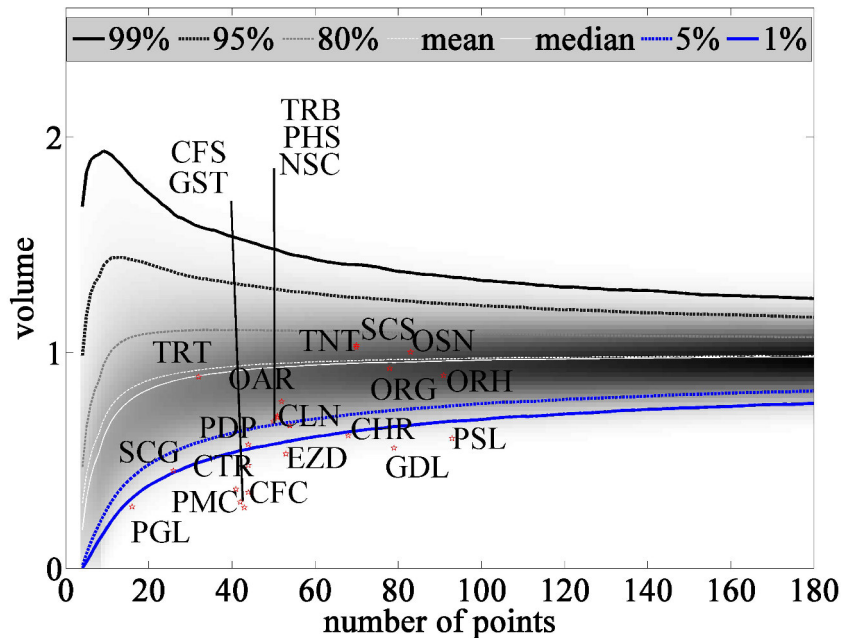


Figure 6.11.: Simulation of the resampling procedure without biological interaction and the short time series, abbreviation of the species can be found in Chapter 3

series did not lead to any differences.

CS: Inclusion of the competitive milieu

ONE was performed in the same way as described in Chapter 5, with the difference that the time series was adapted to the period of zooplankton sampling (1974–2008). All other parts of the procedure were carried out in the same way.

Figure 6.12 shows the factor loadings of the single environmental factors of the first four PCs. Nearly all factors had a significant contribution to the first PC. Only the contributions of the competitive milieu and wind speed were less pronounced. Physical parameters were found on the positive side and nutrients on the negative. Dissolved inorganic nitrogen and salinity had the highest influence on the second PC while the third PC had two factors with a high influence on the positive and on the negative side (positive: phosphate and temperature, negative: interaction milieu and Secchi depth). The fourth PC was dominated by the competitive milieu.

The explained variance (Figure 6.13) is distributed between the PCs in the following way: PC1 represents 30.6%, PC2 18.0%, PC4 11.3%, and PC4 10.8%. The

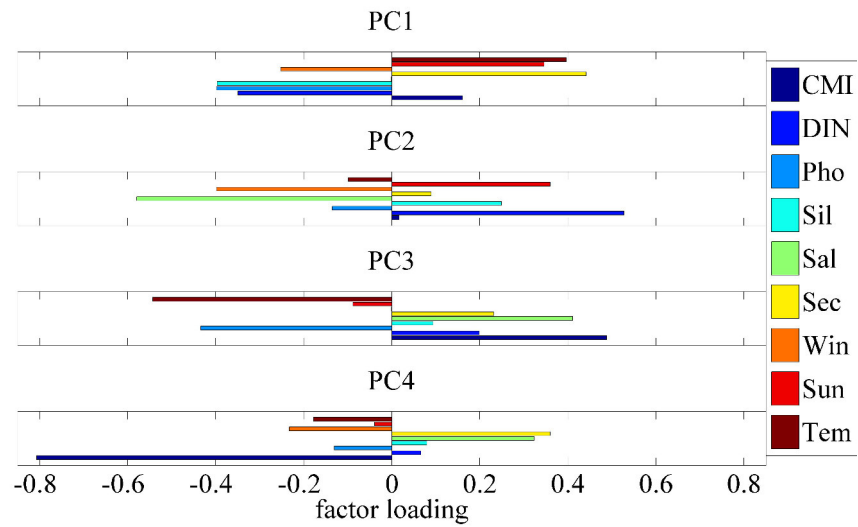


Figure 6.12.: Factor loadings of the first four PCs for the approach with included competitive milieu and the short time series; Tem: temperature, Sun: sunshine duration, Win: wind speed, Sec: Secchi depth, Sal: salinity, Sil: silicate, Pho: phosphate, DIN: dissolved inorganic nitrogen, CMI: competitive milieu

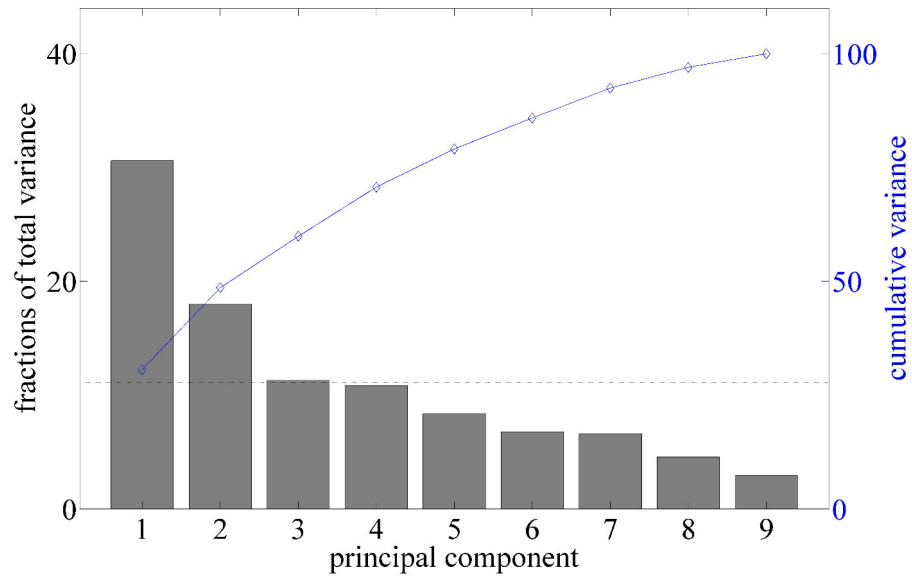


Figure 6.13.: Explained and cumulative variance for the eight PCs for the approach with the competitive milieu and the short time series, dotted line: Kaiser-Guttman rule

fourth principal component was slightly below the Kaiser-Guttman rule. In order to allow a comparison with the other approaches, ONE computed with the shortened time frame was continued with three dimensions.

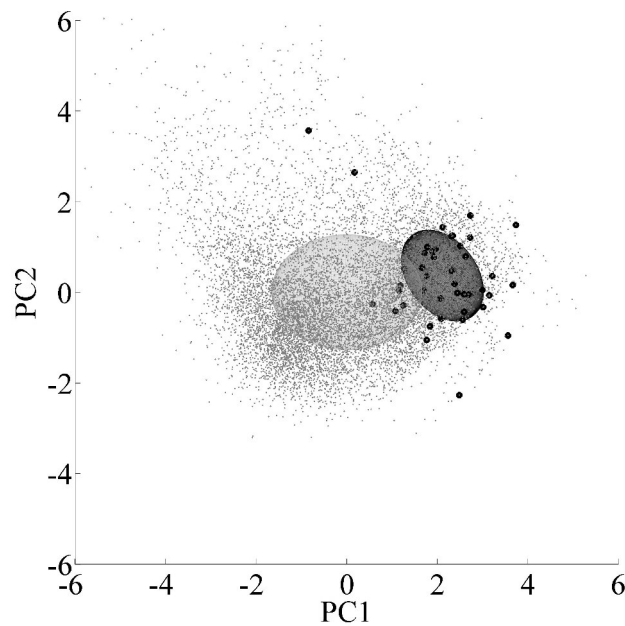


Figure 6.14.: ‘All points’ cluster (grey) and highlighted inflection points (black) with the correlation ellipses (same colour) for the approach with the competitive milieu for *Ceratium fusus* and the short time series

Figure 6.14 shows the ‘all points’ cluster and the inflection point cluster for *Ceratium fusus*. Because of the distribution of the inflection points and the size of the ellipsoid, one can directly see that this species was restricted to special conditions.

Figure 6.15 shows the histogram of the resampling procedure with marked result for *Ceratium fusus*. In contrast to the previous approach, the Poisson-like distribution was visible again and was therefore a result of the inclusion of the interaction milieu in the analysis. The normalized volume for *C. fusus* was significantly small again, and Figure 6.16 shows the result of the resampling simulation. One can see 11 species below the 5% quantile and 10 below the 1% quantile. Again, it was hard to detect species in the upper range, but *Protoperidinium depressum* reached a higher volume than all other species and a comparable high value for all approaches on

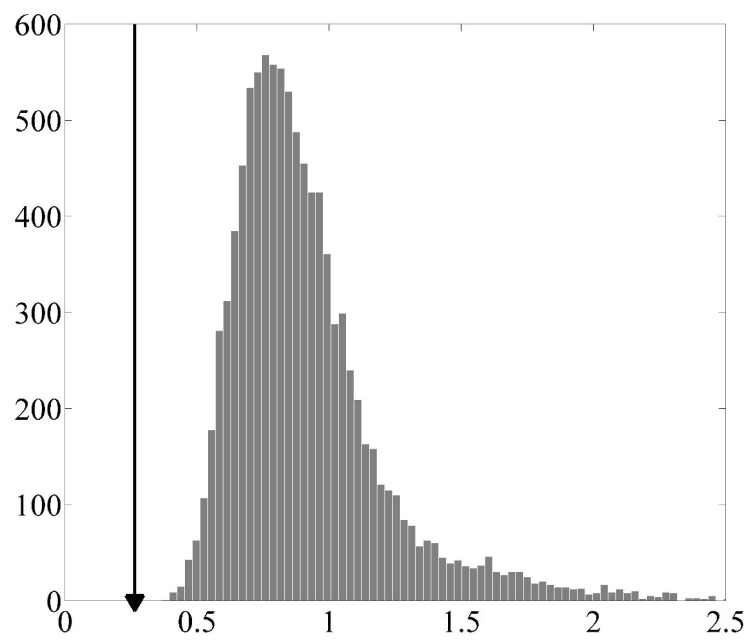


Figure 6.15.: Histogram for the resampling procedure with the competitive milieu and the short time series for *C. fusus*; black arrow points at the volume found for the analysed species

the short time frame. *Paralia sulcata* had its highest value for all approaches on the short time frame.

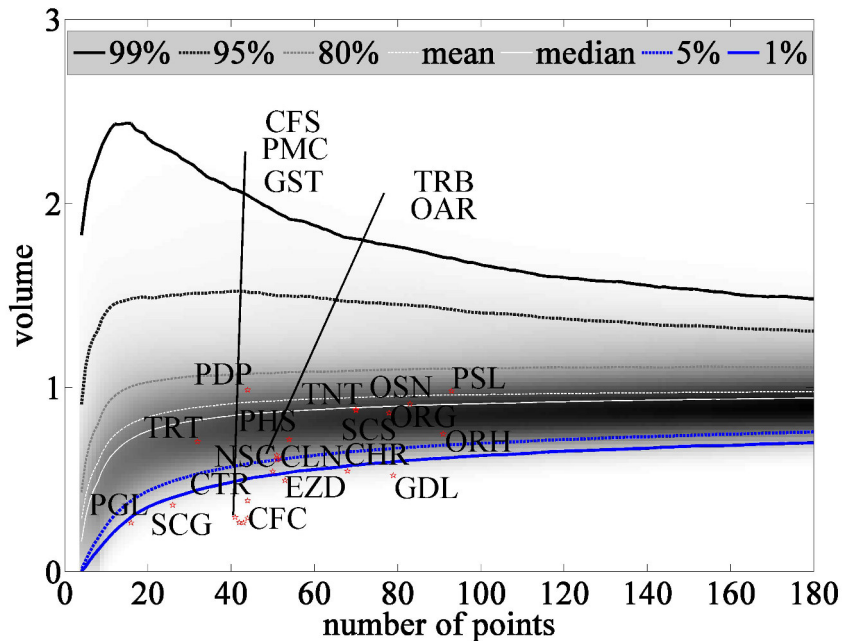


Figure 6.16.: Simulation of the resampling procedure with inclusion of the competitive milieu and the short time series; abbreviation of the species can be found in Chapter 3

Table 6.3 subsumes the result of the computation under the inclusion of the interaction milieu on the shorter time frame. The number of significantly small volumes fell to 11 while a tendency to higher ellipsoid volumes could be identified. The number of inflection points was, due to the same time frame, the same as in the previous step (XS). The lengths of the semi-axes were similar to the previous approaches. The range of specialization showed the same tendency as in Figure 6.16. The high value for *Protoperdinium depressum* was the only remarkable thing. Since this species had its high volumes in the approaches where the competitive milieu was included, this fits to this heterotrophic species when it was able to graze on a number of different prey species.

The grouping of the species was no different from the previous approaches, but a dinoflagellate had the largest ONE volume in this analysis. The other species with large volumes were again diatoms. The order of the species in this approach was

Table 6.3.: Results for the computation with the inclusion of the competitive milieu on the short time series sorted by the volume of the ONE ellipsoid; N: number of inflection points, λ_{max} : length of the longest semi-axis, λ_{min} : length of the shortest semi-axis, diatoms in light grey, dinoflagellates in dark grey and the haptophyte in white

Species	volume ONE ellipsoid	p-value	N	λ_{max}	λ_{min}	range of special-ization
<i>Guinardia striata</i>	0.26321	< 0.001	43	1.3251	0.57382	-1.1109
<i>Porosira glacialis</i>	0.26331	0.0042	16	1.4812	0.51889	-1.1016
<i>Ceratium fuscus</i>	0.26491	< 0.001	42	1.2068	0.59073	-1.1109
<i>Ceratium furca</i>	0.28898	< 0.001	44	1.2486	0.54508	-1.1109
<i>Prorocentrum micans</i>	0.29364	< 0.001	41	1.2745	0.5175	-1.1109
<i>Scrypsiella</i> ssp.	0.36094	0.0039	26	1.9651	0.55803	-1.1022
<i>Ceratium tripos</i>	0.3842	< 0.001	44	1.2165	0.56328	-1.11
<i>Eucampia zodiacus</i>	0.49351	0.0034	53	1.1794	0.82058	-1.1033
<i>Guinardia delicatula</i>	0.52204	< 0.001	79	1.3727	0.8158	-1.1093
<i>Noctiluca scintillans</i>	0.5424	0.0157	50	1.5296	0.70614	-1.076
<i>Ceratium horridum</i>	0.54486	0.0048	68	1.7874	0.58973	-1.1002
<i>Torodinium robustum</i>	0.60715	0.053	51	1.7608	0.77616	-0.99311
<i>Odontella aurita</i>	0.61168	0.0501	52	1.6468	0.63819	-0.99956
<i>Ceratium lineatum</i>	0.62988	0.068	51	1.4005	0.74322	-0.95978
<i>Thalassiosira rotula</i>	0.70525	0.2863	32	1.9483	0.73834	-0.47467
<i>Phaeocystis</i> ssp.	0.7169	0.1865	54	1.5397	0.95452	-0.69644
<i>Odontella rhombus</i>	0.74642	0.1324	91	1.5938	0.76273	-0.81667
<i>Odontella regia</i>	0.86095	0.4106	78	1.6794	0.76898	-0.19844
<i>Skeletonema costatum</i>	0.87379	0.4689	70	1.898	0.73772	-0.068889
<i>Thalassionema nitzschioides</i>	0.87845	0.4795	70	1.7811	0.67331	-0.045333
<i>Odontella sinensis</i>	0.91031	0.5249	83	1.612	0.86614	0.055556
<i>Paralia sulcata</i>	0.98047	0.652	93	1.6862	1.0271	0.338
<i>Protoperidinium depressum</i>	0.9857	0.706	44	2.0656	0.67371	0.458

similar to the approach with the competitive milieu on the long time frame. There were no big differences, indicating once again that the reduction in the time series length had no strong influence on the results of the computation.

CZS: With the competitive milieu and zooplankton

To test for the effects of competition and grazing, a computation with all available biotic and abiotic factors was carried out. The computation was done with 10 environmental factors (Figure 6.17). All environmental factors (except the competitive milieu and salinity) had a high contribution to PC1. Zooplankton, temperature, and sunshine duration had a negative contribution, while wind speed, dissolved inorganic nitrogen, phosphate, and silicate had a positive contribution. The small contribution of salinity and the competitive milieu showed that these two factors were not strongly correlated with the other factors. However, this pattern could be found in most of the other approaches with the inclusion of the competitive milieu (CL, CS), too. PC2 was mainly influenced by dissolved inorganic nitrogen and salinity; PC3 by temperature, zooplankton, phosphate, and the competitive milieu. PC4 was dominated by the competitive milieu.

The distribution of the variances through the PCA is shown in Figure 6.18. PC1, PC2, and PC3 were above the Kaiser-Guttman rule, and PC4 was slightly below (PC1: 29.6 %, PC2: 16.8 %, PC3: 10.7 %, PC4: 9.7 %). Therefore, this approach was continued with three axes.

The ellipsoids in Figure 6.19 show again that the inflection points for *Ceratium fusus* were found in a cluster. Hence, this species had a small niche in this approach, too.

The histogram 6.20 shows the distribution of the randomized resampling procedure, and *Ceratium fusus* had again a significantly small volume. The distribution was comparable to the approach with just the interaction milieu.

Figure 6.21 shows the results for the resampling procedure with included normalized volumes for every species. Eleven species were found below the 1 % and 12 below the 5 % quantile. There was still no detection of a species close to the upper border of the distribution.

Table 6.4 shows the results for the ONE analysis with included zooplankton.

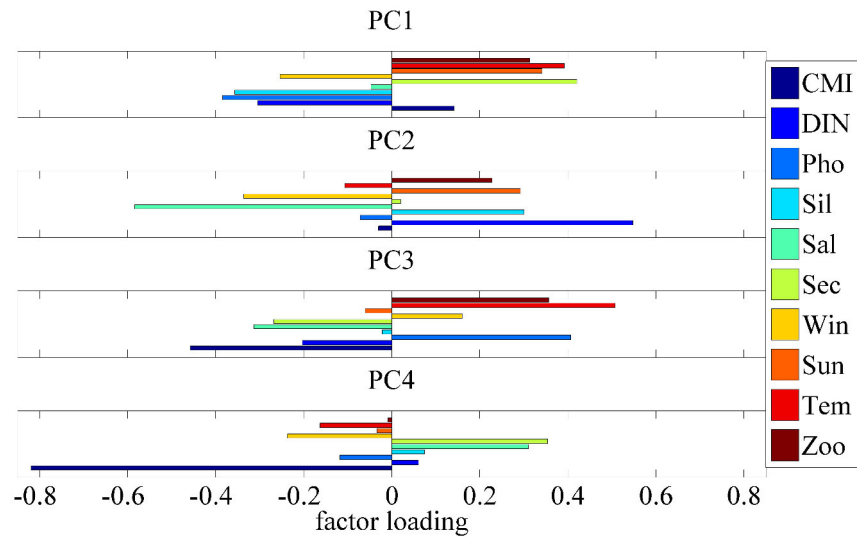


Figure 6.17.: Factor loadings of the first four PCs in the approach with included zooplankton; Zoo: zooplankton, Tem: temperature, Sun: sunshine duration, Win: wind speed, Sec: Secchi depth, Sal: salinity, Sil: silicate, Pho: phosphate, DIN: dissolved inorganic nitrogen, CMI: competitive milieu

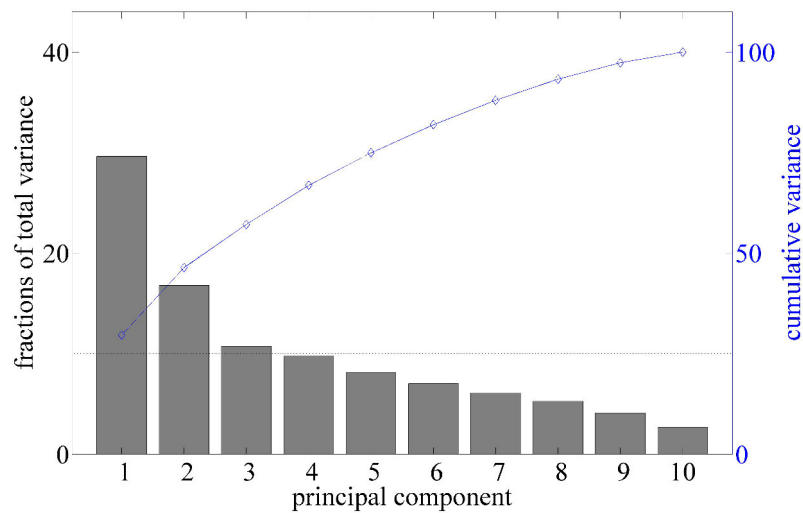


Figure 6.18.: Explained and cumulative variance distributed over the PCs in the approach with included zooplankton; the dotted line shows the Kaiser-Guttman rule

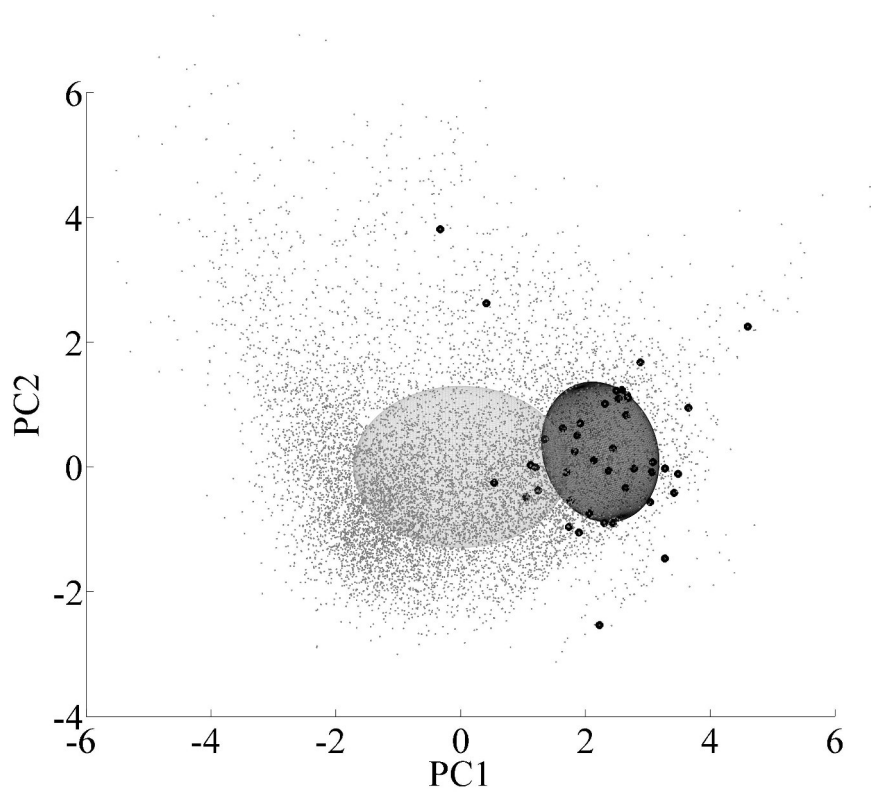


Figure 6.19.: ‘All points’ cluster (grey) and highlighted inflection points (black) with the correlation ellipses (same colour) for the approach with all biotic factors for *Ceratium fusus* on the short time series

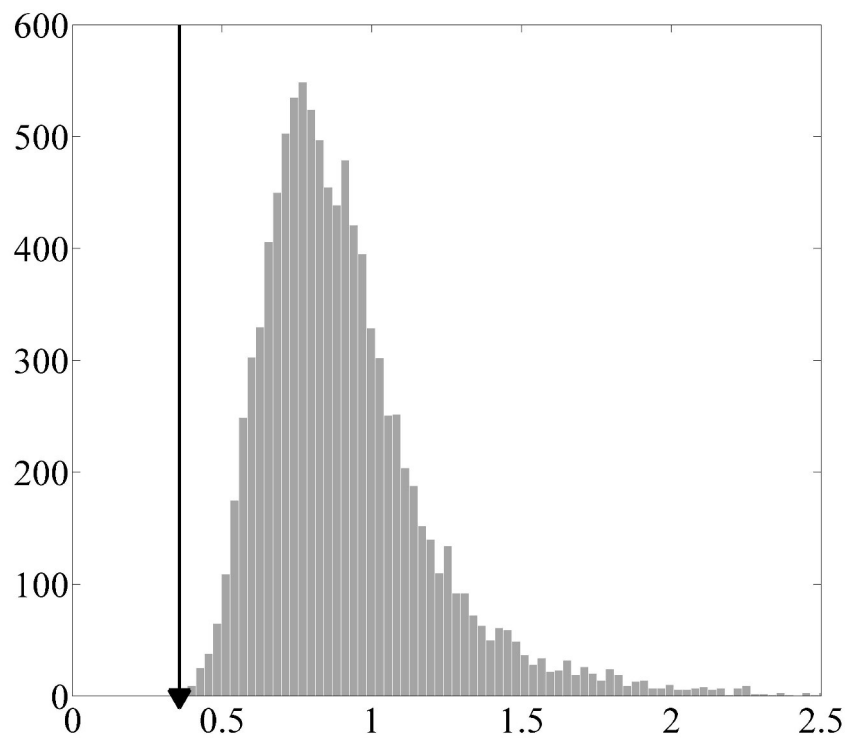


Figure 6.20.: Histogram for the approach with all biotic factors on the short time series; black arrow indicates the volume found for the analysed species

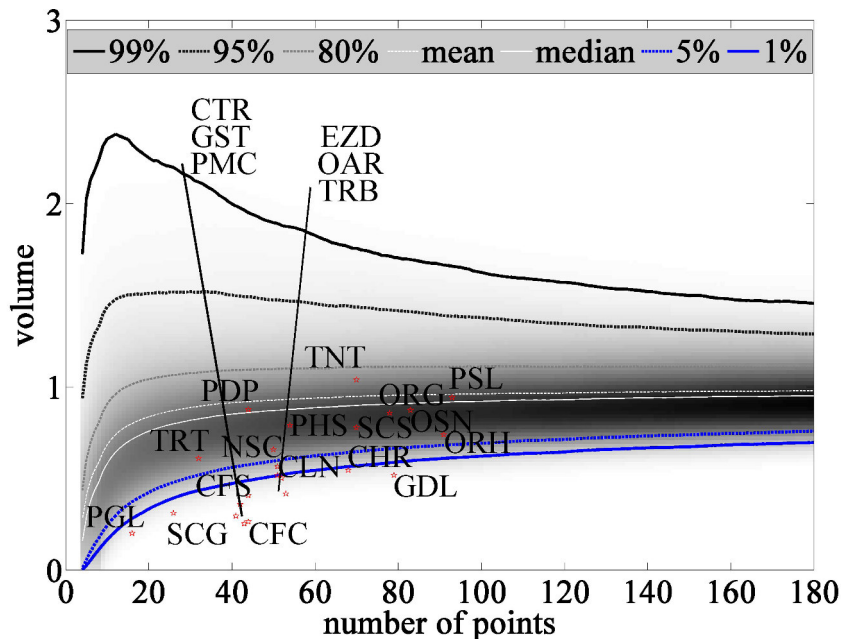


Figure 6.21.: Simulation of the resampling procedure for the approach with included phyto- and zooplankton; abbreviation of the species can be found in Chapter 3

The normalized volumes of the ellipsoids were comparable to the other approaches, and the detected inflection points were the same across the three approaches on the shorter time frame. The range of specialization showed only one high value for *Thalassionema nitzschoides* and a tendency to more specialized species.

The results again showed a clustering of the species, and the upper range of the ONE volumes was dominated by diatoms. This trend was found for every approach. The dinoflagellates were on the lower range again.

6.2.4. Differences and similarities between the approaches with varied environmental factors

This section should help the reader to grasp the essence of the reported results. As shown at the beginning of these comparisons, the investigated approaches were:

- | | | |
|-----|---|-------------------|
| XL: | Without any biological information | ⇒ 1967 until 2008 |
| CL: | With the competitive milieu (Chapter 5) | ⇒ 1967 until 2008 |

6. Variation of the biotic database

Table 6.4.: Results for the computation with inclusion of the interaction milieu and zooplankton on the short time series sorted by the volume of the ONE ellipsoid; N: number of inflection points, λ_{max} : length of the longest semi-axis, λ_{min} : length of the shortest semi-axis, diatoms in light grey, dinoflagellates in dark grey and the haptophyte in white

Species	volume ONE ellipsoid	p-value	N	λ_{max}	λ_{min}	range of special-ization
<i>Porosira glacialis</i>	0.20022	< 0.001	16	1.4621	0.4629	-1.1093
<i>Guinardia striata</i>	0.25211	< 0.001	43	1.3402	0.56295	-1.1109
<i>Ceratium furca</i>	0.26437	< 0.001	44	1.3559	0.49711	-1.1109
<i>Proocentrum micans</i>	0.29408	< 0.001	41	1.3373	0.50765	-1.1109
<i>Scrippsiella</i> ssp.	0.31147	< 0.001	26	1.9769	0.51238	-1.1089
<i>Ceratium fusus</i>	0.35787	< 0.001	42	1.2595	0.71449	-1.1107
<i>Ceratium tripos</i>	0.40637	< 0.001	44	1.3895	0.57753	-1.1093
<i>Eucampia zodiacus</i>	0.41647	< 0.001	53	1.1773	0.72305	-1.1096
<i>Odontella aurita</i>	0.5014	0.0056	52	1.6535	0.57491	-1.0984
<i>Torodinium robustum</i>	0.51704	0.0101	51	1.7685	0.74302	-1.0884
<i>Guinardia delicatula</i>	0.51725	0.0012	79	1.3752	0.8283	-1.1082
<i>Ceratium horridum</i>	0.54547	0.006	68	1.8339	0.59298	-1.0976
<i>Ceratium lineatum</i>	0.564	0.0255	51	1.3902	0.72059	-1.0542
<i>Thalassiosira rotula</i>	0.60837	0.1443	32	1.9112	0.70767	-0.79022
<i>Noctiluca scintillans</i>	0.65671	0.1146	50	1.5382	0.89987	-0.85622
<i>Odontella rhombus</i>	0.73895	0.1198	91	1.6076	0.79409	-0.84467
<i>Skeletonema costatum</i>	0.77723	0.2438	70	1.9028	0.70433	-0.56911
<i>Phaeocystis</i> ssp.	0.79025	0.3283	54	1.6085	0.98992	-0.38133
<i>Odontella regia</i>	0.85711	0.3972	78	1.72	0.79849	-0.22822
<i>Odontella sinensis</i>	0.87158	0.412	83	1.6122	0.87178	-0.19533
<i>Protoperidinium depressum</i>	0.87554	0.5272	44	2.0601	0.68409	0.060667
<i>Paraha sulcata</i>	0.94123	0.554	93	1.6927	1.0097	0.12022
<i>Thalassionema nitzschioides</i>	1.0381	0.7209	70	1.8805	0.74798	0.49111

XS:	Without any biological information	⇒ 1974 until 2008
CS:	With the competitive milieu	⇒ 1974 until 2008
CZS:	With the competitive milieu and zooplankton	⇒ 1974 until 2008.

In the following, every approach will be indicated with the identifier mentioned in the listing above (to repeat the derivation of the identifier: X: without biological data, C: with the competitive milieu, i.e. total phytoplankton, Z: with the zooplankton time series, S: computation with the short period, L: computation with the long period).

The linear combinations of the first three principal components in the different approaches show how the initial variables were represented through the principal components. There were no big differences in the approaches. The reduction to the shorter time frame had no influence, and the linear combinations were nearly the same in the short and long approaches (Figures 6.2 and 5.5 compared to Figures 6.7 and 6.12). By adding the competitive milieu, just a small amount of this information was added to the first and second PCs. However, the third PC received a substantial contribution from the competitive milieu. Because this was the axis with the smallest amount of information included after the PCA for this analysis, this influence was not very pronounced in the results (Figures 6.2 and 6.7 compared to Figures 5.5 and 6.12). The inclusion of the zooplankton had a stronger influence, thus having a considerable contribution to the first three PCs (Figure 6.17). This showed that this time series introduced a great amount of variance into the analysis and explained the change in the results when it was added.

The analysed species were mainly diatoms and dinoflagellates, and the range of specialization (ROS, defined in Section 5.4) showed some important characteristics of these taxa. Figures 6.22 and 6.23 show the ROS for every species from different perspectives. Figure 6.22 shows the distribution of the ROS for each of the five approaches, and some differences could be identified. Some of the dinoflagellates (especially the *Ceratium* species) were always found at the lower limit of the ROS, but some species' values changed considerably between the approaches. Not even one species reached the upper limit of the range of specialization (i.e. $ROS \approx 1$). Nevertheless, across all other approaches, the CL approach showed the highest number of species in the upper part of the ROS with *Protoperidinium depressum* and

Paralia sulcata close to this upper limit. Figure 6.22 shows the differences between the approaches as well as the consequences of changing the environmental dataset for the analyses. The influence of the selected data can be seen clearly. The two approaches without biological information (XL and XS) showed nearly the same results. The ROS for some species were shifted, but the tendency was the same. Just a small influence of the length of the time series was identified in these approaches, but with the inclusion of the competitive milieu (CL and CS), these changes became more pronounced. The CL approach showed the highest number of species in the upper range, and the CS approach identified just three species above the median. This seemed to be comparable to the approach without biological information (XS), but different species were above the median in the CS approach. This showed again the influence of the competitive milieu on the classification. The CL approach was the most interesting one, because the lowest and the highest ROS for all species had the greatest distance. Therefore, the time scale and the competitive milieu had a considerable influence on this approach. By including additionally the zooplankton (CZS), which could only be done for the short time scale, the distance between the smallest and the greatest value was smaller and comparable to the CS approach. This showed that the zooplankton only had a weak influence on the computation.

Figure 6.23 shows the same values as Figure 6.22, but this graph was sorted by the species. The changing values for the species' ROS in the different approaches are shown. Species for which an inclusion of biotic data had a strong effect were identified. Some species showed the same results for all the approaches. The ROS for *Ceratium furca*, *Ceratium fusus*, *Ceratium horridum*, *Ceratium tripos*, *Eucampia zodiacus*, *Guinardia delicatula*, *Guinardia striata*, *Prorocentrum micans*, and *Scrippsiella* ssp. stayed at the lower range for all five approaches. The time series length or the inclusion of biotic time series made hardly any difference for these species. The ROS for *Ceratium lineatum*, *Noctiluca scintillans*, *Odontella regia*, and *Torodinium robustum* varied, but not in a pronounced way. These species showed only small changes. One special characteristic found for these 13 species was that *O. regia* was found close to the centre (near 0) of the ROS and thus needed more special conditions than the species found close to -1.

These 13 species showed a stable ROS due to the timing. These species were found nearly every year at the same time and therefore at comparable conditions.

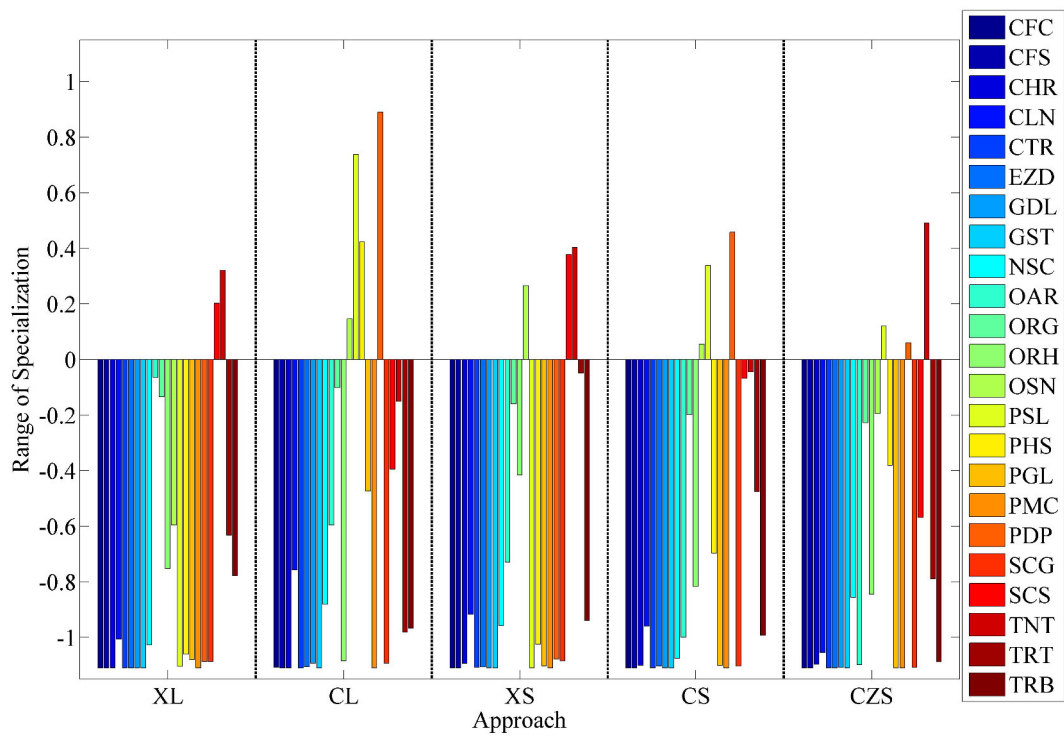


Figure 6.22.: Range of specialization for every approach (x-axis) and every species (colour-coded) from the computed different compositions of the environmental dataset of the previous sections; abbreviation of the species can be found in Chapter 3

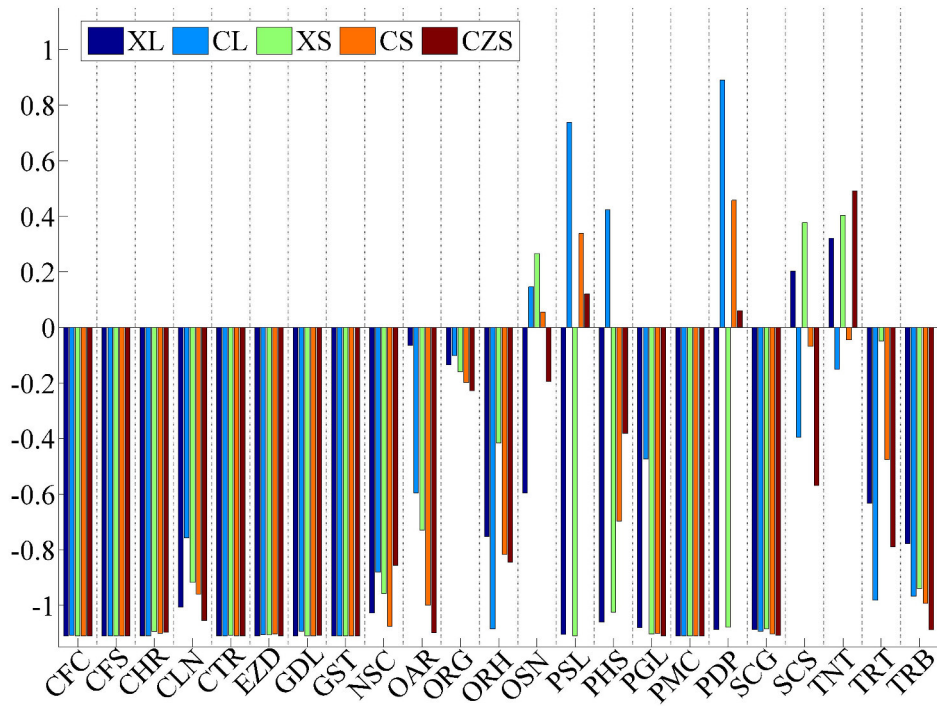


Figure 6.23.: Range of specialization for every species (x-axis) and every approach (colour-coded) from the computed different compositions of the environmental dataset of the previous sections; abbreviation of the species can be found in Chapter 3

This indicated a restriction of these species to special conditions found in all of the environmental factors. The other species showed a greater variation of the ROS for the different computations. *Porosira glacialis* showed an interesting detail: The ROS was at the lower range of the spectrum, except for the CL approach. This showed an influence of the combination of the dataset length and the competitive milieu. This was a consequence of the time of occurrence of the species, because it was only found regularly in the period before 1974. Therefore, the length of the time series had a strong influence on the classification of this species, but this influence was reduced when the competitive milieu was excluded. *Odontella rhombus* showed a variation in the ROS from -1 to -0.4. These extremes were found in the approaches CL and XS; all other ROS were in the range of -0.8. *O. rhombus* had a reduced abundance in the middle part of this time series, which is why the reduction of the length excluded the first abundance period. *Odontella aurita* and *Thalassiosira rotula* showed a strong variation in the ROS, and the values ranged between -1 and 0. Therefore, the results for these species were strongly influenced by the changes of the environmental dataset. The ROS for *O. aurita* showed a stepwise increase with the smallest value for XL and the highest for CZS approach, representing a high influence of the length of the time series on the classification of this species. The ROS for *T. rotula* was smallest in the XS and largest in the CL approach, and the classification of this species was strongly influenced by the biotic data. All aforementioned species never reached a positive range of specialization, and this classified these as species with special needs. Not all of these species were specialists, but their tendencies towards small niches could clearly be identified.

The following species reached a positive ROS in at least one approach. The results for *Odontella sinensis*, *Skeletonema costatum*, and *Thalassionema nitzschioides* were comparable and changed from -0.6 to 0.5. However, there were pronounced differences between the species and the approaches. *O. sinensis* had the smallest ROS in the XL and the largest in the XS approach, while *S. costatum* had the largest ROS in this approach, but the smallest in the CZS approach. *T. nitzschioides*, however, had the largest ROS in the CZS and the smallest in the CL approach. Interestingly, *T. nitzschioides* and *S. costatum* showed the same tendencies, but the results for the CZS approach were contrary. Finding an explanation for these tendencies was not easy, but one could see that *T. nitzschioides* was not influenced by the biotic

milieu. Just with zooplankton and phytoplankton, a high value of the ROS was reached. *S. costatum* showed a strong dependence on the biotic data, and the ROS with / without it was negative / positive. *Phaeocystis* ssp. showed the ROS of -1 (a clear specialist) for the two approaches without the biotic interaction (XL and XS). The only positive value was found for the CL approach. The results for *Paralia sulcata* and *Protoperdinium depressum* were very similar. Both showed the largest ROS in the CL approach and the smallest ROS for approaches without biotic interaction. This indicated an influence of the biological interaction on these species and showed that the length of the time series did not have a strong influence.

Overall, it was hard to interpret the changes resulting from the different compositions of the dataset for the PCA and the subsequent varying niche sizes for the 23 species. By including and excluding the biotic time series and by changing the length, all PCAs were composed differently, visible by the factor loadings, and one could not compare all of them with each other. But a comparison of approaches where only one factor was different showed that the composition of the dataset had a considerable influence on the classification of the species. As mentioned before, excluding time series relevant for the species could result in a dataset that did not represent the conditions found in the habitat. Therefore, the approach with all time series available (CZS) was used for the ecological discussion of the results for all 23 species in the next chapter (Chapter 7). If it was advantageous, the results for the approach with the long time series and the competitive milieu (CL) were added to the discussion.

7. Ecological interpretation of the results

7.1. Consequences of the inclusion of all biotic data for the 23 selected species

In the previous chapter, the different computations and analyses were described and the results were shown. This chapter will focus on the ecological interpretation of the approach with all biotic information (10 dimensional principal component analyses with phytoplankton and zooplankton). This approach was selected to avoid missing important factors not captured by collections of fewer regressor variables. This section will revisit the in Section 3.2 described characteristics of the different species and connects them with the previously presented results for the analysed species. These results will be discussed and compared with data found in literature.

The trophy for all dinoflagellates was assigned after Löder et al. (2011). In the following, the items in brackets will indicate: the volume of the ONE ellipsoid, statistically significant (s.) or statistically not significant (n.s.), the number of inflection points, and the size of the major and minor semi-axes.

Diatoms

Eucampia zodiacus *Eucampia zodiacus* (0.417, s., 53, 1.177, 0.723) was classified as a specialist. Resende et al. (2007, 2005) found a similar result to this classification concerning the temperature range for this species. They showed that this species was more abundant during warmer temperatures. Kraberg et al. (2010) stated that this species could be found across the world in coastal areas mainly in temperate to warm waters in spring and summer. Du and Peterson (2013) found this species to be a dominant member of spring and early summer bloom off the coast in central Oregon, USA. *E. zodiacus* was

also a dominant spring species in a South Korean bay (Baek et al., 2015). But according to Hoppenrath et al. (2009), this species could be found throughout the year at Helgoland and Sylt, North Sea. It had its highest abundance in October and bloomed sometimes in autumn. Growth experiments at different temperatures with species from the Seto Inland Sea, Japan, showed that this species had its optimal growth rate at 20–25 °C (Nishikawa and Yamaguchi, 2006). These, for the Helgoland Roads data, very high temperatures were only reached in the summer. In line with all these findings, the inflection points were found between April and October. Therefore, the specialist characteristics were mainly influenced by the temperature. This species seemed not to be able to grow at lower temperatures, or was at least not able to outcompete other and better adapted species. Varying the dataset for the computation of the PCA had no influence on the results for this species. The niche sizes were small for all approaches.

Guinardia delicatula*, *G. striata Both *Guinardia* species (*G. delicatula*: 0.517, s., 79, 1.375, 0.828, *G. striata*: 0.252, s., 43, 1.340, 0.563) analysed here were classified as specialists by ONE. However, *G. delicatula* showed nearly twice as many inflection points as *G. striata*. The inflection points of *G. delicatula* were concentrated in late spring and summer, and for *G. striata* they were concentrated in the summer and early autumn.

It was shown that *G. delicatula* occurs throughout the year at Helgoland and Sylt, with the highest abundances in summer (Hoppenrath et al., 2009; Schlüter et al., 2012). After Kraberg et al. (2010) *G. delicatula* could be found in late spring and summer, it was present until autumn and appeared earlier in recent years. This tendency towards earlier bloom timing in this dataset could be connected with a shift in the hydrodynamic environment (Schlüter et al., 2012). *G. delicatula* was often one of the dominant species during phytoplankton blooms in other studies from Argentina (Gayoso, 1999), Ireland (Gowen, 1999), the U.K. (Weston et al., 2008), France (Guilloux et al., 2013), and China (Ilyash and Matorin, 2007). Peacock et al. (2014) investigated parasitic infection of *G. delicatula* in the New England shelf, USA, where this species is a typical member of the winter phytoplankton community. They showed that

this species was regularly infected with the nanoflagellate *Cryothecomonas aestivalis* when the water temperature rose above 4°C. This infection was also shown for the species at Helgoland (Drebes et al., 1996) and might play a role in the collapse of the blooms of this species. As mentioned before, Schlüter et al. (2012) showed that changes in the timing of the growth period of *G. delicatula* were influenced by different environmental factors: The start of the growth period was mainly influenced by temperature, Secchi depth, competition, and grazer abundance, whereas the end of the growth period was mainly influenced by sunshine duration, temperature, and grazer abundance. Changes in these factors could shift the start or the end of the growth period to an earlier or later time, reflecting that the species needed special conditions of these factors. For example, warmer water temperature and lower grazer abundance led to earlier blooms (Schlüter et al., 2012). A transfer of this finding to this specialist meant that this species bloomed earlier, because ‘its’ special bloom temperature was reached earlier and that it bloomed earlier because ‘its’ special bloom grazer abundance was reached earlier (zooplankton abundance rises until summer so that earlier means less zooplankton). In summary, one can say that the time of the bloom changed for this species, but the environmental conditions faced at this time did not.

Information about *Guinardia striata* was sparse in the literature, but it was regularly found in summer and autumn in coastal waters and at Helgoland and Sylt (Hoppenrath et al., 2009; Kraberg et al., 2010). An investigation of the phytoplankton community in the English Channel in April, May, and July in 2003 showed that *G. striata* was the dominating or at least one of the dominating species in all samples from May to July (Schapira et al., 2008). Ilyash and Matorin (2007) identified *G. striata* as one of the dominant phytoplankton species in spring and autumn in South China, while Fernandes and Brandini (2004) found this species to be dominant in spring in Southern Brazil. It was hard to say why *G. striata* was classified as a specialist, but it seemed that this species was mainly restricted to the second bloom in late summer or early autumn. This might have been the reason for the small niche and the number of inflection points of about one per year.

Both species, albeit with different abundance and niche volume (however, both had a significantly small volume), were restricted to special environmental conditions, and the size of the optimal niche was insensitive to variations in the analysed combinations of the environmental factors. This shows that both *Guinardia* species were highly adapted to the conditions found during their growth periods.

O. aurita*, *O. regia*, *O. rhombus*, *O. sinensis Three of the *Odontella* species (*O. aurita*: 0.501, s., 52, 1.654, 0.575, *O. regia*: 0.857, n.s., 78, 1.720, 0.798, *O. rhombus*: 0.739, n.s., 91, 1.608, 0.794, *O. sinensis*: 0.872, n.s., 83, 1.612, 0.872) did not yield a statistically significant optimal niche volume. Only *O. aurita* was characterized as a specialist by ONE. The other species were more general as reflected by their diverse timing during the year and the small cell counts in some years. Hoppenrath et al. (2009) mentioned that all the species were found throughout the year at Helgoland. Godhe et al. (2015) analysed the phytoplankton community in the southeast Arabian Sea for 20 years and identified *Odontella* ssp. as an important member. They showed that this genus's abundance was positively correlated with temperature and the Secchi depth. The computation of differently composed datasets had a strong influence on the classification of these species; only *O. regia* was classified in the same way in all approaches. This species was widely distributed in temperate areas (Kraberg et al., 2010) and forms blooms in the Indian River Lagoon, USA (Badylak and Philips, 2004).

O. aurita had the smallest niche sizes for the computations with the long datasets. The niche sizes increased when adding biotic time series to the short and long time series. *O. aurita*, which was a common neritic or littoral species in temperate seas, could become abundant in late winter and early spring (Kraberg et al., 2010). Obrezkova et al. (2015) identified this species dominating in surface sediments in Eastern Russia. *O. aurita* was abundant all year round only in the first years of the HRD (afterwards only winter until spring). Therefore, the sizes of the optimal niche were different for the computation of the long and the short datasets. The substantial decrease in the niche sizes through the addition of the biotic time series reflected that this species

could tolerate a wider range of the abiotic than of the biotic factors. Hence, this species was prone to competition and grazing. Schlüter et al. (2012) analysed this species in combination with *Guinardia delicatula* and *Thalassionema nitzschioides* showing that the start of the growth period was influenced by Secchi depth and total phytoplankton biomass. The end of the growth period was influenced by sunshine duration and the abundance of *Temora longicornis*. Taken these results together with the results of ONE, it was observed that this species is strongly influence by the biotic factors.

O. rhombus was obligate littoral and widely distributed (Kraberg et al., 2010). It was a dominant member in the Bay of Bengal, India (Choudhury and Pal, 2009). The analysis showed a comparable pattern than for *O. aurita*, because this species was not abundant in the middle segment of the HRD. This species was also strongly influenced by the biotic milieu. *O. sinensis* invaded the Atlantic in the beginning of the 20th century and is now considered to be a cosmopolitan species. It could be found throughout the year and could form blooms in summer (Kraberg et al., 2010; Ostensfeld, 1909). Badylak and Phlips (2004) found this species in the Gopalpur Creek, India. Gómez and Souissi (2010), who identified this species regularly in the English Channel from 1997 until 2005, argued that this species did not invade in the beginning of the 20th century. They concluded that the conditions before 1903 were unfavourable for this species and that it was therefore not abundant with high cell counts. The few cells that might have been sampled may have been accidentally identified as *Odontella regia*. The results for the differently composed datasets for *O. sinensis* were comparable for all approaches except for the approach without the biological time series for the long period. This species was less present in the middle segment and more often present in the first and in the last third of the HRD. Therefore, the shortening of the time series excludes the first period when *O. sinensis* was regularly present. The differences in both computations with the long time series showed that the niche of this species was smaller without the biotic time series. Therefore, *O. sinensis* was more specialized regarding the abiotic than the biotic data in the first third of the time series. The niche size remained constant for all other computations.

Paralia sulcata The diatom *Paralia sulcata* (0.942, n.s., 93, 1.693, 1.010) changed its presence period during the course of the time series (Gebühr et al., 2009). It was additionally present in the summer months in the later years of the sampling. Kraberg et al. (2010) explained this species as a cosmopolitan littoral species that can appear in the plankton, mainly during late winter and early spring. *P. sulcata* occurred throughout the year at Helgoland and Sylt (Hoppenrath et al., 2009). Guilloux et al. (2013) found *P. sulcata* as a dominant member of the phytoplankton community in the English Channel from 2000 until 2010. Obrezkova et al. (2015) identified *P. sulcata* as a dominant species in surface sediments in Eastern Russia, and Roelofs (1984) identified this species as a dominant member of sediments in British Columbia, USA. Other regions where this species was found are the Bay of Bengal, Eastern India, where *P. sulcata* was identified as a species of the transition period from winter to summer (Choudhury and Pal, 2009) and in the Bahía Blanca Estuary, Argentina, where *P. sulcata* was found throughout the year in a time series from 1978 until 1991 with low abundances (Gayoso, 1999; Guinder et al., 2013). Hobson and McQuoid (1997) and McQuoid and Nordberg (2003) showed that *P. sulcata* was found across the world and that the environmental conditions could vary strongly in waters where this species was found. Therefore, they concluded that this species is an ecological generalist. They analysed *P. sulcata* in Swedish sediments and used the number and the size of the frustules as an environmental indicator. The usage of *P. sulcata* as an indicator species was done more often in the literature (e.g. Abrantes, 1988; Liu et al., 2013; McQuoid, 2000). Gao et al. (2013) analysed the phytoplankton community in the Southern Yellow Sea, China, where *P. sulcata* was a dominant species of the winter. They showed that *P. sulcata* had the second-broadest niche of all dominant species found during four cruises in 2011. Zong (1997) showed with the help of core analyses that *P. sulcata* had its lower end for optimal growth at a salinity of 10 ‰.

Consistent with the literature, the results of the analysis presented here identify a large optimal niche for *Paralia sulcata*. In this thesis, it was probably because of this change in timing shown in detail by Gebühr et al. (2009). Since

the optimal niche is comparable to an envelope of yearly niche values, it cannot detect changes over time like a yearly niche estimator. However, *P. sulcata* was found at the upper end of the volume spectrum. This was the result of varying conditions due to the change in timing, because this species was abundant in the winter months until 1998 and abundant throughout the year after this year (see Figure A.9). This change led to a wide range of environmental conditions the species had to cope with in the latter years. The sizes of the optimal niche for *P. sulcata* showed a pattern comparable to *Phaeocystis* ssp. and *Protoperidinium depressum* when the environmental factors were changed. The niches were small for the approaches where only abiotic time series were considered, representing that this species was adapted to a small range of these factors. Including the biotic time series resulted in larger niches, showing that *P. sulcata* tolerated a wider range of the biotic factors, but the aforementioned change in the timing of *P. sulcata* made it hard to interpret this pattern. One can argue that the influence of the biotic factors on the niche size was more relevant than the change in timing. This is because on the one hand the change in timing happened in the last few years and on the other hand very small niches were detected when omitting the biotic milieu. Hence, this species faced more or less stable abiotic conditions in the majority of the years through a concentration of the times of fastest growth in the winter months. However, it was able to show high fitness despite a changing and diverse biotic milieu and was able to outcompete other species during this time of the year. A comparable pattern was also shown by Hobson and McQuoid (1997) for the Strait of Georgia, Canada, where *P. sulcata* was able to outcompete other species during the winter months.

Porosira glacialis Although the diatom *Porosira glacialis* (0.200, s., 16, 1.462, 0.463) was found to be a specialist with a small ONE ellipsoid, it was not found often in the Helgoland Roads time series. Hence, this species seemed to be restricted to special conditions. Hoppenrath et al. (2009) explained that this species was abundant at Helgoland from November to August and at Sylt from October to July. Kraberg et al. (2010) stated that this species was abundant in cold to temperate regions and that it was mainly found in winter and spring in

the North Sea. *P. glacialis* was identified as a dominant species in a bloom in the Bellingshausen Sea (Waldron et al., 1995) and in the Weddell Sea (Olguín and Alder, 2011), West Antarctica. In spring 1992 in a transect from the coast to the open ocean in the eastern North Sea, *P. glacialis* was the only species found with high frequencies at the coastal and the oceanic sampling points (Škaloud et al., 2006). In comparison with other species, growth experiments at different temperatures showed nearly no effect on this species (Huseby et al., 2013). *P. glacialis* showed the same growth rates at 0.5 °C and 8.5 °C, indicating an adaptation to cold temperatures. However, the low number of inflection points identified for this species made an interpretation impossible, but showed that this species needed special conditions and was often not able to grow under the conditions found at Helgoland. One can speculate that it was often too warm at Helgoland for this ‘glacial’ species. This species did not show pronounced changes in the niche size when the time series for the computation were composed differently. The niche sizes remained small for all approaches. It was slightly larger only for the approach with the competitive milieu on the long time period.

Skeletonema costatum The species *Skeletonema costatum* (0.777, n.s., 70, 1.903, 0.704) showed an intermediate niche volume and could not be classified as a specialist or generalist. It was found throughout the year except in spring or early summer. It had its highest abundances at Helgoland in October, November, and February and was found at Sylt throughout the year with lowest abundances in late summer and early autumn (Hoppenrath et al., 2009). According to Kraberg et al. (2010), this species could be found at Helgoland throughout the year and it formed blooms in autumn. This species was, for example, additionally abundant in the Sechart Inlet, Canada (Haigh et al., 1992). It was abundant in the lower East River, USA (Samuels et al., 1983). *S. costatum* formed blooms in the Ría de Vigo, Spain (Álvarez-Salgado et al., 2005) and in the Jiaozhou Bay, China (Huo et al., 2001), and was a dominant member of the autumn / winter phytoplankton community in a fjord in southern Chile (Alves-de Souza et al., 2008).

Comparing the abundance pattern with the analysis of the variability of the

environmental conditions (see Subsection 7.2.4) revealed that if a species was present nearly all the time, it did not automatically lead to a large niche. The environmental conditions showed their highest variability (see Figure 7.3) in spring and early summer, and consequently not being present at this time led to the intermediate size of the niche. The timing of the fastest growth was of course not the only factor that influenced the optimal niche, but the seasonality of the environmental conditions undoubtedly had an important role. Additionally, the timing was strongly correlated with the environmental factors (see Section 3.2) and can therefore act as an indicator, because a change in timing was for the species often connected with a change in the environmental conditions, i.e. higher temperature and longer sunshine duration when the timing was shifted to the summer, and higher wind speed and stronger turbidity when the timing was shifted to the winter.

Skeletonema costatum was not present during the periods with low nutrient concentrations in the Helgoland Roads data. Davies and Sleep (1989), Haigh et al. (1992) and Sakshaug and Andresen (1986) showed that this species needs high phosphorous concentrations or is phosphate-limited. Yoder (1979) discovered that silicate is a nutrient that limits the growth of *S. costatum*, and Alves-de Souza et al. (2008) found that the abundance of this species is associated with high silicate. Depletion of both of these nutrients led to the death of *S. costatum* in the Jiaozhou Bay, China, and the decline of the bloom (Huo et al., 2001). This might have been the reason why the species was not abundant in the Helgoland Roads data in late spring and early summer when these nutrients were depleted. Temperature elevation also led to a decline in the abundance of *S. costatum*, but the investigated temperatures were with 16°C to 35°C comparably high to the water temperature at Helgoland (Hyun et al., 2014; Sánchez et al., 1995). Although not especially relevant for the Helgoland Roads data, salinity did not have a strong influence on this species (Mallin, 1994). It could even live under rapid salinity fluctuations (Rijstenbil et al., 1989). Additionally, *Prorocentrum micans* was able to graze on *S. costatum* and reduce its abundance considerably (Du Yoo et al., 2009). While *P. micans* has high abundances in summer at Helgoland, it might be that grazing during

this time on *S. costatum* has an additional effect on the reduction of the cell counts.

This species showed no pronounced change in the niche size when the time series for the computation are composed differently. The niche size for *S. costatum* stayed in the same range.

Thalassionema nitzschioides The diatom *Thalassionema nitzschioides* (1.038, n.s., 70, 1.880, 0.748) was found in the upper range of the niche volumes and was therefore classified as a generalist. It was especially found in the colder months and in spring. Kraberg et al. (2010) described *T. nitzschioides* as a cosmopolitan species found throughout the year at Helgoland and Sylt, its highest abundances being in spring. According to Hoppenrath et al. (2009), it had its highest abundances in winter. *T. nitzschioides* was, for example, additionally abundant at Paraná State, Brazil (Fernandes and Brandini, 2004), in Gopalpur Creek, India (Baliarsingh et al., 2013), and at the Kerguelen Islands, Southern Ocean (Kopczyńska et al., 1998). It was a dominant species in a western Galician ria, Spain (Prego et al., 2007), in the Caspian Sea, Iran (Bagheri et al., 2014), in the South China Sea (Liu and Sun, 2015; Wu et al., 2013), and was forming blooms in the Indian River Lagoon, USA (Badylak and Philips, 2004).

The analysis showed that *T. nitzschioides* was able to grow in diverse conditions, and as shown in the literature, this species was able to grow at coastal and oceanic salinity values (Sahu et al., 2012). Rising temperatures had a positive effect on the growth rate of this species (Lassen et al., 2010), and it was not found in polar waters (Kraberg et al., 2010). This should have reflected an adaptation to warmer temperatures, but this species was not found during the warmest period in the Helgoland Roads data. The warmest period in the HRD was the time when the nutrients were depleted and thus *T. nitzschioides* was not able to be abundant with high cell counts. In agreement with this, Schlüter et al. (2012) showed that the end of the bloom was mainly correlated with nutrient concentrations. They showed that the start and the end of the growth period of *T. nitzschioides* could be connected with some environmental conditions, but temperature only played a minor role.

Thalassiosira rotula The algal species *Thalassiosira rotula* (0.608, n.s., 32, 1.911, 0.708) was found in cold-temperate to warm waters and was observed at Helgoland and Sylt throughout the year with highest abundances in March / April and October (Hoppenrath et al., 2007, 2009). *T. rotula* was considered a cosmopolitan species, frequently found during spring and summer (Kraberg et al., 2010). This species was additionally common during spring in Loch Creran, Scotland (Harris et al., 1995) and in the Loire River plume, France (Lunven et al., 2005). It was found in the Saanich Inlet, Canada (Hobson and McQuoid, 2001), in the Sundarban mangrove forests, Bangladesh (Aziz and Rahman, 2011), and in Australian waters (Hallegraeff, 1984). *T. rotula* was a winter species of the north-eastern Adriatic Sea, Croatia (Godrijan et al., 2013). It was found from May until October in the southern hemisphere in San Matías Gulf, Argentina (Sar et al., 2002).

In the analysis, *T. rotula* showed an irregular timing, which was also found by Widdicombe et al. (2010) for the western English Channel. Krawiec (1982) described *T. rotula* as eurythermal and moderate euryhaline, while Schöne (1972, 1974) showed this experimentally for *T. rotula* from the North Sea. It grew from 4°C to 22°C and from 12‰ to 38‰ salinity. Cloern and Dufford (2005) detected *T. nodulolineata* in the San Francisco Bay over a broad salinity range. Additionally, a broad salinity range can be concluded from the aforementioned distribution of this species. It was not only found in typical marine environments, but also in estuaries, mangroves, and river plumes, all waters with more or less brackish water. When analysing the growth rate of different strains at different temperatures (4, 10, 17.5, 25, and 30°C), it was shown that *T. rotula* grew best at 17.5°C and did not grow at 30°C (Boyd et al., 2013). Single strains reacted differently to the temperatures, but the pattern was comparable. *T. rotula* was only found at the beginning and end of the sampling period of the HRD, but then it was found from spring until the end of autumn. Therefore, along with the aforementioned findings and the relatively large niche, a tendency towards a generalist was seen.

If the dataset for the computation of the PCA was composed differently, the sizes of the optimal niches varied. The smallest niche was found for the ap-

proach with the competitive milieu for the long period, whereas the largest niche was found for the approach without a biological time series for the short time period. This reflected that *T. rotula* was only found in the first and in the last third of the HRD, and that the first abundance cluster was omitted when computing the short period.

Dinoflagellates

Ceratium furca, *C. fusus*, *C. horridum*, *C. lineatum*, *C. tripos* The *Ceratium* spp. (*C. furca*: 0.264, s., 44, 1.356, 0.497, *C. fusus*: 0.358, s., 42, 1.260, 0.714, *C. horridum*: 0.545, s., 68, 1.834, 0.593, *C. lineatum*: 0.564, s., 51, 1.390, 0.721, *C. tripos*: 0.406, s., 44, 1.390, 0.577) are mixotrophic dinoflagellates. All showed a narrow niche and were thus regarded as clear specialists. According to Kraberg et al. (2010), *C. furca*, *C. furca*, and *C. horridum* were found to be cosmopolitan species while *C. lineatum* and *C. horridum* were widely distributed. Based on Hoppenrath et al. (2009), all of these species were widely distributed except *C. lineatum*, which was found to be a northerly species. For example, Figueiras and Pazos (1991) found *C. fusus* and *C. horridum* in three Rías Baixas, Spain, Godrijan et al. (2013) found *C. furca*, *C. fusus*, and *C. tripos* in the Adriatic Sea, Croatia, Baek et al. (2009) found *C. furca* and *C. fusus* in Sagami Bay, Japan, and Gayoso (2001) found *C. horridum*, *C. fusus*, and *C. tripos* in the Golfo Nuevo, Argentina. Hinder et al. (2012) found four and Yallop (2001) found all five species in the northeast Atlantic Ocean.

C. fusus tolerated a wide range of salinity but grew best under the typical coastal values of 24–30 PSU (Baek et al., 2007). It was mainly found in the summer period (Bresnan et al., 2009; Löder et al., 2011; Resende et al., 2007) when spring blooms were over and nutrient stocks were reduced. The dinoflagellates were the dominating phytoplankton group at this time of the year, because their growth was not dependent on the depleted silicate. In line with these findings, Baek et al. (2007) showed that *C. fusus* growth is negatively correlated with nitrate / nitrite and phosphate. Similarly, Godrijan et al. (2013) showed that the abundance of *C. furca*, *C. fusus*, and *C. tripos* was negatively correlated with nitrate / nitrite, silicate, and phosphate (although phosphate

was not statistically significant). This indicated that these species were abundant when these nutrients were reduced. The *Ceratium* species were also dominant in summer due to the required elevated temperatures (Baek et al., 2007, 2009), which are only reached in summer at Helgoland (Dodge and Marshall, 1994). Baek et al. (2008) concluded from their experiments that *C. furca* and *C. fusus* preferred high temperatures and long photoperiods which were only faced in summer. Godrijan et al. (2013) showed that the abundances of *C. furca*, *C. fusus*, and *C. tripos* were positively correlated with temperature. The number and timing of the inflection points found for these species supported the finding that they were adapted to the summer conditions after the diatom spring bloom. These species were adapted to higher temperatures and were able to outcompete other species in summer.

The size of the semi-axes did not show any abnormalities, indicating a comparable spatial shape for the ONE ellipsoids for each of these species. The computation of the different approaches (Chapter 6) did not affect this group of species. Only the computations for *C. lineatum* exhibited small variations, but these variations had no influence on the ecological classification of this species (see Figure 6.23). These species were abundant annually and were not influenced through the in- or exclusion of biotic time series, implying that these species depended more on the abiotic than on the biotic factors, i.e. competition and grazing did not directly influence the building of blooms and the connected inflection points significantly. The aforementioned dependence on elevated temperatures and the fact that they bloom after silicate was depleted by the diatoms supported these findings.

Noctiluca scintillans The dinoflagellate *Noctiluca scintillans* (0.657, n.s., 50, 1.538, 0.900) is heterotrophic. It had an intermediate volume of the optimal niche, but the result was statistically not significant. This meant that a comparable niche size could be found by chance. Therefore, it was not possible to classify this species, neither as a specialist nor as a generalist. *N. scintillans* was widely distributed and formed dense blooms in the German Bight. It could be found throughout the whole year, but had its highest abundances in summer (Hoppenrath et al., 2009; Kraberg et al., 2010). *N. scintillans* bloomed

in Rio Grande do Sul, Brazil (Cardoso, 2012), in the Adriatic Sea (Fonda Umani et al., 2004), in the coastal waters of Oman (Al-Azri et al., 2015), in the Port Blair Bay, Andamans, India (Eashwar et al., 2001), and in Sagami Bay, Japan (Miyaguchi et al., 2006). It was also found in Gopalpur Creek, India (Baliarsingh et al., 2013) and at New South Wales, Australia (Dela-Cruz et al., 2007).

N. scintillans is eurythermal with an optimum at 20–22°C (Huang and Qi, 1997; Lee and Hirayama, 1992; Tada et al., 2004), which might have been one reason why this species had its highest abundances in summer (Löder et al., 2011). This species has different feeding modes (Kiørboe and Titelman, 1998; Shanks and Waters, 1996) and a diverse diet (Fonda Umani et al., 2004; Kiørboe and Titelman, 1998; Prasad, 1958) reflected by the non-significant classification, because it was able to react to different conditions (Zhang et al., 2015). One could have argued that this species should have been classified as a generalist, but competition for nutrients with other species and grazing pressure might prevent this species to find its optimal growth conditions throughout the whole year (Fock and Greve, 2002). This species had to be seen as atypical for the selection of the species in this analysis, because it was, together with *Protoperidinium depressum*, the only heterotrophic species analysed here. The composition of the dataset for the PCA made hardly any difference. On the one hand, the inclusion of the biotic time series should have had an influence, because this predator obviously depended on its prey. On the other hand, it could have been that this species was not preying exclusively on other species but was feeding on other particles like detritus (Tada et al., 2004), copepod eggs (Quevedo et al., 1999), faecal pellets (Kiørboe, 2003), or similar.

Prorocentrum micans The dinoflagellate *Prorocentrum micans* (0.294, s., 41, 1.337, 0.508) had a small optimal niche and was therefore classified as a specialist. *P. micans* was found to be a cosmopolitan species abundant at Helgoland throughout the year with the highest cell counts from July to November and it was able to form blooms (Hoppenrath et al., 2009; Kraberg et al., 2010). Resende et al. (2007) found this species in the Iberian Coastal zone, Portugal,

Godrijan et al. (2013) in the Adriatic Sea, Croatia, and Munir et al. (2013) at Karachi, Pakistan. Alkawri and Ramaiah (2010) identified this species in the waters at the west coast of India. It formed blooms in the Indian River Lagoon, USA (Badylak and Philips, 2004).

P. micans showed the same characteristics as *Ceratium* spp., with its bloom events concentrated around July and August when the spring blooms were over (Löder et al., 2011; Resende et al., 2007; Widdicombe et al., 2010). Hence, the aforementioned interpretation of the results for *Ceratium* spp. could be transferred to *P. micans*. Besides, the variation of the biotic factors had also no influence on this species. *P. micans* also preferred warm waters (Munir et al., 2013; Resende et al., 2007; Sahu et al., 2012). Surprisingly, the competition with *Ceratium* spp. and other dinoflagellates had no influence, although *P. micans* formed blooms simultaneously with some of them. These species could obviously have taken advantage of different food sources and coexisted during their growth period. It was shown that *P. micans* grazed on *S. costatum* (Du Yoo et al., 2009, see page 123 f. of this thesis) and on other species (Jeong et al., 2010). Sahu et al. (2012) showed that *P. micans* and *Ceratium furca* occurred together and that they were typical members of the warm water phytoplankton in Indian waters.

Protoperidinium depressum The heterotrophic dinoflagellate *Protoperidinium depressum* (0.876, n.s., 44, 2.060, 0.684) was classified in a way comparable to *N. scintillans*, but *P. depressum* was not very abundant in the Helgoland Roads data. *P. depressum* was found worldwide and throughout the year in the German Bight with highest abundances from May to October (Hoppenrath et al., 2009). It was found in coastal and oceanic waters and from the Arctic to Antarctic regions (Kraberg et al., 2010). For instance, this species was found at Port Aransas, USA (Buskey et al., 1992), in south-western Ireland (Gribble et al., 2007), in the inner Oslofjord, Norway (Kjaeret et al., 2000), and at the North Arabian Sea shelf, Pakistan (Gul and Nawaz, 2014). Moreover, Hinder et al. (2012) found species of the genus *Prorocentrum* spp. in the Atlantic.

In the years when this species was abundant at Helgoland, it was found from summer until winter with low individual numbers. This possibly implied that

this species was able to adapt to different types of food available, i.e. other phytoplankton species (Menden-Deuer et al., 2005), faecal pellets (Poulsen et al., 2011), or similar. It seemed to have high abundances when there was enough prey or food available (Kjaeret et al., 2000). Therefore, one could not identify special conditions for this species, because it tolerated a wide range of the environmental conditions.

The exclusion of all biotic time series had a strong influence on the classification of this species, reducing the size of the optimal niche significantly. This indicated that *P. depressum* was restricted to a small range of abiotic factors. If the competitive milieu was included and represented in the principal components, the optimal niche was larger. This showed that *P. depressum* was able to tolerate or actually preferred a wide range of these time series, i.e. it was not prey selective. This pattern fitted perfectly to a predator that grazed on other phytoplankton species. Including the zooplankton time series additionally reduced the niche to an intermediate size. This might have been caused by a high grazing pressure on this species. This could have been the reason why this species was only abundant in some years—only in years when it was able to outgrow this loss through predation.

***Scrippsiella* ssp.** The dinoflagellates of the genus *Scrippsiella* ssp.(0.311, s., 26, 1.977, 0.512) showed patterns like the *Ceratium* spp., but were not detected throughout the entire investigation period. Kraberg et al. (2010) mentioned that *Scrippsiella trochoidea* was probably misidentified many times. It is most likely cosmopolitan, but not very abundant in the Southern North Sea. Hoppenrath et al. (2009) also mentioned the problem of misidentification and that *S. trochoidea* was found throughout the whole year at Helgoland with no clear seasonality. *S. trochoidea* was the species of the genus that was mostly mentioned in the literature. Therefore, it was hard to give an overview of the global distribution of the whole genus. However, through the aforementioned misidentification, the following examples for *S. trochoidea* have to be taken with care. *S. trochoidea* and *S. hangoei* were identified in the Baltic Sea (Godhe et al., 2001; Högländer et al., 2004). *S. trochoidea* was found in the Guanabara Bay, Brazil (Villac and Tenenbaum, 2010) and in the Adriatic

Sea, Croatia (Ninčević-Gladan et al., 2015). It was a dominant member of the phytoplankton in the Ghar El Melh Lagoon, Tunisia (Dhib et al., 2013), and formed blooms in the Daya Bay, China (Song et al., 2009).

This genus was only detected during the last 10 years of sampling, and the blooms were around July and August. The same pattern was found by Terenko and Terenko (2009) for *S. trochoidea* in the brackish Black Sea. This suggested that elevated temperature and missing competition through diatoms were more important than salinity for these species, although Terenko and Terenko (2009) analysed only one member of this genus. Some researchers correlated the abundance of *Scrippsiella* ssp. or *S. trochoidea* with environmental factors, and their results supported this hypothesis. Dhib et al. (2013) found out that the abundance of *S. trochoidea* in a north-eastern Mediterranean lagoon was associated with high temperature and salinity. Ninčević-Gladan et al. (2015) found a positive correlation of *S. trochoidea* with temperature (and ammonium) in the coastal waters of the eastern Adriatic Sea. Probably through the restriction of this genus to the environmental conditions found in summer (or to the conditions found after the diatom bloom), it had a small optimal niche and was thus classified as a specialist. Most likely due to the short detection period of this species, the computations with differently composed datasets were almost identical.

Torodinium robustum The mixotrophic species *Torodinium robustum* (0.517, s., 51, 0.769, 0.743) was classified as a specialist. It was found sporadically with no clear seasonality in the Pacific Ocean, Atlantic Ocean, Baltic Sea, and in temperate waters of the Mediterranean Sea (Hoppenrath et al., 2009). It was also found mainly during winter and spring in the Gulf of California, Mexico (Gárate-Lizárraga and Muciño-Márquez, 2013) and from spring to autumn at the Catalan coast, Spain (Reñé et al., 2015). *Torodinium* ssp. was a dominant member of the dinoflagellates in summer in the Bizerte Lagoon, Tunisia (Sakka Hlaili et al., 2008).

It was concluded from the analysis in this thesis that this species seemed to be well adapted to the habitat around Helgoland. Owing to similar lengths of the semi-axes, one was able to identify an almost spherical shape of the ONE el-

lipsoïd for this species, caused by a similar spread of the inflection points in all three dimensions. This was a special characteristic that showed that the times of fastest growth of *T. robustum* depended more on the subordinated linear combinations of the environmental factors than the times of fastest growth of the other species. This species was only found in the last years of sampling, but then it was abundant throughout the year, which might have been the reason for the aforementioned spherical shape. Being abundant throughout the year and having a small niche seemed to be counterintuitive, but it had to have its periods of fastest growth every year at comparable environmental conditions. Overall, this species was able to tolerate a wider range of environmental factors to establish a population with small cell counts, but it needed special conditions to establish a peak when the period of fastest growth was detected. Additionally, the inclusion or exclusion of the biotic time series from computation had only a weak influence on the classification of this species. Therefore, this species was not strongly influenced by competition and grazing.

Haptophyte

***Phaeocystis* ssp.** The haptophyte *Phaeocystis* ssp. (0.790, n.s., 54, 1.609, 0.990) formed blooms, often after the spring diatom bloom and occasionally in autumn (Jordan and Chamberlain, 1997; Loebel et al., 2009). Peperzak et al. (1998) supported these results for the Dutch coastal zone of the North Sea. After Kraberg et al. (2010), two *Phaeocystis* species could have been found in the North Sea: *P. globosa* and *P. pouchetii*. *P. globosa* was found in temperate and tropical waters of both hemispheres. It was abundant at Helgoland from late winter until summer with the highest abundances in late spring or early summer. *P. pouchetii* occurred in cold waters of the northern hemisphere and was abundant in the North Sea in winter and spring (Kraberg et al., 2010). Species of this genus were found mainly in cold to temperate regions, for example, *Phaeocystis antarctica* was a dominant species in the Ross Sea, Antarctica (Arrigo et al., 1999), *Phaeocystis* ssp. was a dominant member of the summer phytoplankton community in the Fram Strait, Arctic Ocean / Atlantic Ocean (Nöthig et al., 2015). It was dominating the phytoplankton in April and May in

the Gulf of Alaska and the Bering Sea, USA (Stauffer et al., 2014), but *Phaeocystis globosa* bloomed in September at the coast of Viet Nam (Hai et al., 2010).

The optimal niche was large when compared to the other species. Therefore, *Phaeocystis* ssp. had to be seen as more generalistic, but omitting the biotic data led to a very small optimal niche. Since *Phaeocystis* ssp. was establishing blooms regularly after the diatom bloom, this pattern could be explained, because blooming regularly after the diatoms indicated stable abiotic environmental conditions. Breton et al. (2006) identified the diatom-*Phaeocystis* succession at the Belgian Coastal Zone every year from 1988 until 2001, although with changing duration and cell counts of the single blooms. Adding the biotic time series again enlarged the niche, implying that *Phaeocystis* ssp. faced a wide range of biotic factors at its inflection points. This wide range was a combination of zooplankton and dinoflagellate abundance and the collapsing diatom bloom.

One reason for the decline of the *Phaeocystis* ssp. bloom might have been a viral infection. For species of this genus, it was repeatedly shown that an infection could reduce the cell counts considerably (e.g. Baudoux et al., 2006; Brussaard, 2004; Haaber and Middelboe, 2009), but *Phaeocystis* ssp. is known for forming colonies (Wang et al., 2010) which might prevent the single species from infection with viruses (Hamm, 2000).

7.2. Analysing an increased number of species to test some general ecological hypotheses

7.2.1. How these species were analysed

The above discussion of the results for 23 selected species led to the formulation of some hypotheses concerning the phytoplankton ecology at Helgoland. To test these hypotheses, a similar analysis with an increased number of species from the Helgoland Roads data was carried out. The 167 species extracted from the original time series were checked. Some of these species could not be used for this analysis,

because the aim was an analysis with all included biotic data. The excluded species were found in a short time period in the Helgoland Roads data or showed too few inflection points. The condition of inclusion used here was that the analysis on the short time frame (1974 until 2008) would be possible with more than 4 inflection points. This was the case for 115 of these 167 species, and the analyses of these 115 species were used for testing three general hypotheses. A complete list of these 115 species can be found in the appendix (see Section A.2). The volume of the ONE ellipsoid for each of the species was computed and used for the subsequent testing of these hypotheses. The competitive milieu, previously established as the sum of 23 species, was adjusted to the new dataset. Consequently, in this section it is composed of the sum of these 115 species, with all other environmental factors remaining the same.

7.2.2. Hypothesis 1: *Species with a small ONE are specialists and thus have a lower number of presence days per year than those with a big ONE*

In ecological terms, a small ecological niche implies that a species is restricted to special environmental conditions and a species with a large ecological niche is not restricted in that way. Hence, the terms ‘specialist’ and ‘generalist’ are used to describe these two types of species (Futuyma and Moreno, 1988). As mentioned before, the concept of the optimal niche followed the same interpretation, albeit with a fitness-based background. If a species was found often in the dataset, the chance of having the inflection points distributed over a huge range of environmental conditions was most likely higher than for a species that was infrequently found. As Ignatiades (1994) concluded from an analysis of the niche breadth of phytoplankton species in the Mediterranean Sea: ”Species with broad breadth were fewer (14% of all species) in number, had low abundance (equivalent to that of the narrow-breadth species) and a low rate of succession, being recorded in nearly all samples (baseline population).” Ignatiades (1994, p. 93). In another work analysing the ecology of rare phytoplankton species from Ignatiades and Gotsis-Skretas (2014), they concluded that the abundance and niche breadth are linked. Besides, Hernández Fariñas et al.

(2015) showed that marginal taxa are more often specialists. Therefore, it was hypothesized that the size of the optimal niche was positively correlated with the number of presence days per year.

Figure 7.1 shows the volume of the ONE ellipsoid versus the mean number of presence days per year, i.e. the days with non-zero abundance. The regression line exhibited a very small trend, but this trend was not statistically significant (p-value = 0.445). It also showed that the presence during the year had no influence on the size of the optimal niche for the species. Therefore, a linear correlation between the annual presence and the size of the optimal niche could not be inferred from the data.

There were some outliers that showed interesting patterns (Figure 7.1). There was one outlier with a large number of mean presence days and a small ONE volume. Additionally, there were some outliers with a small number of presence days and a comparably large ONE volume. These two patterns were counterintuitive and could only be reached at very special conditions. A species that was present often and showed a small optimal niche was most likely found with stable abundances throughout the year and could establish blooms only at special conditions. This was because the ONE did not consider abundance on a stable level—only the period with fastest growth was used for this estimate. The opposite case, a species with a large optimal niche and only a few presence days per year, could be reached when a species formed blooms once per year at varying conditions and was not present or below the detection limit for the rest of the year. These cases were very rare and thus only found for a very small number of species.

Therefore, the classification of the species' niches with the help of the ONE method depended on the inflection points and the corresponding environmental conditions and not on mere presence. This and the aforementioned studies (Hernández Fariñas et al., 2015; Ignatiades, 1994; Ignatiades and Gotsis-Skretas, 2014) implied that methods of niche classification based on the presence of species would result in a different classification and, as mentioned before, that the 'traditional' ecological niche and ONE are two different measures.

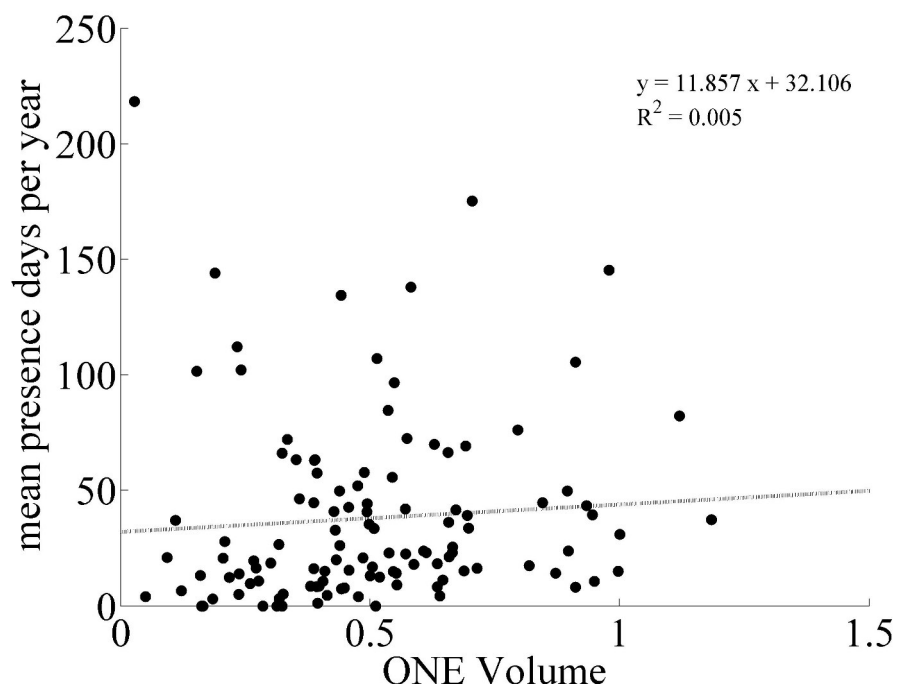


Figure 7.1.: Mean number of presence days per year for all 115 species plotted against the volume of the ONE ellipsoid; linear regression as dashed line and the corresponding formula is presented in the right upper corner of the graph

7.2.3. Hypothesis 2: *The size of the optimal niche is positively correlated with the number of inflection points*

A species that established more than one bloom over the course of the year had the inflection points at different times of the year and hence at different quantities of the environmental conditions. This argument suggested that the niche volumes should have increased with the number of inflection points found for the species. If a species was found to have typically just one inflection point per year and if this inflection point was found at (more or less) the same time, it would likely have led to similar conditions for every year. How variable these conditions were depended on the season (cf. Figure 7.3). Therefore, the optimal niche could have been large or small. But having the inflection points distributed over the whole year and facing a huge amount of different environmental conditions would necessarily have caused a larger niche.

Figure 7.2 shows the volume of the ONE ellipsoid versus the mean number of inflection points per year for every species. A correlation between these two parameters was identified, although the coefficient of determination (R^2) indicated that the regression line did not fit the data adequately. The correlation was statistically significant (p-value = 0.001).

A clear trend could be identified. The two outliers for species with an average of four inflections per year and a small niche pushed the regression line up. Without these outliers, the regression would have been steeper. These two species were only found in one year and had four inflection points in this year, which was why they exhibited this strange pattern. The other extreme values of species having a small number of inflection points per year and a large niche could happen when species established blooms at different environmental conditions in different years. These species did not bloom very often, but when they did, they did not need special conditions. This was the case for a slow-growing species that was not able to form blooms fast and frequently. As expected, the number of inflection points per year had an influence on the size of the optimal niche.

This finding reflected the aforementioned fact that a species with a larger number of inflection points tolerated a wider range of environmental conditions than a species with a small number of inflection points did. Species with more than one inflection

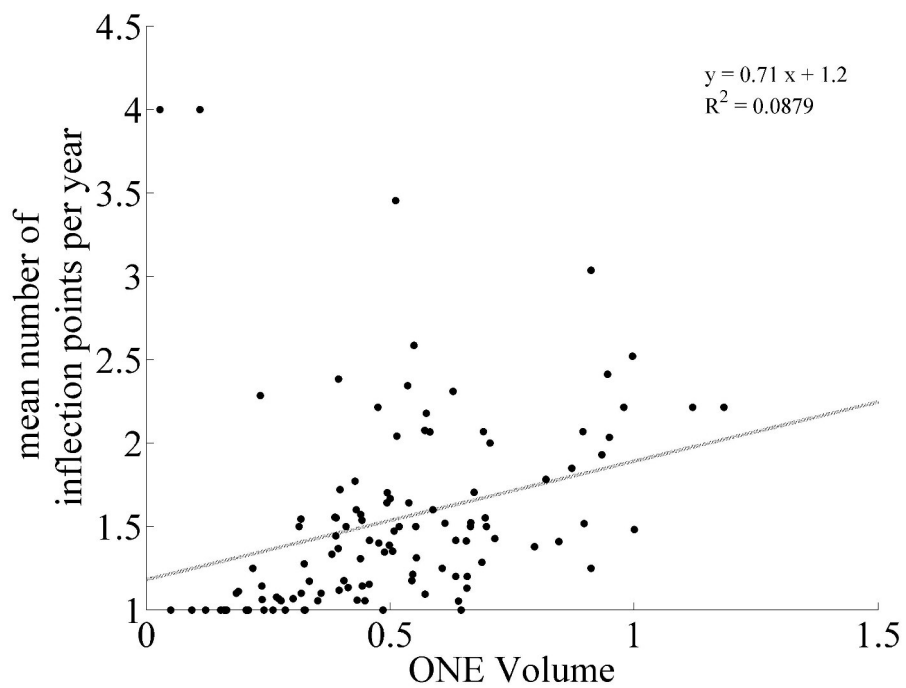


Figure 7.2.: Mean number of inflection points plotted against the volume of the ONE ellipsoid for all 115 species; linear regression as dashed line and the corresponding formula is presented in the right upper corner the graph

point per year were able to grow under different conditions and were thus more likely generalists than species with only one inflection point per year.

7.2.4. Hypothesis 3: *Species with inflection points in summer face more variable environmental conditions than species with inflection points in spring and therefore have a bigger ONE*

The variability of environmental conditions changes during the year. There are periods when the environmental conditions are less variable and periods when the environmental conditions are highly variable (compare Beaugrand, 2003; Hernandez-Farinas et al., 2013; Ionita et al., 2008). Therefore, there was reason to expect that species with inflection points in the nearly static periods would have had a smaller niche and species with their inflection points in the variable period would have had larger niches. To obtain a value for the variability of the environmental conditions, an estimation of an ellipsoid comparable to the ONE ellipsoid was carried out.

Calculating the arithmetic mean day of two groups of inflection points—one group in December and one in January—would result in a mean day in the middle of the year. This would obviously be a problem, because the true average would not be represented. The true mean day should be found at the end of December or the beginning of January. To solve this problem, the mean was calculated with the help of circular statistics (Bell, 2008). This was used to calculate the mean on a circle in the following manner:

The days of the year were mapped onto an angle via $\Phi_j = \frac{t_j}{365} \times 2\pi$ with $t_j \in \{1, \dots, 365\}$ and $j = 1, \dots, N$ where t_j was the day of the j th inflection point and N was the number of inflection points. The mean inflection point day was calculated by $Z = \frac{1}{N} \sum_{j=1}^N e^{i\Phi_j} = |Z| \times e^{i\psi}$, and the mean day of the inflection points was then $\frac{\psi}{2\pi} \times 365$.

The volume of ONE versus this mean day of the inflection points is shown in the left panel of Figure 7.3. The polynomial fit showed that it was more likely to find larger niche volumes in the middle of the year than at the beginning or at the end.

The time window for this sliding window analysis was selected to be 21 days as this was the expected duration of the spring bloom (Kiørboe et al., 1994). For every

window of 21 days (window 1: day 1–21, window 2: day 2–22, window 3: day 3–23, . . .), the 21 values were extracted from each of the first three principal components of the computation with all factors included and the volume of the corresponding ellipsoid was computed in the same manner as explained before (cf. Section 5.4). A large volume indicated that the relevant environmental conditions were variable at this time, because a large volume accounted for a large spread in the extracted values and vice versa. Doing this for every year yielded an annual statistic, and the median (50 % quantile) for every day of the year (1–365) was computed. Additionally, the 5 % and 95 % quantiles were calculated. This led to the graph in the middle panel of Figure 7.3. One can see that the variability rose from mid-March on (Day 75) until Day 120 and decreased slowly thereafter. It reached the initial level towards the end of June (Day 180). A small peak with a following dip in the curve of the median was identified from Day 100 until Day 130, which showed probably the average period of the spring bloom. The 95 % quantile showed the same pattern, but with strong fluctuations. These fluctuations resulted from a small number of years with extreme peaks (thin coloured lines in the middle panel of Figure 7.3).

The right panel in Figure 7.3 was computed in a similar manner, except that the changes in the position of the ellipsoid were computed. Again, the window was set to 21 days, and the values were extracted from the first three principal components. These changes in the position were calculated as the increments (Euclidean distances) of two consecutive ellipsoids' centres. This was done for every year and the median (50 % quantile) for every day of the year was computed. Additionally, 5 % and 95 % quantiles were calculated. This distance was a measure for the change in the position of the ellipsoid per day and, hence, a measure for the day-to-day rate of change. This rate of change showed how the ellipsoids 'jump' in the cloud of the environmental conditions and added another measure for the variability of the environmental conditions. A large day-to-day distance appeared when the conditions were variable or fast changing. When the conditions were less variable or changing slowly, the day-to-day distance became small. Therefore, one could identify the same pattern as in the middle panel of Figure 7.3 with high variability in the second quarter of the year.

To relate the ONE volume to the variability of the environment at the time where the inflection points were extracted, i.e. the mean day of the inflection points, Fig-

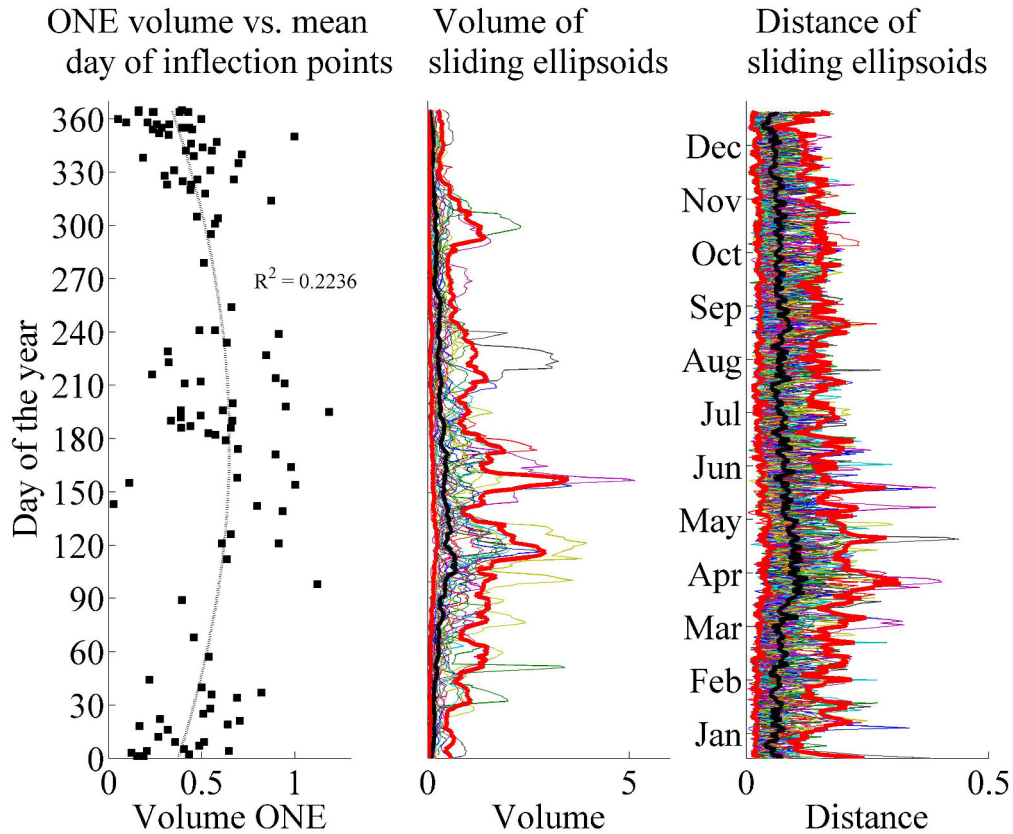


Figure 7.3.: Left panel: ONE volume for every species plotted versus the mean day where these inflection points were found - the line represents a polynomial fit of degree two; middle panel: median volume (black line) of a sliding ellipsoid (details in the text) versus the day of the year with the 5% and 95% quantiles (red lines); right panel: median distance (black line) of the sliding ellipsoid's centre from one day to the next (details in the text) versus the day of the year with the 5% and 95% quantile (red lines); in the two right-hand panels the thin coloured lines show the results for the single years which were used to calculate the quantiles

Figure 7.4 shows the seasonal variability versus the observed ONE volume. The median variability is the black line in the middle panel of Figure 7.3. The statistically significant regression line (p -value < 0.001) in this plot of variability versus the volume shows that it was more likely to have a small ONE when the inflection points were found at times where the environmental conditions fluctuate less. This is represented by the cluster in the lower left corner (Figure 7.4). It was also more likely to have a large ONE when the inflection points were found at times where the conditions showed a high seasonal variability. Corresponding values are found in the upper right corner of Figure 7.4. The lower right and the upper left corners of the graph are sparsely populated, but in the upper left corner some points can be found. For the species in this region, the ONE volume was large and the environmental conditions were fluctuating less. This could be found in the data when a species had a lot of the inflection points in stable regions, which could have led to a large ONE, because in summary the huge number of small variabilities added up to a large niche. There were also only a few points in the lower right region, because if the conditions were fluctuating strongly, it should have been nearly impossible to find species with a small niche at these times. The species found in these special regions of the plot were species which were added through the widening of the species list, except *Odontella rhombus* which was found in the upper left corner (Figure 7.4: ONE volume ≈ 1 , median variability ≈ 0.15). This species was present and had its inflection points in the colder and thus stable months. This supported the hypothesis that this species ‘collected’ the stable conditions, resulting in a large optimal niche. Again, this could be seen as an envelope around many inflections points in stable conditions.

All three panels of Figure 7.3 indicate that the hypothesis could be corroborated. The environmental conditions were more variable in the summer, and it was, therefore, more likely that the species with their inflection points in summer had a large optimal niche. Additionally, Figure 7.4 supported this outcome through the identified trend that the size of the optimal niche was positively correlated with the variability of the environmental conditions. As expected, the results showed that the seasonal aspects had a strong influence on the optimal niche. In that case, the inflection points found over the course of the year considerably affected the size of the optimal niche. Ecologically, species with their fastest growth in a month with high variability were able to tolerate this variability and were, therefore, general-

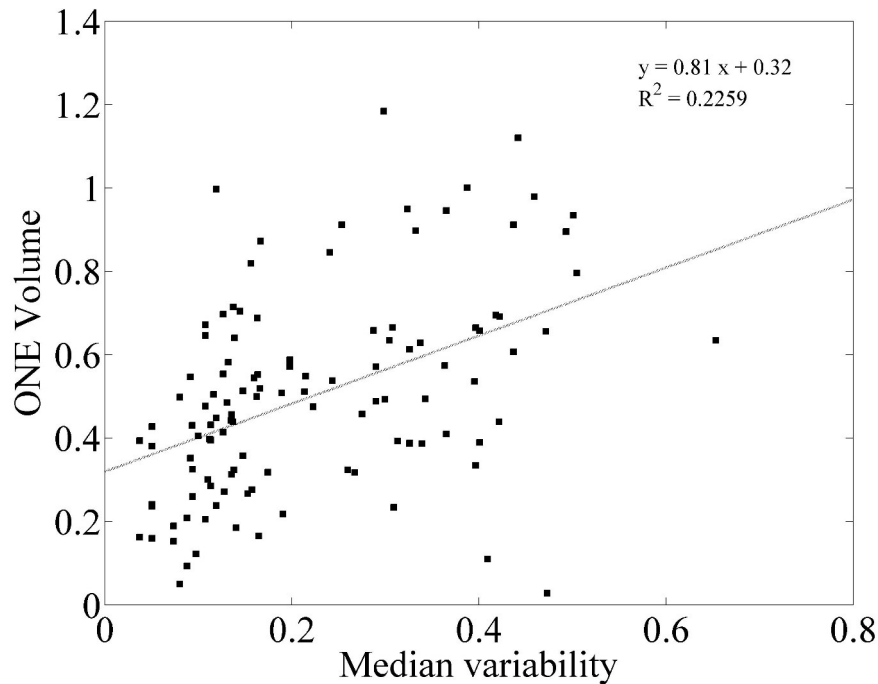


Figure 7.4.: Median variability (black line in the middle panel of Figure 7.3) versus the ONE ellipsoid volume for all 115 species, dashed line: linear regression, the corresponding formula is presented in the right upper corner of the graph

ists. Species with the inflection points in the periods with less variability and low rate of change were presumably restricted to these conditions and were more likely specialists.

Analyzing this large number of species showed that the species were differently influenced by the environment. The specialists were able to grow when the preferred conditions were available, whereas the generalists were not restricted in their needs and could, therefore, grow in a broad range of environmental conditions. Reid et al. (1990) explained blooms in the North Sea with the following statement: "The majority of blooms occur in the summer months of the year but may develop at any time in the growing season given favourable conditions. Different responses to light, temperature, stability and nutrients are likely to be the main factors governing this sequence." (Reid et al., 1990, p. 320). They identified the aforementioned needs of the species and the resulting bloom patterns as one reason for the typical succession

of the phytoplankton in the North Sea and hence around Helgoland.

Analysing the variability of the environment accordingly at the time when the inflection points were found over the course of the year for phytoplankton species revealed that there were obviously different kinds of species. These different kinds—here classified as specialists and generalists—were different not only in their physiological needs to establish blooms but also in their ability to deal with competition. The generalists, or even opportunists, could outcompete a small number of competitors and were able to react with a spontaneous fast growth. The specialists were restricted to a small range of the environmental factors and when the environment did not suit their needs, they were only sparsely abundant. If the environmental factors changed in such a way that their requirements were met, they were able to outcompete the other species and developed a bloom. This showed clearly that both these adaptations (i.e. specialists and generalists) could be advantageous.

Adding the presented analysis of the environmental variability to the aforementioned discussion of the species' classification (see Section 7.1) showed that the variability, as a measure for the range of environmental conditions a species was able to tolerate, allowed for differentiation of the species. The size of the niche, which was an integral part of the niche concept, was positively correlated with this range. This analysis of environmental variability showed once again that ONE has advantages compared to the classical concept. Only species with a very restricted presence time during the year would have been classified in a comparable manner with the classical approach. If a species was present often and produced only one bloom, it was nearly impossible to classify a specialist with the classical method, but ONE was able to identify the special conditions needed by the species to establish a bloom. Therefore, this result is informative and showed that the optimal niche was an ecologically worthwhile adaptation of the classical niche concept.

8. Niche changes against the backdrop of regime shifts in the North Sea

8.1. Changes in the context of the reported regime shifts

8.1.1. Modification of the ONE method

In this chapter, the analysis of the optimal niche will be evaluated in the context of the reported regime shifts (see Section 3.1). Parts of this chapter were published in *Marine Biology* (Freund et al., 2012). At first, a short repetition and an explanation of the modifications implemented for this analysis will be presented.

First, eight abiotic (silicate, phosphate, dissolved inorganic nitrogen, salinity, temperature, Secchi depth, sunshine duration, and wind speed) plus one biotic (interaction milieu, established as the sum of 23 community-forming species) factors of the Helgoland Roads data were treated with a principal component analysis (PCA). The exclusion of zooplankton was done because the time frame of this analysis had to be sufficiently long to assess reported regime shifts with statistical significance. If this analyses were done on the shorter time series, the first reported regime shift would have been out of reach. A subsequent restriction to the first three principal components led to a dimensional reduction. Projecting the time series onto this three-dimensional subspace created a cluster (once again, this ‘all points’ cluster is abbreviated as AP cluster). Second, for illustrative purposes, the extracted species-specific inflection points were highlighted in the AP cluster (to which they belong). This subset of points formed a second cluster, which was previously introduced as the inflection point cluster. Third, the volumes of both these clusters were computed via the estimated correlation ellipsoid. This enabled a comparison of the ‘all

points' ellipsoid and the ONE ellipsoid sizes and was aimed at quantifying what fraction of the AP cluster was populated by a species in times of high fitness. Fourth, statistical significance of the resultant fraction was tested through a resampling procedure, often called Monte Carlo technique, where the species-specific number of inflection points was picked 10 000 times randomly out of the AP cluster, and the corresponding volume fractions were computed. Lastly, the corresponding p-value was computed as the fraction of all resampled volumes smaller than the volume of the ONE ellipsoid.

To check whether the changes in the realized niche could be observed across the reported regime shifts (1978 / 79 and 1988 / 89), the times series was split. Since joint time series for all nine factors were only available for the time range from 1968 to 2008, the multivariate data was split into the segments 1968–1978 and 1979–2008 or, alternatively, into 1968–1988 and 1989–2008. For illustrative purposes, Figure 8.1 shows the inflection point cluster for *Paralia sulcata* with points marked differently for the three different periods 1968–1978, 1979–1988, and 1989–2008. Even though Figure 8.1 suggests a three-interval analysis, only a two-interval comparisons was performed.

The change in the niche volume was estimated through the ratio of the niche volumes for the different periods as $|vol_{period2}/vol_{period1}|$. In addition to niche volumes, niche positions defined as the centroids of correlation ellipsoids estimated from related inflection point clusters were also compared. A shift in the niche position was quantified through the distance between ellipsoid centres as $|pos_{period2} - pos_{period1}|$. This distance was normalized to the longest semi-axis of the corresponding inflection point ellipsoids to reach a comparable result for every species. Therefore, the shift in the niche position for small ellipsoids was normalized with a small value and vice versa. This implied that a small shift for species with small niches was as important as a big shift for a species with a large niche. The statistical significance of the obtained shifts was again tested via a resampling procedure. However, contrary to the treatment described above, the AP cluster was not used for resampling. Instead, the whole inflection point cluster was taken, its list of points was permuted, and the resultant set was split into two. The sizes of these two parts were determined by the number of inflection points found within each period. By this procedure, two volumes and one value for the niche shift (i.e. the distance) were computed with

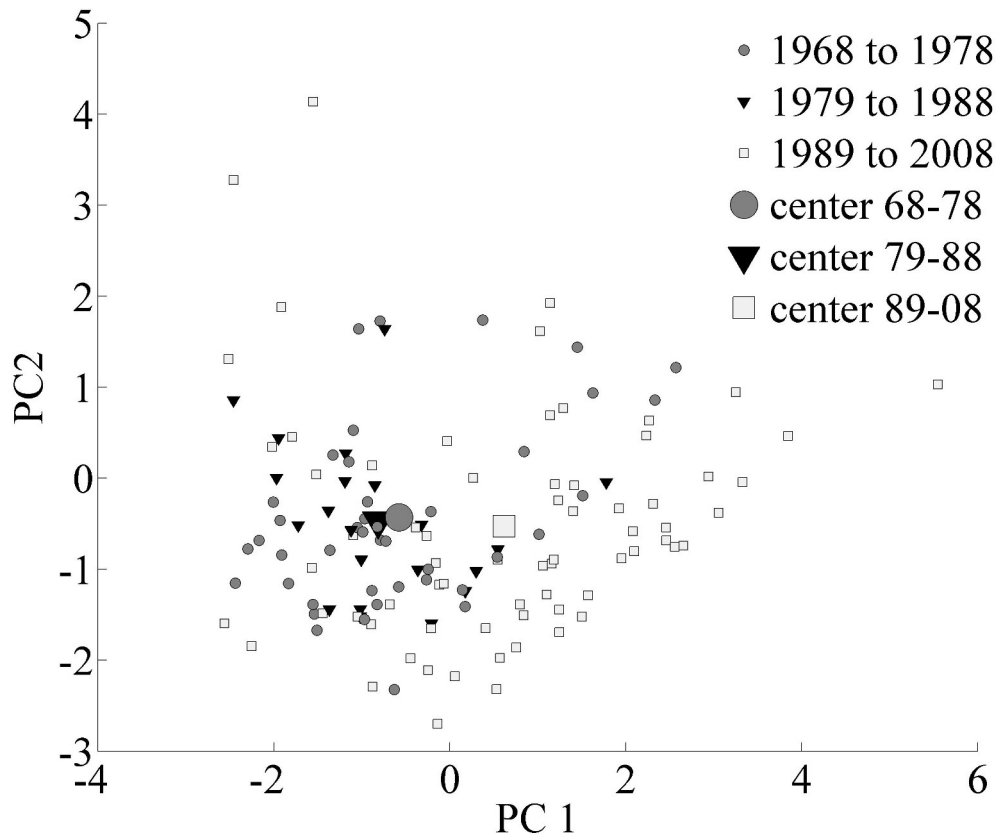


Figure 8.1.: Cluster corresponding to the results for *Paralia sulcata* with different markers for the different sections; the cluster centres for each period are marked by the same but bigger respective symbol

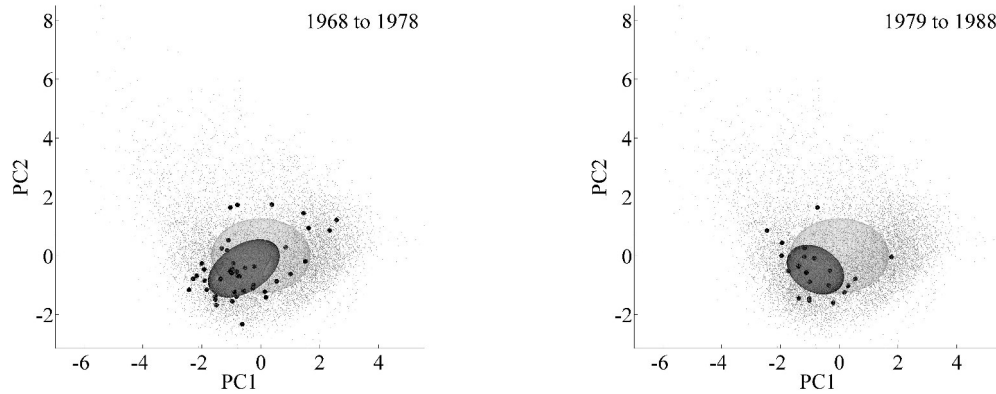
every repetition. As before, calculation of a related p-value was straightforward.

The emphasis was not so much on numbers resulting for volumes and distances as on their statistically significant changes across reported break points. This has to be kept in mind when it comes to interpreting possible changes in the ecological niche. This analysis was done with the same 23 species selected for the approaches in Chapters 5 and 6 (see page 29 f. for a list of these species).

8.1.2. Results

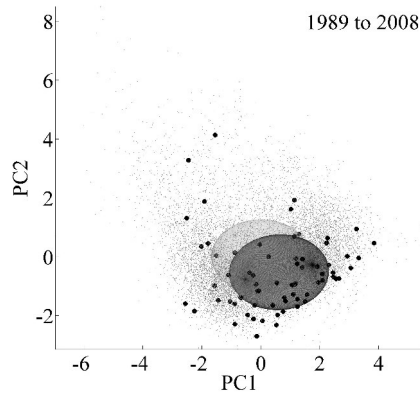
Figure 8.2 shows the changes in the realized niche, represented by the black ellipse, exemplarily for *Paralia sulcata* in three periods (1968–1978, 1979–1988, and 1989–2008). For statistical reasons, as a small number of inflection points would have led to a high estimation error, two approaches were realized with split time series at the reported years for the regime shifts. A realization of an approach with two split points, as shown in Figure 8.2, was therefore not carried out. It appeared that both position and size of the ONE ellipse changed during the course of time for *Paralia sulcata*. This visual impression was confirmed through the above-described resampling statistics and the results for all selected species are listed in Table 8.1.

The changes in the distance and volumes of the niches were identified for all periods, but a conspicuous result was found for the computation of the distance with the split point between the years 1988 and 1989. The majority of the species showed a statistically significant change in the niche position for this split point. Statistically significant changes could be identified for volume and distance for *P. sulcata* and *O. rhombus* in all different segments. Changes in the realized niche for *Ceratium furca* could not be claimed with statistical significance; only one change in niche position (with break point at 1989) was found to be statistically significant. The split point led to statistically significant niche shifts for the majority of the species, except for *G. striata*, *O. aurita*, *Phaeocystis* ssp., *P. glacialis*, and *T. nitzschoides*. The niche position of *S. costatum* shifted statistically significantly for either of both split points, while the niche volume changed statistically significantly only for the latter split point. One could identify an overarching pattern for a change in the niche at the end of the 1980s. There was no clear pattern for a change at the end of the 1970s, neither for the change in position nor for the change in the ellipsoid's volume.



(a) Calculation of the ellipsoids for the first section

(b) Calculation of the ellipsoids for the second section



(c) Calculation of the ellipsoids for the third section

Figure 8.2.: Calculation of the ellipsoids for the different sections for *P. sulcata*; grey points and ellipse: ‘all points’ clusters and correlation ellipses; black circles and ellipses: species-specific inflection points and correlation ellipse; computations were carried out in three dimensions; for better visualization, only two dimensions are shown

Table 8.1.: Distances of niche centres and ratio of niche volumes computed for the two split points (regime shift years 1979 and 1989); diatoms in light grey, dinoflagellates in dark grey and the haptophyte in white; p-values equal to or less than 0.05 are in bold font; *Scrippsiella* spp. could not be analysed, because it had too few inflection points in the first period

Species	Distances				Volumes			
	79-08/68-78	p-value	89-08/68-88	p-value	79-08/68-78	p-value	89-08/68-88	p-value
<i>Ceratium furca</i>	0.27	0.57	1.08	0.01	0.57	0.29	0.53	0.16
<i>Ceratium fusus</i>	1.17	0.07	2.26	< 0.01	0.84	0.48	1.60	0.81
<i>Ceratium horridum</i>	0.46	0.51	1.53	0.1	0.68	0.23	0.96	0.50
<i>Ceratium lineatum</i>	0.62	0.23	1.13	0.1	0.24	< 0.01	0.47	0.07
<i>Ceratium tripos</i>	0.80	0.25	1.88	< 0.01	0.71	0.31	1.67	0.90
<i>Eucampia zodiacus</i>	0.34	0.37	0.92	0.01	0.21	< 0.01	0.73	0.28
<i>Guinardia delicatula</i>	0.60	0.03	1.31	< 0.01	0.24	0.01	0.73	0.24
<i>Guinardia striata</i>	0.93	0.12	0.87	0.12	0.66	0.29	0.75	0.26
<i>Noctiluca scintillans</i>	0.61	0.21	1.33	< 0.01	0.57	0.42	2.42	0.90
<i>Odontella aurita</i>	1.28	0.05	0.86	0.16	0.85	0.46	0.81	0.30
<i>Odontella regia</i>	0.60	0.11	0.75	< 0.01	0.57	0.12	0.60	0.07
<i>Odontella rhombus</i>	1.08	0.01	0.91	0.02	0.27	< 0.01	0.30	< 0.01
<i>Odontella sinensis</i>	1.02	< 0.01	1.11	< 0.01	0.82	0.44	0.83	0.29
<i>Paralia sulcata</i>	0.81	< 0.01	1.19	< 0.01	0.18	0.01	0.15	< 0.01
<i>Phaeocystis</i> ssp.	0.72	0.11	0.68	0.06	1.03	0.73	1.02	0.62
<i>Porosira glacialis</i>	1.15	0.21	1.22	0.18	2.75	0.77	2.13	0.64
<i>Prorocentrum micans</i>	0.66	0.22	1.68	< 0.01	0.48	0.19	1.70	0.82
<i>Protoperidinium depressum</i>	0.73	0.14	1.05	0.01	1.07	0.73	0.98	0.65
<i>Skeletonema costatum</i>	1.66	< 0.01	1.28	0.01	0.54	0.07	0.47	0.01
<i>Scrippsiella</i> ssp.	-	-	-	-	-	-	-	-
<i>Thalassionema nitschioides</i>	0.52	0.39	0.38	0.51	0.50	0.07	0.53	0.03
<i>Thalassiosira rotula</i>	2.33	0.01	1.90	0.04	0.38	0.03	0.68	0.15
<i>Torodinium robustum</i>	0.92	0.28	1.72	0.01	0.36	0.14	0.29	0.02

8.1.3. Discussion

As mentioned above, not only the results for the single species were of interest, but primarily the overarching pattern was used to identify if the regime shifts could be detected in the algal community at Helgoland Roads. Nevertheless, the results for some of the analysed species could be discussed in the context of the changed environment through the reported regime shifts. Statistically significant shifts of the niche were detected mainly for the second split point towards the end of the 1980s. The reported reasons for this second split point were mainly water temperature and weather conditions (Weijerman et al., 2005). The niche volume for *S. costatum* increased after the year 1989. Because this species favoured lower water temperatures (Karentz and Smayda, 1984; Resende et al., 2007), the abundance at the end of the year may have been caused by the changed weather conditions and increased turbulence. *P. sulcata* showed changes of volume and distance for all periods, and as already reported by (Gebühr et al., 2009), this species changed its timing and was also abundant in the summer months over the last years of sampling. This influenced the computation and explained these changes after both split points. The pronounced increase in the niche volume for the two benthic species *O. rhombus* and *P. sulcata* suggested that the regime shift led to increased resuspension through stronger turbulence. *T. rotula* showed statistically significant shifts across both split points and a change in the volume for the split point at 1988 / 1989. This species was only abundant at the beginning and at the end of the time series, and these changes reflected this abundance pattern. The species of the genus *Ceratium* did not show any special characteristics, only *C. lineatum* exhibited a statistically significant result for the volume for the split point at 1978 / 1979. This was a result of the change in the abundance period of this species found at the time of the split point. This species was not found very often in this time series. Before 1979 it was found in winter, summer, and autumn, but after 1979 it was only found in late spring, summer, and early autumn with only very few findings in the winter. The change in the abundance of this species may have been a result of the changed competition and grazing in the context of the reported regime shift (Beaugrand, 2004).

Significant changes in the realized niches for six phytoplankton species were identified across the periods defined by the already reported regime shifts in 1979 and

1989. ONE classified the range of environmental conditions where the species showed their highest fitness. Through a comparative analysis, changes in these conditions that were reflected by changes in the niche size and position were identified. Common to 17 of the 23 investigated species were statistically significant shifts of the niche position at the break in the year 1989. The earlier break point at 1979 did not allow for an overarching statement, but significant changes in the niche position for this break point were found for six species. With respect to the niche volumes, changes across the split point in 1989 were comparable to the earlier year 1979.

For nearly all analysed species, tendencies towards larger niche distances could be detected for the approach with the split point at 1988 / 1989. This suggested changes in the habitat rather than shifts in species timing. This interpretation was supported by Wiltshire et al. (2010, 2008), who described the habitat trends at Helgoland. The shift in the niche for nearly all species with the split point at 1988 / 1989 suggested that the influence of factors that caused this regime shift was more pronounced than for the earlier regime shift. The volumes did not change strongly, which was not very surprising. If the shift in the niche was large, then the niche position had moved considerably in the environmental cluster. If the niche volume remained constant, there could have been some changes in the position of the niche, but the spread of the niche could nevertheless remain the same. Therefore, it was more likely to find statistically significant results for the shift in the niche than for changes in the niche volume. This was again a result of the abovementioned envelope effect, because the volume measured the spread of all inflection points (here for the different periods) and could not resolve the distribution of the single inflection points in the ‘all points’ cluster. Due to this low chance of detection, there were too few species showing a statistically significant trend in the volume to draw an overarching conclusion in view of the reported regime shifts.

8.2. Sliding window analysis

In the previous section, the two-period analysis for reported regime shifts was explained, and the pronounced shifts of the niches through a splitting of the time series were identified. In order to enhance this approach in this section, the split

point segmenting the total observation time was not fixed at the reported regime shift years but a ‘running’ split point analysis was computed with the measure for the niche shift explained in the previous section in which the centres of the species-specific inflection points ellipsoids were computed in the new subspace of the first three principal components. For each split point that divided the time series into two sections, the distance of the ellipsoids’ centres from the first to the second section was computed. The sections were defined by the inflection points and, hence, this analysis was species-specific. Every inflection point was used to cut the time series into two parts, and the distances of the resulting ellipsoids’ centres were computed individually for every species. This ended up in one distance value for every inflection point. Figure 8.3 shows this exemplarily for *Paralia sulcata*, and the values for the distance computed for this species were plotted as the red curve. To assess statistical significance, again a Monte Carlo resampling was applied. The time series of the values found at the inflection points in the first three principal components were jointly permuted and divided into two sections (1^{st} vs. $2^{\text{nd}} - n^{\text{th}}$, $1^{\text{st}} - 2^{\text{nd}}$ vs $3^{\text{rd}} - n^{\text{th}}$, $1^{\text{st}} - 3^{\text{rd}}$ vs. $4^{\text{th}} - n^{\text{th}}$, \dots , $1^{\text{st}} - n-1^{\text{th}}$ vs. n^{th}) and the distance was computed 10 000 times for each of these split points. This resampling once again showed whether the result was statistically significant or not. The resulting resampling statistic was plotted with black lines in Figure 8.3. The two thin lines represent the 5% and 95% quantiles, and the thick black line with symbols represents the median. To find a reliable measure for the shift in the species’ niche, the net distance was calculated where the species-specific distance was normalized to the median distance of the resample statistics. This subtracted the random variability and left the species-specific distance. Hence, this net distance was computed as the difference of the species’ distance (red curve) and the median of the resampling (thick black curve with symbols). The results were plotted as the green line in Figure 8.3.

To extract the year with the largest distance, hence the year indicating the shift most pronouncedly, some criteria had to be applied. A steep decrease at the beginning and a steep increase at the end of the distance plot (not shown) were omitted. This was because of the small number of points in the respective sections. This small number caused large statistical errors in the estimation of the ellipsoid, which was why the first and last eight years of this time series were not considered and the year with the largest net distance between the years 1975 and 2000 was extracted.

Furthermore, *Scrippsiella* ssp. was not used for this analysis, because this species was only abundant in the last 11 years of sampling and, therefore, the period was too short for this analysis. The values and the years with the largest net distance for each species were subsumed in Table 8.2 and ranked with respect to the year of the largest net distance between 1975 and 2000.

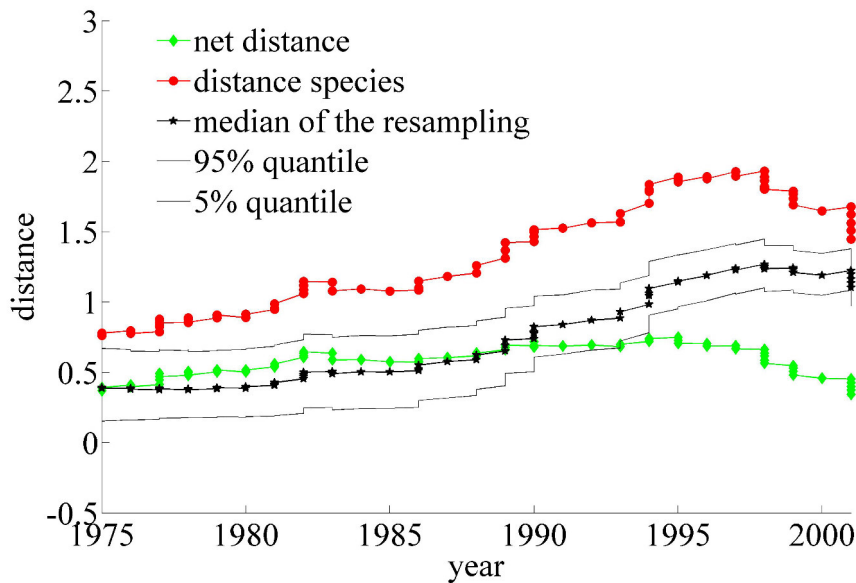


Figure 8.3.: Computation of the ‘running’ split point analysis for *Paralia sulcata* with included resampling statistics; red curve: distance of the ellipsoids for *P. sulcata*; black curve with symbols: median of the resampling procedure; thin black curve: 5% and 95% quantiles of the resampling procedure; green curve: net distance computed as the difference of the species results (red) and the median of the resampling (thick black)

As three breaks were found in the table (marked by blank lines), four groups of species were identified with their largest changes in succeeding years. The first group (*O. aurita*, *P. glacialis*, *G. striata*, *S. costatum*) showed a shift in the years 1975 and 1976, and the second group, consisting of only two species (*O. sinensis*, *C. furca*), in the years 1983 and 1984. The third group (*C. fusus*, *G. delicatula*, *C. lineatum*, *C. tripes*, *P. micans*) showed a shift in the years 1988 and 1989, and the fourth group (the rest of the 23 species, without *Scrippsiella* ssp.) from 1995 until 1999.

The reported regime shift at the end of the 1980s was found with this analysis,

Table 8.2.: Species table with the value and year of the largest change in the distance of the sliding window computation; table ranked with respect to the year; diatoms in light grey, dinoflagellates in dark grey, and the haptophyte in white; blank lines indicate breaks

species	net distance	year
<i>Odontella aurita</i>	0.53107	1975
<i>Porosira glacialis</i>	0.50111	1975
<i>Guinardia striata</i>	0.46027	1976
<i>Skeletonema costatum</i>	0.65257	1976
<i>Odontella sinensis</i>	0.48457	1983
<i>Ceratium furca</i>	0.30483	1984
<i>Ceratium fusus</i>	0.55726	1988
<i>Guinardia delicatula</i>	0.60208	1988
<i>Ceratium lineatum</i>	0.41598	1989
<i>Ceratium tripos</i>	0.42773	1989
<i>Prorocentrum micans</i>	0.46632	1989
<i>Paralia sulcata</i>	0.74635	1995
<i>Phaeocystis</i> ssp.	0.37562	1995
<i>Thalassionema nitzschioides</i>	0.44246	1995
<i>Eucampia zodiacus</i>	0.40156	1996
<i>Odontella regia</i>	0.2325	1996
<i>Noctiluca scintillans</i>	0.48999	1997
<i>Odontella rhombus</i>	0.51758	1998
<i>Protoperidinium depressum</i>	0.77892	1998
<i>Torodinium robustum</i>	0.91202	1998
<i>Ceratium horridum</i>	0.42715	1999
<i>Thalassiosira rotula</i>	0.77089	1999

and it was identified through the third group of species in Table 8.2. The supposed regime shift at the end of the 1990s (Lees et al., 2006; Weijerman et al., 2005) was also found here with this analysis, and it was reflected by the species in the fourth group. It was not possible to find the shift for the year 1979, but a shift for the year 1976 was found instead, which was very close to this reported shift (Beaugrand et al., 2008).

Regime shifts (cf. Section 3.1) are large-scale changes in multiple physical parameters (e.g. climate, hydrography, . . .) and are therefore connected with the ecosystem. Although, the ecosystem can recover or reorganize after this disturbance (Peterson et al., 1998; Wiltshire et al., 2008). These regime shifts cannot be identified through an analysis of a phytoplankton time series alone, but the influence of the regime shifts can possibly be detected in the phytoplankton time series. Phytoplankton depend on environmental conditions, and if these change, the species face changed conditions that affect their dominance and succession. Therefore, this method was used to assist the results found for the same habitat and for the North Atlantic. The regime shifts at the end of the 1980s and the 1990s were connected with oceanic inflow (Reid et al., 2001) and evidences for these shifts were also found through this analysis. The changed conditions through this oceanic inflow had an influence on species adapted to marine and neritic habitats. The marine species faced more favourable conditions and the neritic species more unfavourable conditions. This led to a changed timing of the inflection points for both kinds of species. Additionally, competitors and grazers responded with a changed timing, too. Therefore, these regime shifts had a potentially strong influence on the analysed phytoplankton community and reorganized the phytoplankton succession in the habitat.

Overall, the analysis of the niche shift showed an additional usage of the ONE method and supported the discussed regime shifts.

9. Discussion of the newly developed method

9.1. Summary

In this thesis, a new method to reconstruct the ecological niche of the phytoplankton species was developed and applied to the Helgoland Roads data. This method enabled a classification of the ecological niche from a new perspective. The procedure was defined, and the results were shown and explained in the context of the Hutchinsonian ecological niche. A variation of the computation by combining different biotic factors as environmental variables showed their influence. An ecological interpretation of the obtained results was reached by testing some hypotheses, and it showed the possible impact on phytoplankton ecology. Finally, changes in the ecological niche were studied with respect to the reported regime shifts. A discussion of the advantages and drawbacks of this method, and the present work's contribution to the understanding of phytoplankton ecology will follow in the next section.

9.2. Why the new method?

The newly developed method presented in this work has to be seen as supplementing existing ecological classification (niche describing) methods. What was added to the pool of methods was the new aspect of taking a fitness parameter into account for this classification. This so-called Optimal Niche Estimate (ONE) identified the range of environmental conditions where species performed optimal, i.e. a fitness-based ecological niche. The term 'ONE' reflected the new approach by defining the new niche with a focus on optimal conditions.

As mentioned before, nearly all concepts of niche reconstruction were based on

abundance. A good overview of the applied concepts can be found in Wake et al. (2009), where publications were combined in a special issue following the Arthur M. Sackler Colloquium of the National Academy of Sciences ‘Biogeography, Changing Climates and Niche Evolution’. Wake et al. (2009) started with an comprehensive summary of the history of the niche and recent applications. The other publications were recently applied methods or concepts of niche reconstruction itself. Tingley et al. (2009) focused on a climate-induced change of the Grinnellian niche of birds. They identified a climatic niche for birds and showed that this niche shifted over time. Porter and Kearney (2009) defined a thermal niche using functional traits (characteristics that are expressed in phenotypes of organisms (Díaz et al., 2013)). This niche for endotherms was determined through laboratory experiments analysing the metabolic rate. The determination of the thermal niche was used to find a range of suitable climatological parameters for the species and helped to predict the influence of climate change on these endotherms. Other works in this special issue dealt with the influence of climate change on species’ niche and the biogeography of species (e.g. Vieites et al. (2009), Wiens et al. (2009), Zimmermann et al. (2009)). The number of papers published in the field of niche analysis increased significantly in the last few years (Vaz et al., 2015), and the number of studies will most probably rise further, although the analysis of the ecological niche of phytoplankton species is still not very common. Some recently published papers concerning the ecological niche of phytoplankton analysed the realized niche for a different number of single species using abundance data (Brun et al., 2015; Hernández Fariñas et al., 2015). A comparable limnological study analysing the optimal growth conditions for species in the Lake Garda, Italy, grouped the species into different classes using a PCA and other multivariate statistical methods (Salmaso, 2003). It was shown that the realized niche and the optimal conditions for growth were unique to the analysed habitat, but no connection was made between these two parameters. Another study investigated the ecology of phytoplankton in Australian lakes and used a PCA to group the species (Fabbro and Duivenvoorden, 2000); however, it used the abundance of the species, and no niche was determined. Using an ordination technique to identify similarities between the phytoplankton community at different sampling stations at the Tunisian coast, Feki-Sahnoun et al. (2014) showed that some station had comparable communities. They concluded that because of these similarities

not all stations had to be sampled in the sampling project REPHY. Other methods for the determination of the ecological niche of phytoplankton species had a different understanding of the ecological niche. For example, Wang et al. (2012) determined a niche for different months of a year for species from a Chinese lake. To detect and predict changes in the North Sea, Helaouët et al. (2013) determined a two-dimensional niche for two zooplankton species using data from the Continuous Plankton Recorder. This niche was only based on the abundance and two environmental parameters, Phytoplankton Colour Index and Sea Surface Temperature.

By focusing on fitness, the conditions where species performed best were extracted and, especially for phytoplankton, the optimal proliferation was considered. In this thesis, fitness was understood as the maximal growth rate, but one could consider different fitness parameters as relevant if one would adapt this concept to another group of species.

Barton et al. (2013) explained that functional traits determine the fitness of plankton species and concluded: "The fitness of a particular species, therefore, varies along environmental and biological gradients, producing its characteristic temporal and spatial distribution [...]" (Barton et al., 2013, p. 523). This means that fitness should be considered an important factor for the classification of species when one focuses on its functional traits.

In a comparative approach (Grüner et al., 2011), the newly developed ONE method was compared with a different, yearly niche classification method (outlying mean index or OMI, see Chapter 1). This comparison showed that the yearly niche and the global optimal niche could complement each other. The optimal niche can be interpreted as the average niche over the whole time series and is, so to speak, an envelope of the yearly niches (Figure 9.1). This comparison was done with three species and *P. sulcata* was included. This showed that both approaches had advantages and disadvantages. A drawback of ONE is the restriction to a densely sampled long-term dataset. It would not be possible to work with short time series, because one would find typically two (sometimes just one, sometimes more) inflection points per year, and the computation of the covariance ellipsoids should not be done with less than 20 inflection points. The estimation error would get too high and the results of the computation would not be reliable anymore. Additionally, a densely sampled time series would be needed to hit the time of fastest growth. The advantage of

the long-term and high-frequency sampling of the Helgoland Roads data made this computation possible, and the method showed its power through such a long time series. The OMI has the advantage of reconstructing a yearly niche and opened space for a more detailed perspective on the changes in the ecological niches, but one can argue if this was ecologically meaningful. A yearly niche reflects the range of environmental conditions in which a species is found (it is done by an abundance weighting), and if these conditions change from one year to another, one will detect these changes in the yearly niche. This is most likely not due to the changes in the species specific niche, but just a reflection of the environment. Of course, it can be useful to identify the yearly niches and its changes over the years, but one should also distinguish between fluctuations and persistent changes. The comparison was concluded with the statement that it would be best to combine these two methods for a more detailed insight into the ecology of the species (Grüner et al., 2011).

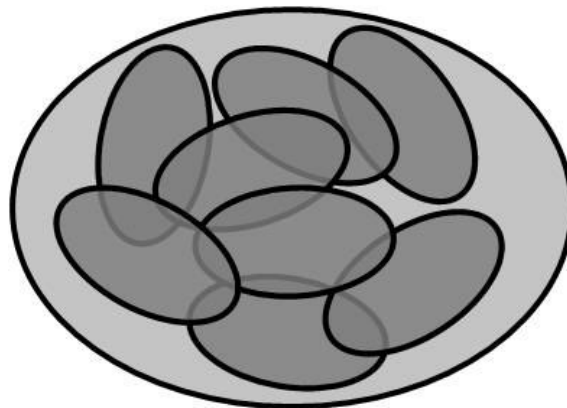


Figure 9.1.: Sketch of the yearly and the global niches; small ellipses are the yearly niches and the large one may be seen as their envelope

An advantage of ONE was the species-specific characteristic. It was not done for functional groups or an artificially constructed groups of species. However, if one were interested in these groups, it could be done in that way as well. The species-specific ONE enabled an understanding of the ecology of phytoplankton species and the phytoplankton community as shown in Sections 7.1 and 7.2. ONE did this in such a way that the sizes of the niches for the species could be compared. Chapter 5 explained how it was done and discussed how the range of specialization was used

for this classification. In the results of ONE, it was shown that it was easier to find species in the lower range, hence species with more special needs. This resulted from the fact that the ONE ellipsoid was compared with the full dynamic range of the environmental conditions, and, therefore, only species covering a small area could have been detected with statistical significance.

Litchman et al. (2012) proposed trait-based niche modelling as a future aspect of the analysis of phytoplankton ecology, especially in a globally changing environment. The combination of major functional traits with a range of environmental factors where a species was abundant could be used to map the ecological niche. This idea correlates somehow with the work presented here, but the idea of ONE was different. Here, an identification of the times where the species had its highest fitness was made, and then the niche for the environmental factors found at these times was constructed.

The analyses were done for the two major groups of phytoplankton in this habitat, the dinoflagellates and the diatoms. These two groups are well studied, and there is a lot of information about their life cycles and morphology. These pieces of information can be found in every standard phycological text book. A short summary of the biology of these groups can be found in the introductory part of Hoppenrath et al. (2009). The advantage of focusing on these groups was the possible transferability of the obtained results to other regions. Additionally, these two groups had considerably different niche characteristics, which enabled testing the new method under different circumstances. Boyd et al. (2013) analysed the thermal niches of different phytoplankton species from polar to tropical waters and also showed that there were only minor differences between species isolated from different waters. Therefore, there are no or only minor differences in the optimal temperatures between species in their and other studies. This showed that the results gained for the Helgoland Roads time series in this work can most likely be transferred to other habitats. Irwin et al. (2012) used the data from the Continuous Plankton Recorder to estimate the realized niches from phytoplankton species. However, they used the presence of the species and the range of the environmental factors at these places. They also showed that the niches for diatoms and dinoflagellates are separate, but that there was a lot of variations between species in this two groups.

One essential part of ONE was the principal component analysis (PCA). This

multivariate technique was used to reduce the dimension of the dataset without losing too much of the total variance. The PCA constructs new variables as linear combinations of the original factors that account for the highest variances in the dataset. The restriction to linear relationships could be a problem if there were many nonlinear correlations in the data. These would not be represented adequately in the new subset of variables and could lead to problems in the newly constructed space. An early test of another linear ordination method, which is not restricted to non-correlated axis for the new subspace, the independent component analysis (ICA, Comon, 1994), made hardly any difference. Therefore, the PCA was used, as it is well known, well investigated, and well implemented in most of the standard statistical software tools available. This had the advantage that the method would be easy to reproduce and could be used by other ecologists as well.

Another point of the PCA is that the construction of the new subspace is reached through a linear combination of the original variables. This enabled a direct interpretation of how much each factor contributed to the first few principal components. By analysing the coefficients of these linear combinations, the so-called factor loadings, an interpretation of the dimension reduction can be made. The PCA is a traditional method, but it is still widely used and the usage of this method in recent studies showed its impact and reliability (Fabbro and Duivenvoorden, 2000; Salmaso, 2003).

The reduction of the dimension can be critical. A test of dimension reduction showed that three dimensions provided the best solutions. In principle, it is not necessary to reduce the dimension to three, but a graphical illustration is difficult beyond. The computation of the ellipsoids could be done in the same way when considering more dimensions, and the results could be interpreted on the same basis as for three dimensions. However, the estimation error has to be seen critical if the dimension is chosen higher.

The computation of inflection points was a straightforward procedure. The only restrictions made were the criteria (mentioned in Chapter 5) devised to extract only significant inflection points, which were: to exclude inflection points at relatively low values of smoothed cell counts, an acceptance threshold at 10 % of the annual maximum was set; only inflection points on the ascending parts of the abundance curve were taken into account; and after one detected inflection point, the abundance curve had to fall below 10 % of the annual maximum before accepting the next point.

The computation of the species-specific inflection point cluster and the normalization to the whole environmental cluster ('all points' cluster) were the big advantages of this method. It was not necessary to interpret the results for different species in a comparative manner. Additionally, the normalization enabled a comparison of results found for different time series. With the introduced range of specialization, a normalized value for the niche size, the niche characteristics for the analysed species could have been shown with one single number.

The inclusion of grazing and competition as an environmental factor was another important thing. These have a high influence on the abundance and growth of the phytoplankton species and should not be ignored in comparative studies. By ignoring these factors, one excludes some of the most important factors for phytoplankton growth. However, these factors are not so relevant for the initial phases of the spring blooms, because zooplankton abundance is still low and the competing phytoplankton species have not yet established a stable population to strongly influence the growth of other species. However, for later blooms (in summer or autumn), these factors are very relevant.

9.3. Advantages of the new method

- The new method offers a fitness-based classification of the phytoplankton species and determines an ecological niche for them. This niche differs considerably from previously developed methods.
- The work presented in this thesis is a contribution to the research carried out with the Helgoland Roads data. The contribution should be seen as an extension of the single-species analysis.
- Through an analysis of 115 species, the ONE method was used to test some general hypotheses.
- A modification of the ONE method enabled a time-resolved analysis checking for consequences of the reported regime shifts.
- A transfer of this method to other research communities would be a possible

perspective. The adaptation to other species can be done in a straightforward way.

- Through the normalization of the optimal niche volume, results from different habitats can be compared directly.

A. Appendix

A.1. Graphs of the 23 selected species

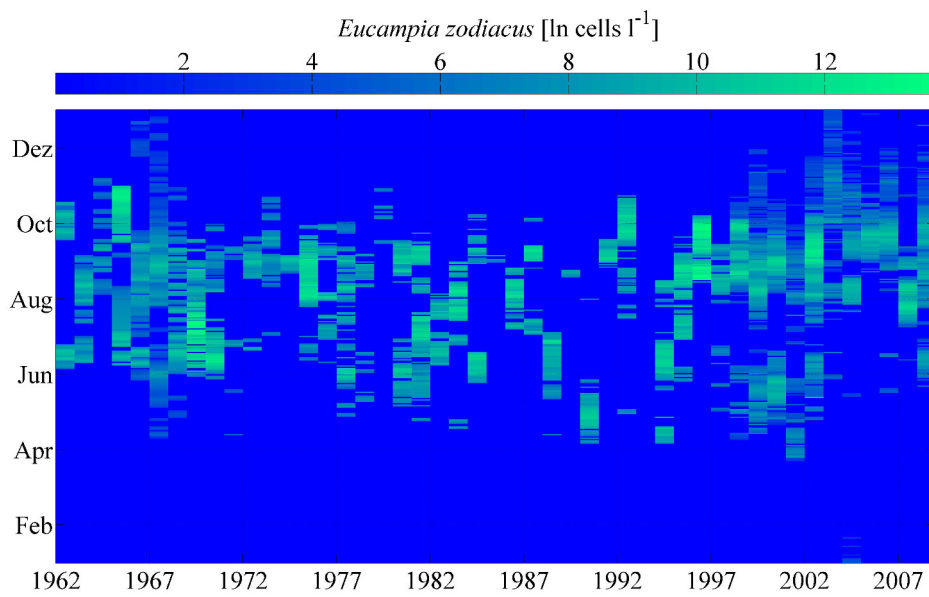


Figure A.1.: Logarithmic abundance of *Eucampia zodiacus* at Helgoland

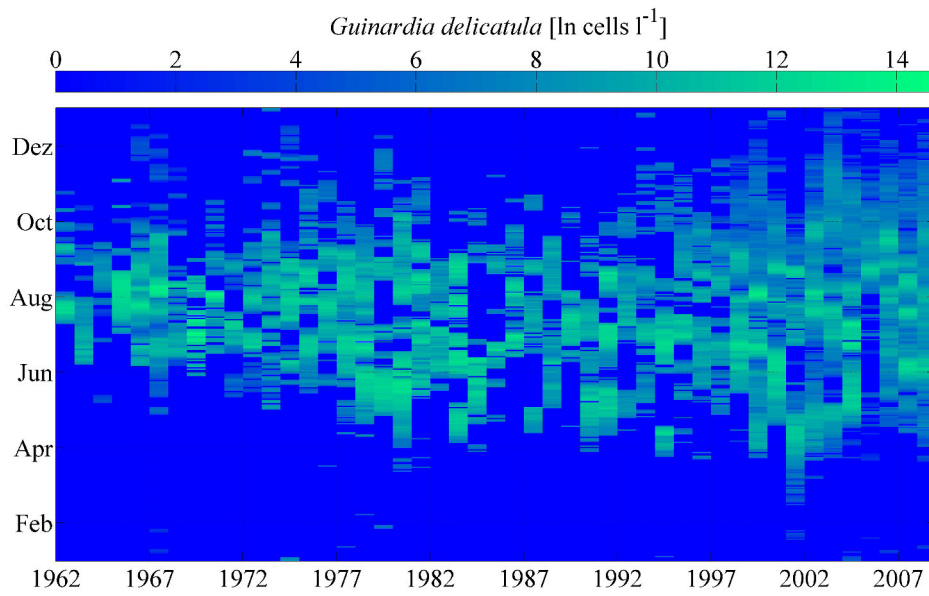


Figure A.2.: Logarithmic abundance of *Guinardia delicatula* at Helgoland

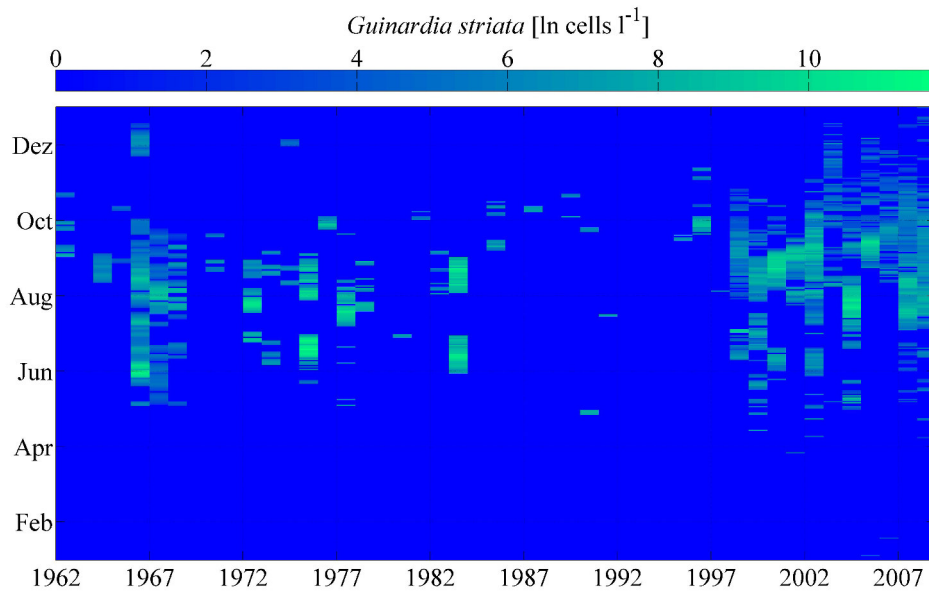


Figure A.3.: Logarithmic abundance of *Guinardia striata* at Helgoland

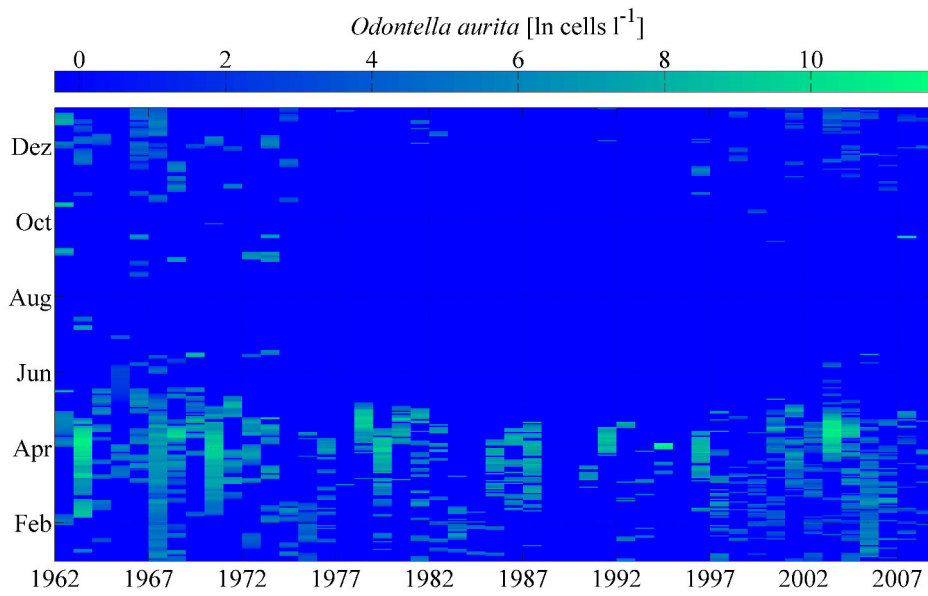


Figure A.4.: Logarithmic abundance of *Odontella aurita* at Helgoland

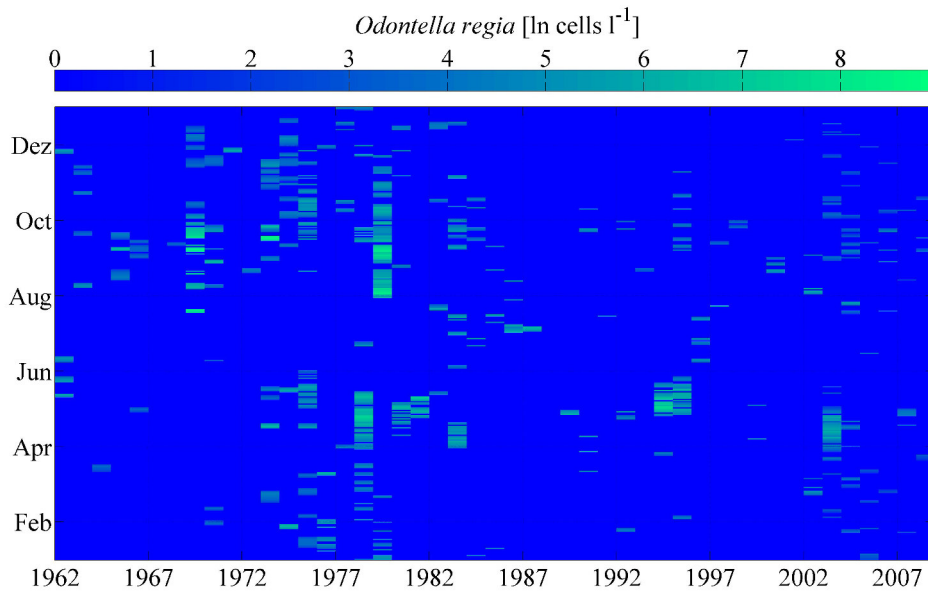


Figure A.5.: Logarithmic abundance of *Odontella regia* at Helgoland

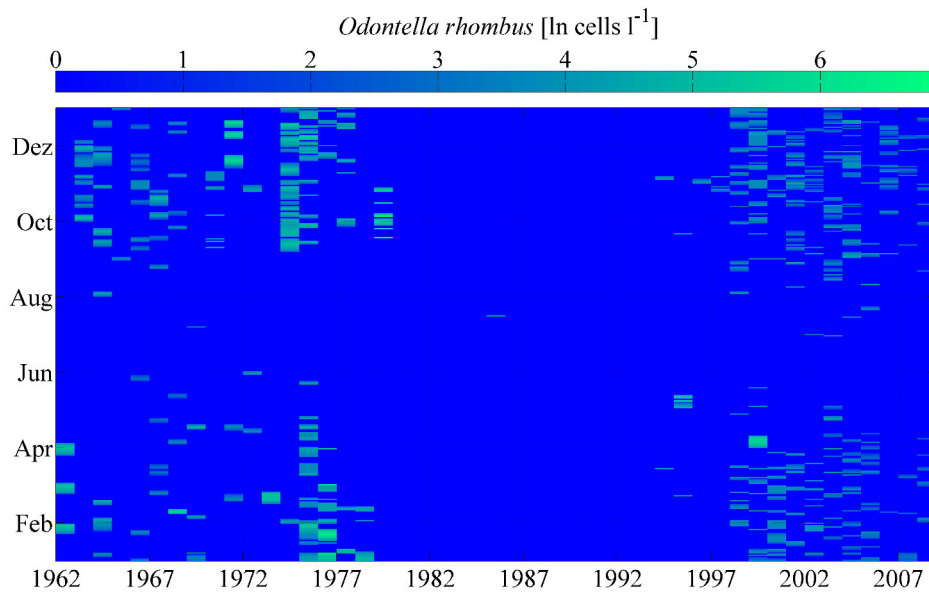


Figure A.6.: Logarithmic abundance of *Odontella rhombus* at Helgoland

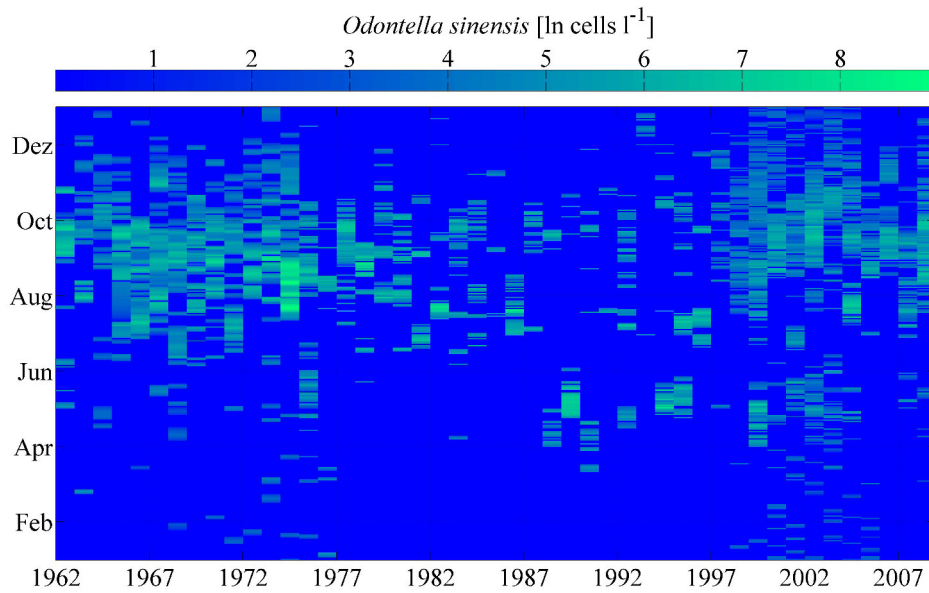


Figure A.7.: Logarithmic abundance of *Odontella sinensis* at Helgoland

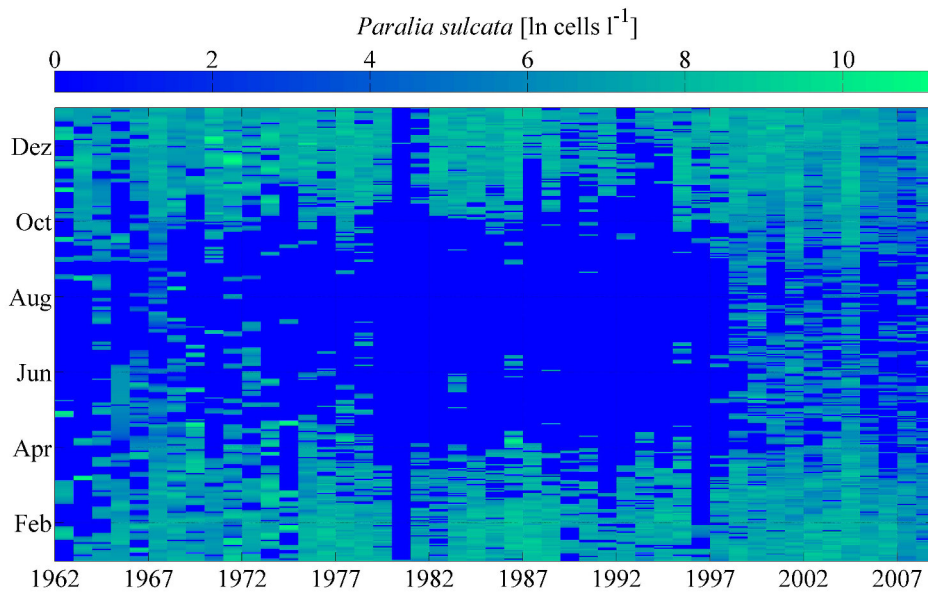


Figure A.8.: Logarithmic abundance of *Paralia sulcata* at Helgoland

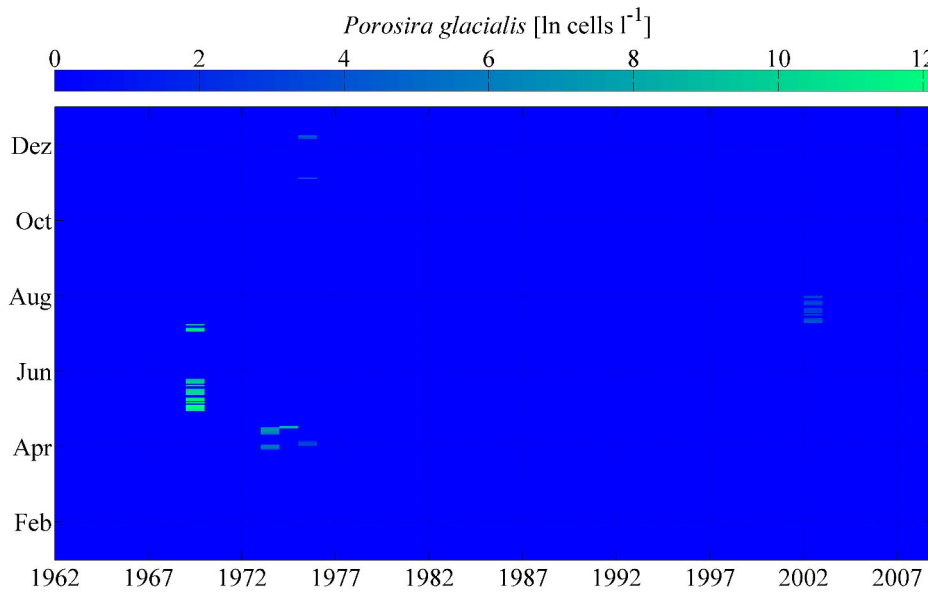


Figure A.9.: Logarithmic abundance of *Porosira glacialis* at Helgoland

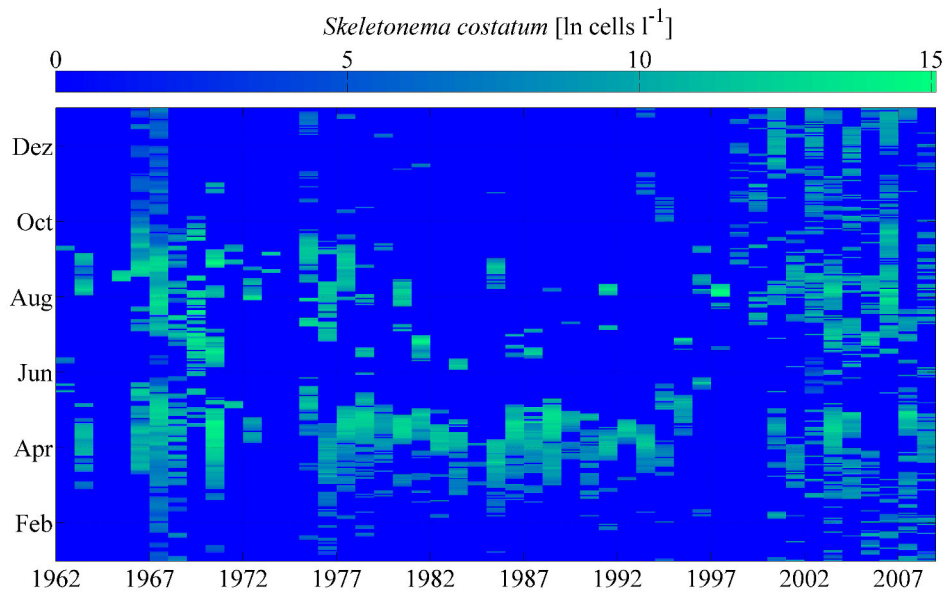


Figure A.10.: Logarithmic abundance of *Skeletonema costatum* at Helgoland

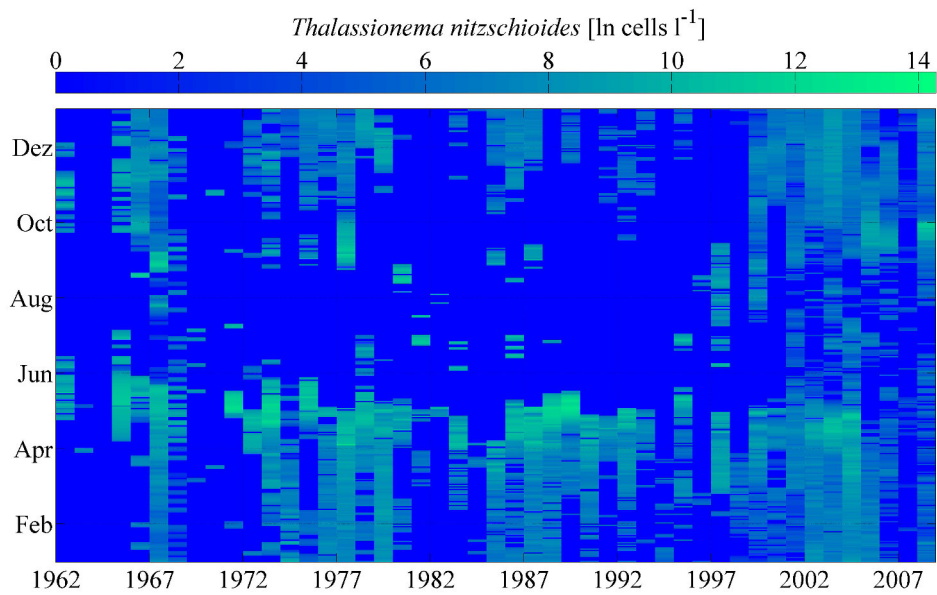


Figure A.11.: Logarithmic abundance of *Thalassionema nitzschioides* at Helgoland

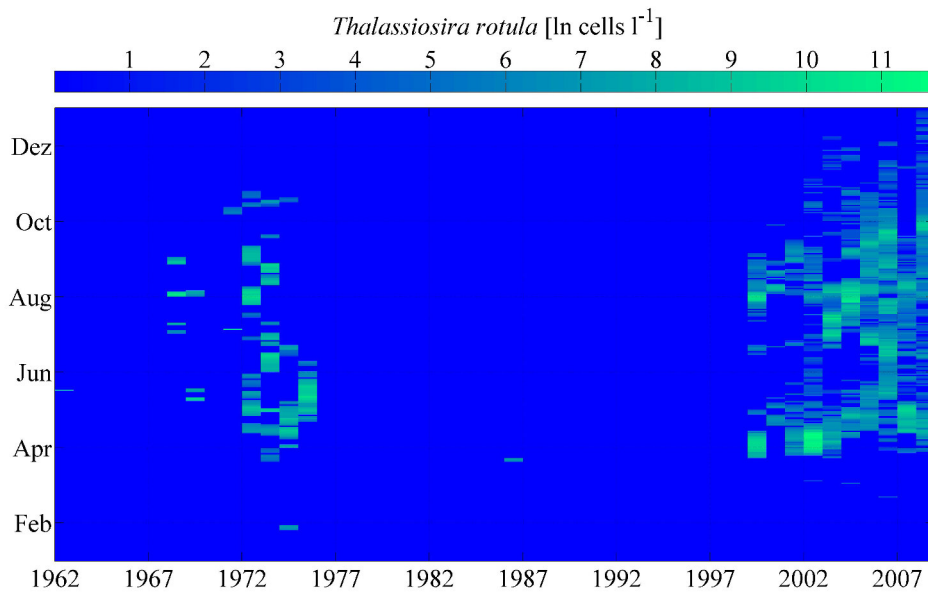


Figure A.12.: Logarithmic abundance of *Thalassiosira rotula* at Helgoland

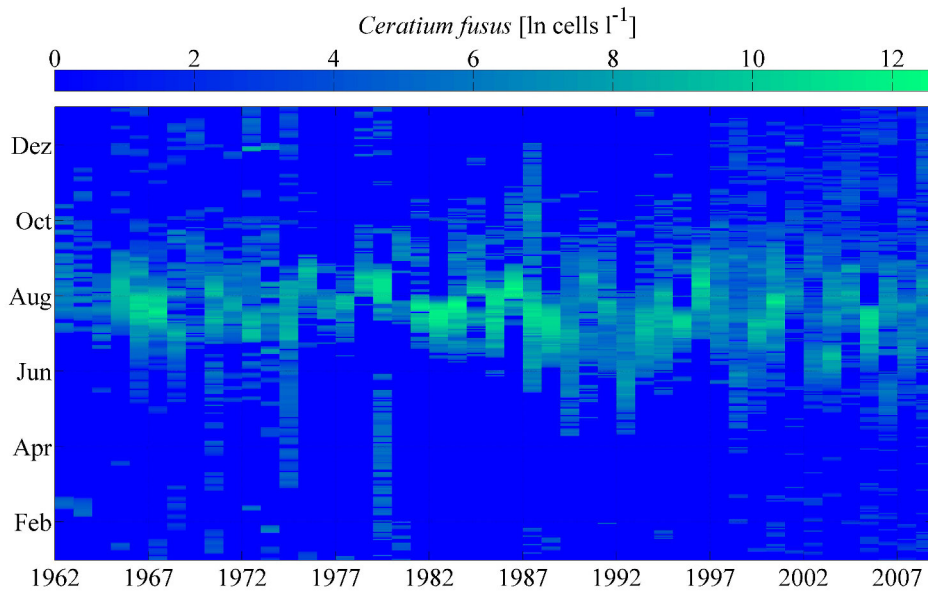


Figure A.13.: Logarithmic abundance of *Ceratium fusus* at Helgoland

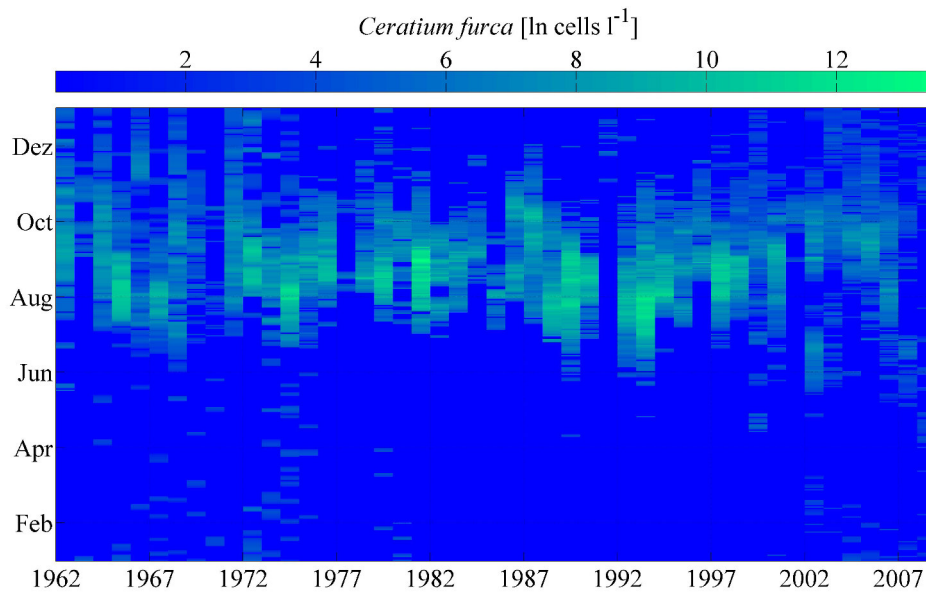


Figure A.14.: Logarithmic abundance of *Ceratium furca* at Helgoland

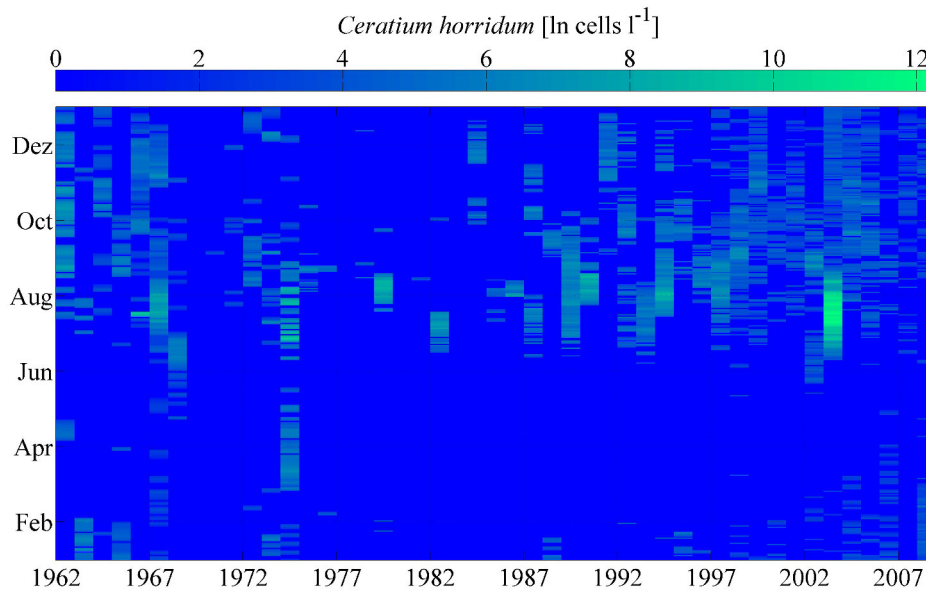


Figure A.15.: Logarithmic abundance of *Ceratium horridum* at Helgoland

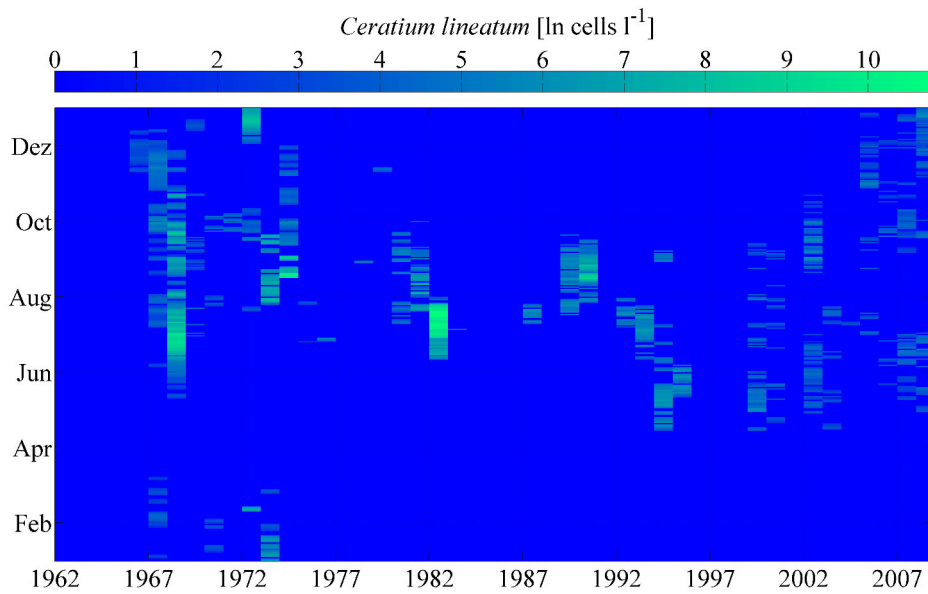


Figure A.16.: Logarithmic abundance of *Ceratium lineatum* at Helgoland

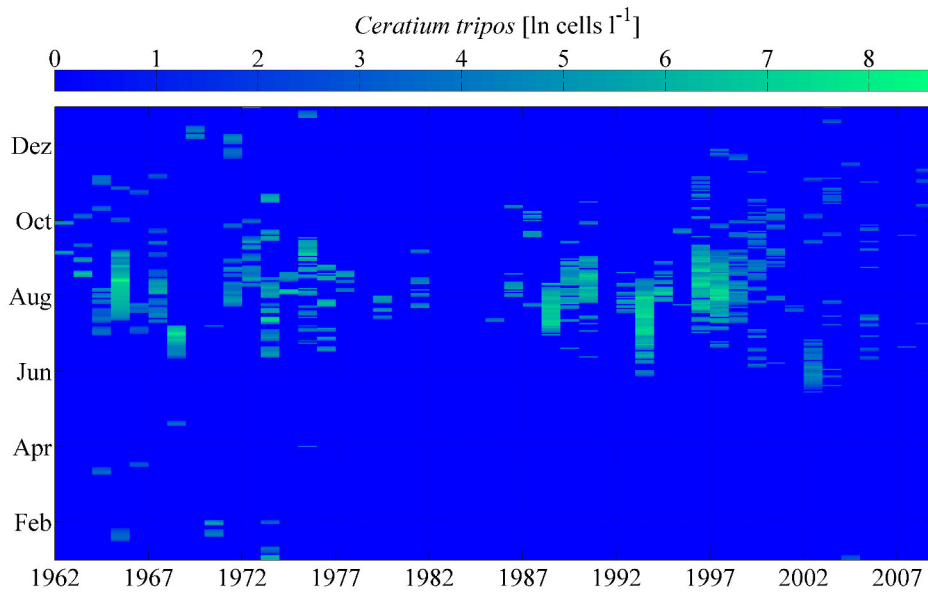


Figure A.17.: Logarithmic abundance of *Ceratium tripos* at Helgoland

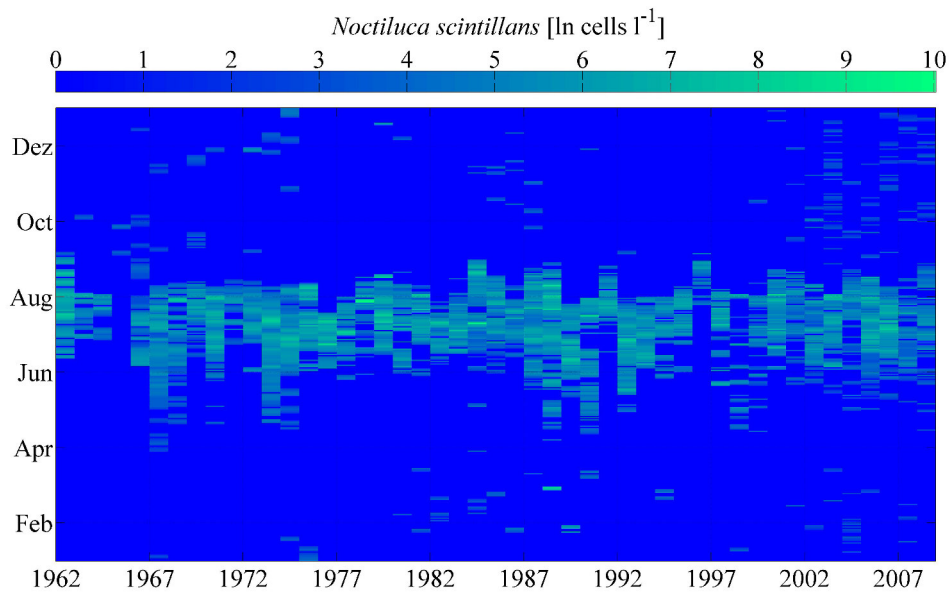


Figure A.18.: Logarithmic abundance of *Noctiluca scintillans* at Helgoland

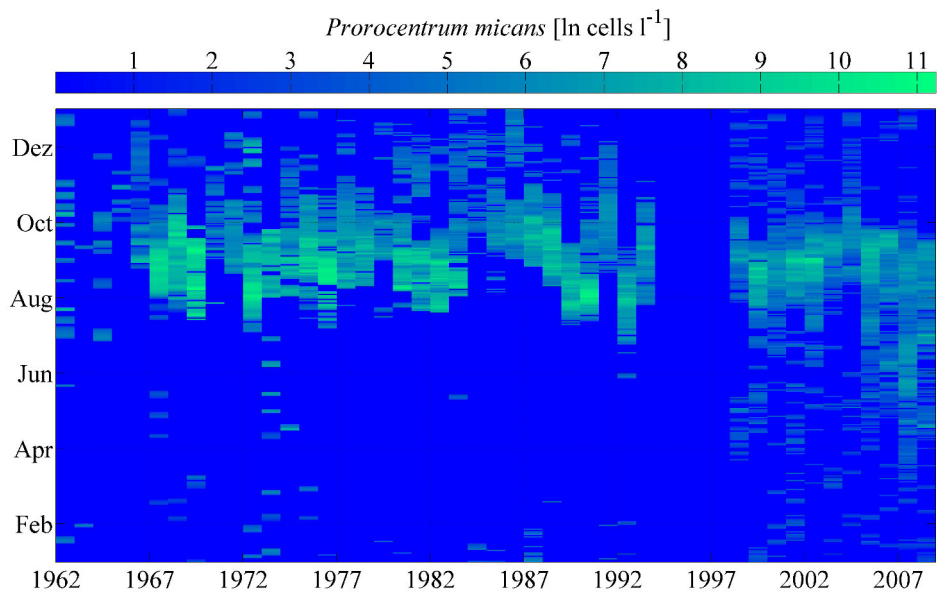


Figure A.19.: Logarithmic abundance of *Prorocentrum micans* at Helgoland

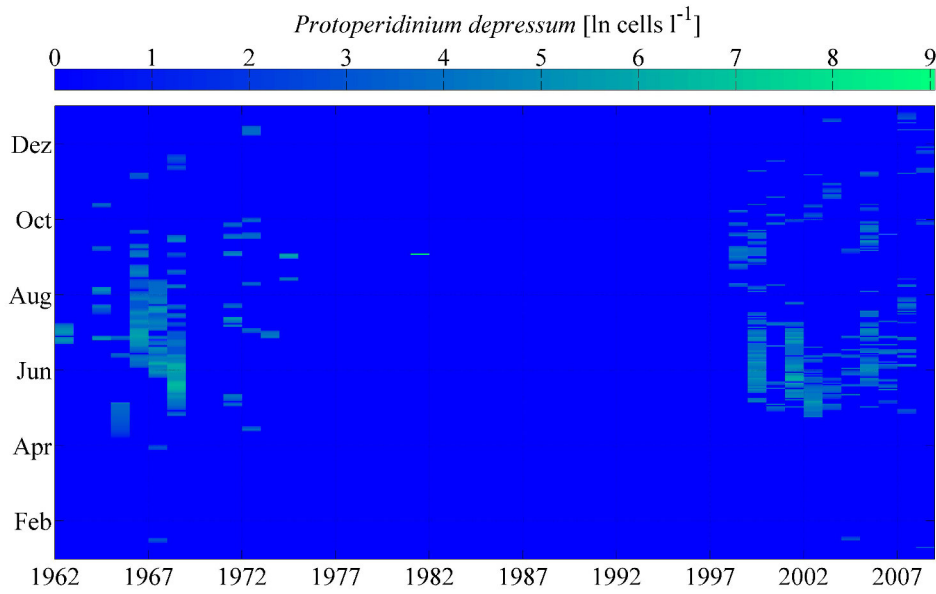


Figure A.20.: Logarithmic abundance of *Protoperidinium depressum* at Helgoland

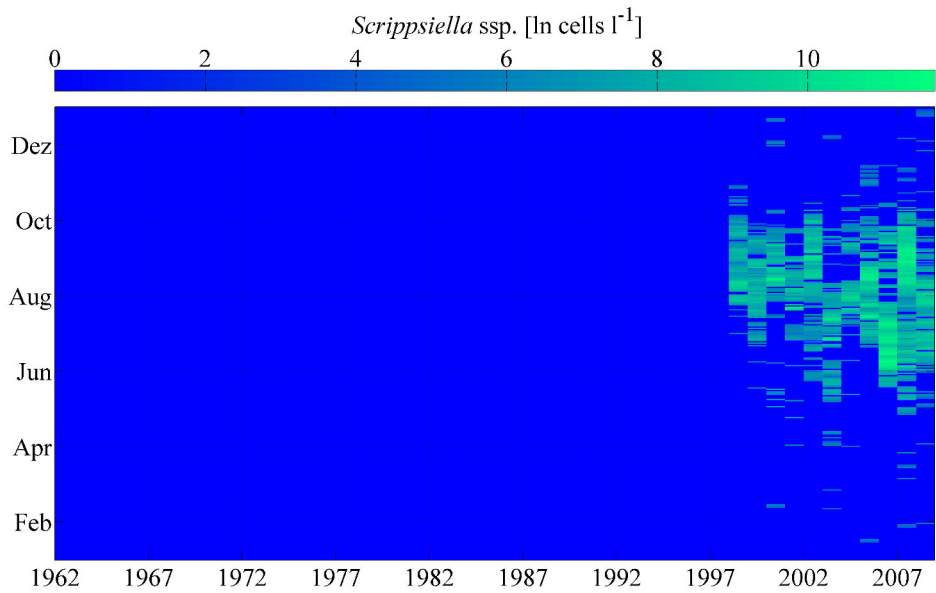


Figure A.21.: Logarithmic abundance of *Scrippsiella* ssp. at Helgoland

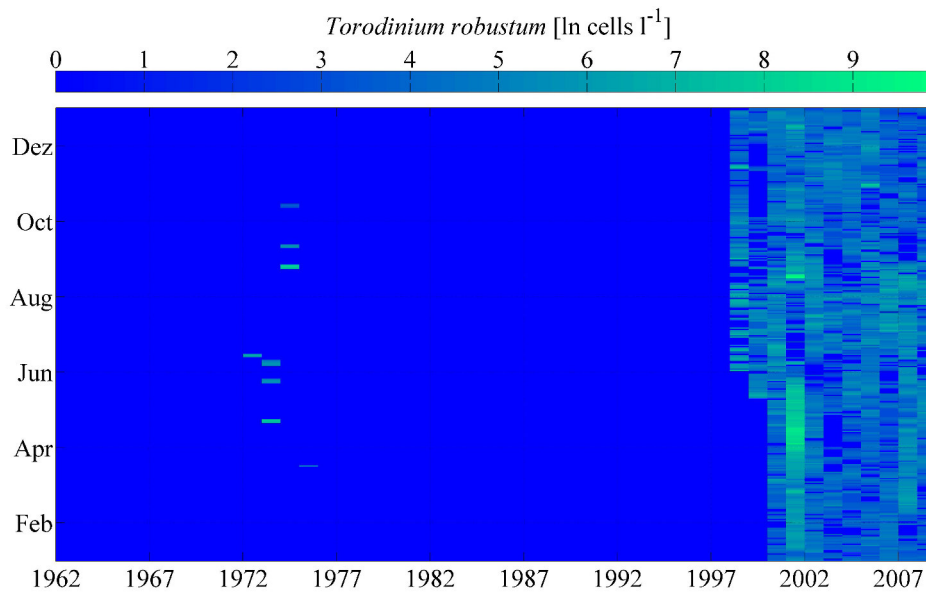


Figure A.22.: Logarithmic abundance of *Torodinium robustum* at Helgoland

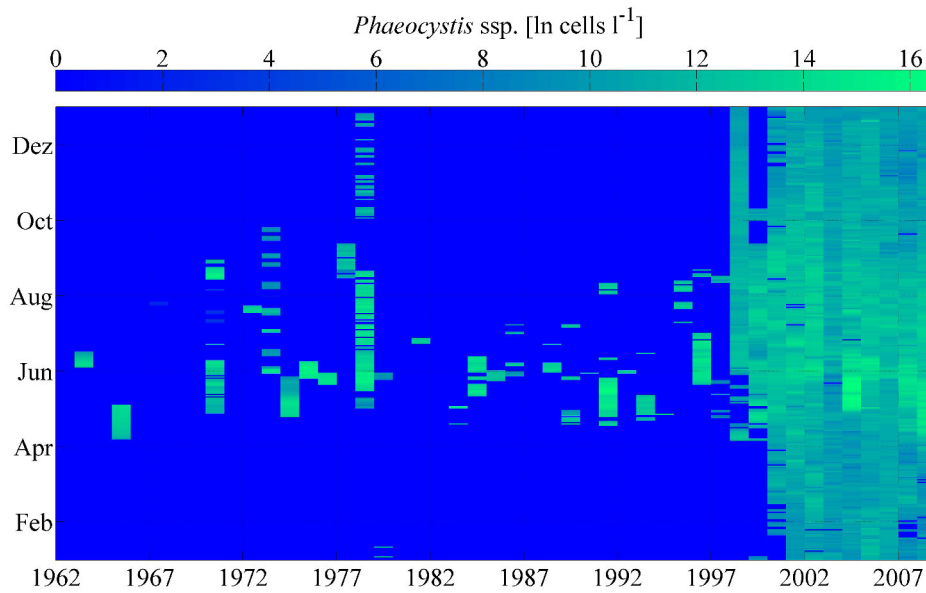


Figure A.23.: Logarithmic abundance of *Phaeocystis* ssp. at Helgoland

A.2. Species list

Actinocyclus ssp

Actinoptychus senarius

Amphidinium ssp

Asterionellopsis glacialis

Asterionellopsis kariana

Bacillariales indeterminata

Bacillaria paxillifer

Bacteriastrum hyalinum

Bellerochea malleus

Biddulphiales indeterminata

Brockmanniella brockmannii

Cerataulina pelagica

Ceratium furca

Ceratium fusus

Ceratium horridum

Ceratium lineatum

Ceratium longipes

Ceratium macroceros

Ceratium tripos

Chaetoceros debilis

Chaetoceros densus

Chaetoceros didymus

Chaetoceros socialis

Chaetoceros ssp

Coccolithophorid indeterminata

Coscinodiscus concinnus

Coscinodiscus granii

Coscinodiscus radiatus

Coscinodiscus ssp

Coscinodiscus wailesii

Cylindrotheca closterium

A. Appendix

Dactyliosolen fragilissimus
Detonula confervacea
Detonula pumila
Dictyocha speculum
Dinophyceae indeterminata
Dinophysis acuminata
Dinophysis acuta
Dinophysis norvegica
Dinophysis rotundata
Dinophysis ssp
Diplopsalis ssp
Dissodinium pseudolunula
Ditylum brightwellii
Eucampia zodiacus
Fragilaria ssp
Gonyaulax ssp
Guinardia delicatula
Guinardia flaccida
Guinardia striata
Gymnodinium mikimotoi
Gymnodinium ssp
Gyrodinium ssp
Gyrosigma ssp
Helicotheca tamesis
Lauderia annulata
Leptocylindrus danicus
Leptocylindrus minimus
Lithodesmium undulatum
Melosira nummuloides
Melosira ssp
Meuniera membranacea
Myrionecta rubra

Navicula ssp
Nitzschia longissima
Noctiluca scintillans
Odontella aurita
Odontella mobiliensis
Odontella regia
Odontella rhombus
Odontella sinensis
Paralia sulcata
Phaeocystis ssp
Pleurosigma ssp
Podosira stelliger
Polykrikos ssp
Porosira glacialis
Proboscia alata
Prorocentrum balticum
Prorocentrum micans
Prorocentrum ssp
Protoperidinium bipes
Protoperidinium brevipes
Protoperidinium claudicans
Protoperidinium conicum
Protoperidinium depressum
Protoperidinium divergens
Protoperidinium pellucidum
Protoperidinium punctulatum
Protoperidinium ssp
Pseudo-nitzschia delicatissima
Pseudo-nitzschia seriata
Pyrophacus ssp
Rhaphoneis amphiceros
Rhizosolenia hebetata

A. Appendix

Rhizosolenia imbricata
Rhizosolenia pungens
Rhizosolenia robusta
Rhizosolenia setigera
Rhizosolenia styliformis
Scrippsiella trochoidea
Silicoflagellates ssp
Skeletonema costatum
Stephanopyxis turris
Thalassionema nitzschioides
Thalassiosira minima
Thalassiosira nordenskiöldii
Thalassiosira punctigera
Thalassiosira rotula
Thalassiosira ssp
Torodinium robustum
Triceratium alternans
Triceratium fавus

List of Figures

1.1. Sketch of different concepts of niche classification; gray: environmental conditions; green: generalist - occupying nearly the whole range of the environmental conditions; blue: specialist or generalist - found at the average environmental conditions (centre) but only in a small range; red: specialist - found in a small range and at the border of the environmental conditions (extended after Gebühr (2010))	18
2.1. Phytoplankton blooms in the North Sea in late October 2011 with brownish sediment clouds close to the coast; NASA images, courtesy Jeff Schmaltz, MODIS Rapid Response Team, Goddard Space Flight Center - detail from the original picture	22
3.1. The island of Helgoland and its position in the German Bight with marked sampling station Helgoland Roads in the inset; map from Teeling et al. (2016, p. 4), Creative Commons Attribution License - https://creativecommons.org/licenses/by/4.0	27
3.2. Sea surface temperature at Helgoland	30
3.3. Secchi depth at Helgoland	31
3.4. Salinity at Helgoland	32
3.5. DIN concentration at Helgoland	33
3.6. Phosphate concentration at Helgoland	33
3.7. Silicate concentration at Helgoland	34
3.8. Sunshine duration at Helgoland	35
3.9. Wind speed at Helgoland	35
3.10. Logarithmic zooplankton abundance at Helgoland	37
3.11. Logarithmic abundances of <i>Eucampia zodiacus</i> at Helgoland	37
3.12. Logarithmic abundances of the <i>Guinardia</i> species at Helgoland	38
3.13. Logarithmic abundances of the <i>Odontella</i> species at Helgoland	39

3.14. Logarithmic abundances of <i>Paralia sulcata</i> at Helgoland	40
3.15. Logarithmic abundances of <i>Porosira glacialis</i> at Helgoland	40
3.16. Logarithmic abundances of <i>Skeletonema costatum</i> at Helgoland	41
3.17. Logarithmic abundances of <i>Thalassionema nitzschioides</i> at Helgoland	41
3.18. Logarithmic abundances of <i>Thalassiosira rotula</i> at Helgoland	42
3.19. Logarithmic abundances of the <i>Ceratium</i> species at Helgoland	43
3.20. Logarithmic abundances of <i>Noctiluca scintillans</i> at Helgoland	44
3.21. Logarithmic abundances of <i>Prorocentrum micans</i> at Helgoland	44
3.22. Logarithmic abundances of <i>Protoperidinium depressum</i> at Helgoland .	45
3.23. Logarithmic abundances of <i>Scrippsiella</i> ssp. at Helgoland	45
3.24. Logarithmic abundances of <i>Torodinium robustum</i> at Helgoland	46
3.25. Logarithmic abundances of <i>Phaeocystis</i> ssp. at Helgoland	46
4.1. Abundance data from <i>C. fusus</i> , upper panel: complete time series of cell counts; middle panel: complete time series of cell counts on a logarithmic scale; lower panel: black - raw cell counts for the year 1976, red - smoothed cell counts for the year 1976	48
4.2. Histogram of the temperatures where <i>Ceratium fusus</i> is present in red; histogram of the temperature for the whole time series in blue . .	50
4.3. Histogram of temperatures weighted with the species abundance for <i>C. fusus</i>	51
4.4. Histogram of temperatures at the local maxima for <i>C. fusus</i> . Only local maxima higher than the acceptance threshold of 1% from the global maximum were taken into account	53
4.5. Illustration of an inflection point; section of the smoothed abundance curve from <i>Ceratium fusus</i> of the year 1987	55
4.6. Histogram of temperatures at the inflection points for <i>C. fusus</i>	56
4.7. Normalized histograms for the different approaches	57
5.1. (a) Sketch of the empirical ‘all points’ cluster in the space defined by the first two principal components, in (b) the inflection points are highlighted as black circles; reduction to two dimensions with a sketch of principal component 1 vs. principal component 2	60
5.2. Extracted inflection point (black circle) for <i>C. fusus</i> in summer 1987; dotted line: 10% of the annual maximum	62

5.3.	Geometrical view of the PCA; a: original dataset, b: original dataset with the principal components, c: transformed dataset with a projection onto two dimensions	63
5.4.	Explained and cumulative variance for the principal components; dotted line shows the Kaiser-Guttman criterion	65
5.5.	Factor loadings of the first four principal components; Tem: temperature, Sun: sunshine duration, Win: wind speed, Sec: Secchi depth, Sal: salinity, Sil: silicate, Pho: phosphate, DIN: dissolved inorganic nitrogen, CMI: competitive milieu	66
5.6.	‘All points’ cluster projected onto the first three principal components resulting from the PCA; for a better visualization, only two dimensions are shown; all environmental factors were used for this computation	68
5.7.	‘All points’ cluster (grey dots) with highlighted inflection points (black circles)	69
5.8.	‘All points’ cluster (grey dots) with corresponding ellipse (grey ellipse) and highlighted inflection points (black circles) with corresponding ellipse (dark ellipse) for <i>Ceratium fusus</i>	70
5.9.	‘All points’ cluster (for better visualization of the ellipses as very tiny grey dots, same distribution as in Figures 5.7 and 5.8) with corresponding ellipse (grey ellipse) and highlighted inflection points (black circles) with corresponding ellipse (dark ellipse) for two different species.	72
5.10.	Histogram of the null hypothesis resulting from the resampling procedure; black arrow indicates the volume found for the analysed species (<i>Ceratium fusus</i>)	74

5.11.	Upper panel: Simulation of the resampling procedure with the original AP cluster; lines show the different quantiles (grey box in the top), the median, and the mean of the normalized volumes. 10 000 resamples were computed with different numbers of points simulating an artificial inflection points ellipsoid (this number is shown on the x-axis). The volume along the y-axis was normalized to the volume of the AP cluster (CFS: <i>C. fusus</i> , ORG: <i>O. regia</i> , PSL: <i>P. sulcata</i>). The range of specialization is indicated on the right side fenced between values -1 and 1. Lower left panel: Simulation of the resampling procedure with different number of points taken out of an AP cluster subset with constructed volume 0.32, i.e. an artificial species with inflection points concentrated in a small region. Blue lines same as in the top panel, green lines reflect the subsamples, and the black squares identify the type II error of 5% and 1% respectively. Lower right panel: Type II error as a function of the number of points; the two curves correspond to the different acceptance thresholds.	76
5.12.	Simulation of the resampling procedure	81
6.1.	Extracted inflection points without and with logarithmic transformed data for <i>Ceratium fusus</i>	83
6.2.	Factor loadings of the first four PCs for the approach without biological interaction; Tem: temperature, Sun: sunshine duration, Win: wind speed, Sec: Secchi depth, Sal: salinity, Sil: silicate, Pho: phosphate, DIN: dissolved inorganic nitrogen	86
6.3.	Explained and cumulative variance for the eight PCs, dotted line: Kaiser-Guttman rule	86
6.4.	‘All points’ cluster (grey) and highlighted inflection points (black) with the correlation ellipses (same colour) for the approach without biological interaction for <i>Ceratium fusus</i>	87
6.5.	Histogram for the resampling procedure without biological interaction for <i>C. fusus</i> , black arrow points at the volume found for the analysed species	88
6.6.	Simulation of the resampling procedure without biological interaction; abbreviation of the species can be found in Chapter 3	90

6.7. Factor loadings of the first four PCs for the approach without biological interaction and shortened time frame; Tem: temperature, Sun: sunshine duration, Win: wind speed, Sec: Secchi depth, Sal: salinity, Sil: silicate, Pho: phosphate, DIN: dissolved inorganic nitrogen	93
6.8. Explained and cumulative variance for the eight PCs for the approach without biological interaction for <i>Ceratium fusus</i> and the short time series, dotted line: Kaiser-Guttman rule	93
6.9. ‘All points’ clusters (grey) and highlighted inflection points (black) with the correlation ellipses (same colour) for the approach without biological interaction for <i>Ceratium fusus</i> and the short time series . .	94
6.10. Histogram for the resampling procedure without biological interaction for <i>C. fusus</i> , black arrow points at the volume found for the analysed species for the approach without biological interaction and the short time series	95
6.11. Simulation of the resampling procedure without biological interaction and the short time series, abbreviation of the species can be found in Chapter 3	97
6.12. Factor loadings of the first four PCs for the approach with included competitive milieu and the short time series; Tem: temperature, Sun: sunshine duration, Win: wind speed, Sec: Secchi depth, Sal: salinity, Sil: silicate, Pho: phosphate, DIN: dissolved inorganic nitrogen, CMI: competitive milieu	98
6.13. Explained and cumulative variance for the eight PCs for the approach with the competitive milieu and the short time series, dotted line: Kaiser-Guttman rule	98
6.14. ‘All points’ cluster (grey) and highlighted inflection points (black) with the correlation ellipses (same colour) for the approach with the competitive milieu for <i>Ceratium fusus</i> and the short time series . . .	99
6.15. Histogram for the resampling procedure with the competitive milieu and the short time series for <i>C. fusus</i> ; black arrow points at the volume found for the analysed species	100

6.16. Simulation of the resampling procedure with inclusion of the competitive milieu and the short time series; abbreviation of the species can be found in Chapter 3	101
6.17. Factor loadings of the first four PCs in the approach with included zooplankton; Zoo: zooplankton, Tem: temperature, Sun: sunshine duration, Win: wind speed, Sec: Secchi depth, Sal: salinity, Sil: silicate, Pho: phosphate, DIN: dissolved inorganic nitrogen, CMI: competitive milieu	104
6.18. Explained and cumulative variance distributed over the PCs in the approach with included zooplankton; the dotted line shows the Kaiser-Guttman rule	104
6.19. ‘All points’ cluster (grey) and highlighted inflection points (black) with the correlation ellipses (same colour) for the approach with all biotic factors for <i>Ceratium fusus</i> on the short time series	105
6.20. Histogram for the approach with all biotic factors on the short time series; black arrow indicates the volume found for the analysed species	106
6.21. Simulation of the resampling procedure for the approach with included phyto- and zooplankton; abbreviation of the species can be found in Chapter 3	107
6.22. Range of specialization for every approach (x-axis) and every species (colour-coded) from the computed different compositions of the environmental dataset of the previous sections; abbreviation of the species can be found in Chapter 3	111
6.23. Range of specialization for every species (x-axis) and every approach (colour-coded) from the computed different compositions of the environmental dataset of the previous sections; abbreviation of the species can be found in Chapter 3	112
7.1. Mean number of presence days per year for all 115 species plotted against the volume of the ONE ellipsoid; linear regression as dashed line and the corresponding formula is presented in the right upper corner of the graph	136

7.2.	Mean number of inflection points plotted against the volume of the ONE ellipsoid for all 115 species; linear regression as dashed line and the corresponding formula is presented in the right upper corner the graph	138
7.3.	Left panel: ONE volume for every species plotted versus the mean day where these inflection points were found - the line represents a polynomial fit of degree two; middle panel: median volume (black line) of a sliding ellipsoid (details in the text) versus the day of the year with the 5 % and 95 % quantiles (red lines); right panel: median distance (black line) of the sliding ellipsoid's centre from one day to the next (details in the text) versus the day of the year with the 5 % and 95 % quantile (red lines); in the two right-hand panels the thin coloured lines show the results for the single years which were used to calculate the quantiles	141
7.4.	Median variability (black line in the middle panel of Figure 7.3) versus the ONE ellipsoid volume for all 115 species, dashed line: linear regression, the corresponding formula is presented in the right upper corner of the graph	143
8.1.	Cluster corresponding to the results for <i>Paralia sulcata</i> with different markers for the different sections; the cluster centres for each period are marked by the same but bigger respective symbol	147
8.2.	Calculation of the ellipsoids for the different sections for <i>P. sulcata</i> ; grey points and ellipse: 'all points' clusters and correlation ellipses; black circles and ellipses: species-specific inflection points and correlation ellipse; computations were carried out in three dimensions; for better visualization, only two dimensions are shown	149
8.3.	Computation of the 'running' split point analysis for <i>Paralia sulcata</i> with included resampling statistics; red curve: distance of the ellipsoids for <i>P. sulcata</i> ; black curve with symbols: median of the resampling procedure; thin black curve: 5 % and 95 % quantiles of the resampling procedure; green curve: net distance computed as the difference of the species results (red) and the median of the resampling (thick black)	154

9.1. Sketch of the yearly and the global niches; small ellipses are the yearly niches and the large one may be seen as their envelope	160
A.1. Logarithmic abundance of <i>Eucampia zodiacus</i> at Helgoland	165
A.2. Logarithmic abundance of <i>Guinardia delicatula</i> at Helgoland	166
A.3. Logarithmic abundance of <i>Guinardia striata</i> at Helgoland	166
A.4. Logarithmic abundance of <i>Odontella aurita</i> at Helgoland	167
A.5. Logarithmic abundance of <i>Odontella regia</i> at Helgoland	167
A.6. Logarithmic abundance of <i>Odontella rhombus</i> at Helgoland	168
A.7. Logarithmic abundance of <i>Odontella sinensis</i> at Helgoland	168
A.8. Logarithmic abundance of <i>Paralia sulcata</i> at Helgoland	169
A.9. Logarithmic abundance of <i>Porosira glacialis</i> at Helgoland	169
A.10. Logarithmic abundance of <i>Skeletonema costatum</i> at Helgoland	170
A.11. Logarithmic abundance of <i>Thalassionema nitzschioides</i> at Helgoland	170
A.12. Logarithmic abundance of <i>Thalassiosira rotula</i> at Helgoland	171
A.13. Logarithmic abundance of <i>Ceratium fusus</i> at Helgoland	171
A.14. Logarithmic abundance of <i>Ceratium furca</i> at Helgoland	172
A.15. Logarithmic abundance of <i>Ceratium horridum</i> at Helgoland	172
A.16. Logarithmic abundance of <i>Ceratium lineatum</i> at Helgoland	173
A.17. Logarithmic abundance of <i>Ceratium tripos</i> at Helgoland	173
A.18. Logarithmic abundance of <i>Noctiluca scintillans</i> at Helgoland	174
A.19. Logarithmic abundance of <i>Prorocentrum micans</i> at Helgoland	174
A.20. Logarithmic abundance of <i>Protoperidinium depressum</i> at Helgoland	175
A.21. Logarithmic abundance of <i>Scrippsiella</i> ssp. at Helgoland	175
A.22. Logarithmic abundance of <i>Torodinium robustum</i> at Helgoland	176
A.23. Logarithmic abundance of <i>Phaeocystis</i> ssp. at Helgoland	176

References

- Abrantes, F. (1988). Diatom productivity peak and increased circulation during latest Quaternary: Alboran Basin (Western Mediterranean). *Marine Micropaleontology*, 13(1):79–96.
- Al-Azri, A. R., Al-Hashmi, K. A., Al-Habsi, H., Al-Azri, N., and Al-Khusaibi, S. (2015). Abundance of harmful algal blooms in the coastal waters of Oman: 2006–2011. *Aquatic Ecosystem Health & Management*.
- Alkawri, A. and Ramaiah, N. (2010). Spatio-temporal variability of dinoflagellate assemblages in different salinity regimes in the west coast of India. *Harmful Algae*, 9(2):153–162.
- Álvarez-Salgado, X. A., Nieto;Cid, M., Piedracoba, S., Crespo, B. G., Gago, J., Brea, S., Teixeira, I. G., Figueiras, F. G., Garrido, J. L., Rosón, G., Castro, C. G., and Gilcoto, M. (2005). Origin and fate of a bloom of *Skeletonema costatum* during a winter upwelling/downwelling sequence in the Ría de Vigo (NW Spain). *Journal of Marine Research*, 63(6):1127–1149.
- Alves-de Souza, C., Gonzalez, M. T., and Iriarte, J. L. (2008). Functional groups in marine phytoplankton assemblages dominated by diatoms in fjords of southern Chile. *Journal of Plankton Research*, 30(11):1233–1243.
- Arrigo, K., Robinson, D., Worthen, D., Dunbar, R., DiTullio, G., VanWoert, M., and Lizotte, M. (1999). Phytoplankton community structure and the drawdown of nutrients and CO₂ in the southern ocean. *Science*, 283(5400):365–7.
- Aziz, A. and Rahman, M. (2011). New record of planktonic diatoms from the Sundarban Mangrove Forests, Bangladesh. *Bangladesh Journal of Botany*, 40(2):163–169.

- Badylak, S. and Phlips, E. J. (2004). Spatial and temporal patterns of phytoplankton composition in subtropical coastal lagoon, the Indian River Lagoon, Florida, USA. *Journal of Plankton Research*, 26(10):1229–1247.
- Baek, S. H., Kim, D., Son, M., Yun, S. M., and Kim, Y. O. (2015). Seasonal distribution of phytoplankton assemblages and nutrient-enriched bioassays as indicators of nutrient limitation of phytoplankton growth in Gwangyang Bay, Korea. *Estuarine, Coastal and Shelf Science*, 163:265–278.
- Baek, S. H., Shimode, S., and Kikuchi, T. (2007). Reproductive ecology of the dominant dinoflagellate, *Ceratium fusus*, in coastal area of Sagami Bay, Japan. *Journal of Oceanography*, 63(1):35–45.
- Baek, S. H., Shimode, S., and Kikuchi, T. (2008). Growth of dinoflagellates, *Ceratium furca* and *Ceratium fusus* in Sagami Bay, Japan: The role of temperature, light intensity and photoperiod. *Harmful Algae*, 7(2):163–173.
- Baek, S. H., Shimode, S., Shin, K., Han, M. S., and Kikuchi, T. (2009). Growth of dinoflagellates, *Ceratium furca* and *Ceratium fusus* in Sagami Bay, Japan: The role of vertical migration and cell division. *Harmful Algae*, 8(6):843–856.
- Bagheri, S., Turkoglu, M., and Abedini, A. (2014). Phytoplankton and Nutrient Variations in the Iranian Waters of the Caspian Sea (Guilan region) during 2003–2004. *Turkish Journal of Fisheries and Aquatic Sciences*, 14(1):231–245.
- Baliarsingh, S. K., Sahu, B. K., Srichandan, S., Sahu, K. C., Lotliker, A. A., and Kumar, T. S. (2013). Seasonal variation of phytoplankton community in Gopalpur Creek: a tropical tidal backwater ecosystem, East Coast of India. *Indian Journal of Geo-Marine Sciences*, 42(5):622–634.
- Barton, A. D., Pershing, A. J., Litchman, E., Record, N. R., Edwards, K. F., Finkel, Z. V., Kiørboe, T., and Ward, B. A. (2013). The biogeography of marine plankton traits. *Ecology letters*, 16(4):522–34.
- Baudoux, A. C., Noordeloos, A. A. M., Veldhuis, M. J. W., and Brussaard, C. P. D. (2006). Virally induced mortality of *Phaeocystis globosa* during two spring blooms in temperate coastal waters. *Aquatic Microbial Ecology*, 44(3):207–217.

- Bauerfeind, E., Hickel, W., Niermann, U., and Westernhagen, H. V. (1990). Phytoplankton biomass and potential nutrient limitation of phytoplankton development in the southeastern North Sea in spring 1985 and 1986. *Netherlands Journal of Sea Research*, 25(1-2):131–142.
- Beaugrand, G. (2003). Long-term changes in copepod abundance and diversity in the north-east Atlantic in relation to fluctuations in the hydroclimatic environment. *Fisheries Oceanography*, 12(4-5):270–283.
- Beaugrand, G. (2004). The North Sea regime shift: Evidence, causes, mechanisms and consequences. *Progress In Oceanography*, 60(2-4):245–262.
- Beaugrand, G., Edwards, M., Brander, K., Luczak, C., and Ibanez, F. (2008). Causes and projections of abrupt climate-driven ecosystem shifts in the North Atlantic. *Ecology letters*, 11(11):1157–68.
- Beaugrand, G. and Ibanez, F. (2004). Monitoring marine plankton ecosystems. II: Long-term changes in North Sea calanoid copepods in relation to hydro-climatic variability. *Marine Ecology Progress Series*, 284:35–47.
- Bell, K. N. I. (2008). *Analysing Cycles in Biology and Medicine: A Practical Introduction to Circular Variables and Periodic Regression*. Razorbill Press, 2nd edition.
- Boersma, M., Grüner, N., Tasso Signorelli, N., Montoro González, P. E., Peck, M. A., and Wiltshire, K. H. (2016). Projecting effects of climate change on marine systems: is the mean all that matters? *Proceedings of the Royal Society B: Biological Sciences*, 283(1823):20152274.
- Boyd, P. W., Rynearson, T. A., Armstrong, E. A., Fu, F., Hayashi, K., Hu, Z., Hutchins, D. A., Kudela, R. M., Litchman, E., Mulholland, M. R., Passow, U., Strzepek, R. F., Whittaker, K. A., Yu, E., and Thomas, M. K. (2013). Marine phytoplankton temperature versus growth responses from polar to tropical waters—outcome of a scientific community-wide study. *PloS one*, 8(5):e63091.

- Brandt, G. and Wirtz, K. W. (2010). Interannual variability of alongshore spring bloom dynamics in a coastal sea caused by the differential influence of hydrodynamics and light climate. *Biogeosciences*, 7(1):371–386.
- Brandt, S. (1999). *Datenanalyse*. Spektrum Akademischer Verlag, 4th edition.
- Bresnan, E., Hay, S., Hughes, S., Fraser, S., Rasmussen, J., Webster, L., Slesser, G., Dunn, J., and Heath, M. (2009). Seasonal and interannual variation in the phytoplankton community in the north east of Scotland. *Journal of Sea Research*, 61(1-2):17–25.
- Breton, E., Rousseau, V., Parent, J.-Y., Ozer, J., and Lancelot, C. (2006). Hydroclimatic modulation of diatom/Phaeocystis blooms in nutrient-enriched Belgian coastal waters (North Sea). *Limnology and Oceanography*, 51(3):1401–1409.
- Brun, P., Vogt, M., Payne, M. R., Gruber, N., O'Brien, C. J., Buitenhuis, E. T., Le Quéré, C., Leblanc, K., and Luo, Y.-W. (2015). Ecological niches of open ocean phytoplankton taxa. *Limnology and Oceanography*, 60(3):1020–1038.
- Brussaard, C. P. D. (2004). Viral Control of Phytoplankton Populations—a Review. *The Journal of Eukaryotic Microbiology*, 51(2):125–138.
- Buskey, E. J., Strom, S., and Coulter, C. (1992). Bioluminescence of heterotrophic dinoflagellates from Texas coastal waters. *Journal of Experimental Marine Biology and Ecology*, 159(1):37–49.
- Cardoso, L. d. S. (2012). Bloom of *Noctiluca scintillans* (Macartney) Kofoid & Swezy (Dinophyceae) in southern Brazil. *Brazilian Journal of Oceanography*, 60(2):265–268.
- Cattell, R. (1966). The Scree Test For The Number Of Factors. *Multivariate Behavioral Research*, 1(2):245–276.
- Choudhury, A. K. and Pal, R. (2009). Phytoplankton and nutrient dynamics of shallow coastal stations at Bay of Bengal, Eastern Indian coast. *Aquatic Ecology*, 44(1):55–71.

- Cloern, J. E. and Dufford, R. (2005). Phytoplankton community ecology: principles applied in San Francisco Bay. *Marine Ecology Progress Series*, 285:11–28.
- Colwell, R. K. and Futuyma, D. J. (1971). On the Measurement of Niche Breadth and Overlap. *Ecology*, 52(4):567–576.
- Comon, P. (1994). Independent component analysis, A new concept? *Signal Processing*, 36(3):287–314.
- Darwin, C. (1859). *On the origin of species by means of natural selection, or the preservation of favoured races in the struggle for life*. John Murray, London, 1st edition.
- Davies, A. G. and Sleep, J. A. (1989). The photosynthetic response of nutrient-depleted dilute cultures of *Skeletonema costatum* to pulses of ammonium and nitrate; the importance of phosphate. *Journal of Plankton Research*, 11(1):141–164.
- Dela-Cruz, J., Middleton, J. H., and Suthers, I. M. (2007). The influence of upwelling, coastal currents and water temperature on the distribution of the red tide dinoflagellate, *Noctiluca scintillans*, along the east coast of Australia. *Hydrobiologia*, 598(1):59–75.
- DeYoung, B., Barange, M., Beaugrand, G., Harris, R., Perry, R. I., Scheffer, M., and Werner, F. (2008). Regime shifts in marine ecosystems: detection, prediction and management. *Trends in ecology & evolution*, 23(7):402–9.
- Dhib, A., Frossard, V., Turki, S., and Aleya, L. (2013). Dynamics of harmful dinoflagellates driven by temperature and salinity in a northeastern Mediterranean lagoon. *Environmental monitoring and assessment*, 185(4):3369–82.
- Díaz, S., Purvis, A., Cornelissen, J. H. C., Mace, G. M., Donoghue, M. J., Ewers, R. M., Jordano, P., and Pearse, W. D. (2013). Functional traits, the phylogeny of function, and ecosystem service vulnerability. *Ecology and evolution*, 3(9):2958–75.

- Dickson, R. R., Meincke, J., Malmberg, S.-A., and Lee, A. J. (1988). The “great salinity anomaly” in the Northern North Atlantic 1968–1982. *Progress In Oceanography*, 20(2):103–151.
- Dodge, J. D. and Marshall, H. G. (1994). Biogeographic analysis of the armored planktonic dinoflagellate *Ceratium* in the North Atlantic and adjacent seas. *Journal of Phycology*, 30(6):905–922.
- Dolédec, S., Chessel, D., and Gimaret-Carpentier, C. (2000). Niche separation in community analysis: A new Method. *Ecology*, 81(10):2914–2927.
- Drebes, G., Kühn, S. F., Gmelch, A., and Schnepf, E. (1996). *Cryothecomonas aestivalis* sp. nov., a colourless nanoflagellate feeding on the marine centric diatom *Guinardia delicatula* (Cleve) Hasle. *Helgoländer Meeresuntersuchungen*, 50(4):497–515.
- Du, X. and Peterson, W. T. (2013). Seasonal Cycle of Phytoplankton Community Composition in the Coastal Upwelling System Off Central Oregon in 2009. *Estuaries and Coasts*, 37(2):299–311.
- Du Yoo, Y., Jeong, H. J., Kim, M. S., Kang, N. S., Song, J. Y., Shin, W., Kim, K. Y., and Lee, K. (2009). Feeding by phototrophic red-tide dinoflagellates on the ubiquitous marine diatom *Skeletonema costatum*. *The Journal of eukaryotic microbiology*, 56(5):413–20.
- Eashwar, M., Nallathambi, T., Kuberaraj, K., and Govindarajan, G. (2001). *Noctiluca* blooms in Port Blair Bay, Andamans. *Current Science*, 81(2):203–206.
- Edwards, M., Beaugrand, G., Reid, P. C., Rowden, A. A., and Jones, M. B. (2002). Ocean climate anomalies and the ecology of the North Sea. *Marine Ecology Progress Series*, 239:1–10.
- Elton, C. (1971). *Animal Ecology*. Methuen & Co. Ltd, London (first published 1927, this is an unchanged reprint).

-
- Fabbro, L. D. and Duivenvoorden, L. J. (2000). A two-part model linking multidimensional environmental gradients and seasonal succession of phytoplankton assemblages. *Hydrobiologia*, 438(1-3):13–24.
- Falkowski, P. (2012). Ocean Science: The power of plankton. *Nature*, 483(7387):S17–20.
- Feinsinger, P., Spears, E. E., and Poole, R. W. (1981). A simple measure of niche breadth. *Ecology*, 62(1):27–32.
- Feki-Sahnoun, W., Hamza, A., Mahfoudi, M., Rebai, A., and Hassen, M. B. (2014). Long-term microphytoplankton variability patterns using multivariate analyses: ecological and management implications. *Environmental science and pollution research*, 21(19):11481–99.
- Fernandes, L. F. and Brandini, F. P. (2004). Diatom associations in shelf waters off Paraná State, Southern Brazil: annual variation in relation to environmental factors. *Brazilian Journal of Oceanography*, 52(1):19–34.
- Figueiras, F. and Pazos, Y. (1991). Microplankton assemblages in three Bias Baixas (Vigo, Arosa and Muros, Spain) with a subsurface chlorophyll maximum: their relationships to hydrography. *Marine Ecology Progress Series*, 76(3):219–233.
- Fock, H. and Greve, W. (2002). Analysis and interpretation of recurrent spatio-temporal patterns in zooplankton dynamics: a case study on *Noctiluca scintillans* (Dinophyceae) in the German Bight (North Sea). *Marine Biology*, 140(1):59–73.
- Fogg, G. E. (1991). The phytoplanktonic ways of life. *New Phytologist*, 118(2):191–232.
- Fonda Umani, S., Beran, A., Parlato, S., Virgilio, D., Zollet, T., Olazabal, A. D., Lazzarini, B., and Cabrini, M. (2004). *Noctiluca scintillans* MACARTNEY in the Northern Adriatic Sea: long-term dynamics, relationships with temperature and eutrophication, and role in the food web. *Journal of Plankton Research*, 26(5):545–561.

- Franke, H.-D., Buchholz, F., and Wiltshire, K. H. (2004). Ecological long-term research at Helgoland (German Bight, North Sea): retrospect and prospect - an introduction. *Helgoland Marine Research*, 58(4):223–229.
- Franke, H.-D. and Gutow, L. (2004). Long-term changes in the macrozoobenthos around the rocky island of Helgoland (German Bight, North Sea). *Helgoland Marine Research*, 58(4):303–310.
- Franks, P. (2002). NPZ Models of Plankton Dynamics: Their Construction, Coupling to Physics, and Application. *Journal of Oceanography*, 58(2):379–387.
- Freund, J. A., Grüner, N., Brüse, S., and Wiltshire, K. (2012). Changes in the phytoplankton community at Helgoland, North Sea: lessons from single spot time series analyses. *Marine Biology*, 159(11, SI):2561–2571.
- Futuyma, D. J. and Moreno, G. (1988). The evolution of ecological specialization. *Annual Review of Ecology and Systematics*, 19(20):207–233.
- Gao, Y., Jiang, Z., Liu, J., Chen, Q., Zeng, J., and Huang, W. (2013). Seasonal variations of net-phytoplankton community structure in the southern Yellow Sea. *Journal of Ocean University of China*, 12(4):557–567.
- Gárate-Lizárraga, I. and Muciño-Márquez, R. E. (2013). New data on the distribution of *Torodinium robustum* and *T. teredo* (Dinophyceae: Gymnodiniales) in the Gulf of California. *Check List*, 9(4):809.
- Gayoso, A. M. (1999). Seasonal Succession Patterns of Phytoplankton in the Bahía Blanca Estuary (Argentina). *Botanica Marina*, 42(4):367–375.
- Gayoso, A. M. (2001). Observations on *Alexandrium tamarense* (Lebour) Balech and Other Dinoflagellate Populations in Golfo Nuevo, Patagonia (Argentina). *Journal of Plankton Research*, 23(5):463–468.
- Gebühr, C. (2010). *Investigations on the ecology of the marine centric diatom *Paralia sulcata* at Helgoland Roads, North Sea, Germany*. PhD thesis, Jacobs University.

- Gebühr, C., Wiltshire, K. H., Aberle, N., van Beusekom, J. E. E., and Gerdts, G. (2009). Influence of nutrients, temperature, light and salinity on the occurrence of *Paralia sulcata* at Helgoland Roads, North Sea. *Aquatic Biology*, 7:185–197.
- Gerdts, G., Wichels, A., Döpke, H., Klings, K.-W., Gunkel, W., and Schütt, C. (2004). 40-year long-term study of microbial parameters near Helgoland (German Bight, North Sea): historical view and future perspectives. *Helgoland Marine Research*, 58(4):230–242.
- Gillbricht, M. (1988). Phytoplankton and nutrients in the Helgoland region. *Helgoland Marine Research*, 42(3):435–467.
- Godhe, A., Narayanaswamy, C., Klais, R., Moorthy, K. V., Ramesh, R., Rai, A., and Reddy, H. V. (2015). Long-term patterns of net phytoplankton and hydrography in coastal SE Arabian Sea: What can be inferred from genus level data? *Estuarine, Coastal and Shelf Science*, 162:69–75.
- Godhe, A., Noren, F., Kuylenstierna, M., Ekberg, C., and Karlson, B. (2001). Relationship between planktonic dinoflagellate abundance, cysts recovered in sediment traps and environmental factors in the Gullmar Fjord, Sweden. *Journal of Plankton Research*, 23(9):923–938.
- Godrijan, J., Marić, D., Tomažić, I., Precali, R., and Pfannkuchen, M. (2013). Seasonal phytoplankton dynamics in the coastal waters of the north-eastern Adriatic Sea. *Journal of Sea Research*, 77:32–44.
- Gómez, F. and Souissi, S. (2010). The diatoms *Odontella sinensis*, *Coscinodiscus wailesii* and *Thalassiosira punctigera* in the European Atlantic: recent introductions or overlooked in the past? *Fresenius Environmental Bulletin*, 19(8):1424–1433.
- Gowen, R. (1999). Are copepods important grazers of the spring phytoplankton bloom in the western Irish Sea? *Journal of Plankton Research*, 21(3):465–483.
- Green, R. H. (1971). A Multivariate Statistical Approach to the Hutchinsonian Niche: Bivalve Molluscs of Central Canada. *Ecology*, 52(4):543.

- Green, R. H. (1974). Multivariate Niche Analysis with Temporally Varying Environmental Factors. *Ecology*, 55(1):73.
- Greve, W., Reiners, F., Nast, J., and Hoffmann, S. (2004). Helgoland Roads meso- and macrozooplankton time-series 1974 to 2004: lessons from 30 years of single spot, high frequency sampling at the only off-shore island of the North Sea. *Helgoland Marine Research*, 58(4):274–288.
- Gribble, K. E., Nolan, G., and Anderson, D. M. (2007). Biodiversity, biogeography and potential trophic impact of *Protoperidinium* spp. (Dinophyceae) off the southwestern coast of Ireland. *Journal of Plankton Research*, 29(11):931–947.
- Grinnell, J. (1914). An account of the mammals and birds of the lower Colorado Valley, with especial reference to the distributional problems presented. *University of California Publications in Zoology*, 12(4):226–304.
- Grinnell, J. (1917). The Niche-Relationships of the California Thrasher. *The Auk*, 34(4):427 – 433.
- Grüner, N., Gebühr, C., Boersma, M., Feudel, U., Wiltshire, K. H., and Freund, J. A. (2011). Reconstructing the realized niche of phytoplankton species from environmental data: fitness versus abundance approach. *Limnology and Oceanography: Methods*, 9:432–442.
- Guilloux, L., Rigaut-Jalabert, F., Jouenne, F., Ristori, S., Viprey, M., Not, F., Vault, D., and Simon, N. (2013). An annotated checklist of Marine Phytoplankton taxa at the SOMLIT-Astan time series off Roscoff (Western English Channel, France): data collected from 2000 to 2010. *Cahiers de Biologie Marine*, 54(2):247–256.
- Guinder, V. A., Popovich, C. A., Molinero, J. C., and Marcovecchio, J. (2013). Phytoplankton summer bloom dynamics in the Bahía Blanca Estuary in relation to changing environmental conditions. *Continental Shelf Research*, 52:150–158.
- Gul, S. and Nawaz, M. F. (2014). The Dinoflagellate Genera *Protoperidinium* and *Podolampas* from Pakistan’s Shelf and Deep Sea Vicinity (North Arabian Sea). *Turkish Journal of Fisheries and Aquatic Sciences*, 14(1):91–100.

-
- Gutiérrez-Rodríguez, A., Latasa, M., Scharek, R., Massana, R., Vila, G., and Gasol, J. M. (2011). Growth and grazing rate dynamics of major phytoplankton groups in an oligotrophic coastal site. *Estuarine, Coastal and Shelf Science*, 95(1):77–87.
- Guttman, L. (1954). Some necessary conditions for common-factor analysis. *Psychometrika*, 19(2):149–161.
- Haaber, J. and Middelboe, M. (2009). Viral lysis of *Phaeocystis pouchetii*: implications for algal population dynamics and heterotrophic C, N and P cycling. *The ISME journal*, 3(4):430–41.
- Haeckel, E. (1866). *Generelle Morphologie der Organismen. Allgemeine Grundzüge der organischen Formen-Wissenschaft, mechanisch begründet durch die von Charles Darwin reformirte Descendenz-Theorie*. Generelle morphologie der organismen. G. Reimer, Berlin, Germany, bd. 2 edition.
- Hagmeier, E. (1998). Aus der Geschichte der Biologischen Anstalt Helgoland (BAH). *Helgoländer Meeresuntersuchungen*, 52(S1):2–105.
- Hai, D.-N., Lam, N.-N., and Dippner, J. W. (2010). Development of *Phaeocystis globosa* blooms in the upwelling waters of the South Central coast of Viet Nam. *Journal of Marine Systems*, 83(3-4):253–261.
- Haigh, R., Taylor, F., and Sutherland, T. (1992). Phytoplankton ecology of Sechart Inlet, a fjord system on the British Columbia coast. I. General features of the nano- and microplankton. *Marine Ecology Progress Series*, 89(2-3):117–134.
- Hallegraeff, G. M. (1984). Species of the Diatom Genus *Thalassiosira* in Australian Waters. *Botanica Marina*, 27(11):495–513.
- Hamm, C. (2000). Architecture, ecology and biogeochemistry of *Phaeocystis* colonies. *Journal of Sea Research*, 43(3-4):307–315.
- Handl, A. (2002). *Multivariate Analysemethoden*. Springer, Berlin.
- Harris, A., Medlin, L., Lewis, J., and Jones, K. (1995). *Thalassiosira* species (Bacillariophyceae) from a Scottish sea-loch. *European Journal of Phycology*, 30(2):117–131.

- Hausser, J. (1995). *Säugetiere der Schweiz. Mammifères de la Suisse. Mammiferi della Svizzera*. Birkhäuser Verlag, Berlin, Germany, 1st edition.
- Heino, J. and Soininen, J. (2006). Regional occupancy in unicellular eukaryotes: a reflection of niche breadth, habitat availability or size-related dispersal capacity? *Freshwater Biology*, 51(4):672–685.
- Helaouët, P., Beaugrand, G., and Edwards, M. (2013). Understanding long-term changes in species abundance using a niche-based approach. *PloS one*, 8(11):e79186.
- Hernández Fariñas, T., Bacher, C., Soudant, D., Belin, C., and Barillé, L. (2015). Assessing phytoplankton realized niches using a French national phytoplankton monitoring network. *Estuarine, Coastal and Shelf Science*, 159:15–27.
- Hernandez-Farinas, T., Soudant, D., Barille, L., Belin, C., Lefebvre, A., and Bacher, C. (2013). Temporal changes in the phytoplankton community along the French coast of the eastern English Channel and the southern Bight of the North Sea. *ICES Journal of Marine Science*, 71(4):821–833.
- Hesse, K.-J., Liu, Z., and Schaumann, K. (1989). Phytoplankton and fronts in the German Bight. *Scientia Marina*, 53:187–196.
- Hickel, W. (1998). Temporal variability of micro- and nanoplankton in the German Bight in relation to hydrographic structure and nutrient changes. *ICES Journal of Marine Science*, 55(4):600–609.
- Hinder, S. L., Hays, G. C., Edwards, M., Roberts, E. C., Walne, A. W., and Gravenor, M. B. (2012). Changes in marine dinoflagellate and diatom abundance under climate change. *Nature Climate Change*, 2(4):271–275.
- Hobson, L. and McQuoid, M. (1997). Temporal variations among planktonic diatom assemblages in a turbulent environment of the southern Strait of Georgia, British Columbia, Canada. *Marine Ecology Progress Series*, 150(1-3):263–274.

-
- Hobson, L. and McQuoid, M. (2001). Pelagic diatom assemblages are good indicators of mixed water intrusions into Saanich Inlet, a stratified fjord in Vancouver Island. *Marine Geology*, 174(1-4):125–138.
- Höglander, H., Larsson, U., and Hajdu, S. (2004). Vertical distribution and settling of spring phytoplankton in the offshore NW Baltic Sea proper. *Marine Ecology Progress Series*, 283:15–27.
- Hooper, H. L., Connon, R., Callaghan, A., Fryer, G., Yarwood-Buchanan, S., Biggs, J., Maund, S. J., Hutchinson, T. H., and Sibly, R. M. (2008). The ecological niche of *Daphnia magna* characterized using population growth rate. *Ecology*, 89(4):1015–1022.
- Hoppenrath, M. (2004). A revised checklist of planktonic diatoms and dinoflagellates from Helgoland (North Sea, German Bight). *Helgoland Marine Research*, 58(4):243–251.
- Hoppenrath, M., Beszteri, B., Drebes, G., Halliger, H., Van Beusekom, J. E. E., Janisch, S., and Wiltshire, K. H. (2007). *Thalassiosira* species (Bacillariophyceae, Thalassiosirales) in the North Sea at Helgoland (German Bight) and Sylt (North Frisian Wadden Sea) - a first approach to assessing diversity. *European Journal of Phycology*, 42(3):271–288.
- Hoppenrath, M., Elbrächter, M., and Drebes, G. (2009). *Marine Phytoplankton: Selected Microphytoplankton Species from the North Sea Around Helgoland and Sylt*. Schweizerbart'sche Verlagsbuchhandlung, Stuttgart.
- Huang, C. and Qi, Y. (1997). The abundance cycle and influence factors on red tide phenomena of *Noctiluca scintillans* (Dinophyceae) in Dapeng Bay, the South China Sea. *Journal of Plankton Research*, 19(3):303–318.
- Huo, W. Y., Yu, Z. M., Zou, J. Z., Song, X. X., and Hao, J. H. (2001). Outbreak of *Skeletonema costatum* red tide and its relations to environmental factors in Jiaozhou Bay. *Ocean. Limnol. Sinica*, 32:311–318.

- Huseby, S., Degerlund, M., Eriksen, G. K., Ingebrigtsen, R. A., Eilertsen, H. C., and Hansen, E. (2013). Chemical diversity as a function of temperature in six northern diatom species. *Marine drugs*, 11(11):4232–45.
- Hutchinson, G. E. (1957). Concluding Remarks - Cold Spring Harbour Symposium. *Quantitative Biology*, 22:415–427.
- Hutchinson, G. E. (1978). *An Introduction to Population Ecology*. Yale University Press.
- Huthnance, J. (1991). Physical oceanography of the North Sea. *Ocean and Shoreline Management*, 16(3-4):199–231.
- Hyun, B., Choi, K.-H., Jang, P.-G., Jang, M.-C., Lee, W.-J., Moon, C.-H., and Shin, K. (2014). Effects of Increased CO₂ and Temperature on the Growth of Four Diatom Species (*Chaetoceros debilis*, *Chaetoceros didymus*, *Skeletonema costatum* and *Thalassiosira nordenskiöldii*) in Laboratory Experiments. *Journal of Environmental Science International*, 23(6):1003–1012.
- ICES (1983). Flushing times of the North Sea. *Cooperative Research Report 123*.
- Ignatiades, L. (1994). Species dominance and niche breadth in bloom and non-bloom phytoplankton populations. *Oceanologica Acta*, 17(1):89–96.
- Ignatiades, L. and Gotsis-Skretas, O. (2014). The contribution of rare species to coastal phytoplankton assemblages. *Marine Ecology*, 35(1):132–145.
- Ilyash, L. V. and Matorin, D. N. (2007). Features of the spatial distribution of phytoplankton in Nhatrang Bay of the South China Sea during the rainy season. *Oceanology*, 47(6):788–796.
- Ionita, M., Lohmann, G., Rimbu, N., and Wiltshire, K. (2008). The influence of large-scale atmospheric circulation on the variability of salinity at Helgoland Roads station. *Tellus A*, 60(5).
- Irwin, A. J., Nelles, A. M., and Finkel, Z. V. (2012). Phytoplankton niches estimated from field data. *Limnology and Oceanography*, 57(3):787–797.

-
- Jeong, H. J., Yoo, Y. D., Kim, J. S., Seong, K. A., Kang, N. S., and Kim, T. H. (2010). Growth, feeding and ecological roles of the mixotrophic and heterotrophic dinoflagellates in marine planktonic food webs. *Ocean Science Journal*, 45(2):65–91.
- Ji, R., Edwards, M., Mackas, D. L., Runge, J. A., and Thomas, A. C. (2010). Marine plankton phenology and life history in a changing climate: current research and future directions. *Journal of plankton research*, 32(10):1355–1368.
- Johnson, R. H. (1910). *Determinate evolution in the color-pattern of the lady-beetles*. Carnegie Institution of Washington, Washington, DC.
- Jolliffe, I. T. (2002). *Principal component analysis*. Springer, New York, 2nd edition.
- Jordan, R. and Chamberlain, A. (1997). Biodiversity among haptophyte algae. *Biodiversity and Conservation*, 6(1):131–152.
- Kaiser, H. (1960). The application of electronic computer to factor analysis. *Educ. Psychol. Meas.*, 20:141–151.
- Karentz, D. and Smayda, T. (1984). Temperature and seasonal occurrence patterns of 30 dominant phytoplankton species in Narragansett Bay over a 22-year period (1959-1980). *Marine Ecology Progress Series*, 18(3):277–293.
- Kjørboe, T. (2003). High turnover rates of copepod fecal pellets due to *Noctiluca scintillans* grazing. *Marine Ecology Progress Series*, 258:181–188.
- Kjørboe, T., Lundsgaard, C., Olesen, M., and Hansen, J. L. S. (1994). Aggregation and sedimentation processes during a spring phytoplankton bloom: A field experiment to test coagulation theory. *Journal of Marine Research*, 52(2):297–323.
- Kjørboe, T. and Titelman, J. (1998). Feeding, prey selection and prey encounter mechanisms in the heterotrophic dinoflagellate *Noctiluca scintillans*. *Journal of Plankton Research*, 20(8):1615–1636.
- Kjaeret, A., Naustvoll, L., and Paasche, E. (2000). Ecology of the heterotrophic dinoflagellate genus *Protoperdinium* in the inner Oslofjord (Norway). *SARSIA*, 85(5-6):453–460.

- Kopczyńska, E. E., Fiala, M., and Jeandel, C. (1998). Annual and interannual variability in phytoplankton at a permanent station off Kerguelen Islands, Southern Ocean. *Polar Biology*, 20(5):342–351.
- Kraberg, A., Baumann, M., and Dürselen, C. D. (2010). *Coastal Phytoplankton: Photo Guide for Northern European Seas*. Pfeil, München.
- Kraberg, A. C., Wasmund, N., Vanaverbeke, J., Schiedek, D., Wiltshire, K. H., and Mieszkowska, N. (2011). Regime shifts in the marine environment: the scientific basis and political context. *Marine pollution bulletin*, 62(1):7–20.
- Krawiec, R. W. (1982). Autecology and clonal variability of the marine centric diatom *Thalassiosira rotula* (Bacillariophyceae) in response to light, temperature and salinity. *Marine Biology*, 69(1):79–89.
- Lassen, M. K., Nielsen, K. D., Richardson, K., Garde, K., and Schlüter, L. (2010). The effects of temperature increases on a temperate phytoplankton community — A mesocosm climate change scenario. *Journal of Experimental Marine Biology and Ecology*, 383(1):79–88.
- Lee, A. J. (1980). North Sea: Physical Oceanography. In Banner, F. T., Collins, M. B., and Massie, K. S., editors, *The North-West European Shelf Seas: the Sea Bed and the Sea in Motion II. Physical and chemical oceanography, and physical resources*, pages 467–493. Elsevier.
- Lee, J. K. and Hirayama, K. (1992). Effects of salinity, food level and temperature on the population growth of *Noctiluca scintillans* (Macartney). *Bulletin of the Faculty of Fisheries - Nagasaki University (Japan)*, 71:163–168.
- Lees, K., Pitois, S., Scott, C., Frid, C., and Mackinson, S. (2006). Characterizing regime shifts in the marine environment. *Fish and Fisheries*, 7(2):104–127.
- Lindeboom, H., Raaphorst, W., Beukema, J., Cadée, G., and Swennen, C. (1995). (Sudden) Changes in the North Sea and Wadden Sea: oceanic influences underestimated? *Deutsche Hydrographische Zeitschrift*, (2):86–100.

-
- Litchman, E., Edwards, K., Klausmeier, C., and Thomas, M. (2012). Phytoplankton niches, traits and eco-evolutionary responses to global environmental change. *Marine Ecology Progress Series*, 470:235–248.
- Litchman, E. and Klausmeier, C. A. (2008). Trait-Based Community Ecology of Phytoplankton. *Annual Review of Ecology, Evolution, and Systematics*, 39(1):615–639.
- Liu, D., Shen, X., Di, B., Shi, Y., Keesing, J., and Wang, Y. (2013). Palaeoecological analysis of phytoplankton regime shifts in response to coastal eutrophication. *Marine Ecology Progress Series*, 475:1–14.
- Liu, H. and Sun, J. (2015). Netz-Phytoplankton Diversity in the western and southern regions of the South China Sea. *Oceanological and Hydrobiological Studies*, 44(4):530–538.
- Llewellyn, C. A., Tarran, G. A., Galliene, C. P., Cummings, D. G., De Menezes, A., Rees, A. P., Dixon, J. L., Widdicombe, C. E., Fileman, E. S., and Wilson, W. H. (2008). Microbial dynamics during the decline of a spring diatom bloom in the Northeast Atlantic. *Journal of Plankton Research*, 30(3):261–273.
- Löder, M. G. J., Kraberg, A. C., Aberle, N., Peters, S., and Wiltshire, K. H. (2011). Dinoflagellates and ciliates at Helgoland Roads, North Sea. *Helgoland Marine Research*, pages 1–13.
- Loebl, M., Colijn, F., van Beusekom, J. E., Baretta-Bekker, J. G., Lancelot, C., Philippart, C. J., Rousseau, V., and Wiltshire, K. H. (2009). Recent patterns in potential phytoplankton limitation along the Northwest European continental coast. *Journal of Sea Research*, 61(1-2):34–43.
- Lorenzen, C. J. (1972). Extinction of Light in the Ocean by Phytoplankton. *ICES Journal of Marine Science*, 34(2):262–267.
- Lunven, M., Guillaud, J. F., Youéno, A., Crassous, M. P., Berric, R., Le Gall, E., Kérouel, R., Labry, C., and Aminot, A. (2005). Nutrient and phytoplankton distribution in the Loire River plume (Bay of Biscay, France) resolved by a new Fine Scale Sampler. *Estuarine, Coastal and Shelf Science*, 65(1-2):94–108.

- MacGillivray, M. L. and Kaczmarska, I. (2012). Genetic differentiation within the *Paralia longispina* (Bacillariophyta) species complex. *Botany*, 90(3):205–222.
- Mallin, M. A. (1994). Phytoplankton Ecology of North Carolina Estuaries. *Estuaries*, 17(3):561.
- McGarigal, K., Cushman, S., and Stafford, S. (2000). *Multivariate statistics for wildlife and ecology research*. Springer, New York, 1st edition.
- McGill, B. J., Enquist, B. J., Weiher, E., and Westoby, M. (2006). Rebuilding community ecology from functional traits. *Trends in ecology & evolution*, 21(4):178–85.
- McQuoid, M. (2000). The tythropelagic diatom, *Paralia sulcata*, as paleoindicator species in coastal marine environments. *Journal of Phycology*, 36(s3):47.
- McQuoid, M. and Nordberg, K. (2003). The diatom *Paralia sulcata* as an environmental indicator species in coastal sediments. *Estuarine, Coastal and Shelf Science*, 56(2):339–354.
- Menden-Deuer, S., Lessard, E., Satterberg, J., and Grünbaum, D. (2005). Growth rates and starvation survival of three species of the pallium-feeding, thecate dinoflagellate genus *Protoperidinium*. *Aquatic Microbial Ecology*, 41(2):145–152.
- Metropolis, N. and Ulam, S. (1949). The Monte Carlo Method. *Journal of the American Statistical Association*, 44(247):335–341.
- Mieruch, S., Freund, J., Feudel, U., Boersma, M., Janisch, S., and Wiltshire, K. (2010). A new method of describing phytoplankton blooms: Examples from Helgoland Roads. *Journal of Marine Systems*, 79(1-2):36–43.
- Miyaguchi, H., Fujiki, T., Kikuchi, T., Kuwahara, V. S., and Toda, T. (2006). Relationship between the bloom of *Noctiluca scintillans* and environmental factors in the coastal waters of Sagami Bay, Japan. *Journal of Plankton Research*, 28(3):313–324.

-
- Munir, S., Burhan, Z.-u.-n., Naz, T., Siddiqui, P. J. A., and Morton, S. L. (2013). Morphotaxonomy and seasonal distribution of planktonic and benthic *Prorocentrales* in Karachi waters, Pakistan Northern Arabian Sea. *Chinese Journal of Oceanology and Limnology*, 31(2):267–281.
- Newsome, S. D., Martinez del Rio, C., Bearhop, S., and Phillips, D. L. (2007). A niche for isotopic ecology. *Frontiers in Ecology and the Environment*, 5(8):429–436.
- Ninčević-Gladan, Ž., Bužančić, M., Kušpilić, G., Grbec, B., Matijević, S., Skejić, S., Marasović, I., and Morović, M. (2015). The response of phytoplankton community to anthropogenic pressure gradient in the coastal waters of the eastern Adriatic Sea. *Ecological Indicators*, 56:106–115.
- Nishikawa, T. and Yamaguchi, M. (2006). Effect of temperature on light-limited growth of the harmful diatom *Eucampia zodiacus* Ehrenberg, a causative organism in the discoloration of *Porphyra thalli*. *Harmful Algae*, 5(2):141–147.
- Nöthig, E.-M., Bracher, A., Engel, A., Metfies, K., Niehoff, B., Peeken, I., Bauerfeind, E., Cherkasheva, A., Gäbler-Schwarz, S., Hardge, K., Kiliyas, E., Kraft, A., Mebrahtom Kidane, Y., Lalande, C., Piontek, J., Thomisch, K., and Wurst, M. (2015). Summertime plankton ecology in Fram Strait—a compilation of long- and short-term observations. *Polar Research*, 34(23349).
- Obrezkova, M. S., Kolesnik, A. N., and Semiletov, I. P. (2015). The diatom distribution in the surface sediments of the Eastern Arctic seas of Russia. *Russian Journal of Marine Biology*, 40(6):465–472.
- Olguín, H. F. and Alder, V. A. (2011). Species composition and biogeography of diatoms in antarctic and subantarctic (Argentine shelf) waters (37–76°S). *Deep Sea Research Part II: Topical Studies in Oceanography*, 58(1-2):139–152.
- Ostenfeld, C. H. (1909). Immigration of a Plankton Diatom into a quite new Area within recent years; *Biddulphia sinensis* in the North Sea Waters. *Internationale Revue der gesamten Hydrobiologie und Hydrographie*, 2(3):362–374.

- Paul, C., Barofsky, A., Vidoudez, C., and Pohnert, G. (2009). Diatom exudates influence metabolism and cell growth of co-cultured diatom species. *Marine Ecology Progress Series*, 389:61–70.
- Peacock, E., Olson, R., and Sosik, H. (2014). Parasitic infection of the diatom *Guinardia delicatula*, a recurrent and ecologically important phenomenon on the New England Shelf. *Marine Ecology Progress Series*, 503:1–10.
- Peperzak, L., Colijn, F., Gieskes, W. W. C., and Peeters, J. C. H. (1998). Development of the diatom-Phaeocystis spring bloom in the Dutch coastal zone of the North Sea: the silicon depletion versus the daily irradiance threshold hypothesis. *Journal of Plankton Research*, 20(3):517–537.
- Peterson, G., Allen, C. R., and Holling, C. S. (1998). Original Articles: Ecological Resilience, Biodiversity, and Scale. *Ecosystems*, 1(1):6–18.
- Pierce, L. L. and Running, S. W. (1988). Rapid Estimation of Coniferous Forest Leaf Area Index Using a Portable Integrating Radiometer. *Ecology*, 69(6):1762–1767.
- Pither, J. and Aarssen, L. W. (2005). Environmental specialists: their prevalence and their influence on community-similarity analyses. *Ecology Letters*, 8(3):261–271.
- Porter, W. P. and Kearney, M. (2009). Size, shape, and the thermal niche of endotherms. *Proceedings of the National Academy of Sciences of the United States of America*, 106(Supplement 2):19666–72.
- Poulsen, L., Moldrup, M., Berge, T., and Hansen, P. (2011). Feeding on copepod fecal pellets: a new trophic role of dinoflagellates as detritivores. *Marine Ecology Progress Series*, 441:65–78.
- Prasad, R. R. (1958). A note on the occurrence and feeding habits of *Noctiluca* and their effects on the plankton community and fisheries. *Proceedings of the Indian Academy of Sciences - Section B*, 47(6):331–337.

-
- Prego, R., Guzmán-Zuñiga, D., Varela, M., DeCastro, M., and Gómez-Gesteira, M. (2007). Consequences of winter upwelling events on biogeochemical and phytoplankton patterns in a western Galician ria (NW Iberian peninsula). *Estuarine, Coastal and Shelf Science*, 73(3-4):409–422.
- Quevedo, M., Gonzalez-Quiros, R., and Anadon, R. (1999). Evidence of heavy predation by *Noctiluca scintillans* on *Acartia clausi* (Copepoda) eggs off the central Cantabrian coast (NW Spain). *Oceanologica Acta*, 22(1):127–131.
- Raabe, T. and Wiltshire, K. (2009). Quality control and analyses of the long-term nutrient data from Helgoland Roads, North Sea. *Journal of Sea Research*, 61(1-2):3–16.
- Radach, G. (1992). Ecosystem Functioning in the German Bight under Continental Nutrient Inputs by Rivers. *Estuaries*, 15(4):477.
- Radach, G. and Pätsch, J. (2007). Variability of continental riverine freshwater and nutrient inputs into the North Sea for the years 1977–2000 and its consequences for the assessment of eutrophication. *Estuaries and Coasts*, 30(1):66–81.
- Raven, P. H., Evert, R. F., and Eichhorn, S. E. (2000). *Biologie der Pflanzen*. de Gruyter, Berlin, New York, 3 edition.
- Reid, P. C., Holliday, N. P., and Smyth, T. J. (2001). Pulses in the eastern margin current and warmer water off the north west European shelf linked to North Sea ecosystem changes. *Marine Ecology Progress Series*, 215:283–287.
- Reid, P. C., Lancelot, C., Gieskes, W. W. C., Hagmeier, E., and Weichart, G. (1990). Phytoplankton of the North Sea and its dynamics: A review. *Netherlands Journal of Sea Research*, 26(2-4):295–331.
- Reinsch, C. (1967). Smoothing by spline functions. *Numerische Mathematik*, 10(3):177–183.
- Reñé, A., Camp, J., and Garcés, E. (2015). Diversity and Phylogeny of Gymnodiniales (Dinophyceae) from the NW Mediterranean Sea Revealed by a Morphological and Molecular Approach. *Protist*, 166(2):234–63.

- Resende, P., Azeiteiro, U., Goncalves, F., and Pereira, M. (2007). Distribution and ecological preferences of diatoms and dinoflagellates in the west Iberian Coastal zone (North Portugal). *Acta Oecologica*, 32(2):224–235.
- Resende, P., Azeiteiro, U., and Pereira, M. J. (2005). Diatom ecological preferences in a shallow temperate estuary (Ria de Aveiro, Western Portugal). *Hydrobiologia*, 544(1):77–88.
- Riegman, R., Noordeloos, A. A. M., and Cadee, G. C. (1992). Phaeocystis blooms and eutrophication of the continental coastal zones of the North Sea. *Marine Biology*, 112(3):479–484.
- Rijstenbil, J. W., Mur, L. R., Wijnholds, J. J., and Sinke, J. J. (1989). Impact of a temporal salinity decrease on growth and nitrogen metabolism of the marine diatom *Skeletonema costatum* in continuous cultures. *Marine Biology*, 101(1):121–129.
- Rink, B., Grüner, N., Brinkhoff, T., Ziegelmüller, K., and Simon, M. (2011). Regional patterns of bacterial community composition and biogeochemical properties in the southern North Sea. *Aquatic Microbial Ecology*, 63(3):207–222.
- Roelofs, A. (1984). Distributional patterns and variation of valve diameter of *Paralia sulcata* in surface sediments of Southern British Columbia Inlets. *Estuarine, Coastal and Shelf Science*, 18(2):165–176.
- Rolinski, S., Horn, H., Petzoldt, T., and Paul, L. (2007). Identifying cardinal dates in phytoplankton time series to enable the analysis of long-term trends. *Oecologia*, 153(4):997–1008.
- Rudnick, D. L. and Davis, R. E. (2003). Red noise and regime shifts. *Deep-Sea Research Part I: Oceanographic Research Papers*, 50(6):691–699.
- Sahu, G., Satpathy, K. K., Mohanty, A. K., and Sarkar, S. K. (2012). Variations in community structure of phytoplankton in relation to physicochemical properties of coastal waters, southeast coast of India. *Indian Journal of Geo-Marine Sciences*, 41(3):223–241.

- Sakka Hlaili, A., Grami, B., Niquil, N., Gosselin, M., Hamel, D., Troussellier, M., and Hadj Mabrouk, H. (2008). The planktonic food web of the Bizerte lagoon (south-western Mediterranean) during summer: I. Spatial distribution under different anthropogenic pressures. *Estuarine, Coastal and Shelf Science*, 78(1):61–77.
- Sakshaug, E. and Andresen, K. (1986). Effect of light regime upon growth rate and chemical composition of a clone of *Skeletonema costatum* from the Trondheimsfjord, Norway. *Journal of Plankton Research*, 8(4):619–637.
- Salmaso, N. (2003). Life strategies, dominance patterns and mechanisms promoting species coexistence in phytoplankton communities along complex environmental gradients. *Hydrobiologia*, 502(1-3):13–36.
- Samuels, W. B., Kleppel, G. S., and McLaughlin, J. J. A. (1983). Population growth patterns of *Skeletonema costatum* and nutrient levels in the lower East River, New York, U.S.A. *Hydrobiologia*, 98(1):35–43.
- Sánchez, S., de la Casa, J. A., Martínez, M. E., and Molina, E. (1995). The influence of temperature on the growth and fatty-acid composition of *Skeletonema costatum* in a batch photobioreactor. *Journal of Chemical Technology and Biotechnology*, 62(2):148–152.
- Sar, E. A., Sunesen, I., and Lavigne, A. S. (2002). The diatom genus *Thalassiosira*: species from the northern San Matías Gulf (Río Negro, Argentina). *Nova Hedwigia*, 74(3):373–386.
- Schapira, M., Vincent, D., Gentilhomme, V., and Seuront, L. (2008). Temporal patterns of phytoplankton assemblages, size spectra and diversity during the wane of a *Phaeocystis globosa* spring bloom in hydrologically contrasted coastal waters. *Journal of the Marine Biological Association of the UK*, 88(04):649–662.
- Schlüter, M. H., Kraberg, A., and Wiltshire, K. H. (2012). Long-term changes in the seasonality of selected diatoms related to grazers and environmental conditions. *Journal of Sea Research*, 67(1):91–97.

- Schlüter, M. H., Merico, A., Wiltshire, K. H., Greve, W., and Storch, H. (2008). A statistical analysis of climate variability and ecosystem response in the German Bight. *Ocean Dynamics*, 58(3-4):169–186.
- Schöne, H. K. (1972). Experimentelle Untersuchungen zur Ökologie der marinen Kieselalge *Thalassiosira rotula*. I. Temperatur und Licht. *Marine Biology*, 13(4):284–291.
- Schöne, H. K. (1974). Experimentelle Untersuchungen zur Ökologie der marinen Kieselalge *Thalassiosira rotula*. II. Der Einfluß des Salzgehaltes. *Marine Biology*, 27(4):287–298.
- Shanks, A. and Waters, K. (1996). Feeding by a heterotrophic dinoflagellate (*Noctiluca scintillans*) in marine snow. *Limnology and Oceanography*, 41(1):177–181.
- Shi, X., Liu, X., Liu, G., Sun, Z., and Xu, H. (2012). Application of phytoplankton communities for monitoring water quality in the Hangzhou section of Jing-Hang Grand Canal, southern China. *Fundamental and Applied Limnology / Archiv für Hydrobiologie*, 180(1):11.
- Shigesada, N. and Okubo, A. (1981). Analysis of the self-shading effect on algal vertical distribution in natural waters. *Journal of Mathematical Biology*, 12(3):311–326.
- Škaloud, P., Řezáčová, M., and Ellegaard, M. (2006). Spatial distribution of phytoplankton in Spring 2004 along a transect in the eastern part of the North Sea. *Journal of Oceanography*, 62(5):717–729.
- Slawnych, M., Laszlo, C., and Hershler, C. (1997). Motor unit number estimation: Sample size considerations. *Muscle & Nerve*, 20(1):22–28.
- Smayda, T. J. (1997a). Harmful algal blooms: Their ecophysiology and general relevance to phytoplankton blooms in the sea. *Limnology And Oceanography*, 42(5, Part 2):1137–1153.
- Smayda, T. J. (1997b). What is a bloom? A commentary. *Limnology And Oceanography*, 42(5):1132–1136.

-
- Soberón, J. (2007). Grinnellian and Eltonian niches and geographic distributions of species. *Ecology letters*, 10(12):1115–23.
- Soberón, J. and Nakamura, M. (2009). Niches and distributional areas: concepts, methods, and assumptions. *Proceedings of the National Academy of Sciences of the United States of America*, 106 Suppl(Supplement 2):19644–50.
- Song, X., Huang, L., Zhang, J., Huang, H., Li, T., and Su, Q. (2009). Harmful algal blooms (HABs) in Daya Bay, China: an in situ study of primary production and environmental impacts. *Marine pollution bulletin*, 58(9):1310–8.
- Stauffer, B. A., Goes, J. I., McKee, K. T., do Rosario Gomes, H., and Stabeno, P. J. (2014). Comparison of spring-time phytoplankton community composition in two cold years from the western Gulf of Alaska into the southeastern Bering Sea. *Deep Sea Research Part II: Topical Studies in Oceanography*, 109:57–70.
- Stips, A., Bolding, K., Pohlmann, T., and Burchard, H. (2004). Simulating the temporal and spatial dynamics of the North Sea using the new model GETM (general estuarine transport model). *Ocean Dynamics*, 54(2):266–283.
- Tada, K., Pithakpol, S., and Montani, S. (2004). Seasonal variation in the abundance of *Noctiluca scintillans* in the Seto Inland Sea, Japan. *Plankton Biology and Ecology (Japan)*.
- Teeling, H., Fuchs, B. M., Bennke, C. M., Krüger, K., Chafee, M., Kappelmann, L., Reintjes, G., Waldmann, J., Quast, C., Glöckner, F. O., Lucas, J., Wichels, A., Gerds, G., Wiltshire, K. H., and Amann, R. I. (2016). Recurring patterns in bacterioplankton dynamics during coastal spring algae blooms. *eLife*, 5(April2016).
- Telford, R. J., Vandvik, V., and Birks, H. J. B. (2006). How many freshwater diatoms are pH specialists? A response to Pither & Aarssen (2005). *Ecology letters*, 9(4):E1–5; discussion E6–12.
- ter Braak, C. J. F. (1986). Canonical Correspondence Analysis: A New Eigenvector Technique for Multivariate Direct Gradient Analysis. *Ecology*, 67(5):1167–1179.

- ter Braak, C. J. F. and Verdonschot, P. F. M. (1995). Canonical correspondence analysis and related multivariate methods in aquatic ecology. *Aquatic Sciences*, 57(3):255–289.
- Terenko, L. and Terenko, G. (2009). Dynamics of *Scrippsiella trochoidea* (Stein) Balech 1988 (Dinophyceae) blooms in Odessa Bay of the Black Sea (Ukraine). *Oceanological and Hydrobiological Studies*, 38(S2):107–112.
- Tillmann, U., Hesse, K.-J., and Tillmann, A. (1999). Large-scale parasitic infection of diatoms in the Northfrisian Wadden Sea. *Journal of Sea Research*, 42(3):255–261.
- Tingley, M. W., Monahan, W. B., Beissinger, S. R., and Moritz, C. (2009). Birds track their Grinnellian niche through a century of climate change. *Proceedings of the National Academy of Sciences of the United States of America*, 106(Supplement 2):19637–43.
- Townsend, D. W., Cammen, L. M., Holligan, P. M., Campbell, D. E., and Pettigrew, N. R. (1994). Causes and consequences of variability in the timing of spring phytoplankton blooms. *Deep Sea Research Part I: Oceanographic Research Papers*, 41(5–6):747–765.
- Tsiftsis, S., Tsiripidis, I., Karagiannakidou, V., and Alifragis, D. (2008). Niche analysis and conservation of the orchids of east Macedonia (NE Greece). *Acta Oecologica*, 33(1):27–35.
- Tyler, J. E. (1968). The Secchi disc. *Limnology and Oceanography*, 13(1):1–6.
- Vanvoorhis, C. R. W. and Morgan, B. L. (2007). Understanding Power and Rules of Thumb for Determining Sample Sizes. *Tutorials in Quantitative Methods*, 3(2):43–50.
- Vaz, U. L., Cunha, H. F., and Nabout, J. C. (2015). Trends and biases in global scientific literature about ecological niche models. *Brazilian journal of biology = Revista brasleira de biologia*, 75(4 Suppl 1):17–24.

-
- Vieites, D. R., Nieto-Román, S., and Wake, D. B. (2009). Reconstruction of the climate envelopes of salamanders and their evolution through time. *Proceedings of the National Academy of Sciences of the United States of America*, 106(Supplement 2):19715–22.
- Villac, M. C. and Tenenbaum, D. R. (2010). The phytoplankton of Guanabara Bay, Brazil. I. Historical account of its biodiversity. *Biota Neotropica*, 10(2):271–293.
- Wake, D. B., Hadly, E. A., and Ackerly, D. D. (2009). Biogeography, changing climates, and niche evolution: Biogeography, changing climates, and niche evolution. *Proceedings of the National Academy of Sciences of the United States of America*, 106(Supplement 2):19631–6.
- Waldron, H. N., Attwood, C. G., Probyn, T. A., and Lucas, M. I. (1995). Nitrogen dynamics in the Bellingshausen Sea during the Austral spring of 1992. *Deep Sea Research Part II: Topical Studies in Oceanography*, 42(4-5):1253–1276.
- Wang, X., Tang, K., Wang, Y., and Smith, W. (2010). Temperature effects on growth, colony development and carbon partitioning in three *Phaeocystis* species. *Aquatic Biology*, 9(3):239–249.
- Wang, Z., Li, Z., and Li, D. (2012). A niche model to predict *Microcystis* bloom decline in Chaohu Lake, China. *Chinese Journal of Oceanology and Limnology*, 30(4):587–594.
- Warner, A. and Hays, G. (1994). Sampling by the continuous plankton recorder survey. *Progress In Oceanography*, 34(2-3):237–256.
- Weijerman, M., Lindeboom, H., and Zuur, A. (2005). Regime shifts in marine ecosystems of the North Sea and Wadden Sea. *Marine Ecology Progress Series*, 298:21–39.
- Werner, P. (1993). Zur Vorgeschichte der Gründung der Königlichen Biologischen Anstalt auf Helgoland. *Helgoländer Meeresuntersuchungen*, 47(S1):1–23.

- Weston, K., Greenwood, N., Fernand, L., Pearce, D. J., and Sivyer, D. B. (2008). Environmental controls on phytoplankton community composition in the Thames plume, U.K. *Journal of Sea Research*, 60(4):246–254.
- Widdicombe, C. E., Eloire, D., Harbour, D., Harris, R. P., and Somerfield, P. J. (2010). Long-term phytoplankton community dynamics in the Western English Channel. *Journal of Plankton Research*, 32(5):643–655.
- Wiens, J. A., Stralberg, D., Jongsomjit, D., Howell, C. A., and Snyder, M. A. (2009). Niches, models, and climate change: assessing the assumptions and uncertainties. *Proceedings of the National Academy of Sciences of the United States of America*, 106(Supplement 2):19729–36.
- Wiltshire, K. H. (2004). Editorial. *Helgoland Marine Research*, 58(4):221–222.
- Wiltshire, K. H. and Dürselen, C.-D. (2004). Revision and quality analyses of the Helgoland Reede long-term phytoplankton data archive. *Helgoland Marine Research*, 58(4):252–268.
- Wiltshire, K. H., Kraberg, A., Bartsch, I., Boersma, M., Franke, H.-D., Freund, J., Gebühr, C., Gerds, G., Stockmann, K., and Wichels, A. (2010). Helgoland Roads, North Sea: 45 Years of Change. *Estuaries and Coasts*, 33(2):295–310.
- Wiltshire, K. H., Malzahn, A. M., Wirtz, K., Greve, W., Janisch, S., Mangelsdorf, P., Manly, B. F. J., and Boersma, M. (2008). Resilience of North Sea phytoplankton spring bloom dynamics: An analysis of long-term data at Helgoland Roads. *Limnology and Oceanography*, 53(4):1294–1302.
- Wiltshire, K. H. and Manly, B. F. J. (2004). The warming trend at Helgoland Roads, North Sea: phytoplankton response. *Helgoland Marine Research*, 58(4):269–273.
- Wu, R., Gao, Y., Fang, Q., Chen, C., Lan, B., Sun, L., and Lan, D. (2013). Diatom assemblages in surface sediments from the South China Sea as environmental indicators. *Chinese Journal of Oceanology and Limnology*, 31(1):31–45.

- Yallop, M. (2001). Distribution patterns and biomass estimates of diatoms and autotrophic dinoflagellates in the NE Atlantic during June and July 1996. *Deep Sea Research Part II: Topical Studies in Oceanography*, 48(4-5):825–844.
- Yoder, J. A. (1979). A comparison between the cell division rate of natural populations of the marine diatom *Skeletonema costatum* (Greville) Cleve grown in dialysis culture and that predicted from a mathematical model. *Limnology and Oceanography*, 24(1):97–106.
- Zhang, S., Liu, H., Chen, B., and Wu, C. (2015). Effects of diet nutritional quality on the growth and grazing of *Noctiluca scintillans*. *Marine Ecology Progress Series*, 527:73–85.
- Zimmermann, N. E., Yoccoz, N. G., Edwards, T. C., Meier, E. S., Thuiller, W., Guisan, A., Schmatz, D. R., and Pearman, P. B. (2009). Climatic extremes improve predictions of spatial patterns of tree species. *Proceedings of the National Academy of Sciences of the United States of America*, 106(Supplement 2):19723–8.
- Zong, Y. (1997). Implications of *Paralia Sulcata* Abundance in Scottish Isolation Basins. *Diatom Research*, 12(1):125–150.

Danksagung, Lebenslauf, Erklärung

Danksagung

Die Anfertigung einer solchen Arbeit kann nie ohne fremde Hilfe und Unterstützung geschehen, deshalb möchte ich mich im Folgenden bei verschiedenen Personen bedanken.

Ich danke PD Dr. Jan A. Freund für die Betreuung und Unterstützung bei der Anfertigung dieser Dissertation und dafür, dass er mir während meiner Zeit am ICBM jederzeit für Fragen und zur Diskussion zur Verfügung stand.

Bei Prof. Dr. Karen H. Wiltshire möchte ich mich ebenfalls für die Betreuung und die Unterstützung bedanken. Natürlich gilt ihr mein Dank auch dafür, dass sie mir ermöglichte mit den außergewöhnlichen Helgoland Reede Daten zu arbeiten.

Zusätzlich danke ich Prof. Dr. Ulrike Feudel für die Möglichkeit, dass ich diese Arbeit in ihrer Arbeitsgruppe am ICBM anfertigen konnte.

Ich danke der gesamten Arbeitsgruppe „Theoretische Physik und Komplexe Systeme“ am ICBM für die Diskussion und kritische Betrachtung meiner Ergebnisse. Besonders danken möchte ich Jens, Christian und Klemens.

Allen anderen Kollegen und Kolleginnen am ICBM und der Biologischen Anstalt Helgoland danke ich für die professionelle und konstruktive Zusammenarbeit.

Lebenslauf

Persönliche Daten

Name: Nico Grüner

Geburtsdatum und -ort: 19. September 1979 in Emsdetten, Deutschland

Staatsangehörigkeit: deutsch

Schulische Ausbildung

Grundschule: 1986 – 1990 St. Joseph Grundschule Emsdetten

Gymnasium: 1990 – 2000 Gymnasium Martinum Emsdetten

Abschluss: Abitur

Studium

Wintersemester 2000/2001 bis März 2007: Studium der Biologie mit Hauptfach Zoologie an der Westfälischen Wilhelms-Universität Münster. Diplomarbeit im Institut für Zoophysiology zu dem Thema: „Stoffwechselphysiologische Anpassungen des Wattwurms *Arenicola marina* an saisonale und latitudinale Temperaturänderungen“.

Praktische Tätigkeiten

07.2012 – 06.2016 Wissenschaftlicher Mitarbeiter am Referenzzentrum für Hepatitis C und dem Konsiliarlaboratorium für Tollwut im Institut für Virologie am Universitätsklinikum Essen, Universität Duisburg-Essen.

09.2007 – 04.2012 Wissenschaftlicher Mitarbeiter in der Arbeitsgruppe Theoretische Physik im Institut für Chemie und Biologie des Meeres an der Carl-von-Ossietzky Universität Oldenburg mit einer engen Kooperation mit der Biologischen Anstalt Helgoland.

Publikationsliste

Boersma, Maarten, **Nico Grüner**, Natália Tasso Signorelli, Pedro E. Montoro González, Myron A. Peck, and Karen H. Wiltshire, ‘Projecting Effects of Climate Change on Marine Systems: Is the Mean All That Matters?’, Proceedings of the Royal Society B: Biological Sciences, 283 (2016), 20152274

Grüner, Nico, Oumaima Stambouli, and R Stefan Ross, ‘Dried Blood Spots–Preparing and Processing for Use in Immunoassays and in Molecular Techniques.’, *Journal of visualized experiments?: JoVE*, 97 (2015)

Grüner, Nico, S. Viazov, K. Korn, A. Knöll, M. Trippler, J.F. Schlaak, and others, ‘Performance Characteristics of the VERSANT Hepatitis C Virus RNA 1.0 (kPCR) Assay’, *International Journal of Medical Microbiology*, 305 (2015), 627–635

Ross, R. Stefan, Bernd Wolters, Bernd Hoffmann, Lutz Geue, Sergei Viazov, **Nico Grüner**, and others, ‘Instructive Even after a Decade: Complete Results of Initial Virological Diagnostics and Re-Evaluation of Molecular Data in the German Rabies Virus “outbreak” Caused by Transplantations’, *International Journal of Medical Microbiology*, 305 (2015), 636–643

Krawczyk, Adalbert, Christian Hintze, Jessica Ackermann, Birgit Goitowski, Martin Trippler, **Nico Grüner**, and others, ‘Clinical Performance of the Novel DiaSorin LIAISON(®) XL Murex: HBsAg Quant, HCV-Ab, HIV-Ab/Ag Assays.’, *Journal of clinical virology*, 59 (2014), 44–49

Ross, R, Oumaima Stambouli, **Nico Grüner**, Ulrich Marcus, Wei Cai, Weidong Zhang, and others, ‘Detection of Infections with Hepatitis B Virus, Hepatitis C Virus, and Human Immunodeficiency Virus by Analyses of Dried Blood Spots - Performance Characteristics of the ARCHITECT System and Two Commercial Assays for Nucleic Acid Amplification’, *Virology Journal*, 10 (2013), 72

Freund, Jan A., **Nico Grüner**, Sabrina Brüse, and KarenH. Wiltshire, ‘Changes in the Phytoplankton Community at Helgoland, North Sea: Lessons from Single Spot Time Series Analyses’, *Marine Biology*, 159 (2012), 2561–2571

Rocker, Dagmar, Thorsten Brinkhoff, **Nico Grüner**, Marco Dogs, and Meinhard Simon, ‘Composition of Humic Acid-Degrading Estuarine and Marine Bacterial Communities’, *FEMS Microbiology Ecology*, 80 (2012), 45–63

Grüner, Nico, Christina Gebühr, Maarten Boersma, Ulrike Feudel, Karen H. Wiltshire, and Jan A. Freund, 'Reconstructing the Realized Niche of Phytoplankton Species from Environmental Data: Fitness versus Abundance Approach', *Limnology and Oceanography: Methods*, 9 (2011), 432–442

Rink, Beate, **Nico Grüner**, Thorsten Brinkhoff, Katja Zieglmüller, and Meinhard Simon, 'Regional Patterns of Bacterial Community Composition and Biogeochemical Properties in the Southern North Sea', *Aquatic Microbial Ecology*, 63 (2011), 207–222

Schröer, Mareike, Astrid C. Wittmann, **Nico Grüner**, Hans-Ulrich Steeger, Christian Bock, Rüdiger Paul, and Hans-O. Pörtner, 'Oxygen Limited Thermal Tolerance and Performance in the Lugworm *Arenicola Marina*: A Latitudinal Comparison', *Journal of Experimental Marine Biology and Ecology*, 372 (2009), 22–30

Erklärung

Hiermit erkläre ich, dass ich diese Dissertation selbstständig verfasst und keine anderen als die angegebenen Hilfsmittel genutzt habe. Alle wörtlich oder inhaltlich übernommenen Stellen habe ich als solche gekennzeichnet.

(Ort, Datum)

(Nico Grüner)